

**The Distribution of Stratospheric
Water Vapour as Measured by
the Microwave Limb Sounder**

Ewan S. Carr

**Doctor of Philosophy
The University of Edinburgh
1996**



Declaration

This thesis has been composed by myself, and all work reported herein is my own except where otherwise stated.

Acknowledgements

I would like to thank Bob Harwood for supervising this research and providing invaluable guidance and encouragement throughout. My thanks also to all members of the Meteorology Department, both past and present, who made working at Edinburgh such a relaxing and rewarding experience. Last, and certainly not least, thanks to my friends and family who have supported me over the last few years; it was greatly appreciated. The work was financially supported by the Science and Engineering Research Council.

Abstract

On September 12, 1991 the Upper Atmosphere Research Satellite (UARS) was launched. It carried a number of instruments one of which was the Microwave Limb Sounder (MLS) (Barath et al., 1993). MLS obtains near-global simultaneous measurements of several atmospheric trace species at heights throughout the middle atmosphere. One of the species measured is water vapour.

This thesis describes the zonal-mean climatology of the MLS water vapour measurements in the stratosphere (~ 16 to 50 km) and compares it to previous satellite measurements of H_2O from the Limb Infrared Monitor of the Stratosphere (LIMS) and the Stratospheric and Aerosol Gas Experiment II (SAGE II) (e.g. Russell et al., 1984, Chiou et al., 1993)). Some of main features of the distribution in MLS data, the increase in mixing ratio with height, the presence of a tropical minimum in the lower stratosphere, are consistent with these previous results. The extensive dehydration that occurs in the antarctic polar vortex during winter is comprehensively observed for the first time in UARS data. Water vapour measurements in the arctic winter vortex do not show any significant dehydration.

Temporal and spatial variations are also discussed and it is shown that the zonal-mean variability in the lower tropical stratosphere is primarily annual and is modulated by the quasi-biennial oscillation (QBO) in zonal-mean winds. This modulation means that the time between maxima and minima is either shorter or longer than one year according to the phase of the QBO. At higher latitudes, the variability in the lower stratosphere is marked by periods of descent (and dehydration) in the winter polar vortices. In the upper stratosphere, there is a clear semi-annual oscillation in tropical mixing ratios which compares well to the variability in zonal-mean winds in these regions. The location of the maximum amplitude of the H_2O oscillation moves seasonally between hemispheres. At higher latitudes the variability is annual and is marked by periods of stronger winter descent than in the lower stratosphere, consistent with calculations of high-latitude descent rates (e.g. Schoeberl et al., 1992). The annual variations are complicated by the fact that air is drier in the mesosphere than in the stratosphere so that descent from aloft first brings wet air (and thus maxima) and then dry air (and minima).

Finally, a synoptic case study is given that looks, in detail, at the antarctic and arctic winter conditions encountered by MLS during 1992/93. Evidence is shown to suggest the presence of type II polar stratospheric clouds (PSC) in the antarctic winter and type I PSC in the arctic winter.

Contents

Abstract	iv
1 Atmospheric Water Vapour	1
1.1 Introduction	1
1.2 Discussion of early H ₂ O measurements	4
1.3 Temporal variability at a fixed location	10
1.3.1 Mastenbrook and Oltmans (1983)	10
1.3.2 Cluley and Oliver (1978)	12
1.3.3 Hyson (1983)	12
1.4 Conclusions	13
2 Mechanisms for stratospheric variability	14
2.1 The Brewer-Dobson Theory	14
2.2 The SAO and QBO	15
2.3 Dehydration in the winter vortices	16
2.4 Possible Longer Term Trends	18
3 Previous satellite measurements of stratospheric water vapour	20
3.1 Introduction	20
3.2 The Nimbus 7 Mission	21
3.2.1 Limb Infrared Monitor of the Stratosphere (LIMS)	21
3.2.2 Stratospheric and Mesospheric Sounder (SAMS)	23
3.3 Zonal-mean cross sections of LIMS H ₂ O	24
3.4 Water vapour budget from LIMS/SAMS	27
3.4.1 Introduction	27
3.4.2 Total water from LIMS and SAMS	28
3.5 Stratospheric and Aerosol Gas Experiment II (SAGE II)	28
3.6 Atmosphere Trace Molecule Spectroscopy Experiment (ATMOS)	31
3.7 Comparison of LIMS, SAGE II and ATMOS water vapour	31
3.7.1 Latitudinal variations of LIMS and SAGE II H ₂ O	34
3.7.2 Temporal variations of LIMS/SAMS/SAGE II H ₂ O	37
3.8 Summary	44

4	Microwave Limb Sounder (MLS): Description and validation of its H₂O measurements	46
4.1	The Upper Atmosphere Research Satellite (UARS) Program	46
4.2	Description of MLS and its measurement technique	47
4.3	Other UARS instruments that measure H ₂ O	50
4.3.1	Improved Stratospheric and Mesospheric Sounder (ISAMS)	50
4.3.2	Cryogenic Limb Array Etalon Spectrometer (CLAES)	51
4.3.3	The Halogen Occultation Experiment (HALOE)	51
4.4	Validation of MLS Water Vapour	52
4.4.1	Estimates of Water Vapour Precision	52
4.4.2	Comparison of results from each method	55
4.5	Accuracy of MLS H ₂ O	57
4.6	Summary of Precision and Accuracy	59
4.7	Correlative comparison	60
4.7.1	Frost point hygrometer data	60
4.7.2	Ground-based microwave data	60
4.7.3	FIRS-2 data	63
4.7.4	Halogen Occultation Experiment (HALOE) data	64
4.7.5	Summary of comparison with correlative data	64
4.8	Some problems with v0003 retrievals	66
4.9	Summary	68
5	Monthly and zonally averaged H₂O (v0003) from MLS	69
5.1	Zonal-Mean Climatology of MLS H ₂ O	69
5.2	Comparison with LIMS and SAGE II H ₂ O	77
5.2.1	Data description and quality	77
5.2.2	Percentage differences	78
5.3	Summary	84
6	Variability of Stratospheric MLS H₂O	88
6.1	Introduction	88
6.2	Seasonal scale variations in MLS H ₂ O	88
6.2.1	Lower stratospheric variations	88
6.2.2	Upper stratospheric variations	116
6.3	Summary	132
7	Arctic and Antarctic dehydration case studies	134
7.1	Introduction	134
7.2	Polar Stratospheric Clouds	135
7.2.1	Type I	135
7.2.2	Type II	135
7.2.3	Type III	136
7.2.4	Importance in ozone destruction	136
7.3	Case Study I: August 30 to September 3	137
7.3.1	Introduction	137

7.3.2	Discussion	142
7.3.3	The cooling influence of a tropospheric anti-cyclone	147
7.3.4	Summary	154
7.4	Case Study 2: February 12 to February 16	154
7.4.1	Introduction and overview of winter 1992/93	154
7.4.2	Discussion	155
7.4.3	The cooling influence of a tropospheric anti-cyclone	164
7.4.4	Summary	166
7.5	Conclusions from Case Studies	166
8	Summary and Conclusions	171
	References	176

Chapter 1

Atmospheric Water Vapour

1.1 Introduction

The Earth's atmosphere is believed to have formed around four and a half billion years ago and has evolved to the stage where its present composition is primarily nitrogen (78.1 %) and oxygen (20.9 %) with trace amounts of the noble gases, carbon dioxide, methane, ozone and water vapour (see Table 1.1)

Constituent	Content (fraction of total molecules)
Nitrogen (N ₂)	0.7808 (75.51% by mass)
Oxygen (O ₂)	0.2095 (23.14% by mass)
Argon (A)	0.0093 (1.28% by mass)
Water Vapour (H ₂ O)	0-0.04
Carbon Dioxide(CO ₂)	325 parts per million
Neon (Ne)	18 parts per million
Helium (He)	5 parts per million
Krypton (Kr)	1 parts per million
Hydrogen(H)	0.5 parts per million
Ozone (O ₃)	0-12 parts per million

Table 1.1: Composition of earth's atmosphere below 100 km (*Atmospheric Science - A brief survey*, Academic Press, 1977, p5)

This thesis is concerned mainly with water vapour measurements in the stratosphere, and in particular those made from the Microwave Limb Sounder (MLS), an instrument launched aboard the Upper Atmosphere Research Satellite in 1991. The main results of the thesis will be in chapters 5-7.

In Chapter 5, the general features of the zonal-mean water vapour distribution will be described and will be compared to measurements from previous satellite studies.

In Chapter 6, the variability of MLS water vapour will be examined in more detail by making use of time-series in various latitudinal bands and at various stratospheric levels.

In Chapter 7, two winter case-studies are described. In each of these five-day studies the stratosphere was very cold and water vapour may have been expected to condense to form ice-cloud.

The first three chapters will introduce and describe the earliest measurements of stratospheric water vapour, initially those made *in-situ* (Chapter 1) and then, those made from satellite instruments (Chapter 3). The conclusions and limitations of these measurements are also described. Bridging the *in-situ* and satellite measurement descriptions is a short chapter on the likely dynamical and chemical mechanisms that can affect the stratospheric water vapour distribution (Chapter 2).

The fourth chapter will describe the MLS instrument and give an overview of the quality, in terms of error analysis, of its stratospheric water vapour data.

We begin first, however, by looking at why the study of water vapour is important.

Water vapour is present throughout the atmosphere but its concentration varies dramatically with altitude and geographical location. In the troposphere (altitudes up to ~ 12 km) water vapour is abundant with concentrations of up to several thousand ppmv. However, in the stratosphere and mesosphere (12 to 80 km) concentrations are approximately a factor 1000 smaller. At higher altitudes water vapour decreases further, primarily through destruction by photolysis.

Water vapour, although lacking the attention that ozone and carbon dioxide have attracted, forms an integral part of both the chemistry and dynamics of the atmosphere and hence is amongst the most frequently studied of the atmospheric trace constituents.

Water vapour is a major greenhouse gas which means that any significant increase in its atmospheric content should lead to an increase in the surface temperature of the earth. Several global models have predicted a global warming of

4 degrees Kelvin (K) with doubling of carbon dioxide with 40% of this warming due to additional water vapour (Hansen et al., 1984). A doubling of stratospheric water vapour could by itself cause a rise of 1 K in the surface temperature. However recent modelling work by Rind and Lonergan (1995) suggest that this increase is an overestimate and the true value may be 30% less than first thought. However since the models employed presently have trouble in dealing with issues such as cloudiness there is a great deal of uncertainty as to the impact of increased amounts of greenhouse gases in the atmosphere.

Water vapour also plays an essential part in the mechanism by which ozone is depleted in the polar stratosphere (in fact, in the polar vortex). It has been known for a number of years (Solomon, 1988) that the presence of polar stratospheric cloud (PSC) is required for the heterogeneous depletive chemistry to occur. PSC's were thought to be composed of both nitric acid tridydrate (NAT) and water vapour, although more recent work has cast doubt on their exact crystalline structure (Toon and Tolbert, 1995) but their formation is known to be dependent on both water vapour concentration and temperature. Thus a better knowledge of water vapour concentration may help in determining more accurately the presence of PSC and the subsequent depletion of ozone. Since PSC form at very low temperatures (Toon, 1986) the ice-crystals formed can grow large enough to precipitate. This leads to dehydration in the polar vortex and leads to strong variations in the distribution across the vortex. Since water vapour is mostly conserved elsewhere the dehydration creates an ancillary role as a tracer for motions of extravortical air since, when the vortex breaks up, dehydrated air can be followed as it is transported to lower latitudes.

Another reason why water vapour is extensively measured is because, being relatively inert, it makes an excellent tracer for studies of tropical and mid-latitude atmospheric dynamics particularly those concerned with troposphere-stratosphere exchange.

Also, although more important in the troposphere, accurate knowledge of water vapour content is vital in weather prediction models, particularly in the tropics (Mason, 1986).

Before discussing water vapour measurements from the Microwave Limb Sounder we look at previous measurements of stratospheric water vapour, starting with the

earliest *in situ* results and then progressing to the satellite measurements of the Limb Infra-Red Monitor of the Stratosphere (LIMS) (Gille and Russell, 1984) and the Stratospheric and Aerosol Gas Experiment II (SAGE II) (Rind et al, 1993).

1.2 Discussion of early H₂O measurements

Many of the water vapour measurements made in last fifty years have been reviewed by Mastenbrook (1968), Harries (1976), Penndorf (1978) and Elssaeser (1983). A brief revision of their work and other measurements not discussed by them is given below.

The earliest measurements of stratospheric humidity were made in 1943 over Southern England (Dobson et.al., 1946) and were obtained using a manually operated frost point hygrometer aboard an aircraft; the technique whereby the water vapour content of an air sample is established directly from the frost (or dew) point of that sample. The flights, continuing for around eleven years, provided the largest body of water vapour data for many years to come and made up what became known as Meteorological Research Flight (MRF) data.

Note that, to maintain consistency concentrations of water vapour will be given in ‘parts per million by volume (ppmv)’. Hence the discussion of some of the early water vapour measurements may cite numerical values different from those contained in the literature which are given in terms of the mass mixing ratio.

The majority of these early flights obtained measurements for only the lowest stratospheric levels; aircraft ascents rarely got higher than 40,000 ft (~12 km). Later flights in 1954 and 1955 reached 50,000 ft (~15 km). The measurements are summarised fully in Tucker (1957) and show in general the humidity in the stratosphere, at middle northern latitudes, to be much lower than in the troposphere. An essentially constant stratospheric mixing ratio of 3.2 ppmv was obtained for all levels to 50,000 ft (~15 km)

During, and after, the eleven years that the MRF campaign was in operation other investigators also sought to measure stratospheric water vapor. A large number of these measurements were also made at middle northern latitudes.

Barrett et al (1950) used the same technique as above but to obtain mea-

measurements at higher altitudes (to 100,000 ft, ~ 30 km) the instrument was carried aboard a large plastic balloon. The mixing ratios were an order of magnitude higher than those obtained during the MRF flights. Similar results were obtained by Barclay et al (1960) and Brown et al. (1961) who found average mixing ratios at 27 km to be 59 ppmv and 64 ppmv respectively. Furthermore Murcay et al. (1962) and Hayashi (1961) reported mixing ratios nearly an order of magnitude higher than the MRF results. The results from Hayashi were particularly important, at that time, as they represented two years worth of soundings. Only the measurements of Houghton and Seeley (1960), at this time, bore any resemblance to the early results of Dobson et al.. They used an aircraft borne infrared solar spectrometer to infer mixing ratios of ~ 3.2 ppmv for the region 150–31 hPa (13–25 km) and 6.4 ppmv for the region above 31 hPa.

The widely divergent results, especially in the upper stratosphere, provoked a great deal of argument in part due to the fact that the two largest bodies of data (MRF and Hayashi (1961)) showed mixing ratios that were consistently an order of magnitude different. Of course there was bound to be some degree of natural variability due to the different locations and times that measurements were made. However these would only have a relatively small effect. Frost point measurements made over Iceland (Brewer, 1955) and North-Africa (Helliwell and MacKenzie, 1958), using the same instrument as in the MRF campaign, yielded essentially similar results to that of the MRF measurements over England indicating that the order of magnitude difference with Hayashi's results was unlikely to be entirely due to natural variability.

Mastenbrook (1965) attempted to reconcile at least some of the early differences by considering the possibility of artificial enhancement of water vapour levels due to instrument and/or balloon outgassing. Assuming this as a root cause of the problem he described soundings that took place in 1962 and 1963 in which great care was taken to limit any contamination. The results showed mixing ratios of between 1.5 and 6.5 ppmv at stratospheric levels up 90,000 ft (~ 27 km); results in the lower stratosphere being in close agreement with the MRF values. Other subsequent studies, taking care to avoid the contamination problem, obtained mixing ratios comparable in size with those from the MRF flights and those from Mastenbrook (e.g. Murcay 1969)

Harries (1976) comprehensively reviewed measurements of stratospheric water vapour which occurred in the late sixties and early seventies and also highlighted the great difficulties in determining an accurate vertical profile with the measurements of the time. He stresses the point that, when different techniques are used to measure different quantities at different times, locations and altitudes, a useful comparison is difficult. Moreover the task of deciding which measurements suffered from systematic errors added to this difficulty. However bearing this in mind he pooled the majority of the results from these studies and determined an average northern mid-latitude vertical profile. The profile shows a slight increase in height with mass mixing ratios of between 3.0 and 3.5 ppmv in the range 10-20 km and between 4.0 and 4.8 ppmv between 25 and 45 km. Harries attributes this increase to the possible oxidation of methane to form water vapour and indeed later results discussed below will show that methane oxidation is an important source of stratospheric water vapour, particularly at higher altitudes.

Harries also attempted to deduce the variation of water vapour with latitude. He surmised a distribution whereby a maximum existed in the low stratosphere near the equator with mixing ratios decreasing polewards to 35°N(S); there were few measurements at latitudes beyond this. This was proved later to be incorrect but illustrated both the lack of quality in the data of the time and the danger in drawing global conclusions from relatively few measurements from different instruments.

Penndorf (1978) questioned Harries's method of averaging and comparing datasets (Ellsaesser, 1980) and in his review adopted a different strategy whereby all soundings with mixing ratios greater than 14.5 ppmv (at altitudes > 15 km) were ignored. He then summarised the remaining profiles by observational technique. The main conclusions from his analysis were that,

- The majority of data sets supported a near constant mixing ratio (between 3.2–6.4 ppmv for a mean northern mid-latitude profile) from the tropopause to 30–35 km
- Three independent northern hemisphere datasets showed evidence of an annual cycle in the lower stratosphere, there was some evidence for a long term increase in stratospheric mixing ratios during the years

1954 to 1973 of about 1.4 ppmv per decade.

- Although several of the data sets reported an equatorial maximum in the lower stratosphere Penndorf felt that there were not enough measurements to deduce any firm conclusions about latitudinal gradients.

Ellsaesser (1980, 1983) summarised some later in situ measurements and in general these show a minimum in the lower stratosphere (near 20 km) with mixing ratios increasing with height to the stratopause. Moreover the increase in height is not as large as in previous measurements described by Harries.

In summary, with a couple of exceptions, a large number of the water vapour measurements were of a poor quality and measured too much water. In the late seventies and eighties measurement techniques improved and others evolved (e.g. surface-based microwave measurements). Profiles converged leading to greater confidence in the vertical distribution of stratospheric water vapour. However, although some degree of consensus was reached on the extent of aridity and on the general vertical shape of an H₂O profile, a certain amount of conflict remained between what was expected and what was actually observed.

The distribution of stratospheric water vapour was first hypothesised by Brewer and Dobson (the 'Brewer-Dobson hypothesis' (BD)) in the light of their humidity measurements over Southern England (Brewer, 1949, Dobson et al., 1946). They postulated that the observed dryness could be explained by a freeze-drying mechanism at the tropical tropopause; temperatures here are lower than in polar and temperate regions. They also argued, using additional information on ozone concentrations at high latitudes, for a general circulation where air ascends over the tropics and descends at higher latitudes. Although this theory was, and still is, regarded as a good first order approximation to the zonal-mean circulation, there remained a few contentious issues.

Ellsaesser (1974) suggested that the mean tropical tropopause temperature was too warm to account for the observed dryness.

Another area of confusion lay in the discovery of Kley et al (1979) of a stratospheric minimum (or hygropause as Kley termed it) well above the tropopause. If the BD theory was the sole mechanism for drying stratospheric bound air then either the theory needed revising or the measurements from Kley were simply

wrong. Future *in situ* measurements were consistent with the results of Kley et al. and the reality of a hygropause was considerably strengthened when satellite measurements from the Limb Infrared Monitor of the Stratosphere (LIMS) were analysed (see third chapter). The zonal-mean-latitude height cross-sections of water vapour showed a well-defined minimum in the lower stratosphere persistent in all seven months of data. These minima were not located where LIMS measured temperature minima and thus gave notice of the fact that Brewer and Dobsons' theory needed revision. There was no reason to doubt that zonal-temporal averaging yields a result consistent with that of BD but there was reason to doubt that the vertical transport mechanism was not the slow continuous one suggested by BD. Several authors proposed modifications of the BD hypothesis.

Johnston and Solomon (1979) investigated the role that intense tropospheric mid-latitude thunderstorms play and reported that overshooting cumulonimbus clouds can at times penetrate the tropopause. The tops of these clouds can be 10K colder than the surrounding air and it is thought that this may act to give a net-reduction in local water vapour in the lower stratosphere. This, they suggested, would act to supplement the drying regime in the tropics.

Newell and Gould-Stewart (1981) had a different approach, firstly marking all mixing ratios less than a certain value and then trying to find the times and places where the tropopause temperatures were cold enough to account for water vapour concentration. By taking the lower limit of stratospheric mixing ratio to be 3.5 ppmv (approximately the minimum values reported by Mastenbrook) they looked for 100 hPa temperatures less than -82.4°C - the frost point of the minimum mixing ratio at 100 hPa. The 100hPa pressure surface was chosen as being representative of the tropical tropopause. They discovered that the areas that fulfilled their criteria were over the tropical Pacific, northern Australia, Indonesia and Malaysia during the November to March period and over the Bay of Bengal and India during the Monsoon. They suggest that the bulk of the air entering the stratosphere from the troposphere occurs in these areas ("the stratospheric fountain") during the periods mentioned above.

Danielsen (1982) accepted Newell and Gould-Stewarts' proposed stratospheric inflow areas as likely regions of dehydration but he felt that the criteria they used did not assure a sufficient condition that slow mean ascents are physically

realisable. In fact, he suggests that the dehydration process may be physically independent of the mean motions inferred from the monthly averaged temperatures used by Newell and Gould-Stewart.

Danielsen assessed the impact that large tropical cumulonimbus clouds had on the lower stratosphere and in particular whether they could be expected to act as a “dehydration engine”.

Cumulonimbus (Cb) clouds that penetrate the stratosphere frequently form large ($> 200 \text{ km}^2$) ice-filled anvils at their top. These are formed when, during rapid convection, air at the top of the Cb cloud collapses and meets the still ascending air beneath it. The result is large-scale horizontal divergence. Assuming these two opposing flows mix, Danielsen predicted a temperature profile with two temperature minima, one related to the mean tropopause temperature and the other 1-2 km higher due to the adiabatic gradient (-10 Kkm^{-1}) in the cloud anvil. The dehydration arises from the fall-out of large ice crystals which form at the top of the cloud. Observations of temperature at Panama (summer) and Micronesia (winter) appeared to confirm the profile predicted by Danielsen, the winter and early spring period in the Micronesia region having the maximum dehydration potential.

Danielsen believed this mechanism would account for the minimum found by Kley et al (1979,1980) which was above the tropical tropopause. However Robinson and Atticks-Schoen (1987) disputed this theory as, in over 16000 temperature soundings studied, they found no profiles consistent with those implied by Danielsen nor any appropriate to a turret. They suggested that to test Danielsen’s hypothesis, measurements from high-altitude aircraft were required and these became available in 1987 with the initiation of the NASA-instigated Stratosphere-Troposphere Exchange Project (STEP - see Russell et al, 1987)

The tropical phase of STEP was designed to study the transport of air between the troposphere and stratosphere (Danielsen, 1993). Measurements were made from a high flying sub-sonic aircraft and instruments aboard were able to make accurate measurements of both water vapour and ice-crystals. The measurements were made over the Western Pacific Ocean region from mid-January to mid-February 1987. This region was chosen as being a likely location to observe the deep tropical convection (and subsequent dehydration) predicted by Danielsen

in 1982. The results showed evidence that irreversible transport (and dehydration) of tropospheric air to the lower tropical stratosphere does occur and occurs through similar convective processes to the one predicted by Danielsen in 1982. Danielsen (1993) describes these convective processes in more detail.

Furthermore, recent measurements of tropical stratospheric water vapour and temperature described by Ovarlez et al. (paper submitted to *Quarterly Journal of the Royal Met. Soc.*, 1996) are consistent with Danielsen's hypothesis; the temperature profiles showed double minima spaced ~ 1 km apart.

In summary, the exact mechanism (or mechanisms) which dries air entering the stratosphere is still a contentious issue and, although many of the arguments proposed above are plausible, there is no firm evidence as yet that confirms one of them to be absolutely correct. We will return to the issue of the hygropause (or water vapour minimum) later in the thesis.

We now turn to the limited information gained on the variability of the pre-satellite water vapour measurements.

1.3 Temporal variability at a fixed location

As mentioned above, any conclusions about latitudinal variations were impossible because of the wide divergence in measurement techniques, the measurements themselves and the times the measurements were made. Thus, in this section we deal solely with temporal variations at particular measurement sites. There were only three datasets, as far as I am aware, of any significant length and these are described below

1.3.1 Mastenbrook and Oltmans (1983)

One of the longest records of water vapour data was made from measurements over Washington (39°N) and Boulder (40°N) over the period 1964-1995 (Mastenbrook 1968, Mastenbrook and Oltmans 1983, Oltmans and Hofmann, 1995). Measurements over Washington continued until 1980 when the project was transferred to Boulder.

Soundings were made monthly and ranged approximately from the upper troposphere/lower stratosphere to ~ 25 km (vertical resolution ~ 2 km). Conservative

error estimate were given as $\pm 15\%$. The mean stratospheric concentrations at Boulder were similar to those at Washington but showed a lot less scatter, particularly in the lower stratosphere, and hence the two data sets must be treated separately (Mastenbrook and Oltmans, 1983).

Figure 1.1 (taken from Mastenbrook & Oltmans) shows the average annual variation of the soundings, over Washington, from 1964–1976. A clear and well-defined annual cycle is present with the lowest mean mixing ratios observed throughout January to March (at 14–16 km). By August/September the minimum mixing ratios are ~ 0.3 ppmv higher than earlier in the year and reside at ~ 19 km. The mean concentration in the lower stratosphere was found to be 4.0–4.2 ppmv with slight evidence of an increase in mixing ratios with height.

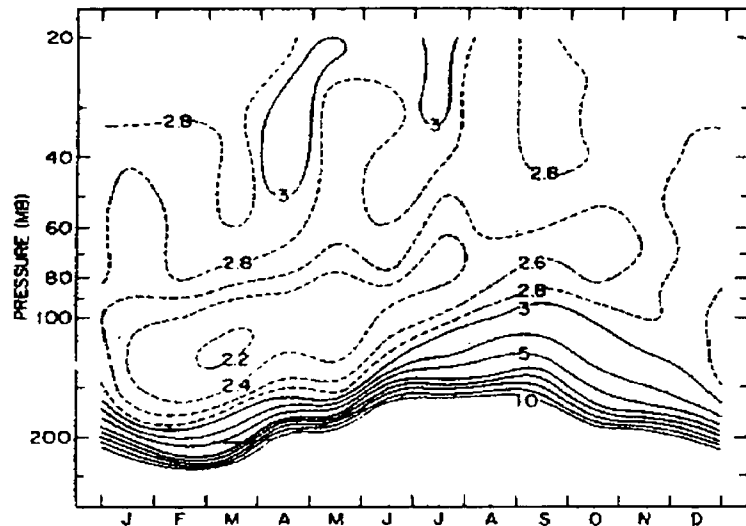


Figure 1.1: Annual variation of stratospheric water vapour derived from soundings made over Washington from 1964-1976. Note that the figure shows concentrations in terms of the mass mixing ratio

At 60 hPa (~ 19 km) they suggest that the variation over the entire data set follows a quasi-biennial oscillation with a longer term non-linear trend acting to increase mixing ratios during the sixties and to decrease them thereafter to the end of the record. The decrease in the latter part of the record is consistent with the results of Hyson (1983) and Cluley and Oliver (1978) discussed below

The data for Boulder show a distinct seasonal cycle with the lowest mixing ratios, in the lower stratosphere, in winter and the highest mixing ratios in summer.

The mean-cycle, over the entire record, is similar to that derived from satellite results (McCormick et al., 1993 – see later). As discussed above, there is a long-term increase in mixing ratios over Boulder ($\sim 0.3\text{--}0.5\%$ above 20 km) which is consistent with the estimates of the yearly growth rate of stratospheric methane.

1.3.2 Cluley and Oliver (1978)

The data discussed by Cluley and Oliver (1978) were obtained using a frost point hygrometer flown aboard an aircraft. Measurements were reported for sixty flights made over southern England between 1972 and 1976. Overall systematic errors were estimated at $\pm 8\%$ on each measurement.

They concluded that the average humidity in the lower stratosphere during the period 1972–1976 was 5.0 ± 0.5 ppmv. Moreover, an annual cycle, with amplitude 0.6 ppmv, was present in the data with a maxima in December. Furthermore some evidence is given for the existence of a 2–3 year cycle but as the dataset covers only four years the evidence is scant at best.

They also compared their results with those from other workers and concluded that mixing ratios in the lower stratosphere increased over the period 1954–1974 but that the increase did not appear to be linear with time. From 1974–1976 the average mixing ratios decreased, consistent with results of Mastenbrook and Oltmans (1983).

1.3.3 Hyson (1983)

Hyson (1983) presented water vapour data from Mildura (34°S), Australia over the period 1974–1979. The measurements were made using a far-infrared radiometer flown aboard an aircraft and covered the years 1973 to 1979. Vertical coverage was from $\sim 10\text{--}21$ km. No explicit error estimates are given.

The average concentration of water vapour in the 15–21 km layer, over the entire record, was 4.0 ppmv. However the average mixing ratio decreased by ~ 1 ppmv over the 1972–1976 to 1976–1979 time periods.

Moreover tentative evidence for a QBO signal in the lower stratospheric water vapour was given but the data record on which he bases his conclusions was short (6 years). He also suggested, based on 100 hPa temperatures at Darwin, a causal

relationship between tropical tropopause temperatures and stratospheric water vapour concentration.

1.4 Conclusions

The earliest results of successfully measured stratospheric water vapour showed that the stratosphere was drier than anticipated. In general, later measurements showed that the dryness was maintained throughout the stratosphere with mixing ratios increasing with height. Typical mixing ratios of between ~ 3.0 ppmv and ~ 6.0 ppmv were observed. Results from Mastenbrook and Oltmans (1983) and others showed that water vapour mixing ratios varied seasonally with the lowest values observed in winter and the highest values in summer. Also, tentative evidence existed for other trends such as a quasi-biennial oscillation (Hyson, 1983) and a longer non-linear trend where mixing ratios increased throughout the 1960's and decreased throughout the 1970's (Cluley and Oliver, 1978, Mastenbrook and Oltmans, 1983). There were not enough good-quality measurements, at geographically widespread locations, to infer conclusions on latitudinal gradients.

The mechanism by which air is dried on entering the stratosphere is only understood on a basic level (Brewer, 1949) and although several theories have sought to explain the observed distribution (e.g. Danielsen, 1982) there remains no definitive answer at present.

We now move on to discuss water vapour measurements made from instruments carried aboard satellites. These instruments revealed significant new information about the stratospheric distribution of water vapour. Before this discussion is a short chapter, describing some of the possible mechanisms that can affect the H_2O distribution.

Chapter 2

Mechanisms for stratospheric variability

This is a short chapter describing some of the dynamical and chemical phenomena which might be expected to affect the distribution of stratospheric water vapour.

2.1 The Brewer-Dobson Theory

Dobson et al (1946) noted that lower stratospheric water vapour measurements over Southern England were comparable to the saturation mixing ratios at the tropical tropopause. This led them to hypothesise that the primary source of stratospheric water vapour was via an upwelling in the extreme coldness of the the tropical tropopause.

As briefly mentioned in Chapter 1 (section 1.2), Brewer (1949) supplemented this argument with a proposed meridional circulation which would transport air upwards and polewards once in the stratosphere. The two theories amalgamated into what became known as the Brewer-Dobson hypothesis. The hypothesis, as a first order approximation, has stood the test of time.

Thus one would expect the water vapour content of an air parcel entering the stratosphere to be marked by the temperature at which it passes through the tropical tropopause. Several investigators sought to find relationships between tropopause temperatures and stratospheric water vapour mixing ratios. Some were unsuccessful (e.g Cluley and Oliver, 1978), while others (e.g. McCormick et al., 1993, Mastenbrook and Oltmans, 1983) noted that the annual variation in lower stratospheric water vapour was consistent with the variation in tropical

tropopause temperatures.

Recent work by Mote et al. (1995) has provided direct evidence to suggest that tropical tropopause temperatures clearly mark the water content of air parcels entering the stratosphere. Their work will be discussed later in the chapter.

Other features of the atmospheric circulation that can affect stratospheric water vapour distribution are the quasi-biennial and semi-annual oscillations (the QBO and SAO respectively).

2.2 The SAO and QBO

The quasi-biennial oscillation is a downwardly propagating quasi-periodic reversal of the equatorial zonal-mean winds and temperatures. It occurs in the stratosphere between 20 and 35 km and descends slowly (~ 1 km/month) with a period varying between 23 and 34 months. It was first noticed independently by Reed (1961) and Veryand and Ebdon (1961) and a theory explaining it appeared in 1968 (Lindzen and Holton, 1968, see also Holton and Lindzen, 1972). This theory essentially proposed that the oscillation is driven from below by the interaction of both vertically propagating Kelvin waves and mixed Rossby-gravity waves with the zonal flow. It is thought that the damping of Kelvin waves may give rise to the westerly phase of the QBO, while mixed Rossby-gravity waves account for the easterly phase.

Since, near the equator, temperatures and zonal winds are in approximate thermal wind balance, a circulation develops so that this balance is maintained against the accelerations produced by the damped waves. This means that during a period when the magnitude of the easterly wind is increasing with height, the vertical velocities in the Hadley circulation are enhanced and act to transport air out of the lower stratosphere faster than during a period of increasing westerlies when the Hadley circulation is reduced. In the sub-tropics the circulation is reversed so that where enhanced upward motion is observed over the equator downward motion is observed in latitudes immediately polewards. Thus we note that the QBO may act to delay or accelerate air parcels in the Brewer-Dobson cell. Moreover, since there is a well established QBO in tropical tropopause temperatures (Angell and Korshover, 1978) the water content of these air parcels may

also bear some signature of their stratospheric-entry temperature.

Quasi-biennial oscillations have been observed in column ozone for many years (Angell and Korshover, 1973, Hasebe, 1984) and for other stratospheric constituents such as nitrogen dioxide (Zawodny and McCormick, 1991). Evidence has been presented for a QBO in water vapour data (Hyson, 1983, Mastenbrook and Oltmans, 1983) but it is tentative at best.

The SAO is also well established (Andrews, 1987) and is the twice yearly reversal of the equatorial zonal-mean wind in the upper stratosphere and mesosphere. The oscillation propagates downwards (at ~ 1 km/month) from the mesosphere to approximately 35 km, where the quasi-biennial oscillation then dominates. The effects on the circulation are similar to those contributed by the QBO lower down, in that air ascends in cool regions and descends in warm regions. Semi-annual oscillations have been observed in many measurements of stratospheric constituents and show up clearly in tropical time series (e.g. Carr et al., 1995, Chiou and McCormick, 1994) and they also manifest themselves in the familiar “double-peaked” structure of middle atmosphere zonal-mean tracer distributions (e.g. Jones and Pyle, 1984).

2.3 Dehydration in the winter vortices

During southern hemisphere winter (\sim May to September) temperatures in the polar vortex can become low enough that water vapour condenses and forms polar stratospheric clouds (PSC)- important platforms for heterogeneous chemical processes that destroy ozone. The question of whether this air is “permanently” dehydrated, through fall-out of the ice-particles, or whether it is rehydrated, through evaporation, before the vortex breaks up has been the subject of much investigation and to some extent the issue is still unresolved.

Stanford (1973) first proposed the idea that the dehydration during winter in the antarctic polar stratosphere could act as a sink for water vapour (see also Ellsaesser (1974)). He surmised, quite reasonably, that the extreme coldness of the polar vortex would lead to local dehydration through the transition of water vapour to ice-crystals. His theory assumed that the stratospheric residence time of these ice-crystals was such that they would fall out to the troposphere (where

their subsequent evaporation would be practically unnoticeable) before the vortex breaks up and temperatures increase. This would then enable dry air to mix in with air from lower latitudes and account for, at least part of, the aridity of the stratosphere (It should be noted that, at this time, the latitudinal gradients of stratospheric water vapour remained uncertain and in fact most of the literature pointed towards mixing ratios decreasing away from the equator to a minimum over the poles). Although Douglass and Stanford (1982) pointed out that the mass of dehydrated air in the antarctic winter stratosphere could only have a relatively small effect when diluted into the entire hemisphere, observations of water vapour made over Antarctica in 1987 (Kelly et al (1989)) show dehydrated air beyond the “boundary” of the vortex spreading to lower latitudes. Moreover, initial results from HALOE [v0016] suggested that polar dehydration had a significant affect on the middle latitude distribution (Tuck et al., 1993). Results from the National Center for Atmospheric Research Community Climate Model (CCM2) were also consistent with this fact (Mote et al., 1993). However Mote (1995) described how, coincidentally, problems in both the model results and in the retrieved HALOE water vapour measurements [v0016] led to the appearance of overly dry middle latitude air in the lower stratosphere. Using a newer and improved version of HALOE data [v0017] and having also corrected the errors in his model *Mote* concluded that there appeared to be little effect on the middle-latitude distribution of water vapour following vortex break up. It is worth bearing in mind, however, that there is an inter-annual variability in the strength and severity of the polar vortex and that this variability may also be modulated by the QBO (Gray and Ruth, 1993). Thus, in any study concerned with the transport/mixing of extra-vortical air to middle latitudes, care should be taken that conclusions are not over generalised. For example, in one year the vortex may be of such a duration so as to allow the complete sedimentation of ice-crystals from the stratosphere. When this vortex breaks up, clearly there is a larger possibility of dehydrated air spreading to mid-latitudes than in a year when the vortex is weak and of a shorter duration.

Another important factor related to this is the descent of air that occurs during both northern and southern winters at high latitudes (Lahoz et al., 1994 and Russell et al., 1993b). This would cause an increase in mixing ratios in the lower

and middle stratosphere and a decrease higher up (where mesospheric air, low in water vapour, descends into the upper stratosphere).

2.4 Possible Longer Term Trends

It has been widely publicised that the global-mean surface temperature of the earth may be rising (Jones, 1994). The main reason for the rise in surface temperature is thought to be due to the increased emissions of greenhouse gases, although is still subject to controversy.

One of the greenhouse gases, methane, contributes to the water vapour budget of the stratosphere through its oxidation and so any increase in its global concentration can be expected, over time, to increase stratospheric water vapour mixing ratios (Blake and Rowland, 1988).

Although recent evidence has suggested that the growth rate of methane emissions has decreased dramatically over the last few years (Steele et al., 1992)) water vapour data over Boulder (40N) suggests that mixing ratios, between 20-25 km, increased, from 1981 to 1994 ($0.3\text{--}0.5\% \text{yr}^{-1}$), in a manner consistent with that predicted from an increase in methane ($0.7\% \text{yr}^{-1}$) (Oltmans and Hofmann, 1995). Below 20 km, the increase in mixing ratios is larger and part of this may be due to the global mean temperature rise in the troposphere. The increases, in both vertical layers, were significant at the 95 % level.

Comparison of UARS measurements of methane and water vapour from 1992 with those of NIMBUS 7, in 1979, are largely inconclusive because of the large error overlap. However, the more recent values of total water are, in general, larger (~ 0.5 ppmv) and tentatively support the rise in water vapour described above. Moreover, in a further chapter it will be shown that some of the differences between LIMS and the Microwave-Limb Sounder (MLS) zonal-mean measurements can be attributed to the rise in atmospheric methane during the 13–14 year gap between measurements.

Another factor that may eventually play an important role is the emission from supersonic aircraft. It is not implausible to assume that in years to come the number of supersonic aircraft in lower stratospheric air-space will increase. Rind and Lonergan (1995) have estimated, using a global climate model, that for a hypo-

thetical fleet of such high-speed aircraft in the northern upper troposphere/lower stratosphere water vapour increased by up to 0.8 ppmv in the flight path and up to 0.2 ppmv globally. However, it should be noted that there are additional complexities in this scenario. For example, since supersonic aircraft are likely to fly near the tropopause and the effects of any emission are expected to be greatest there (Rind and Lacis, 1993) then any increase of H₂O would tend to decrease the local tropopause temperature and hence possibly feedback on stratosphere/troposphere exchange processes.

We now turn to a discussion of water vapour measurements made from satellite instruments.

Chapter 3

Previous satellite measurements of stratospheric water vapour

3.1 Introduction

Measurements from satellite-borne instruments changed the emphasis of research into stratospheric water vapour. Although investigation of the vertical distribution of water vapour remained, and still remains, an important topic of research, satellite technology widened the field so that conclusions could be made on both the vertical and horizontal structure of stratospheric water vapour. Moreover, because satellite instruments had better horizontal coverage than *in situ* and ground-based devices, for the first time conclusions were possible on spatial variations.

Furthermore, some of the questions that prevailed prior to the launch of these satellite instruments could now be answered. For example, the existence of the hygropause in the lower stratosphere had still to be confirmed. Also, the variation with latitude was still very much unknown (Harries, 1976).

In this chapter these points will be looked at in the light of satellite measurements from three instruments, two of them flown aboard the Nimbus 7 spacecraft in 1978/79; the Limb Infrared Monitor of the Stratosphere (LIMS) (Gille and Russell, 1984) and Stratospheric and Mesospheric Sounder (SAMS) (Drummond et al., 1980). More recent measurements from the Stratospheric and Aerosol and Gas Experiment II (SAGE II) (Rind et al., 1993), launched in October 1984, are also discussed.

3.2 The Nimbus 7 Mission

3.2.1 Limb Infrared Monitor of the Stratosphere (LIMS)

The first satellite instrument to successfully measure near-global stratospheric water vapour was the Limb Infrared Monitor of the Stratosphere (LIMS) which was launched aboard the NIMBUS 7 spacecraft in October 1978.

LIMS operated for approximately seven months and throughout that time provided measurements of temperature, water vapour, ozone, nitrogen dioxide and nitric acid. Areal coverage extended from 84° N to 64°S. The vertical range covered most of the stratosphere (100 hPa (16 km) to 1 hPa (50 km)) with precision 0.2–0.3 ppmv and accuracy 20–30 % (above 50 hPa) and $\sim 40\%$ (below 50 hPa) .

The instrument, a six channel radiometer, used the technique of thermal infrared emission limb scanning to obtain radiance profiles (vertical resolution ~ 5 km) across the atmospheric limb of the earth. Measurements of water vapour were deduced from radiances received by the channel centred at $6.9 \mu\text{m}$ (Gille and Russell, 1984).

Effects of spacecraft motion and variations in radiance bias error were found to occur during some orbits and as these problems more readily manifested themselves in single profiles more confidence was placed in zonal-mean results, obtained by averaging profiles around a latitude circle. Moreover only nighttime results were recommended for scientific study since measurements made during the day were affected by non-local thermodynamic equilibrium phenomena (Kerridge and Remsberg 1989).

So that the LIMS data could be validated a wide range of in-situ (and other remotely sensed) correlative measurements were undertaken. Data were obtained at middle and high latitudes throughout the LIMS measuring period so as to encounter a variety of atmospheric conditions. Comparison of these correlative measurements with zonal mean profiles from LIMS revealed differences of less than 30% throughout most of the stratosphere. Furthermore, since in general the vertical distribution of LIMS and correlative water vapour profiles was similar (both showed an increase in mixing ratios with height) a general confidence in the data was established. Further comparisons with *in-situ* data, at the first and second International Water Vapor Intercomparisons of 1981 and 1983 (Figures

3.1 and 3.2), strengthened this confidence. LIMS zonal-mean profiles at 32°N are in general straddled by the *in-situ* ones. The exception to this at the lowest altitudes in the profiles where LIMS water vapour is known to be slightly too dry (Remsberg et al., 1990).

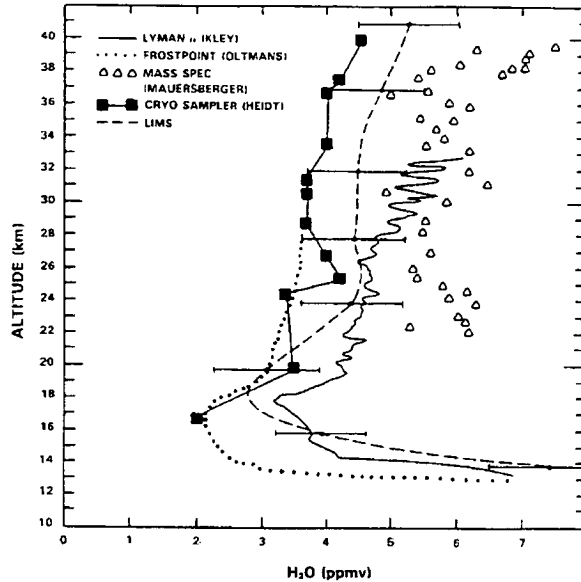


Figure 3.1: Results from the *in-situ* samplers of the 1st International Water Vapor Intercomparison, held over Texas on May 7 1981. LIMS zonal mean profile is for 32°N averaged for May 6–10, 1979 (taken from *WMO 1986*)

Attention is now turned to a discussion of the LIMS latitude-height zonal-mean cross sections and the information they provided.

One of the most important general results of the LIMS mission, and the Nimbus 7 project in general, was the identification of the near-global distribution and budget of stratospheric water vapour (Jones et al., 1986). The near global and continuous nature of the LIMS measurements meant that a great deal of information was yielded on spatial and (to a lesser extent) temporal variations.

Furthermore, since SAMS, also aboard NIMBUS 7, measured methane it was possible to measure the role that methane oxidation played in supplying a source of stratospheric water vapour.

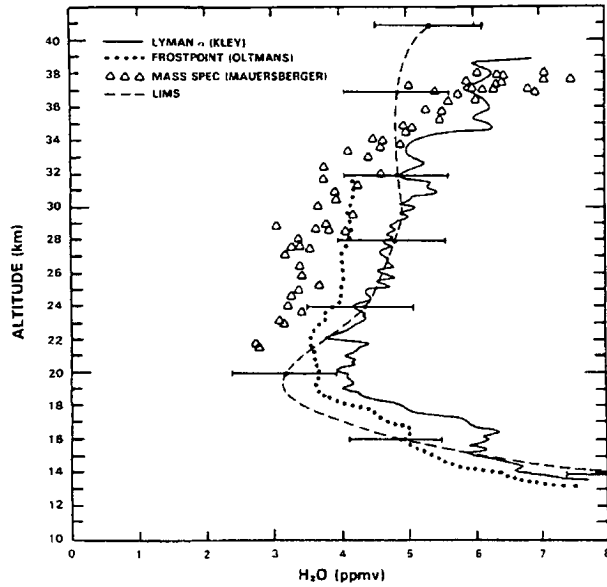


Figure 3.2: Results from the *in-situ* samplers of the 2nd International Water Vapor Intercomparison, held over Texas on October 11 1983. LIMS zonal mean profile is for 32°N averaged for October 27–31, 1978 (taken from *WMO 1986*)

3.2.2 Stratospheric and Mesospheric Sounder (SAMS)

SAMS, an infrared limb viewing instrument, deduced a number of stratospheric and mesospheric constituents, including water vapour and methane (Drummond et al., 1980). Methane measurements were made at heights between ~ 20 hPa to ~ 1.0 hPa with latitudinal coverage of between 50°S and 70°N each day. The zonal-mean measurements of methane have an accuracy of $\sim 20\%$ or better throughout the stratosphere. More detailed discussion of the error budget can be found in Jones and Pyle, 1984).

The H₂O measurements were poor because the transmittance behavior of the water vapour channel was not as expected. Investigations by Mutlow (1984) and Davis (1987) failed to identify the problem. Hence only information on short terms trends and latitudinal variations was possible (Munro and Rodgers (1994)

We now describe some of the main features of the water vapour distribution as revealed by each of the two instruments.

3.3 Zonal-mean cross sections of LIMS H₂O

Figure 3.3 shows zonal-mean distributions of LIMS H₂O for the months from November 1978 to May 1979. The gaps that appear in some plots around the tropical lower stratosphere represent areas where cloud emission, temperature bias errors or uncertainties in interfering O₂ emissions significantly affected retrieval (Rinsland et al.,1982).

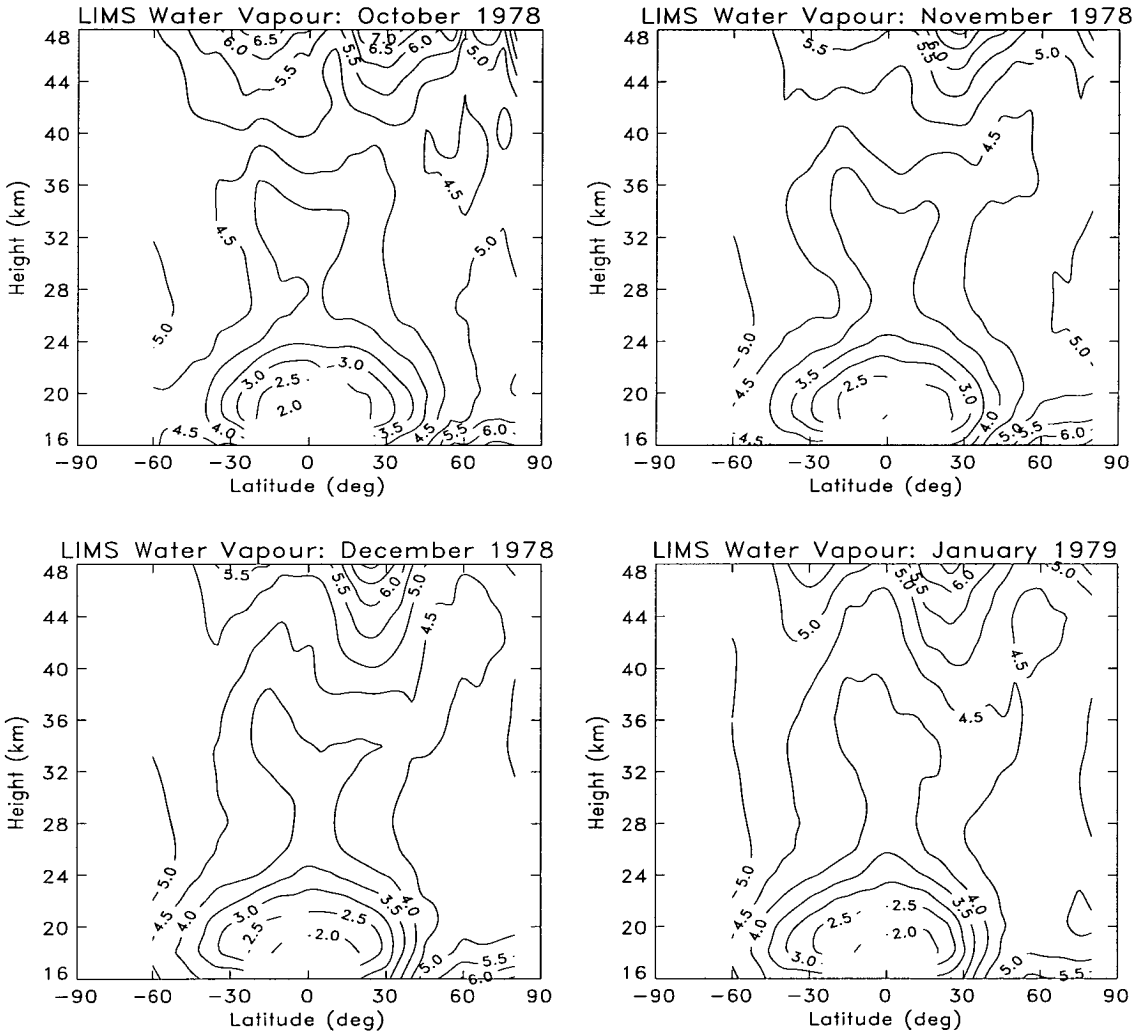


Figure 3.3: Zonal mean water vapour results from LIMS for October 1978 to May 1979. Contour levels are given at 0.5 ppmv intervals

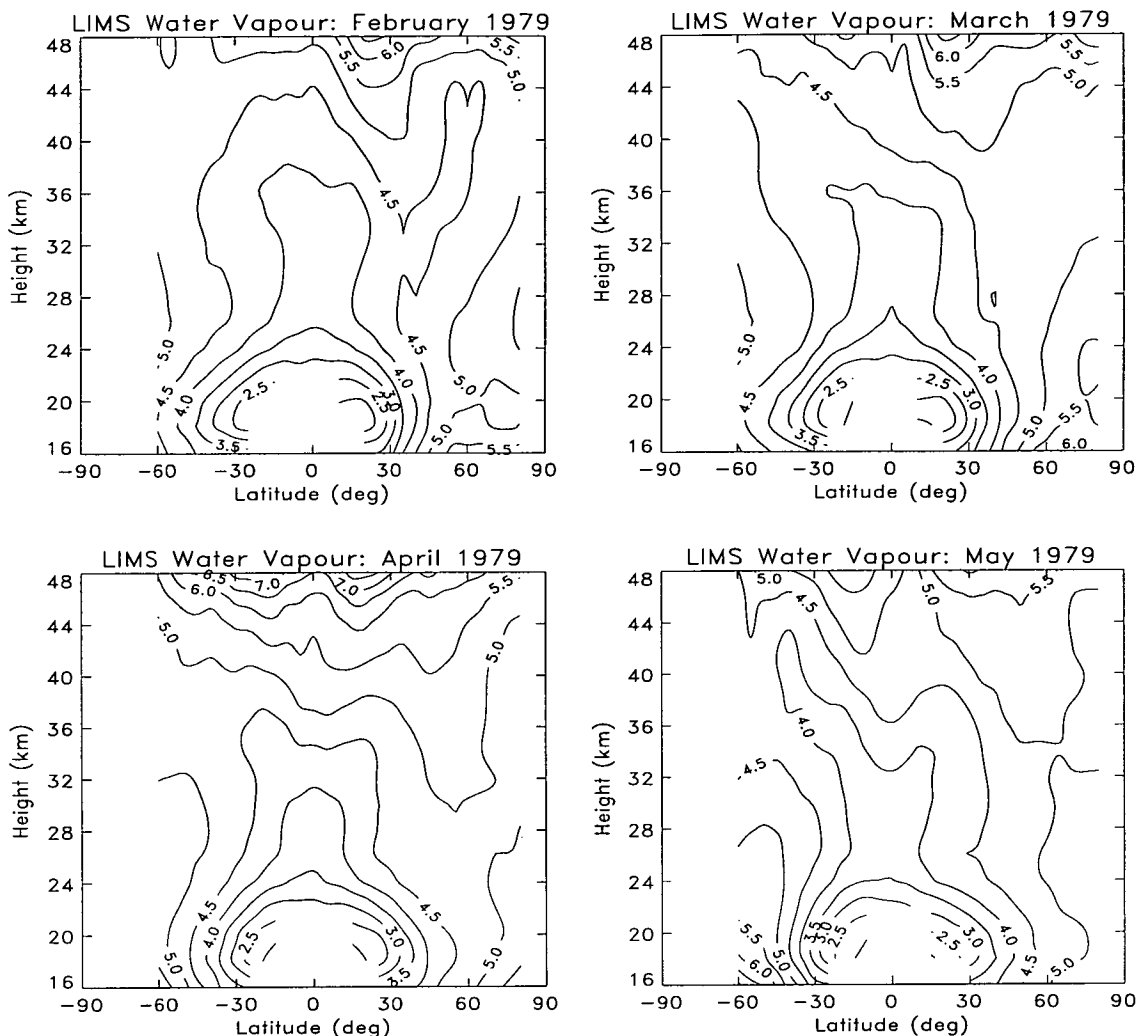


Figure 3.3: Continued

Generally mixing ratios of between 2.5 and 6.5 ppmv were observed with the lowest values in the tropical lower stratosphere. The degree of vertical stratification is similar to results reported by Kley et al. and others as reported above. There is an increase in mixing ratios with height (and latitude) in the tropics and sub-tropics and an essentially constant mixing ratio of 5 ppmv for profiles outwith these areas. The increase in mixing ratio with height is consistent with methane oxidation as a source of water vapour (Jones et al., 1986). Note that the poleward gradient in mixing ratio is the opposite of that shown by earlier authors and highlighted by Harries (1976).

The plots also let us imply certain features of the mean meridional circulation, in both the lower and middle stratosphere. Firstly, the shape of the water vapour

(and temperature - not shown) contours is qualitatively consistent with Brewer-Dobson's hypothesis (Dobson et al., 1946) that air enters the stratosphere above the tropics and then descends at higher latitudes. For example, in November 1978 the 4.5 ppmv contour extends upwards over the equator implying ascent. It then has a tendency to extend into both hemispheres, the larger branch being towards the (winter) north pole. Six months later, in May 1979, where the larger branch is now towards the south (again the winter) pole. This feature, discussed by Remsberg et al. (1984), is supported by the LIMS zonal-mean temperature distributions (not shown) for each month which show "cold" contours in the region of each upward branch.

There is also an asymmetry about the equator in the poleward limits of the low mixing ratios in the lower stratosphere. In November the region of water vapour below 20 km, demarked by the 4.5 ppmv contour, extends from $\sim 60^\circ\text{S}$ to $\sim 45^\circ\text{N}$. In March, during the equinox, there is little asymmetry, then by May the opposite case is observed with the 4.5 ppmv contour extending further north than south. Remsberg et al. (1984) noted that the poleward limits of this asymmetry occur near the position of the tropopause gap for summer ($\sim 45^\circ\text{N}$) and winter ($\sim 30^\circ\text{S}$). They suggest that this may possibly indicate some mixing of wetter tropospheric air into the stratosphere during these times.

The minimum mixing ratios in the lower stratospheric tropics discussed above are a clear and persistent feature apparent in all seven months of the data. Russell et al. (1984) suggest that this is the so called hygropause found by Kley et al. (1979,1982). Although they believe that the feature in LIMS water vapour is real, they point out a couple of caveats that affect both the altitude and dryness of this minimum. Firstly, because retrieval in low-latitudes suffers due to cloud contamination, the areas where low mixing ratios exist are biased towards cloud free events, since any contaminated data are excluded from the zonal average. The net effect of this is to make tropical mixing ratios too low (Remsberg et al., 1990). Secondly, as mixing ratios change relatively slowly above the minimum and relatively rapidly below it, the finite field of view ($\sim 4\text{ km}$) of the water vapour channel results in the retrieved water minimum being 1–2 km too high.

Another important question that analysis of LIMS and SAMS data answered to a great extent was whether stratospheric water vapour mixing ratios were

consistent with methane oxidation being a source of stratospheric water vapour (Jones et al., 1986).

3.4 Water vapour budget from LIMS/SAMS

3.4.1 Introduction

Although it was noted thirty years ago that methane oxidation could be an important part of the stratospheric water vapour budget, (Bates and Nicolet, 1965) the lack of any simultaneous methane and water vapour measurements made confirmation of the theory impossible. Furthermore the divergence observed in many of the water vapour results made it difficult to understand how methane oxidation could supply the necessary mixing ratios.

In an attempt to iron out these difficulties an analysis was carried out using only data from experiments where water vapour and methane profiles were measured simultaneously (WMO 1982). The analysis assumed that no diffusive mixing took place after an air parcel had entered the stratosphere and also that all air parcels entered the stratosphere with the same hydrogen content. The methane oxidation cycle is complex but it is thought that one molecule of methane should yield approximately two molecules of water. Assuming this as a basic axiom the analysis of WMO (1982) argued that the quantity $R = -2([\text{CH}_4]_z - [\text{CH}_4]_{\text{base}})/([\text{H}_2\text{O}]_z - [\text{H}_2\text{O}]_{\text{base}})$ should equal 1, where $[]_z$ represents a mixing ratio at height z . In other words the enhancement of water vapour at any height (z) from its entry level is entirely due to the oxidation of methane at that level (z).

Since 'R' was less than 1 for all the cases examined the methane oxidation hypothesis appeared to be inadequate in explaining the observed water vapour distribution.

Measurements from LIMS and SAMS allowed a reinvestigation of this problem (Jones et al., 1986) since there was almost continuous measurement of both methane and water vapour for seven and a half months (methane was measured until June 1983).

3.4.2 Total water from LIMS and SAMS

The overlap in vertical coverage of LIMS and SAMS allowed calculations of total hydrogen to be made between 20 hPa and 1 hPa ($\sim 25\text{--}50$ km). Total hydrogen can be defined as \mathcal{H} , where $\mathcal{H} = 2[\text{CH}_4] + [\text{H}_2\text{O}] + [\text{H}_2]$.

Jones et al. (1986) initially ignored changes in H_2 (often assumed by many authors to have a constant mixing ratio of 0.5 ppmv) and used $\hat{\text{H}} = 2[\text{CH}_4] + [\text{H}_2\text{O}]$ as their measure of total hydrogen. They felt this was a more sensible approach than the method used in WMO (1982) which, they thought, was inherently flawed since by subtracting quantities of a similar size it would be more sensitive to errors.

After describing briefly the water vapour and methane fields they showed fields of total hydrogen for January, March and May which are reproduced below (Figure 3.4).

The values in each of the three months are approximately constant (6.0–6.5 ppmv) and although there is some structure present the large gradients that appeared in the individual fields are not present. Moreover since the total estimated uncertainty in $\hat{\text{H}}$ is ~ 1 ppmv the structure may not be real.

As $\hat{\text{H}}$ appeared to be a conserved quantity Jones et al. felt that it pointed towards methane oxidation as being the only source of stratospheric water vapour.

A consideration of the variations in H_2 , produced by the Lyman- α radiation, are qualitatively consistent with the minima at 1 hPa in figure 3.4, indicating descent of H_2 -rich and H_2O -poor air from the mesosphere (Figure 3.5)

We now briefly describe two other satellite instruments that measured stratospheric water vapour; the Stratospheric and Aerosol Gas Experiment II (SAGE II) and Atmosphere Trace Molecule Spectroscopy (ATMOS). Following the instrument descriptions is a comparison with some results from LIMS and an investigation into the temporal variations revealed by satellite measurements

3.5 Stratospheric and Aerosol Gas Experiment II (SAGE II)

Another satellite instrument to measure stratospheric water vapour was the Stratospheric Aerosol and Gas Experiment II (SAGE II). It was launched aboard the Earth Radiation Budget Satellite (ERBS) on October 5 1984 (Rind et al., 1993)

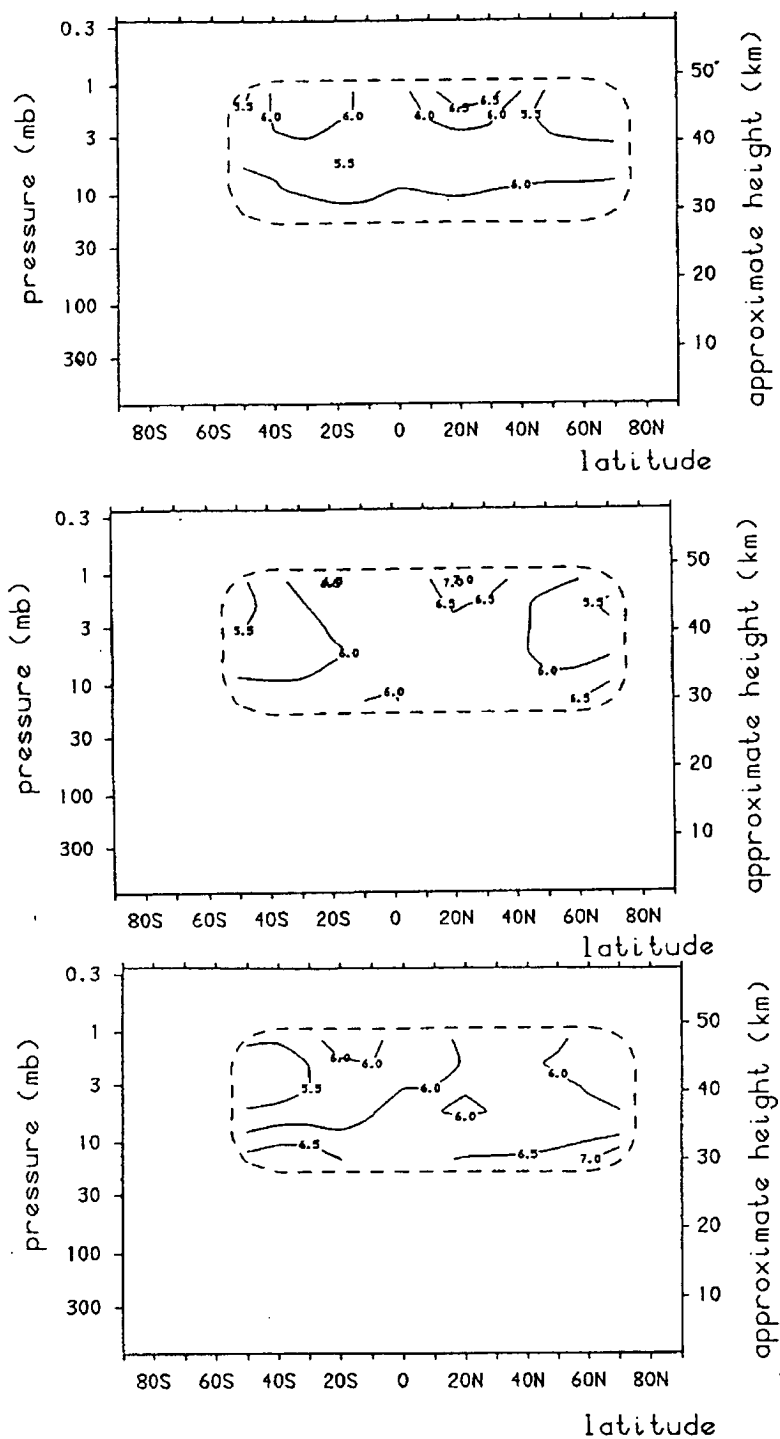


Figure 3.4: $\hat{H} = 2[\text{CH}_4] + [\text{H}_2\text{O}]$ in ppmv calculated from LIMS and SAMS data (top) January 1979; (middle) March 1979; (bottom) May 1979. Taken from *Jones et al.*, 1986

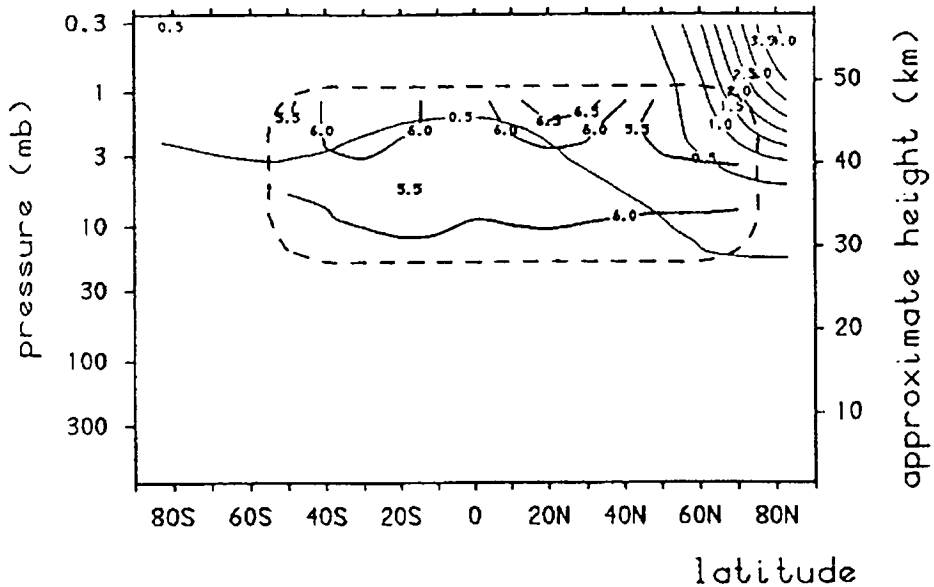


Figure 3.5: \hat{H} in ppmv for January 1979 (thick lines), and calculations of winter H_2 . Taken from *Jones et al.*, 1986

and has been successfully measuring several atmospheric constituents since then. Several years' worth of data have now been archived at the National Space Sciences Data Center (NSSDC).

The SAGE II instrument uses the technique of solar occultation to provide vertical profiles of, amongst others, stratospheric water vapour. The water vapour measurements are deduced from radiances received by the H_2O channel at $0.94 \mu m$ and have a vertical resolution of $\sim 2 km$. Each day, about thirty profiles are obtained. Fifteen of these profiles are made at sunrise and fifteen at sunset. The profiles in each sunset or sunrise group are measured at approximately the same latitude and are separated by 24° in longitude. Near global coverage from $80^\circ N$ to $80^\circ S$ and from 40 km down to cloud tops is achieved approximately every month. Measurements have a vertical resolution of 1–2 km and have a relative error of less than 20% throughout most of the stratosphere. Measurements in low latitudes were affected greatly by heavy aerosol contamination following the eruption of Ruiz in November 1985 and, to a lesser extent, the eruption of El Chichon in 1982.

SAGE II provided a great deal of useful information regarding periodic and long-term variation in water vapour which will be discussed in more detail later

in the chapter.

3.6 Atmosphere Trace Molecule Spectroscopy Experiment (ATMOS)

The Atmosphere Trace Molecule Spectroscopy (ATMOS) experiment was flown aboard Spacelab 3 in 1985 and although it operated for only seven days (April 30 to May 6) provided useful results (Gunson et al., 1990). Like SAGE II, the ATMOS instrument used the technique of solar occultation to deduce vertical profiles of stratospheric water vapour. Measurements were made at an average latitude of 28°N for sunset occultations and 48°S for sunrise occultations. The vertical resolution was approximately 3 km up to 45 km and 4.2 km above 45 km. 1- σ uncertainties were between ~ 0.5 and ~ 1.0 ppmv for sunset occultations and between ~ 0.7 and 2.2 ppmv for sunrise occultations.

3.7 Comparison of LIMS, SAGE II and ATMOS water vapour

In this section we consider, in a similar fashion to Chiou et al. (1993), a comparison of the zonal-mean results from LIMS with those from SAGE II and ATMOS. Note that, although the LIMS monthly averages shown are comprised of significantly more profiles than for SAGE II, the number of profiles in each average is such that the precision is high in each case.

Figures 3.6 and 3.7 show the average ATMOS profiles for 28°N and 48°S. Also plotted are the corresponding monthly averages for LIMS and SAGE II at 30°.

At 28°N there is very good agreement in both vertical gradient and in mixing ratio. LIMS values are lower than SAGE II and ATMOS throughout the profile but agree more closely if the recommendation of Remsberg (1990) to increase LIMS mixing ratios by 10 % in the middle and upper stratosphere is adopted.

The position of the minimum (or hygropause) differs for each instrument. This is partly due to natural variability and partly to the fact that the vertical gradient of water vapour is large in this region and hence the relatively poor vertical resolution of the measurements makes it impossible to accurately resolve

the true vertical structure.

The SAGE II and ATMOS measurements have a finer vertical resolution than LIMS and this may be why they show slightly better agreement.

Note also the apparent decrease in the SAGE II mixing ratios over 1986-1989. Possible reasons are natural atmospheric variability and/or also perhaps a lessening of the effects of aerosols following the eruption of Mount Ruiz in 1985. The former seems unlikely since Chiou (*personal communication*, 1995) has noted that there is a negative trend in SAGE II mixing ratios over the entire seven year SAGE II record. The reasons for this are currently being investigated.

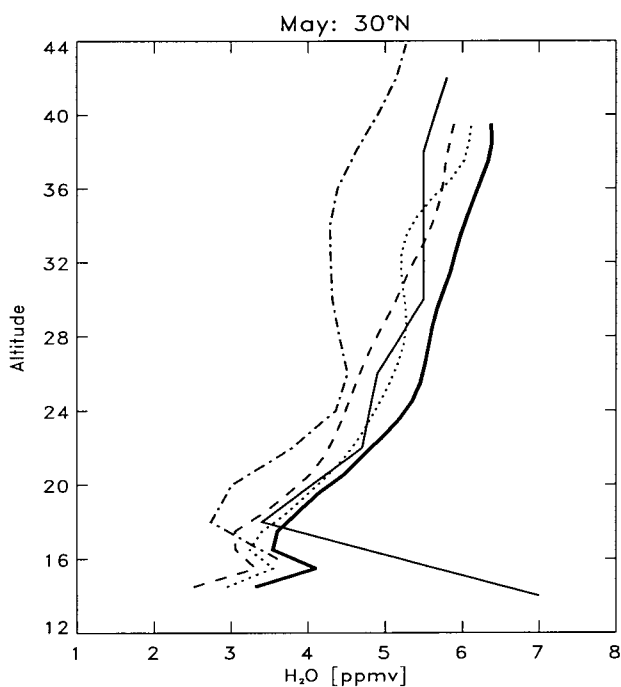


Figure 3.6: Intercomparison for May near 30°N of SAGE II, LIMS and ATMOS. SAGE II(1986-heavy solid)); SAGE II (1987-dotted); SAGE II (1989-dashed); LIMS 1979 (dot-dashed) and light solid line, ATMOS 1985. Note that the ATMOS profile was actually measured at 28°N

Comparison of the 48°S ATMOS profile with SAGE II (50°S) shows a similar picture with general agreement in vertical structure and mixing ratio above ~22 km. Below ~22 km ATMOS mixing ratios are larger and show a local maximum at ~18 km. Below ~18 km the ATMOS mixing ratios decrease to the bottom of the profile at ~14 km where the average mixing ratio is ~3.5 ppmv. SAGE II profiles, for each of the years, show minima at ~16 km of between 2.7 and

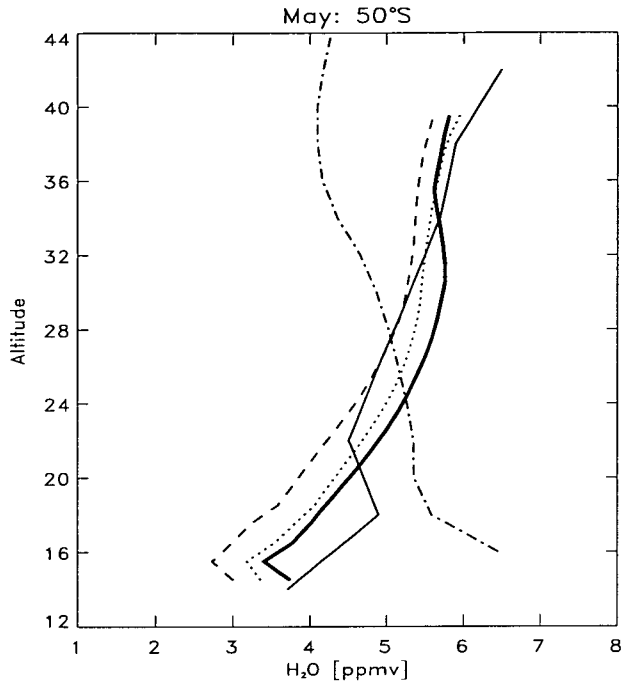


Figure 3.7: Same as Figure 3.6 except for May, 50°S. Note the ATMOS profile was actually measured at 48°S

3.5 ppmv.

The LIMS profile is highly suspect since the profile actually decreases with height. As the vertical gradient of this profile is of the opposite sign to practically every modern (after 1980) water vapour measurement it indicates a problem with LIMS retrievals. The values in the lower stratosphere (below ~18 km) are more likely to be suspect since errors are largest here. The differences between LIMS and SAGE II and ATMOS are reduced somewhat by allowing for the 10 % increase in LIMS mixing ratios above 28 km recommended by Remsberg (1990).

Chiou et al. (1993) also compare SAGE II and LIMS zonal-mean latitude-height cross-sections and show further monthly mean profiles for latitude regions where ATMOS did not measure. Monthly mean profiles for May and November at 10°N, 40°N and 50°S were described. The results are briefly summarised below.

At 10°N the shape of the profiles from LIMS and SAGE II is similar in both November and May but as with the other latitude bands LIMS mixing ratios were consistently lower than those from SAGE II. Above ~24 km LIMS mixing ratios, in both months, are a near-constant 25 % larger. Below ~24 km differences become larger and reach 50% at the lower limit of the profile (~16 km). Mixing

ratios from each instrument typically lie between ~ 3.0 and 6.0 ppmv

At 40°N the profiles for both months were essentially the same as the profiles described above for 28°N with LIMS and SAGE II agreeing very well throughout most of the stratosphere with the largest differences above 28 km where LIMS mixing ratios are known to be too large.

At 50°S there is good agreement in November but in May, as stated previously, there are large discrepancies ($> 50\%$) throughout most of the profile.

Chiou et al. (1993) also attempted to compare the latitudinal structure of SAGE II water vapour with that of LIMS

3.7.1 Latitudinal variations of LIMS and SAGE II H_2O

A more qualitative comparison of SAGE II and LIMS data can be seen in Figures 3.8 and 3.9 which show zonal-mean latitude height cross sections for the months of November and May. Note that the SAGE II figures are not “snapshots” but are composed by collecting the 30 profiles made each day, at different latitudes, until full latitude coverage has been achieved. This takes approximately one month. Consequently the plots do not show exactly the same thing as LIMS and the averages comprise significantly less profiles than LIMS.

Although there are a number of features common to the distributions of both datasets there are also many differences. Some of these similarities and differences are outlined below.

The general features of each of the distributions are relatively similar in that both datasets show; minimum mixing ratios in the tropical lower stratosphere; an increase in mixing ratio with height; a general increase in mixing ratio, in the middle stratosphere, towards each pole; a tendency for dry air to extend more towards the winter hemisphere. There are also a number of differences.

One of the main differences is in the height and mixing ratio of the hygropause. LIMS measures a broad minimum of approximately 2.5 ppmv throughout the tropics at ~ 18 km. SAGE II data shows extremely sharp gradients in the tropics with mixing ratios smallest over the equator (~ 3.0 ppmv) at 16 km. SAGE II also show minima of ~ 3.0 ppmv at higher latitudes at ~ 14 km. These minima are inconsistent with the Brewer-Dobson hypothesis and are not a feature in the LIMS distribution.

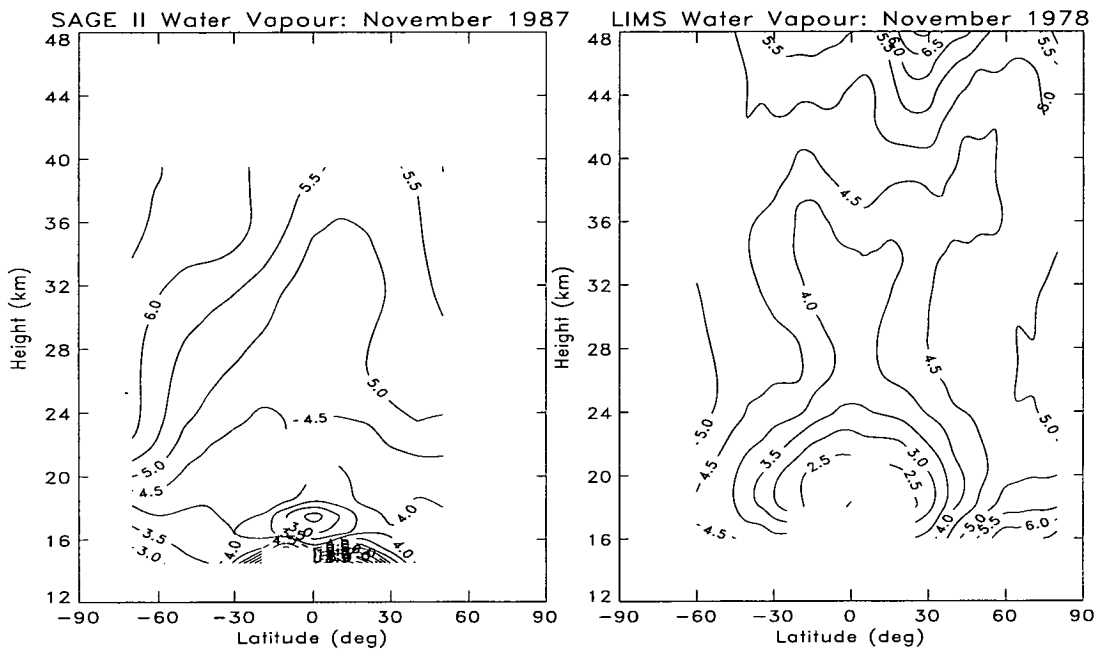


Figure 3.8: Altitude latitude cross sections of LIMS and SAGE II water vapour mixing ratio (ppmv) for November 1978 and 1987 respectively. Typical precision values for SAGE II zonal-mean measurements are between 0.4–0.8 ppmv. Typical precision values for LIMS are between 0.2–0.4 ppmv

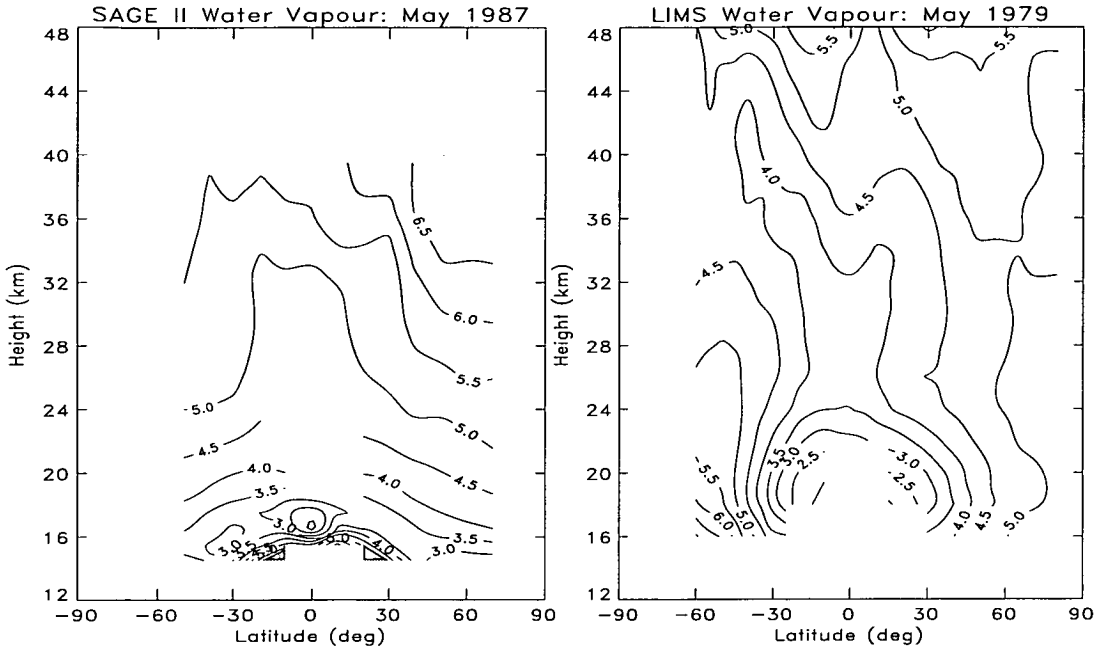


Figure 3.9: Altitude latitude cross sections of LIMS and SAGE II water vapour mixing ratio (ppmv) for May 1979 and 1987 respectively. Typical precision values for SAGE II zonal-mean measurements are between 0.4–0.8 ppmv. Typical precision values for LIMS are between 0.2–0.4 ppmv

Another difference is in the severity of the latitudinal gradients in the lower stratosphere. SAGE II mixing ratios show very little change towards each pole whereas in LIMS data there are sharp increases, below ~ 24 km, in both hemispheres. At higher altitudes there is slightly better agreement where the gradients in LIMS are less severe.

Furthermore, SAGE II does not show the double-peak structure in the tropics at ~ 40 km that LIMS does.

Further work could investigate whether the fact that the SAGE II distribution is not a true zonal-mean could explain some of the differences observed. This could be done by redrawing the LIMS distributions so that, in some way, they would mimic the way in which the SAGE II averages were composed.

To summarise, LIMS and SAGE II paint a generally consistent picture with some shared features such as tropical minimum in the lower stratosphere. Many of the differences are within the accuracy of measurements (Chiou et al., 1993) but there are some differences at higher latitudes, in the lower stratosphere, where

SAGE II mixing ratios are significantly lower than those from LIMS. The reason for this is unknown at present.

Limited results from ATMOS at 28°N and 48°S agree fairly well with both SAGE II and LIMS. LIMS values are lower than both SAGE II and ATMOS everywhere with the exception of high-latitude data in May where lower stratospheric mixing ratios from LIMS have large errors.

The temporal variations of LIMS, SAMS and SAGE II measurements are now addressed.

3.7.2 Temporal variations of LIMS/SAMS/SAGE II H₂O

LIMS H₂O

Although only seven months of LIMS measurements were made they still revealed some useful insights into how stratospheric water vapour varies over time.

The variability (in this case meaning the standard deviation of daily zonal-mean profiles about the monthly mean) in zonal-mean water vapour from LIMS is generally small throughout most of the stratosphere (< 0.2 ppmv), the largest variability occurring in high latitudes of the winter hemisphere, where standard deviations commonly reach 1.0 ppmv.

The variability at 50 hPa (~ 20 km) is small in the tropics (< 0.3 ppmv) with the smallest mixing ratios found around January and February, consistent with the idea of the driest air entering the stratosphere in northern hemisphere winter. There are large latitudinal gradients that remain fairly uniform with time in low and middle latitudes. The largest variability is found at high northern latitudes and is consistent with the greater planetary wave activity that occurs in these regions (Figure 3.10). At 10 hPa the latitudinal gradients are less severe and as before the greatest variability is observed at high northern latitudes. Because of the length of the data-record nothing conclusive can be said about the seasonal trends.

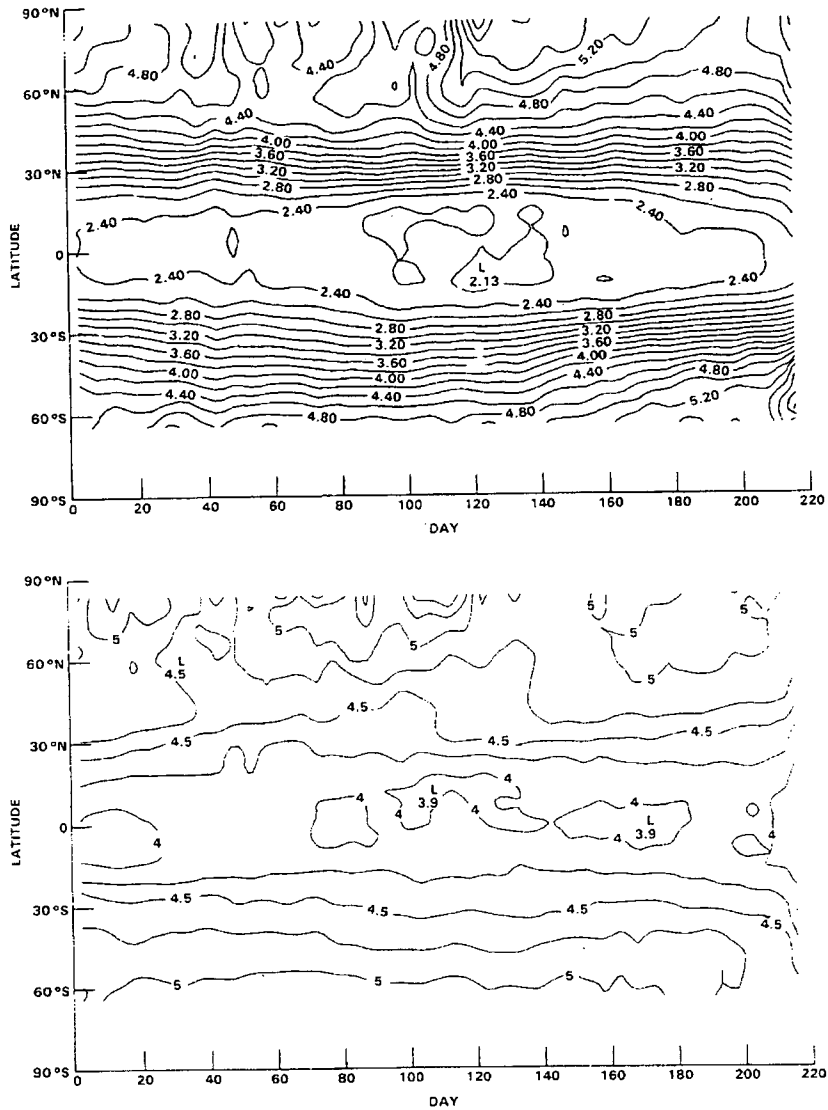


Figure 3.10: LIMS 5-day mean water vapour at 50 (top panel) and 10 hPa (lower panel). (WMO, 1986). Day 40, 80 and 120 are December 2nd 1978, January 11th 1979 and February 20th 1979 respectively. Contour levels at 0.25 ppmv intervals.

SAMS H₂O

SAMS measured water vapour for three years (1979 to 1981). Nothing can be said about absolute values of mixing ratios and long-term trends in the data, since there was an inherent problem with the relevant radiometer which lead to a systematic drift in the raw transmittance data.

However, Munro and Rogers (1994) document a couple of features of the seasonal variation namely a middle to high latitude summer maximum at ~5-10 hPa

with polewards decrease in volume mixing ratios in the winter hemisphere.

SAGE II H₂O

The most extensive source of water vapour data, from satellites, has come from the SAGE II instrument (Rind et al, 1993), which has been measuring water vapour since October 1984. Characteristics of the variability over three years (1986–1988) have been reported by McCormick et al. (1993). Their work is described below.

Two mid-latitude bands (30°N–40°N & 30°S–40°S) and two high latitude bands (50°N–60°N & 50°S–60°S) were chosen for the analysis; data in equatorial latitudes suffered due to aerosol contamination and poor retrieval in general.

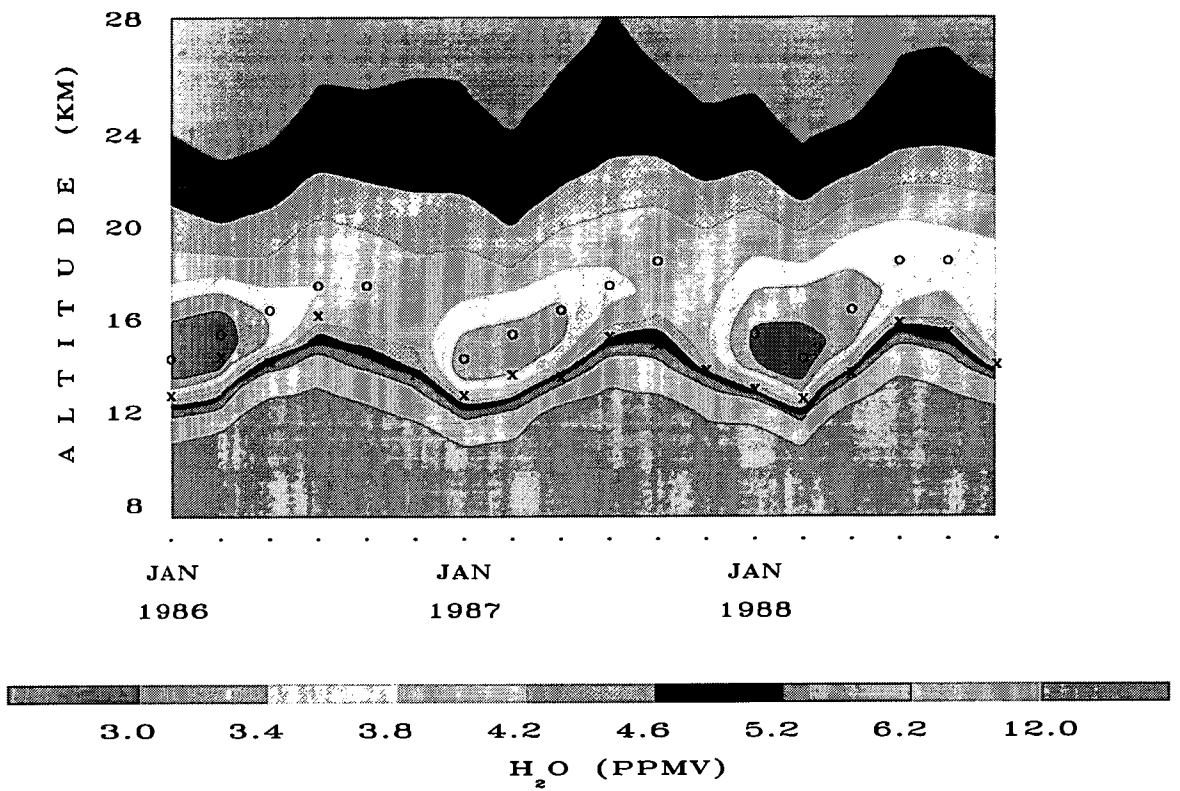
Figure 3.11 shows the time-height cross-section for the ~30°N–~40°N region. It shows a minimum of ~3.0 ppmv in the lower stratosphere from ~15–16 km (~100 hPa). The minimum mixing ratios increase in magnitude until April/May of each year. Correspondingly the altitude of the hygropause (the minimum mixing ratio in a vertical profile) shifts upwards during this period (as does the tropical tropopause). The authors compare their results with those of Mastenbrook and Oltmans (1983) mentioned above and find general agreement in the seasonal variation. Both datasets also exhibit similar amplitudes in the annual variability of the lower stratosphere, 0.6 ppmv at 17.5 km (~70 hPa) for SAGE II and 0.4 ppmv at 90 hPa for Mastenbrook's data (Mastenbrook, 1974).

The ~30°S–~40°S measurements are similar (figure 3.12) in that the yearly minimum occurs at approximately the same time indicating that air in these regions may have originated from the same tropical source(s). The driest air does appear slightly later in the southern hemisphere and the authors suggest this may be because the air is actually dried in the northern tropics (Danielsen, 1982, Danielsen, 1993).

A similar picture is observed in the two high latitude bands (Figures 3.13 and 3.14) with minimum values seen around March/April, some two or three months later than in the lower latitude bands, implying quasi-horizontal transport from the tropics

At higher altitudes (and latitudes), the amplitude of the annual variability diminishes and for heights above ~32 km the variability, particularly in the tropics,

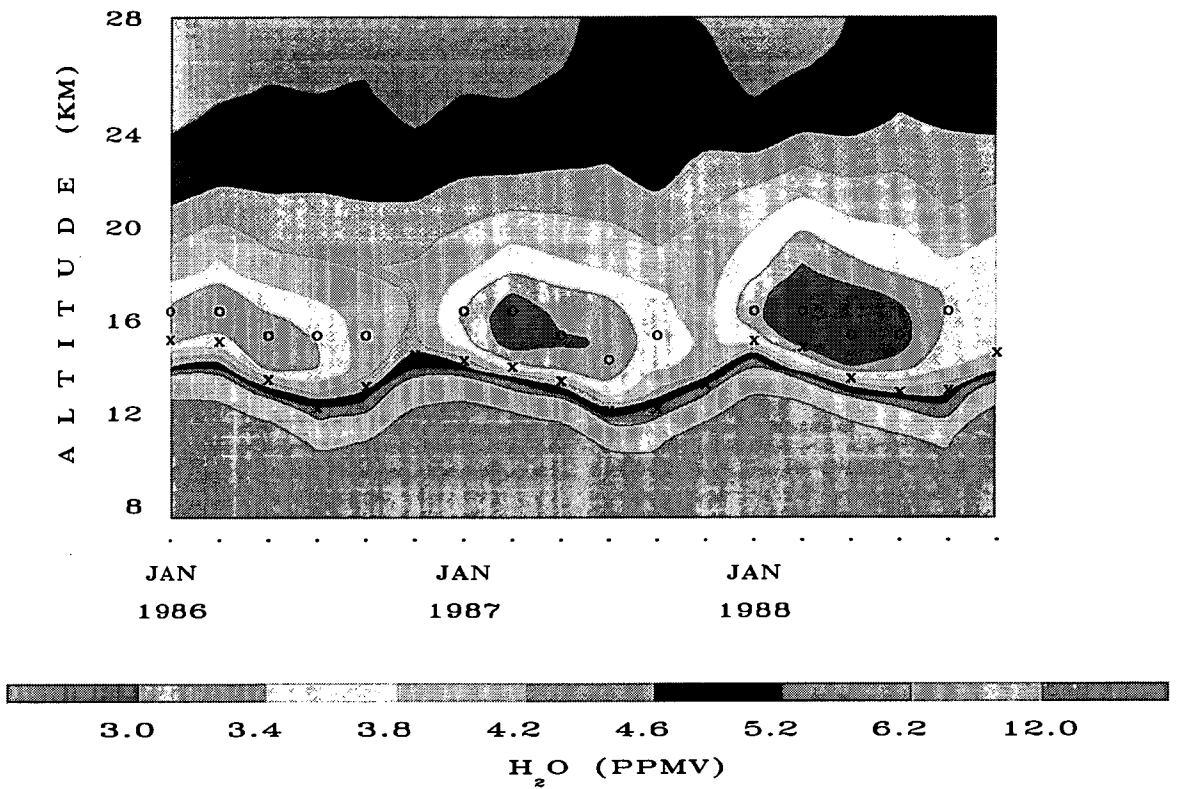
SAGE-II H₂O(1986-88, 30N-40N)



x = tropopause; o = hygropause.

Figure 3.11: SAGE II water vapour (ppmv) in the latitude band 30N-40N. Crosses indicate average tropopause height and circles indicate average hygropause height. From *McCormick et al.*, 1993

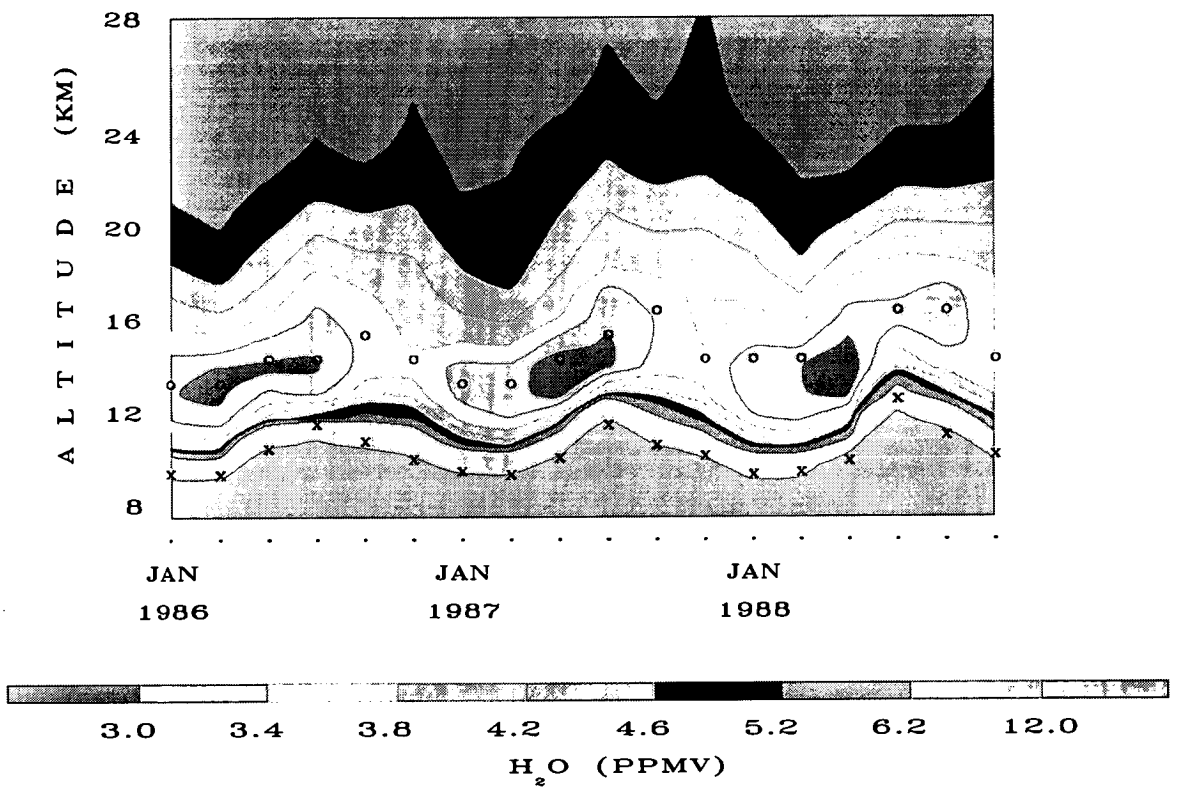
SAGE-II H₂O(1986-88, 30S-40S)



x = tropopause; o = hygropause.

Figure 3.12: SAGE II water vapour (ppmv) in the latitude band 30S-40S. Crosses indicate average tropopause height and circles indicate average hygropause height. From *McCormick et al.*, 1993

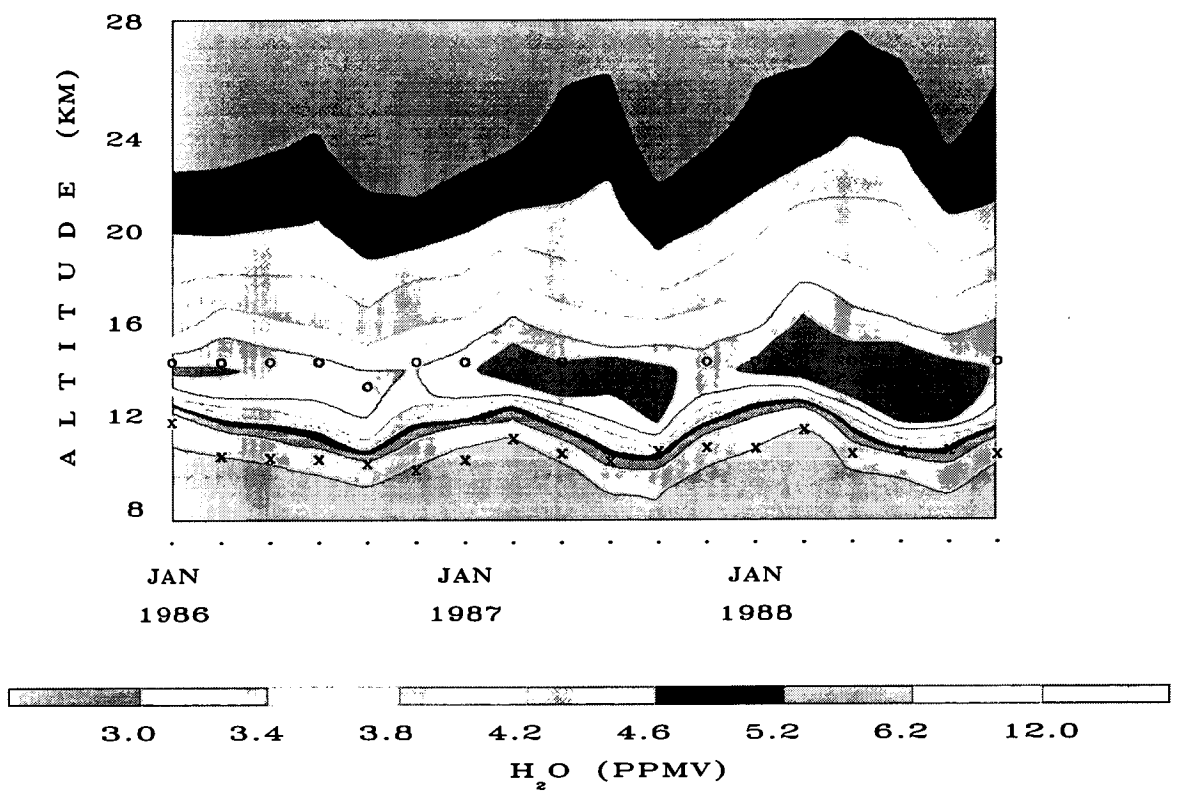
SAGE-II H₂O(1986-88, 50N-60N)



x = tropopause; o = hygropause.

Figure 3.13: SAGE II water vapour (ppmv) in the latitude band 50N-60N. Crosses indicate average tropopause height and circles indicate average hygropause height. From *McCormick et al.*, 1993

SAGE-II H₂O(1986-88, 50S-60S)



x = tropopause; o = hygropause.

Figure 3.14: SAGE II water vapour (ppmv) in the latitude band 50S-60S. Crosses indicate average tropopause height and circles indicate average hygropause height. From *McCormick et al.*, 1993

is predominantly semi-annual (McCormick and Chiou, 1993).

One aspect of the long-term variability in SAGE II data which remains unexplained is that lower stratospheric mixing ratios in the tropics monotonically decrease over the entire length of the data record.

3.8 Summary

In this chapter satellite measurements, prior to the launch of the Microwave Limb sounder, have been described. The main conclusions are as follows

- Typical mixing ratios are between 3.0 ppmv and 6.5 ppmv with the lowest mixing ratios found in the lower and middle atmosphere.
- Satellite measurements of stratospheric water vapour generally show an increase in mixing ratio with height consistent with methane oxidation being the main source of stratospheric water vapour. Measurements from LIMS, and to a lesser extent SAGE II, show that mixing ratios increase rapidly away from the tropics particularly in the lower stratosphere (below ~ 24 km).
- The zonal-mean distributions qualitatively support the Brewer-Dobson hypothesis and are consistent with the in-situ measurements reported by Kley et al. (1982, 1979) showing a minimum in the lower stratospheric tropics above the tropical tropopause. The altitude, magnitude and latitudinal extent of this minimum varies between instruments highlighting the difficulty in accurately measuring water vapour in regions where the vertical distribution possesses large gradients.
- The limited information on temporal variations that LIMS provided showed that the lowest mixing ratios in the lower tropical stratosphere occurred in northern winter. Outwith the tropics the greatest variability, in lower and middle stratospheric regions, was at high northern latitudes particularly during northern winter. SAGE II data provided a great deal more information and confirmed the clear annual signal in the lower stratosphere first observed in the *in-situ* data of Mastenbrook (1968).

The amplitude of this annual signal is similar in both datasets; 0.6 ppmv at 17.5 km (~ 70 hPa) for SAGE II and 0.4 ppmv at 90 hPa for Mastenbrooks' data (see also Mastenbrook, 1974).

At higher latitudes there is a weaker annual signal, which is two or three months out of phase with the variation at lower latitudes, suggesting transport from the tropics. At higher altitudes (above 18 km) there was no sign of the tropical influence at higher latitudes, suggesting that less horizontal transport was occurring. At higher latitudes in the tropics the annual signal diminishes and is replaced by a semi-annual oscillation.

In the following chapter water vapour measurements from the Microwave Limb Sounder (MLS), flown aboard the Upper Atmosphere Research Satellite (UARS), are introduced.

Chapter 4

Microwave Limb Sounder (MLS): Description and validation of its H₂O measurements

In this chapter the MLS instrument is described and, in particular, details are given on how its water vapour measurements are made and how accurate they are believed to be.

4.1 The Upper Atmosphere Research Satellite (UARS) Program

In 1976 a congressional mandate was issued to NASA to develop and then initiate a comprehensive research program aimed at understanding more fully the chemical and physical processes occurring in the upper atmosphere of the earth. NASA quickly set up a number of ground, aircraft and balloon projects to study activity in the stratosphere, mesosphere and lower thermosphere. In addition, out of the need for measurements of a more global and continuous nature NASA investigated using free-flying spacecraft which could achieve this. From this research emerged the Upper Atmosphere Research Satellite Program (Reber, 1990).

The satellite (Figure 4.1) was to be the first to carry out a systematic study of the Earth's upper atmosphere and would carry ten instruments specifically chosen so that a pre-defined set of scientific objectives could be met. Namely to comprehensively study chemical and dynamical processes in the stratosphere and mesosphere, to understand the atmospheric changes following natural and man-

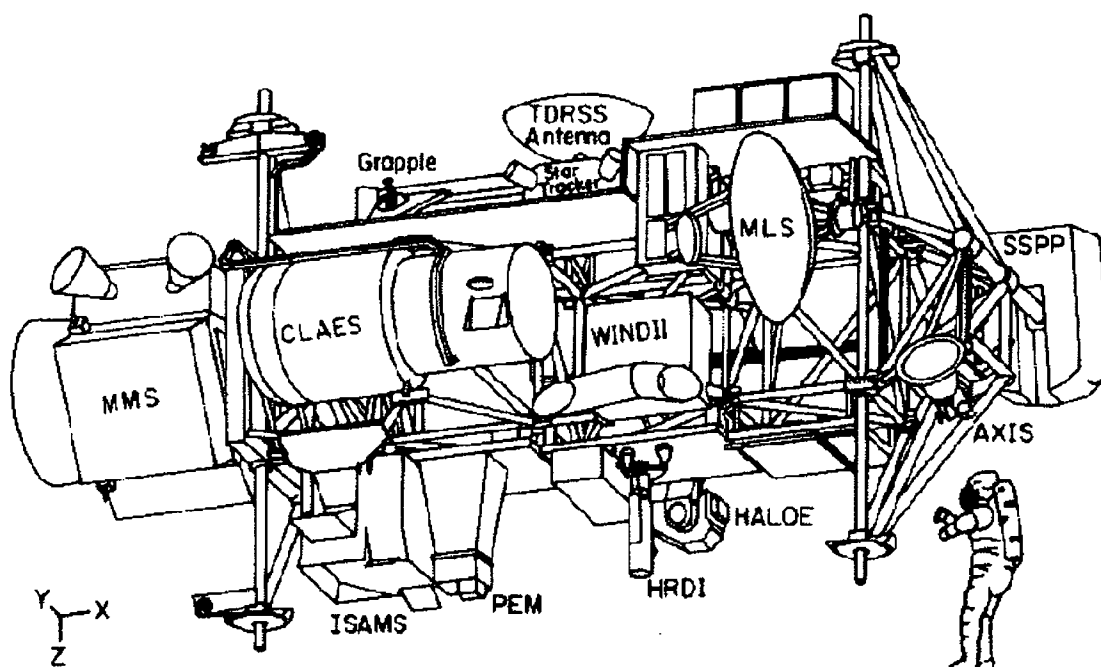


Figure 4.1: Schematic of the Upper Atmosphere Research Satellite(UARS). Courtesy of the British Atmospheric Data Centre.

made chemical (and the related dynamical) perturbations (e.g. volcanoes and release of CFC's) and to improve our knowledge of the role of the upper atmosphere in climate change.

4.2 Description of MLS and its measurement technique

One of the instruments flown aboard UARS was the Microwave Limb Sounder (MLS), developed jointly between the Jet Propulsion Laboratory in the USA and two groups in the UK based at Heriot-Watt University and the Rutherford-Appleton Laboratory. Prior work with the instrument included aircraft (Waters et al., 1980) and balloon (Waters et al., 1984, Robbins et al., 1990) experiments.

The primary measurement objectives of UARS MLS (Barath et al., 1993) were to measure ozone (O_3 over 15–80 km), chlorine monoxide (ClO over 15–45 km), water vapour (H_2O over 15–85 km), temperature (30–60 km) and pressure

(30–60 km). Secondary consideration was given to measuring hydrogen peroxide (H_2O_2), nitric acid (HNO_3) and volcanically ejected sulphur dioxide (SO_2). Note that H_2O_2 was subsequently found to be present in the atmosphere in insufficient concentrations for proper measurement.

An important feature of MLS, lacking in previous satellite stratospheric missions, was that its measurements were unaffected by ice-clouds (e.g. polar stratospheric clouds or PSC's) or aerosol particles (such as those injected into the stratosphere following the eruption of Mount Pinatubo in June 1991).

MLS measures thermal limb emissions at millimeter wavelengths and uses them to obtain simultaneous global measurements of the species (and temperature and pressure) defined above.

There are three radiometers aboard MLS, at 63 GHz, 183 GHz and at 205 GHz (Table 4.1). Water vapour and ozone are measured using information received by the 183 GHz radiometer. Ozone is also measured independently using radiances received by the 205 GHz radiometer.

Radiometer	LO Frequency (GHz)	Wavelength (mm)	Primary Measurement
1	63.282	4.74	Pressure & temperature
2	203.267	1.48	ClO , H_2O_2 & O_3
3	184.778	1.62	H_2O & O_3

Table 4.1: The Microwave Limb Sounder (MLS) Radiometers (LO - local oscillator)

Figure 4.2 shows the calculated limb emission in the spectral region 182–187 GHz which includes both the primary and image spectral sidebands of band 5 (and 6) for the 183 GHz radiometer. More details on the spectroscopy of the ~ 183 GHz H_2O line can be found in Waters et al. (1976, 1993a). Radiances from band 5 are used to retrieve water vapour and are dominated by the emission from the 183.3 GHz H_2O line received by the primary (signal) sideband. The image sideband contains few lines of any strength thus ensuring a ‘clean’ measurement of the 183 GHz emission; the signal received by the radiometer contains a contri-

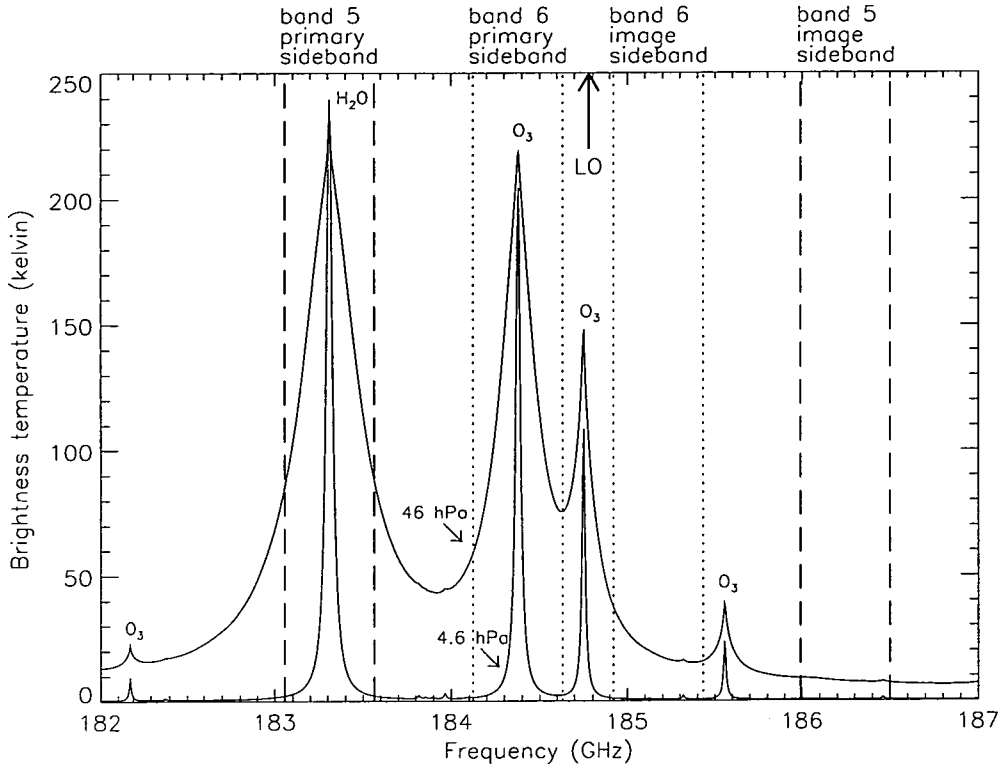


Figure 4.2: Emission spectra for 182–187 GHz. Spectra for tangent pressures of 46 hPa and 4.6 hPa are shown (Lahoz et al., 1996)

bution from both the primary and image sidebands (Jarnot et al., 1994).

There are 15 channels spanning the 510 MHz width of band 5 and for each of these channels a ratio defining the response of the primary and image sidebands is calculated. The ratio is usually close to 1 for most channels. The centre channel of each band is channel 8.

Water vapour profiles are inferred from the intensity, spectral characteristics and vertical variation of the radiances received by each channel. Generally speaking, measurements in the lower stratosphere are derived from radiances in the wing channels. At higher altitudes, the retrieval uses radiances towards the channel 8.

Radiances are measured as the instrument vertically scans the atmospheric limb of the earth and are retrieved, for the “version 3” data used in the bulk of this thesis, onto a grid regularly spaced in a log-pressure “height” co-ordinate with 3 points per decade of pressure. The retrieval algorithm uses a combination of these measured radiances and *a priori* measurement information to derive profiles

of mixing ratio with vertical and horizontal resolution of approximately 5 km and 400 km respectively.

The retrieval also marks each retrieved profile with a quality flag. If the majority of the water vapour measurements at each height level in the profile are satisfactorily retrieved then the flag is given as ‘G’ (good). Only data flagged as ‘G’ are used in this thesis.

The *a priori* information (or ‘climatology’) used in retrieving MLS water vapour is primarily based on zonal-mean LIMS data in the stratosphere and ground-based microwave data for the mesosphere. The climatology is used to constrain the retrieved values so that where there is little measurement information the retrieval relaxes towards the appropriate *a priori* value.

Measurements of MLS water vapour were made for approximately 19 months (from September 20 1991 to April 25 1993) when the 183 GHz radiometer failed. No data were available from June 2 to July 15 1992 due to a solar array problem on UARS.

Each day MLS coverage extends from $\sim 34^\circ$ in one hemisphere to $\sim 80^\circ$ in the other. The satellite performs a 180° yaw maneuver approximately every 36 days (a ‘UARS month’) so that the high-latitudinal observation switches between hemispheres. Within each of these 36 day periods the orbit of UARS slowly precesses with respect to local solar time thus enabling daytime and nighttime measurements at any latitude for each UARS month.

4.3 Other UARS instruments that measure H₂O

Three other instruments aboard UARS measure stratospheric water vapour: the Halogen Occultation Experiment (HALOE) (Russell et al., 1993a), the Improved Stratospheric and Mesospheric Sounder (ISAMS) (Taylor et al., 1993) and the Cryogenic Limb Array Etalon Limb Sounder (CLAES) (Roche et al., 1993).

4.3.1 Improved Stratospheric and Mesospheric Sounder (ISAMS)

ISAMS measures thermal limb emissions for several gases in the infrared region of the spectrum. From these emissions concentrations are derived, at heights

throughout the stratosphere and mesosphere, of the gases involved. Measurements have a vertical resolution of ~ 2.4 km and a horizontal spacing of ~ 200 km along the tangent track. The viewing geometry is similar to MLS, with the satellite yaw maneuver allowing coverage of between 34°N(S) to 80°S(N) in alternate yaw-periods.

ISAMS water vapour measurements were made between late-September 1991 and July 1992 and suffered from various retrieval difficulties such as non-local thermodynamic equilibrium (LTE) effects and aerosol contamination. The ISAMS team recommend that, for the current software version (v0009), only nighttime data between 7 hPa and 0.3 hPa be used. Due to the limitation imposed by this recommendation, and the shortness of data-record, ISAMS H_2O will not be discussed in thesis. Suffice to say, that between 7 hPa and 0.3 hPa, ISAMS and MLS generally show good agreement at all latitudes (Goss-Custard et al., 1996). In future versions of ISAMS H_2O some of these problems may be remedied.

4.3.2 Cryogenic Limb Array Etalon Spectrometer (CLAES)

CLAES also uses infrared limb emissions to remotely measure atmospheric trace gases. It measures, amongst other gases, water vapour. Measurements have vertical and horizontal resolution of ~ 2.5 km and ~ 500 km respectively. Latitudinal coverage was between 34° and 80° , switching between hemispheres at each yaw maneuver. Measurements were made from October 1 1991 to May 5 1993, when the cryogen finally evaporated.

Water vapour measurements from the current retrieval (v0007) suffer, like ISAMS, from non-LTE effects and are thus largely ignored in this thesis.

Another instrument, aboard UARS, that measures water vapour is HALOE.

4.3.3 The Halogen Occultation Experiment (HALOE)

HALOE is a limb occultation instrument which measures atmospheric absorption of solar infrared radiation. It samples the atmosphere twice very orbit; once at sunrise and once at sunset. Fifteen orbits are made each day, thus giving rise to 15 sunrise profiles at one latitude and 15 sunset profiles at another, different, latitude. Profiles in each sunrise or sunset group are separated by $\sim 24^\circ$ in longitude. As



the orbit precesses the latitudes at which measurements gradually change and near-global coverage is obtained approximately every few weeks.

Measurements of water vapour are made from ~ 100 hPa (~ 16 km) to ~ 0.01 hPa (~ 80 km) with a vertical resolution of approximately 2 km (Russell et al., 1993). Comparison of HALOE measurements with a variety of ground-based and balloon-borne instruments indicate an accuracy of $\leq \pm 10\%$ in the height range 100 hPa to 0.1 hPa (~ 16 km to 65 km). Above 0.1 hPa there is more uncertainty since correlative measurements at those altitudes are relatively sparse. The limited results at these heights show correlative measurements 15-20% larger than HALOE. Some HALOE H₂O measurements are shown later, in Chapter 5.

The precision of measurements is 5% in much of the stratosphere. Retrievals in the early part of the mission were limited to heights above 25 km due to the injection of aerosols into the stratosphere following the eruption of Mount Pinatubo in June 1991.

More detail on the validation of HALOE water data is given in Harries et al. (1995).

Attention is now turned to a discussion of the quality of the water vapour measurements from the Microwave Limb Sounder (MLS)

4.4 Validation of MLS Water Vapour

A validation document for MLS water vapour has recently been written (Lahoz et al., 1996). The document discusses in more detail the comparison made with correlative measurements. It also highlights the present state of the MLS (v0003) measurements and pinpoints possible areas where improvements can be made. Some of its main findings regarding precision, accuracy and comparison with correlative data are given below.

4.4.1 Estimates of Water Vapour Precision

A precision or uncertainty associated with each water vapour measurement is computed, along with the measurement itself, by the retrieval algorithm. The precision at each retrieved level in a profile is just a measure of the repeatability of measurement (i.e. if one made the same measurement, say, 1000 times then

the precision, at each pressure level, is the value of the standard deviation around the mean of those 1000 measurements). The estimated precision is comprised of contributions from random noise and also various systematic errors.

The precision obtained by the retrieval algorithm is calculated by propagating the precisions of the radiance measurements, the estimated uncertainties in the constrained parameters and the estimated inaccuracies in the forward model through the retrieval algorithm.

For each of these calculated precisions an error ratio is defined. This is the quotient of the measurement precision and the *a priori* uncertainty. The *a priori* uncertainty is set to 2 ppmv everywhere.

The ratio gives an indication of the dependence of the retrieval on information from the climatology. For example, if the ratio exceeds 0.5 the retrieved mixing ratio has an approximate contribution from the *a priori* which exceeds 25 %.

There are other techniques which can be used to estimate the precision of the water vapour measurements. Lahoz et al. (1996) presented three alternative methods of estimating the precision of MLS water vapour retrievals. They are described below.

Method 1

This method adopted the general technique of Rodgers (1990) whereby the different contributions to the total uncertainty may be estimated. Equation (1) below is for the total error in a retrieval. Contributions from each error source may be obtained from manipulation of the equation.

$$\hat{\mathbf{x}} - \mathbf{x} = [T(\bar{\mathbf{x}}, \hat{\mathbf{b}}, \hat{\mathbf{c}}) - \bar{\mathbf{x}}] + \mathbf{D}_y \mathbf{K}_b \epsilon_b + \mathbf{D}_y \epsilon_y + (\mathbf{A} - \mathbf{I})(\mathbf{x} - \bar{\mathbf{x}}), \quad (4.1)$$

where

$\bar{\mathbf{x}}$ is the reference state of the atmosphere (for MLS $\bar{\mathbf{x}} = \mathbf{x}_a$, the *a priori* state),
 $\hat{\mathbf{b}}$ is an estimate of the forward model parameters \mathbf{b} ,
 $\hat{\mathbf{c}}$ is an estimate of the inverse model parameters \mathbf{c} , e.g. *a priori* data,
the matrix \mathbf{K}_b , known as the model parameter *influence function*, is the sensitivity of the model radiances to the forward model parameter vector \mathbf{b} ,
 ϵ_b is the error vector of \mathbf{b} ,

ϵ_y is the measured radiance error vector.

The *transfer function*, T , relates the retrieved state \hat{x} to the unknown true state x by $\hat{x} = T(x, b, c)$.

The *contribution function*, D_y , is the sensitivity of the retrieval to the measurements y .

The *averaging kernel* matrix, A , is defined by

$$A = \frac{\partial \hat{x}}{\partial x} = D_y K_x,$$

where K_x is the influence function (also known as the weighting function) matrix of the atmospheric state, i.e. the sensitivity of the model radiances to a change in the state of the atmosphere. For more information on error characterisation see Suttie (1995).

The method was run on typical mid-latitude retrievals and yielded precision estimates based only on the root-sum-square (**rss**) of the random errors which include uncertainties in measurement noise, temperature, tangent pressure and other parameters affecting the H₂O retrieval.

Figure 4.3 shows the three major contributors to the random error together with the root-sum-square (**rss**) of all the random errors (solid line)

In the lower stratosphere the **rss** is dominated by the uncertainty in retrieved tangent pressure, which comprises practically the entire certainty in the H₂O retrieval (~ 0.4 ppmv). In the upper stratosphere and lower mesosphere measurement noise increases as does the uncertainty in temperature.

Method 2

The second method involved calculating the variability of profiles near the orbit turning points (80S(N)) in the summer hemisphere. The sampling is densest at these points and so the atmospheric variability should be small. The root-mean-square difference of 241 pairs of close profiles (< 2 hours & < 150km apart) were averaged to give estimated values of precision. The dashed line in Figure 4.4, labelled '2', shows these estimates.

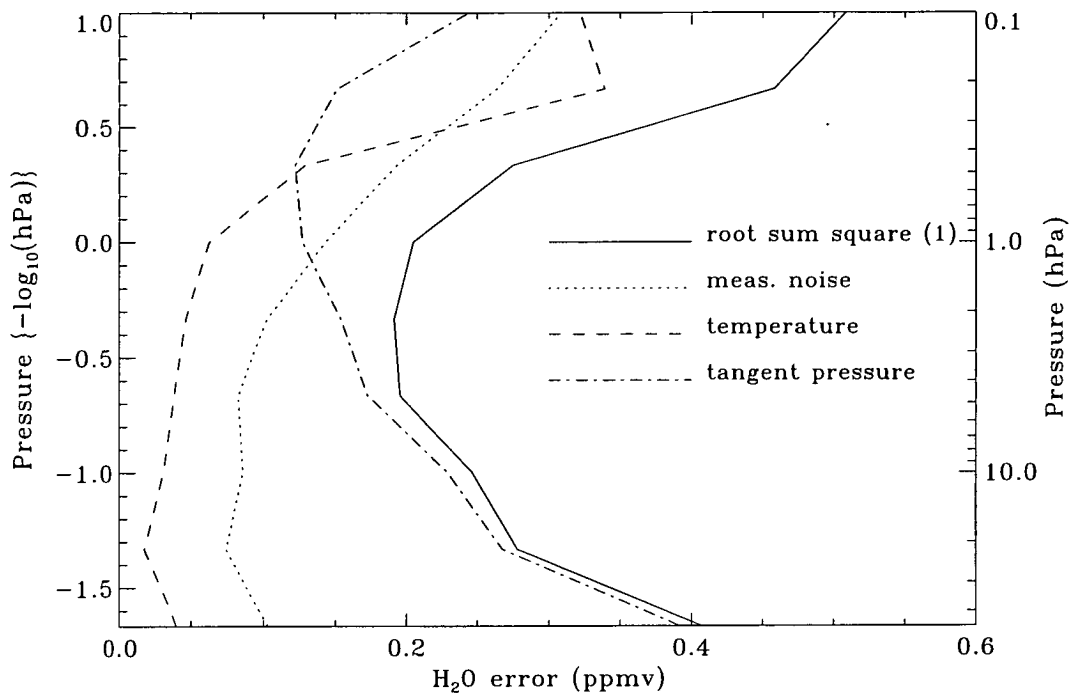


Figure 4.3: Estimated random errors associated with the retrieval of MLS H₂O. The units are ppmv. Line (1) is an estimate of precision given by method 1

Method 3

Finally, the third method involved calculating the standard deviation of the mean of all profiles in the latitude range 5°N-5°S for each of the 442 days that the 183 GHz radiometer operated. The variabilities that are observed by this method are the sum of the variabilities produced by the atmospheric variability and the variabilities produced by the instrument precision. Hence the numbers produced in this study are an upper bound on the precision of the instrument. Insofar as the variability of the atmosphere is small between 5°N and 5°S the numbers should also be good estimates of the precision.

4.4.2 Comparison of results from each method

Figure 4.4 shows the results of each of these methods.

Methods 2 and 3 (M2 and M3) give near identical results from 46hPa to 10 hPa. M2 estimates are higher than those from M3 by less than 0.05 ppmv from to 0.46 hPa. Above 0.46 hPa estimates from the two methods gradually diverge

with those from M3 being larger.

At 46 hPa Method 1 (M1) overestimates results from M2 and M3 by ~ 0.2 ppmv. From 46 hPa to 4.6 hPa, the M1 values decrease from 0.4 to 0.2 ppmv. Above 4.6 hPa values generally increase, reaching 0.5 ppmv at 0.1 hPa.

The poorer estimate of the lower stratospheric precision yielded by Method 1 may be due to a systematic component in the tangent pressure uncertainty which, as mentioned above, dominates the uncertainty in the water vapour retrieval in this region. It might then be expected that this method is actually superior to methods 2 and 3, not poorer, since it acknowledges the tangent pressure uncertainty. However, it is my understanding that *Lahoz et al* feel that the uncertainty is not a random effect and so therefore has no bearing on precision estimates.

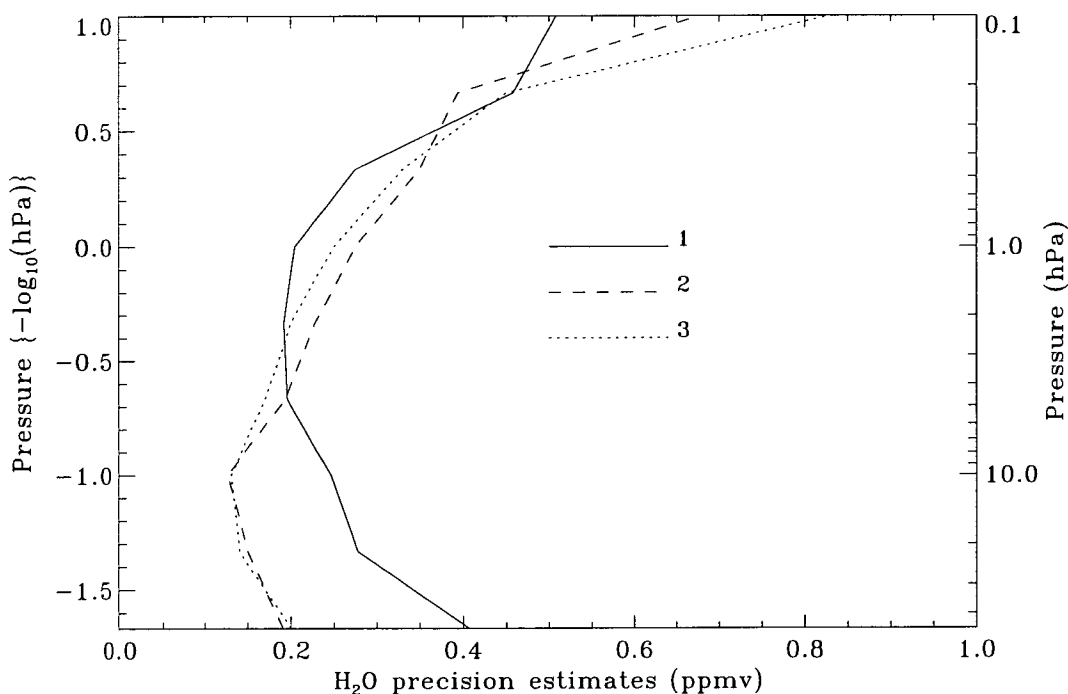


Figure 4.4: Precision estimates for MLS Version 3 H₂O. Method 1: from formal error analysis, method 2: variability of retrieved profiles near to the orbit turning points in the summer hemisphere, method 3: variability of retrieved profiles in the tropics. The units are ppmv. (Lahoz et al., 1996)

Note that precision values calculated by the retrieval algorithm are larger than the values calculated for each of the methods above. This is because the retrieval algorithm include factors such as the uncertainty in the *a priori* error and also

takes account of the linear nature of the measurements.

Lahoz et al. (1996) adopted the precision estimates yielded by Method 3 as the best measurement of the true instrument precision since these estimates should be an upper bound on the instrumental noise.

We now turn to a brief description of the systematic errors which can affect the H₂O retrieval. Quantification of these errors is necessary so that the accuracy of the water vapour measurements can be addressed.

4.5 Accuracy of MLS H₂O

The main systematic uncertainties are in tangent pressure, temperature, retrieval numerics, radiance scaling and the field of view direction. Figure 4.5 shows these uncertainties along with rss of these uncertainties. More detail on the relative importance of each error source can be found in Lahoz et al. (1996).

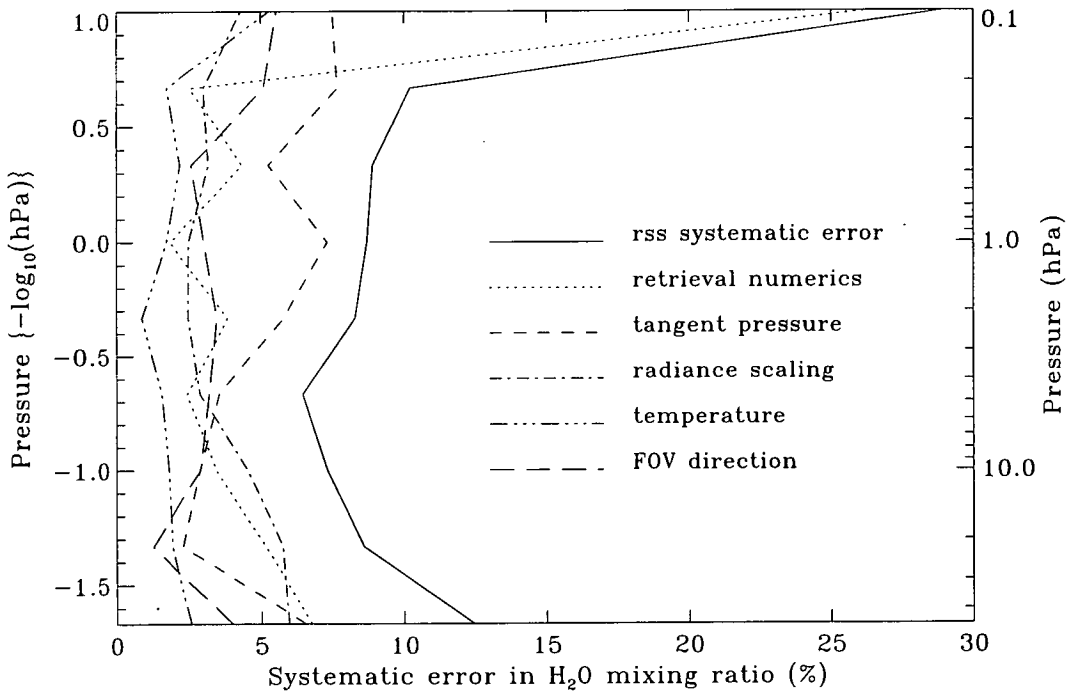


Figure 4.5: Estimated systematic uncertainties associated with the retrieval of MLS H₂O. Taken from Lahoz et al. (1996)

In general, the uncertainties in tangent pressure are the major source of uncertainty in the upper stratosphere and lower mesosphere. At other altitudes no

single source of error dominates, contributions ranging from 2–5% for each of the factors mentioned above.

There are other less important sources of systematic error which only have a slight affect on the retrieval (less than $\sim 1.0\%$). These are discussed in Lahoz et al. (1996)

To give an estimate of the total uncertainty in the water vapour measurements the precision values from Method 1 above (the “random” uncertainty) are added to the rss of the major and minor systematic uncertainties stated above and to the estimated smoothing error. The smoothing error is the error that results from the failure of the retrieval to reproduce the true atmospheric state.

Figure 4.6 shows each of these uncertainties as well as an estimation of the accuracy of the MLS water vapour retrievals; defined as the rss of each component of the sum (at each pressure level) above.

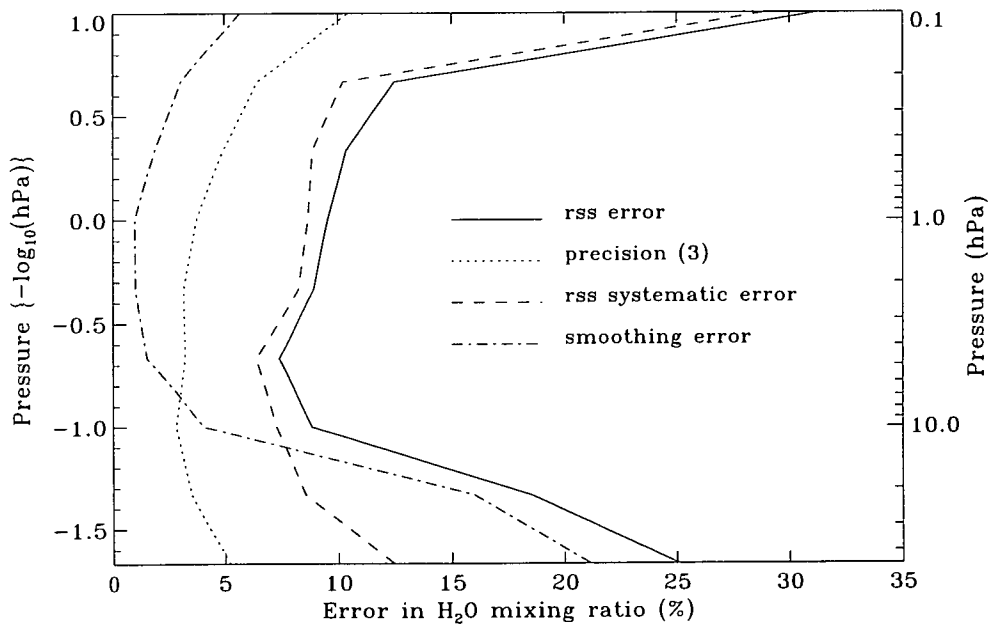


Figure 4.6: Estimated uncertainties associated with the retrieval of MLS H₂O. rss error: root-sum-square of precision, systematic error and smoothing error, precision (3): estimate of precision using method 3 (see text), rss systematic error: root-sum-square of estimated systematic errors, smoothing error: contribution of the *a priori* errors. Taken from Lahoz et al. (1996)

4.6 Summary of Precision and Accuracy

Table 4.2 gives a summary of the precision and accuracy of MLS water vapour measurements in the pressure range 46 hPa to 0.2 hPa. Beyond that range the precision and accuracy degrades to levels which probably make the measurements unsuitable for most scientific studies. Note also that the numbers given below only reflect the general quality of the MLS measurements; precision estimates do vary according to season and location (see section 4.8).

Pressure (hPa)	Single Profile Precision (1)		Accuracy (2)	
	(ppmv)	(percent)	(ppmv)	(percent)
0.22	0.45	7	0.9	13
0.46	0.33	5	0.7	11
1	0.25	4	0.7	10
2.2	0.20	3	0.6	9
4.6	0.17	3	0.5	8
10	0.13	3	0.5	9
22	0.14	4	0.8	19
46	0.20	5	1.2	25

Table 4.2: MLS Version 3 H₂O data summary. (1) The estimated precisions are based on the observed variability of retrievals in the tropics (see Lahoz et al., 1996). (2) The estimated accuracies are based on the error analysis presented in section 4 of Lahoz et al. (1996)

To summarise, version 3 MLS water vapour retrievals are estimated to be ~20–25 % accurate in the lower stratosphere and ~10 % in the upper stratosphere. Single profile precision is estimated to be ~0.2 ppmv in the stratosphere except during polar winter conditions at 46 and 22 hPa where the retrieval is sensitive to the low temperatures present.

MLS water vapour is now compared to data from some correlative data sets. Some small differences are found which are larger than the uncertainties detailed above and this suggests that there remains some unaccounted for uncertainties in the MLS retrieval of water vapour.

4.7 Correlative comparison

MLS data were compared with measurements from four different observing systems namely a frost point hygrometer, an infrared spectrometer (both balloon borne), a ground based microwave spectrometer and data from another UARS instrument, HALOE.

4.7.1 Frost point hygrometer data

A frost point hygrometer (FGH) was flown, on a balloon, at different times and locations as part of a systematic campaign to provide a large database (Oltmans, *unpublished data*) of correlative measurements that could be used to validate water vapour measurements from MLS.

The instrument has an altitude range from the ground to ~ 28 km with a vertical resolution of 250 m. The precision and accuracy of these measurements is 10 % in the stratosphere. A total of twelve profiles from five measurement sites were used in the comparison and were chosen to coincide as nearly as possible with measurements from MLS. Figure 4.7 shows a typical water vapour profile from one of these sites (Hilo, Hawaii, 19.7°N). The closest three MLS profiles are shown for comparison.

The limited overlap in the vertical coverage of the FGH and MLS means that a comparison can only be usefully made at the 46 hPa and 22 hPa levels only. At 46 hPa the mean difference between the MLS and the balloon data (mean of all 12 profiles) is 0.2 ppmv while the root mean square (*rms*) difference (is 0.5 ppmv. At 22 hPa, only 6 profiles reached 22 hPa and the mean difference is 0.1 ppmv and the *rms* difference is 0.4 ppmv. Lahoz et al. (1996) conclude that the systematic bias between the two data sets is smaller than 0.2 ppmv and that the random differences are within the quoted uncertainties. However they point out that none of the profiles used are at a latitude polewards of 45° .

4.7.2 Ground-based microwave data

Comparisons were made with measurements from a ground-based microwave radiometer based at Table Mountain (34.4°N , 243.0°E).

The instrument has an altitude range from 30 to 80 km and has a vertical

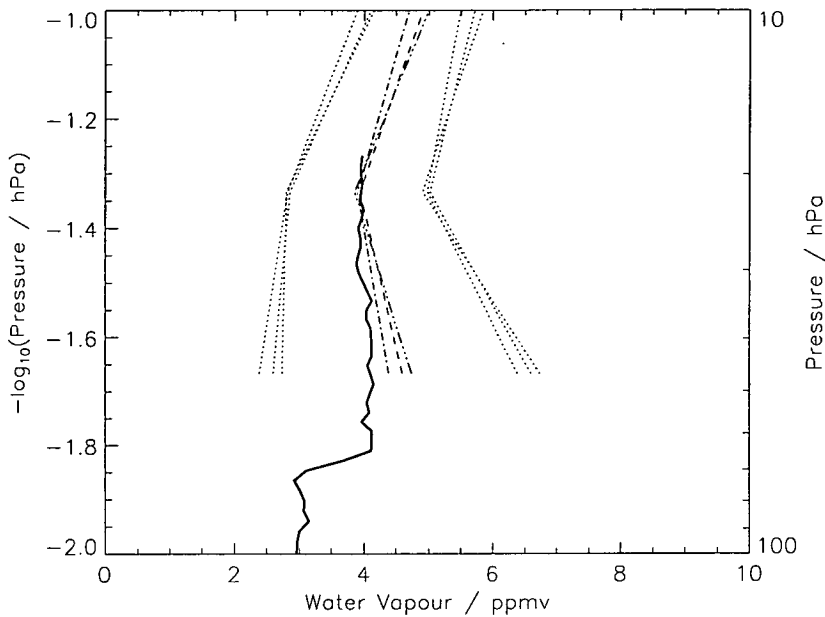


Figure 4.7: A typical water vapour profile measured by a balloon mounted frost point hygrometer (solid line). The balloon was launched from a site in Hawaii at latitude 19.4°N , longitude 155°W , on 24 March 1992. Several MLS profiles for nearby locations ($\sim 23^{\circ}\text{N}$, 160°W) are shown by dashed and dot-dash lines, their error bars are shown by dotted lines. The balloon profile is within the MLS errors at 46 and 22 hPa (Lahoz et al., 1996).

resolution of ~ 15 km (c.f. ~ 5 km for MLS). The total absolute error of the measurements is $\sim 10\%$ over the range 40–70 km (Nedoluha et al., 1995). Data are retrieved on a height grid and then interpolated to a pressure grid using NMC temperature and pressure fields.

Figure 4.8 shows the the mean difference (MLS – ground-based) and the rms difference of MLS (v0003) and the ground-based data for 186 days throughout the period 23rd January – 13th October 1992. The *rms* difference is not much greater than the mean difference, suggesting that much of the difference between the two data sets is systematic. The ground-based data are less accurate at lower altitudes in the profile; some of the difference at 2.2 hPa and perhaps 1.0 hPa may be attributed to this. MLS values at mesospheric levels 0.46 and 0.22 hPa are ~ 1.0 ppmv larger than the ground based data, which is just outside the accuracies calculated above (0.7 ppmv at 0.46 hPa, 0.9 ppmv at 0.22 hPa). At 0.1 hPa the MLS values are unphysically large and are an artifact of the retrieval.

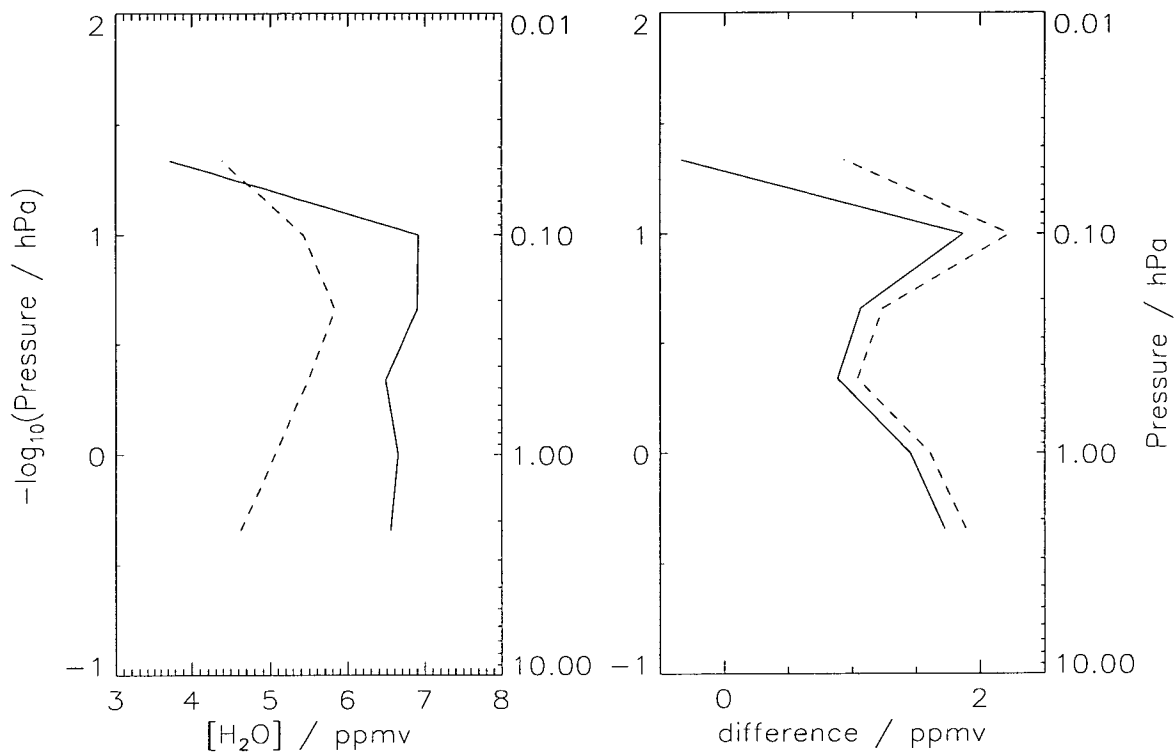


Figure 4.8: Comparison of MLS Version 3 water vapour with the Version 2 data from the ground-based microwave instrument. Data are from the period of 23rd January 1992 to 13th October 1992; a total of 186 days for which both MLS and ground-based measurements were available. The left hand plot shows mean profiles; the solid line is MLS data, the dashed line ground-based. The right hand plot shows the mean difference, MLS – ground-based (solid) and the rms difference (dashed).

4.7.3 FIRS-2 data

Comparisons were also made with measurements from an infra-red emission Fourier transform spectrometer. This was carried by a balloon (Johnson et al. 1994). Its vertical range is approximately 100–3 hPa, with a sampling interval of approximately 4 km. During the period when the 183 GHz was operational three profiles were obtained. Figure 4.9 shows one such profile along with a near coincident MLS one. As with the frost-point hygrometer, the profiles agree well in the lower stratosphere. The MLS profile becomes greater than the FIRS-2 profile as height increases with a difference of 1.6 ppmv at ~3 hPa.

The accuracy of MLS at this altitude is approximately 0.6 ppmv. These features are repeated in the other two FIRS-2 flights.

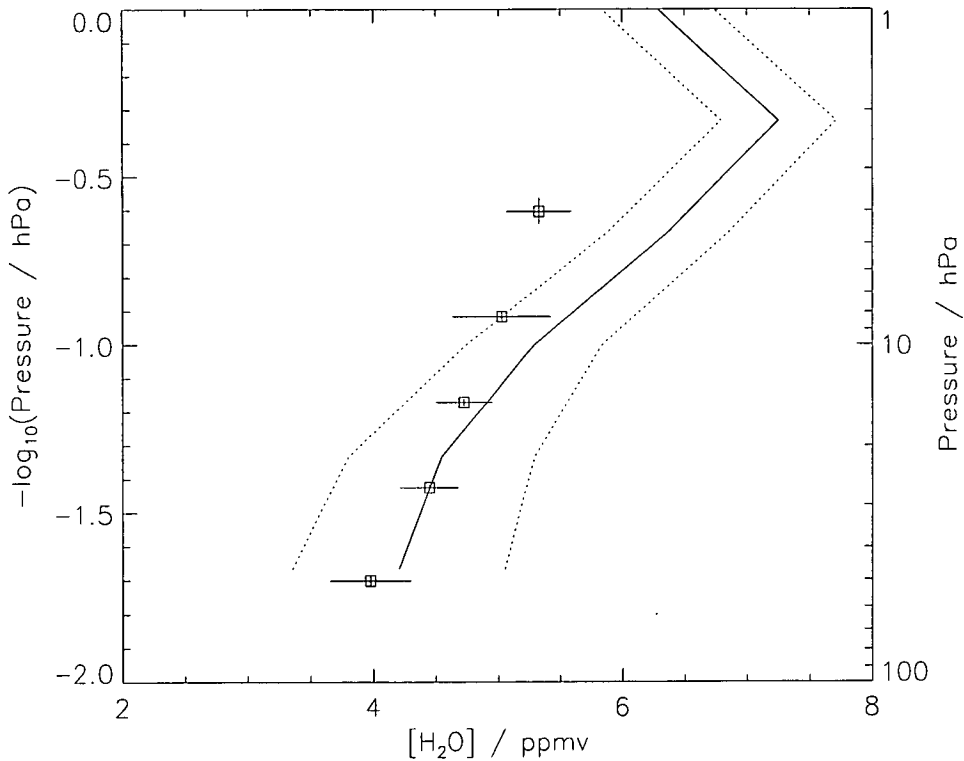


Figure 4.9: Water vapour profiles measured by MLS (solid line) compared with FIRS II (squares) on 29 September 1992. The MLS profile is at latitude 37.5 °N, longitude 103.2 °W, the FIRS II profile is at latitude 36.9 °N, longitude 100.4 °W.

4.7.4 Halogen Occultation Experiment (HALOE) data

Since the MLS and HALOE instruments have different observational patterns comparison between the two is limited to certain times and places. During periods when the observational patterns did overlap (usually ~ 20 days) MLS data were used in such a way as to imitate the way in which HALOE samples the atmosphere (Lahoz et al., 1996). This was done by locating MLS profiles that surrounded, and were in the neighbourhood of, the daily average latitudes from HALOE sunset and sunrise measurements. Linear interpolation was then used to find an average MLS profile at each of the two average HALOE latitudes for each day in the overlap period. The zonal-mean differences (MLS-HALOE) were then calculated. The differences for one such overlap period are shown in Figure 4.10.

The period covered by this comparison is 21st January to 8th February 1993. The latitudinal coverage is from 30°N at the beginning of the period to 50°S at the end of the period. The zonal mean difference is expressed in units of ppmv. The comparison in the figure uses MLS data from ascending orbit tracks only (i.e. where the orbit tracks follow a northerly path). The results of this particular comparison are typical of those from other periods which have been studied.

In general, the zonal-mean differences (MLS – HALOE) show little latitudinal variation. Differences range from ~ 0.5 ppmv (10 %) in the lower stratosphere (46 hPa to 10 hPa) to between 1.0 and 1.5 ppmv (10–20 %) higher up (4.6 hPa to 1 hPa). Note that at 46 hPa the MLS values can sometimes be slightly less than those of HALOE. These differences are comparable with the estimated MLS errors for regions where this occurs. The differences higher up are generally larger than the estimated MLS error.

4.7.5 Summary of comparison with correlative data

MLS water vapour data and correlative measurements show good agreement in the lower stratosphere but higher up MLS values are typically 1.0–1.5 ppmv (10–20 %) higher than all of the correlative measurements. These differences are outside the accuracy of measurements calculated above and suggest that the error analysis above may not have included all possible systematic effects. Of course another possibility is that since the measurements being compared were not made at ex-

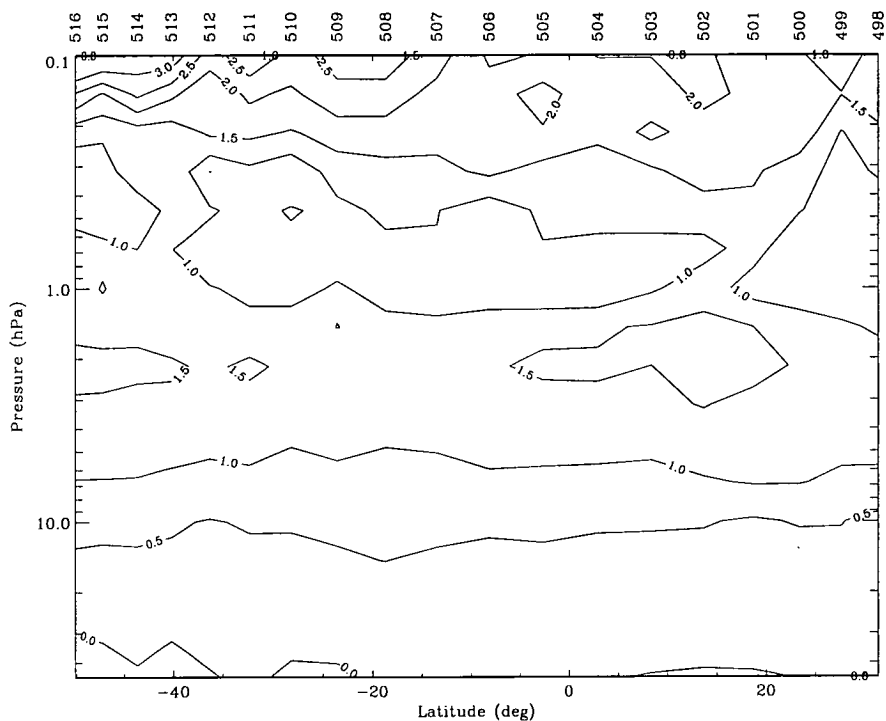


Figure 4.10: Zonal mean differences (MLS – HALOE in ppmv) between MLS Version 3 H₂O and HALOE Version 17 H₂O for the period 21st January 1993 to 8th February 1993. The numbers along the top of the plot are the UARS day numbers for which each zonal mean difference profile was calculated. Data are plotted at the average latitude of the HALOE measurements for each day.

actly the same time and place there will be some degree of natural variability between them.

4.8 Some problems with v0003 retrievals

There are a number of additional problems with the v0003 retrievals and these are mentioned briefly below.

Occasionally there are profiles of water vapour which the retrieval has flagged as good but which, clearly, are not. This may indicate that the “flagging” criterion is not strict enough. The examples of this which have been clearly identified all appear to arise from a coding error in the level 1 software (used to produce calibrated radiances for each channel). This problem has been corrected in the next version of the retrieval.

One problem that has been identified that occurs in all of the MLS measurements is a small systematic dependence on the UARS yaw-cycle. The water vapour measurements show evidence of this effect most clearly in tropical time-series at 22 hPa (Figure 6.2). Just before and after each yaw maneuver there is a small glitch of ~ 0.1 ppmv in the average mixing ratio. The reason for this is currently being investigated.

Another problem of the retrieval, which occurs frequently is the retrieval of unphysically high values at 0.1 hPa (~ 65 km). Sometimes values as large as 10 ppmv are retrieved. This is thought to be due to the non-linearity in the centre channel of band 5 which is saturated at this height. The present retrieval algorithm ignores radiances which come from ray paths that are optically thick. In this thesis no water vapour measurements are shown or used at this height. For more detail on this problem see Suttie (1995).

A similar and more serious problem occurs in the polar winter measurements of water vapour at 46 hPa (and to a lesser extent, 22 hPa) where frequently the retrieved mixing ratios have a large contribution from the *a priori* (i.e. a large error ratio). This is due to a problem in dealing with ray path opacity and with the very low temperatures present. As stated above, the current retrieval does not use any radiances that come from ray paths judged to be optically thick. Essentially, this means that for lower stratospheric measurements in the cold-polar vortex,

less information is available for the retrieval and hence there is more reliance on the *a priori* (Suttie, 1995). Tests have indicated that slackening the criterion for accepting these radiances improves the retrieval at 46 hPa but creates problems higher up, particularly at 22 hPa. Moreover since these radiances are related non-linearly to water vapour a non-linear retrieval algorithm is needed to utilise fully all the received radiances. Dr Hugh Pumphrey of the Department of Meteorology at Edinburgh University has demonstrated such an algorithm with which it should be possible to retrieve water vapour at 100 hPa and also for measurements to have a better vertical resolution. However the method is computationally expensive and so it is likely to be used mainly in time periods and locations that are scientifically interesting and where linear retrieval is particularly poor (e.g. episodes of stratospheric polar dehydration)

The latest version (v0004) of operational reprocessing began in early 1996 with progress made, at both Edinburgh and JPL, in improving the retrieval of water vapour. More accurate oxygen line widths have led to a reduction in retrieved stratospheric H₂O mixing ratios. Initial comparison between the test version of v0004 and v0003 MLS water vapour showed zonal-mean differences (v0003 – v0004) of 0.1–0.2 ppmv in the lower stratosphere and differences of 0.3–0.4 ppmv in the upper stratosphere. This improvement reduced some of the differences between MLS and correlative data which previously existed.

Another improvement has been in the water vapour *a priori* data. The v0003 *a priori* values are too large in the upper troposphere and are unrealistic in the mesosphere. To counter this, the v0004 retrievals use data which, we believe, more accurately reflect the true concentration of atmospheric H₂O. In the upper troposphere, the *a priori* is now mainly SAGE II data and in the mesosphere it is mainly HALOE data.

Further work at JPL has been to develop tropospheric retrievals of water vapour. Although MLS is not specifically designed to measure tropospheric water vapour it is possible to do so using the ClO spectral band. As the field of view of this band is scanned down through the troposphere the dominant contribution to the measured signal is from water vapour. In practice this means that measurements of water vapour can be deduced at heights as low as 7 km at high latitudes and 12 km in the tropics (Read et al., 1994). These retrievals will be potentially

useful in studies of tropospheric-stratospheric exchange.

4.9 Summary

In this chapter we have reviewed the capacity of UARS instruments to measure water vapour. CLAES and ISAMS are both, in principle, capable of measuring the global distribution of H₂O but, using existing retrieval software, their observations are, when compared to MLS, limited in their vertical extent. MLS water vapour measurements (v0003) have single profile precision of better than 0.2 ppmv throughout most of the stratosphere (except during polar winter in the lowermost stratosphere). The accuracy of measurements in the lower stratosphere (46 and 22 hPa) is estimated to be within 25% and is twice as good at higher stratospheric levels (10 – 1.0 hPa).

Currently, MLS is the only instrument giving global coverage and therefore promises to show features of the water vapour distribution not previously observed.

In the next chapter the zonal-mean water vapour distributions are shown, for the first time, and their main features described.

Chapter 5

Monthly and zonally averaged H₂O (v0003) from MLS

In this chapter and the next two the main results from the Microwave Limb Sounder (MLS) water vapour measurements (version 3) are presented, beginning, in the next section, with zonal mean results from each yaw period (called hereafter a ‘UARS-month’).

5.1 Zonal-Mean Climatology of MLS H₂O

In Figure 5.1 the zonal-mean latitude-height cross sections of MLS water vapour are presented for the first time.

Each plot in the figure is a zonal-average of the measurements made during each UARS-month (~36 days). Data were first screened to remove profiles flagged by the retrieval as ‘bad’. The remaining profiles were then binned every 4° in latitude. The number of profiles used to make up each latitudinal average was at least 1000 (more near the turning points) so the zonal mean precision of the measurements is expected to be very high. The number of bad profiles removed, before each latitudinal mean was calculated, was an insignificant number (generally less than 1 % of the total number) compared to the number of good profiles and thus we can be confident that the results in each bin are representative of the measurements in a whole yaw-period. Note that very little data were available between June and mid-July 1992 due to an instrumental problem. Consequently there is no zonal-mean distribution shown for yaw period 8.

Since the UARS satellite performs a 180° yaw maneuver approximately every

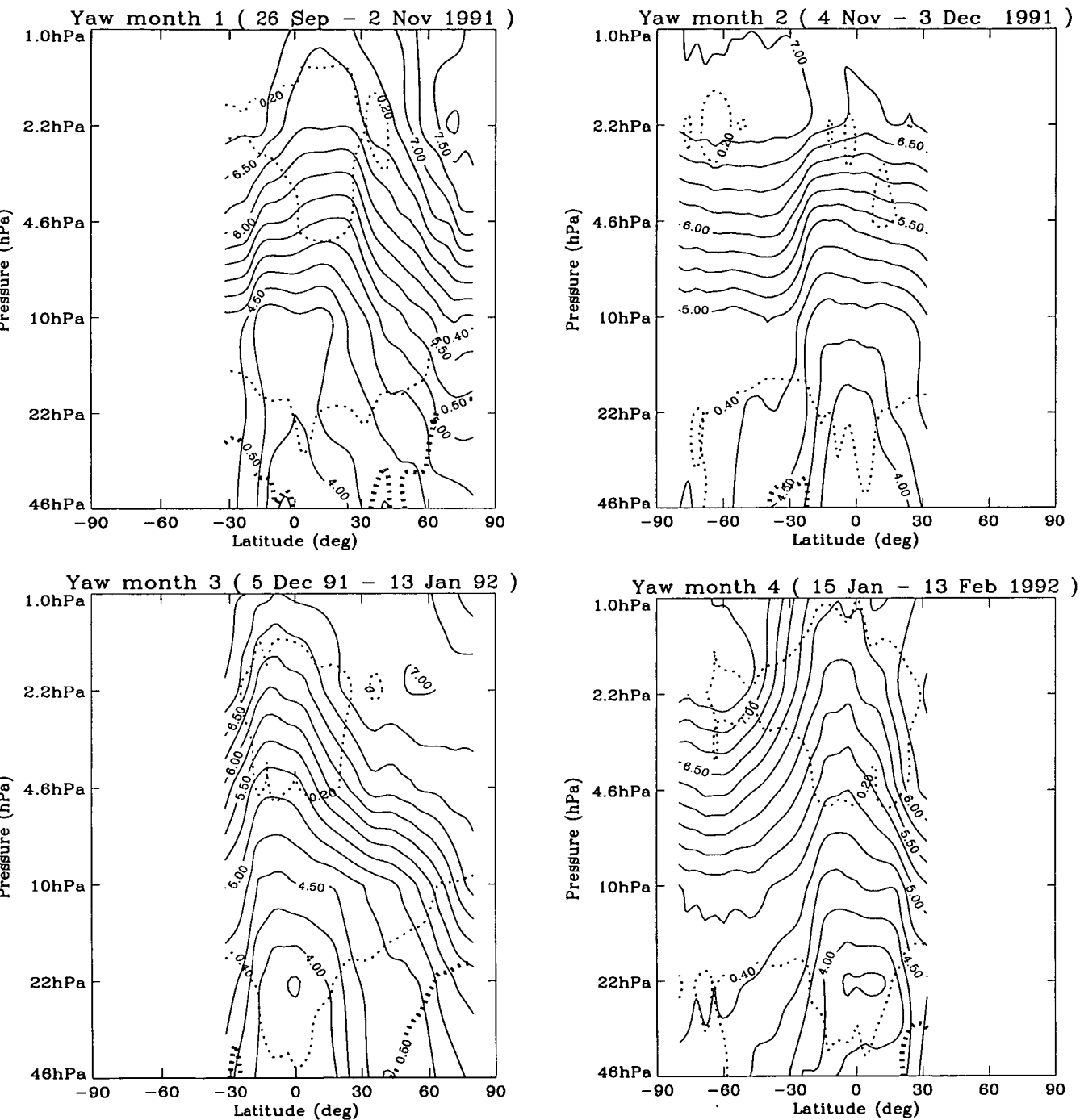


Figure 5.1: Zonal-mean latitude height cross-sections of MLS water vapour (ppmv) for all UARS months from September 1991 to April 1993. Broken contours represent error ratio values of 0.2 (dotted), 0.4 (dashed) and 0.5 (heavy dashed) respectively.

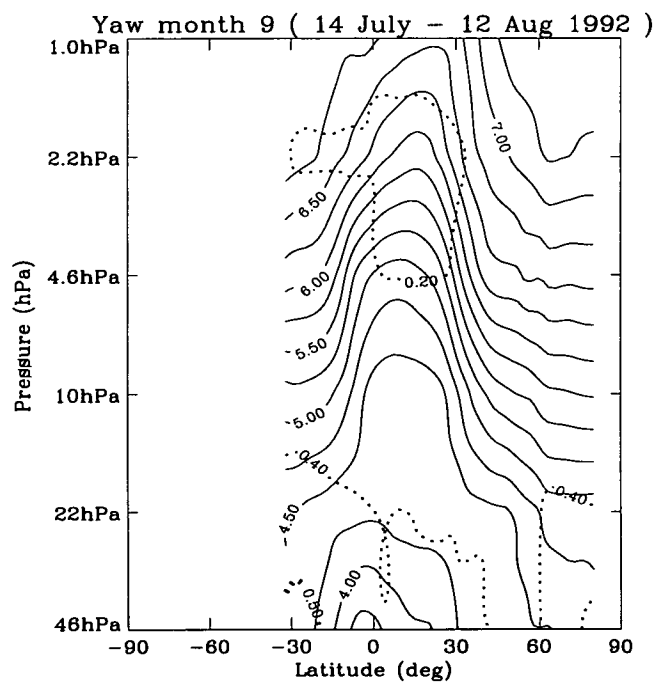
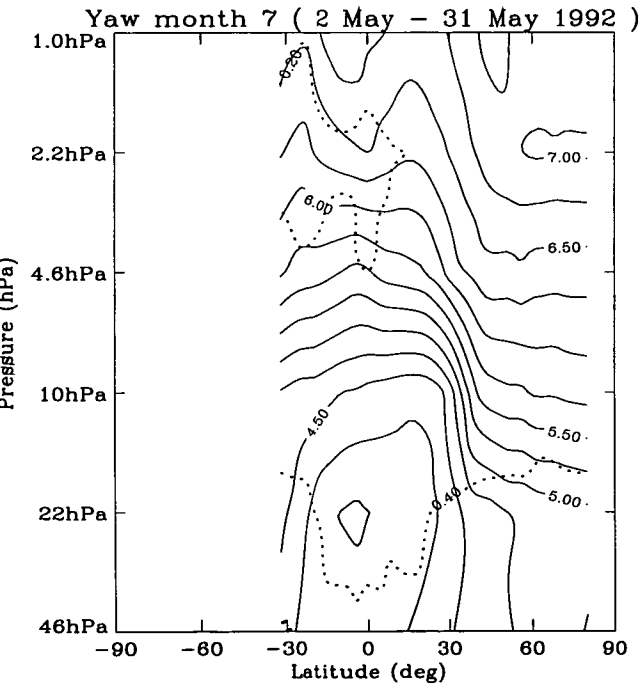
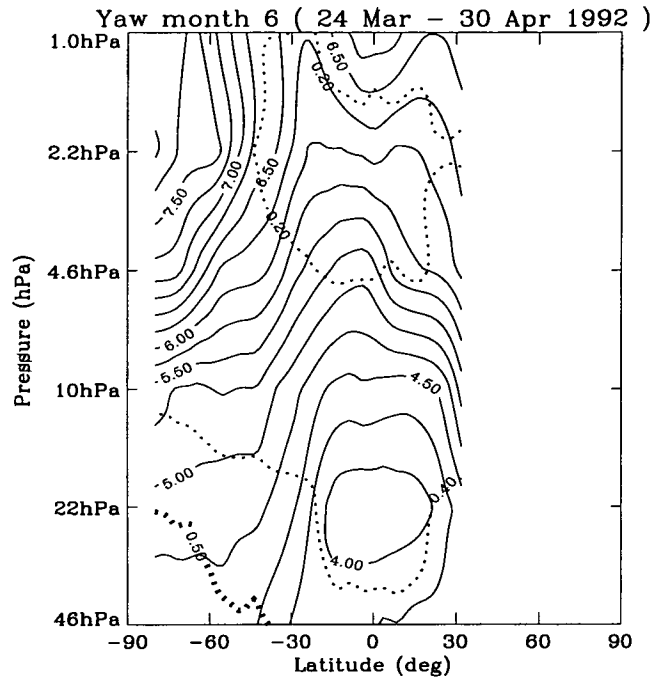
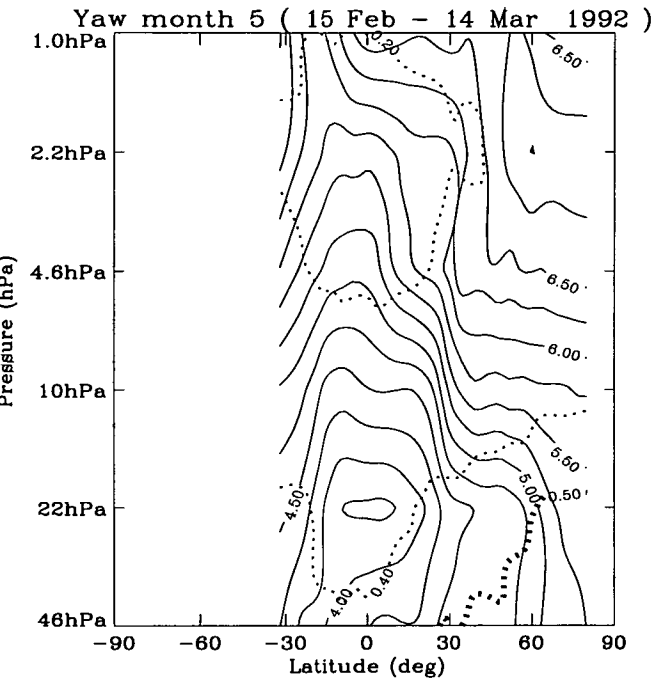


Figure 5.1: (continued)

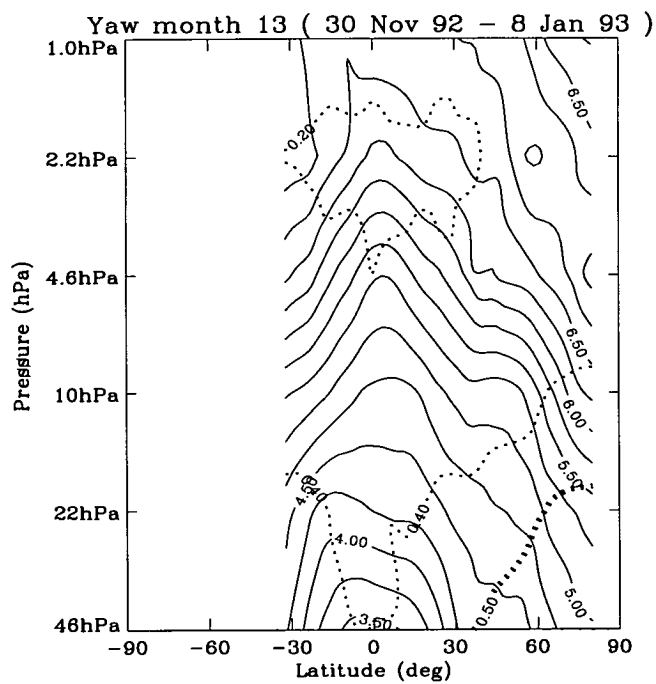
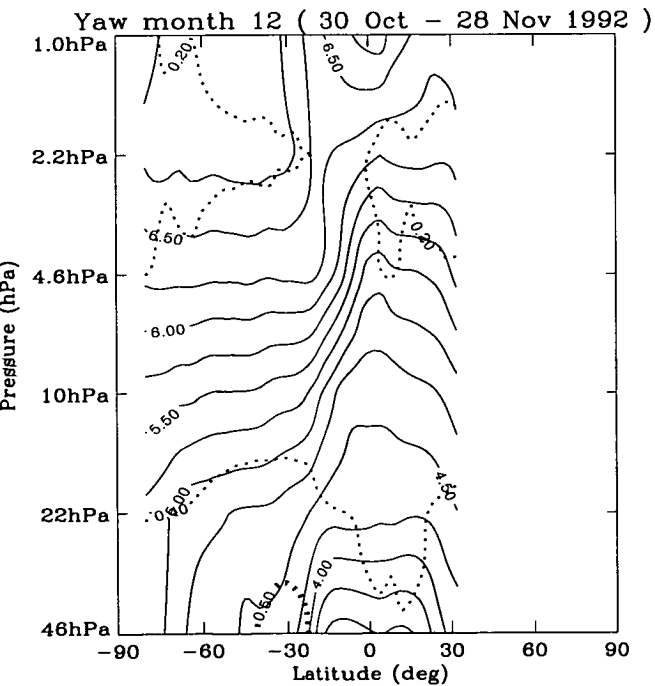
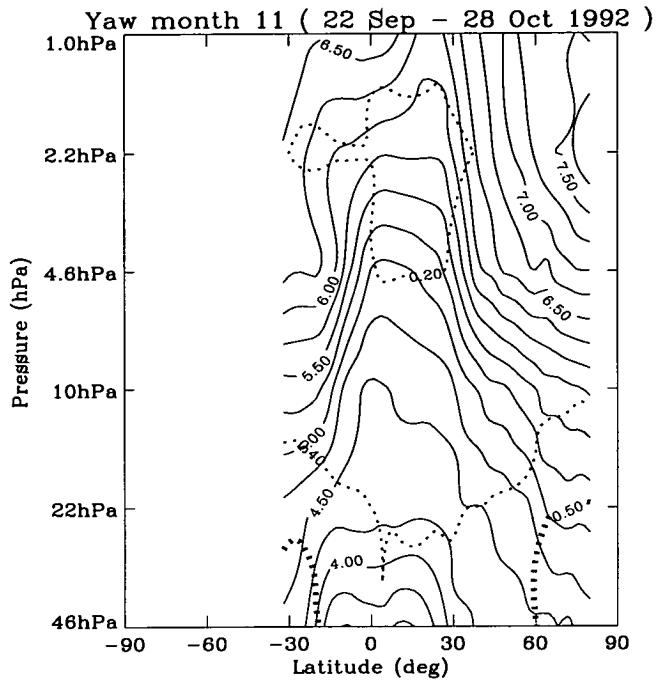
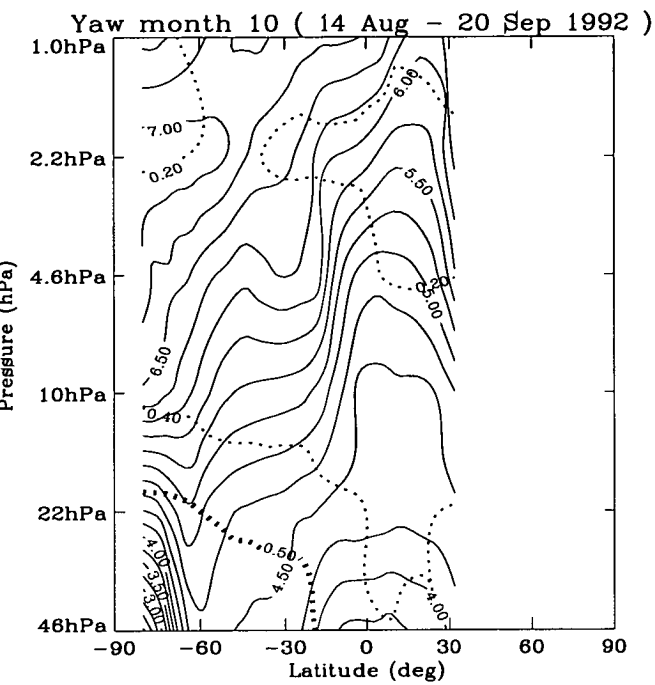


Figure 5.1: (continued)

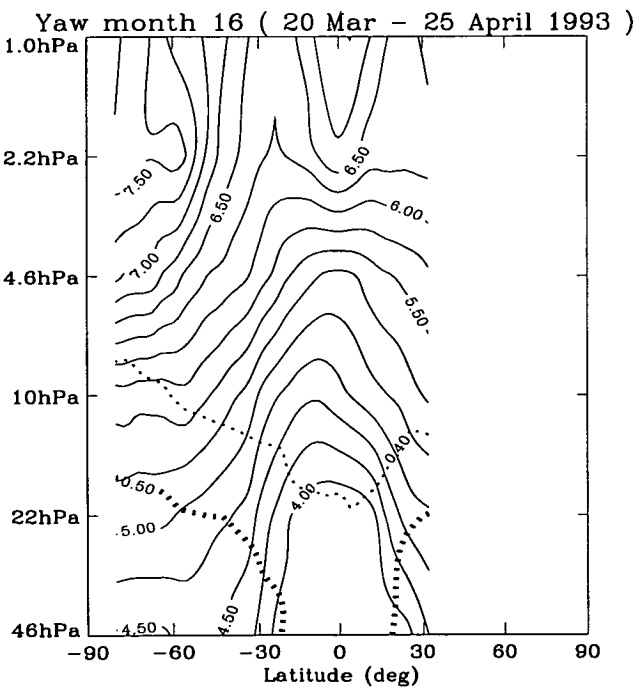
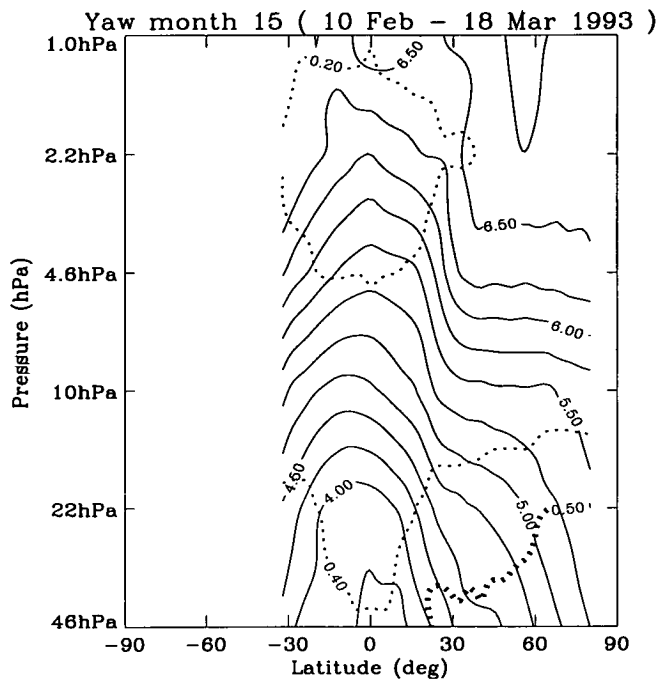
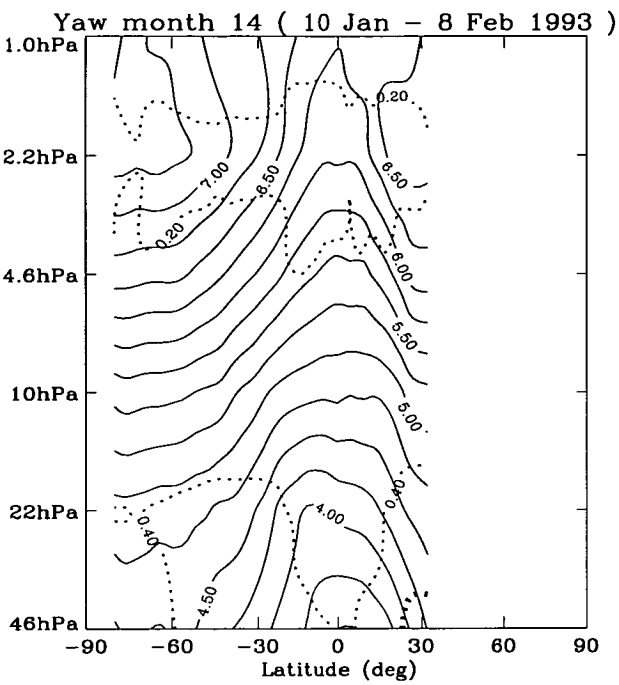


Figure 5.1: (continued)

36 days this means that high-latitude measurements, in each hemisphere, are only available at alternate yaw months. The latitudinal coverage in each zonal-mean plot thus switches between 34°S–80°N and 80°S–34°N.

The reason for averaging data every UARS-month and not every calendar month is that it avoids any complications due to the yaw maneuvers. For example, although in a calendar month there may be measurements at high-northern and high-southern latitudes the measurements are bound to have been at least several days apart and thus any averages shown at high-latitudes would be unrepresentative of the conditions over the entire month.

Superimposed on each plot in the figure are zonal-mean error ratio (ER) contours at $ER = 0.2, 0.4$ and 0.5 . The 0.5 contour is represented by the heavy dotted line. Recall that the error ratio is the ratio of the MLS precision to the *a priori* uncertainty and gives an indication of the dependence of the retrieval on information from the *a priori*. An error ratio greater than 0.5 is sometimes set as the limit beyond which the retrieval is too biased by the *a priori* (Lahoz et al., 1996).

Initial inspection of the MLS water vapour cross sections reveals a number of features present in the LIMS and SAGE II datasets discussed previously (Chapter 3). The mixing ratios, on the whole, increase with height throughout the retrieved levels in the stratosphere (from ~ 4.0 ppmv to ~ 7.0 ppmv between 46 hPa and 1 hPa). Also the distribution is such that the mixing ratios increase towards each pole from a broad minimum in the lower stratospheric tropics.

The well-defined and persistent region of minimum values in the lower tropical stratosphere is present for all 15 yaw months of data. The mixing ratios of these minimum values typically lie between 3.5 and 4.0 ppmv (c.f. 2.5–3.0 ppmv for LIMS, 3.0–3.5 ppmv for SAGE II) and periodically occur at either the 46 hPa and 22 hPa pressure surfaces. The movement of the minimum between these levels appears abrupt in the plots but this is to some extent an artifact of the retrieval grid having adjacent grid points at these positions. Inspection of HALOE data (not shown) which are retrieved on a finer grid indicate that the minimum sometimes occurs on the intermediate level at 32 hPa. Note also that the minimum in the retrieved MLS profile at 22 hPa (~ 25 km) is unlikely to represent the true stratospheric minimum (or hygropause) since the majority of earlier measurements

document a hygropause altitude several kilometres below this (e.g. Remsberg et.al., 1984), in fact at altitudes where MLS H₂O retrievals are not currently available. The height variation of these minima and the tropical stratospheric variation of MLS water vapour in general has been reported recently by Carr et al (1995). The mechanism behind the variation and a possible explanation for the elevated hygropause has been suggested by Mote et al. (1996). The main thrust of their argument is that when a nominal air parcel crosses the tropopause it retains a “mark” of its stratospheric entry temperature and, as it rises upwards through the (lower) stratosphere, it is relatively unaffected by horizontal mixing. So, during northern winter periods (November-January) when the tropopause is cold, water vapour values that enter the stratosphere are relatively dry and in the months that follow are transported upwards in the Brewer-Dobson cell. The minima in MLS water vapour at 22 hPa that occur at certain times during the year was suggested by Carr et al (1995) to be essentially remnants of the same minima that crossed the 46 hPa isobar earlier in the year. *Carr et al* also reported that the transport of mixing ratios from 46 to 22 hPa was modulated by the QBO. Work from both of these papers will be described in more detail in Chapter 6.

There is a large variability in the shape of the upwards bulge in the contours, as may be seen by fixing attention on the 5 ppmv contour, which sometimes is rather flat (e.g. Yaw month 7) and at other times is sharply curved possibly indicating a narrower region of ascent flanked by downwelling in the subtropics (e.g. Yaw month 9). The distributions in Figure 5.1 also give evidence to suggest that the upward branch of the Brewer-Dobson circulation moves seasonally between the southern and northern hemisphere. For example, in UARS-month 4 (January 15 - February 13, 1992) the upwards bulge in contours in the lower stratospheric tropics is more marked south of the equator. Correspondingly, in UARS-month 10 (August 14 - September 20, 1992) the tropical contours are raised higher on northern side of the equator.

The zonal-mean distributions in some UARS-months also show signs of a double-peaked structure in the upper stratospheric tropics. This is most clear in UARS-months 6, 7 and 15 (March/April 1991/92) at ~ 1 hPa (~ 50 km) with minima in the distribution at $\sim 30^\circ\text{S}$ and $\sim 30^\circ\text{N}$ and a maximum over the equator.

This feature is generally consistent with measurements of trace species from

SAMS (Jones and Pyle, 1984, Gille et al., 1987), LIMS (Remsberg et al., 1984) and SAGE II (see section 5.2) although in these cases the ‘double-peak’ was observed slightly lower in the stratosphere. The peaks do occur at the approximately the same time of year though. Both MLS and LIMS/SAMS measurements show that peaks are strongest in April.

It was demonstrated by Gray and Pyle (1987) that there is a clear relationship between the double-peaked structure in tracer data and the semi-annual oscillation of the equatorial zonal-mean wind. At the time of the maximum westerly shear, in April, the circulation associated with the SAO is downwards and at its strongest (Andrews et al., 1987). In the case of the MLS water vapour distribution this would explain the equatorial maxima and subtropical minima at 1 hPa in UARS-months 6, 7 and 15 (March/April 1991/92).

There are other interesting features in the zonal-mean MLS distributions that will be discussed more fully in future chapters. A brief synopsis of these features is given below.

The distribution in yaw month 1 is interesting in that low values (note the 4.25 contour in the lower stratospheric tropics) extend over a greater height range than in other yaw months, reaching 10hPa or higher. Analysis of individual maps throughout this yaw period show that there is a region of low mixing ratios centred over $\sim 15\text{S}$ at ~ 10 hPa in October 1991. Low mixing ratios are also observed at this latitude at 4.6 and 2.2 hPa in November and December. Time series at different heights and latitude bands are consistent with this being a real feature which could be connected to the Pinatubo eruption. The eruption discharged a huge amount of aerosol into the atmosphere (e.g Treppe et al., 1993) and acted to perturb the lower and middle stratosphere. One effect was a pronounced temperature increase in the lower stratosphere for several months following the eruption (Labitzke and McCormick, 1992). Vertical velocities in the Brewer-Dobson circulation were enhanced. Indeed had it not been for buffering of the circulation at this time they may have been even greater (Kinne et al., 1992). The measurements in this period are looked at more closely in the next chapter.

The zonal-mean cross-section for yaw month 10 (14 August - 20 September 1992) shows large-scale dehydration at southern high latitudes in the lower stratosphere. MLS, and HALOE (Tuck et al, 1993), are the first satellite instruments

to have measured this phenomenon, previously only observed in *in-situ* data (e.g. Kelly et al., 1989).

However, note also that the error ratio is larger than 0.5 throughout this dry region. As discussed in an earlier chapter the high error ratio indicates that retrieval is poor in this area of the stratosphere. Ricaud et al. (1995) discuss the water vapour distribution for a 5-day period during this yaw month and suggest, by using non-linearly retrieved MLS water vapour data, that water vapour mixing ratios were low because polar stratospheric clouds (PSC) had formed. This idea was supported by measurements of temperature, which were low enough for PSC to form and from the existence of high values of CLAES aerosol extinction coefficients in this area. Mergenthaler et al. (1993) suggest that CLAES aerosol measurements can be used to indicate the presence of PSC. The measurements in this period are examined more closely in Chapter 6.

We now look more quantitatively at how the zonal mean distributions from MLS compare with those from LIMS and SAGE II. (Note that a comparison of MLS and HALOE water vapour is being undertaken by another Ph.D. student in the department and so will not appear in this thesis. However differences are generally between $\sim 10\text{-}20\%$ with MLS being higher.)

5.2 Comparison with LIMS and SAGE II H₂O

In this section zonal-mean latitude-height cross sections are compared for two monthly periods.

5.2.1 Data description and quality

The MLS data used in this comparison are from 2–31 May 1992 (a complete north looking UARS-month) and from 1–28 November 1992 (the bulk of the data from the south looking UARS-month Oct 30–Nov 28). It is estimated that MLS water vapour measurements are accurate to within 20–25% in the lower stratosphere and to within $\sim 10\%$ in the upper stratosphere (Lahoz et al., 1996).

The LIMS data shown are from November 1978 and May 1979 (Figure 5.2) and have been gridded every 5° in latitude from 60°S to 80°N. Grid points in the vertical are every 2 km with coverage from 16 km to 48 km. The estimated accu-

racy of the zonal-mean measurements above 50 hPa (~ 20 km) is approximately 20-30 % and 40 % at altitudes below (Russell et al., 1984)

The SAGE II data shown are from November and May of 1987 and 1989 (Figures 5.3 and 5.4) and have been gridded every 10° in latitude from 70°S to 70°N . Grid points in the vertical are every 1 km with coverage from 16.5 km to 39.5 km. The estimated accuracy of zonal-mean measurements is better than 25 % (Chiou et al., 1993) except at the lowest latitudes where some residual aerosol loading from the Mount Ruiz in late 1985 affected retrievals. This has a more pronounced effect in 1987 than in 1989.

When comparing MLS water vapour measurements with those from SAGE II and LIMS, the MLS data have been interpolated, where possible, onto the grid of each instrument's measurements.

5.2.2 Percentage differences

In the section 5.1 it was shown that the zonal-mean measurements from MLS shared many qualitative features of the distributions in LIMS and SAGE II data. Here we consider a more quantitative approach and examine the percentage differences between measurements.

MLS v LIMS

MLS average mixing ratios are generally less than 20 % greater than LIMS throughout the stratosphere in both November and May (Figure 5.5). These differences are also within the accuracy of both instruments.

MLS mixing ratios are more than 20 % greater than LIMS in:-

- 1) the lower stratospheric tropics where, as was stated in Chapter 3, the combination of the coarse field-of-view of the satellite instruments and the rapidly changing mixing ratios make it difficult to accurately resolve the true vertical structure.
- 2) the tropics between ~ 36 and 40 km in both November and May where MLS values are between 40 and 50 % greater. One reason for the differences in these regions is that LIMS measures low values of water over a greater vertical range than MLS with mixing ratios of 4.0–4.2 ppmv observed at ~ 36 km. The MLS

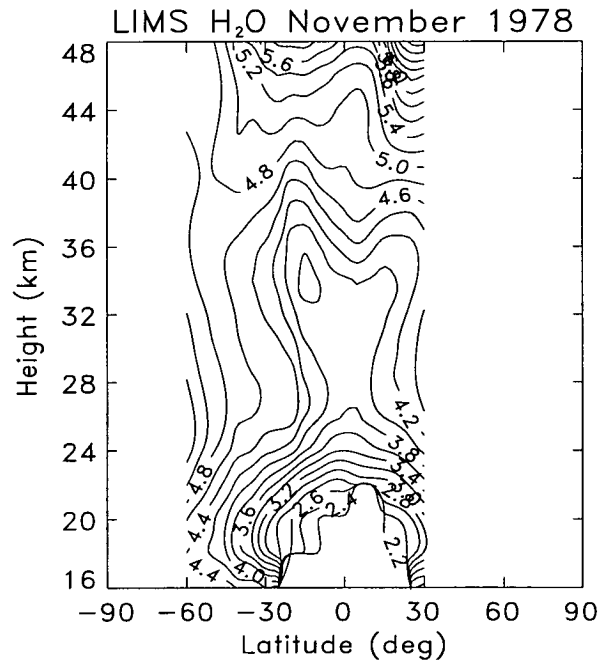
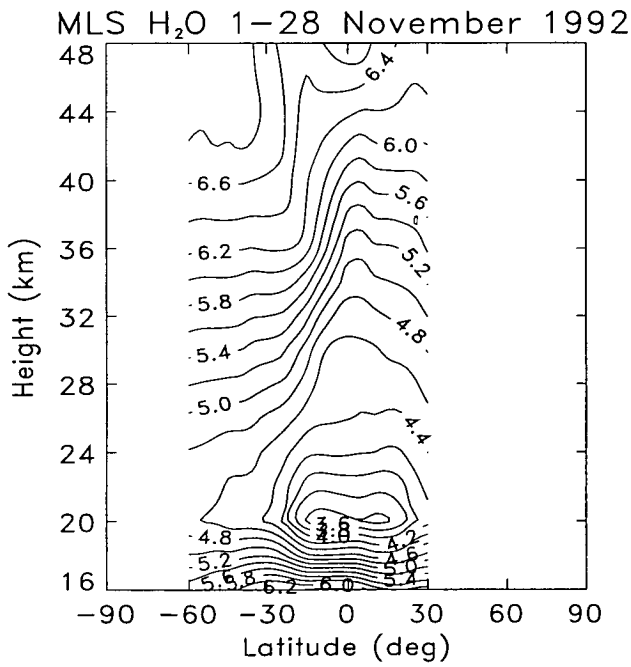
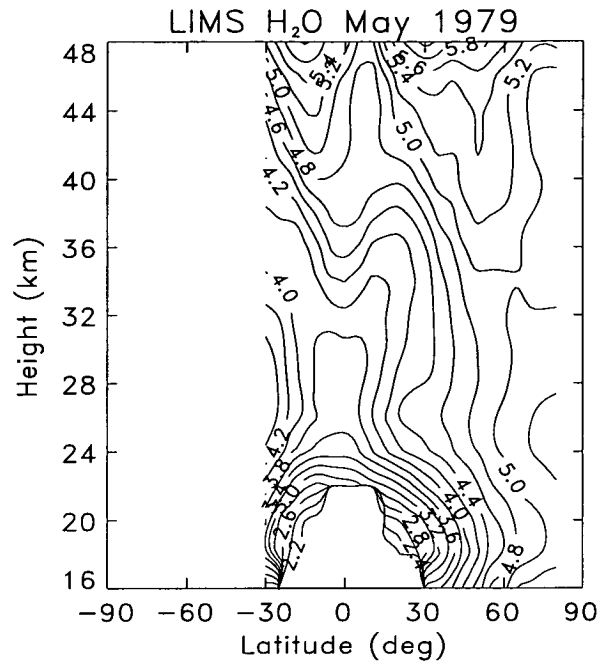
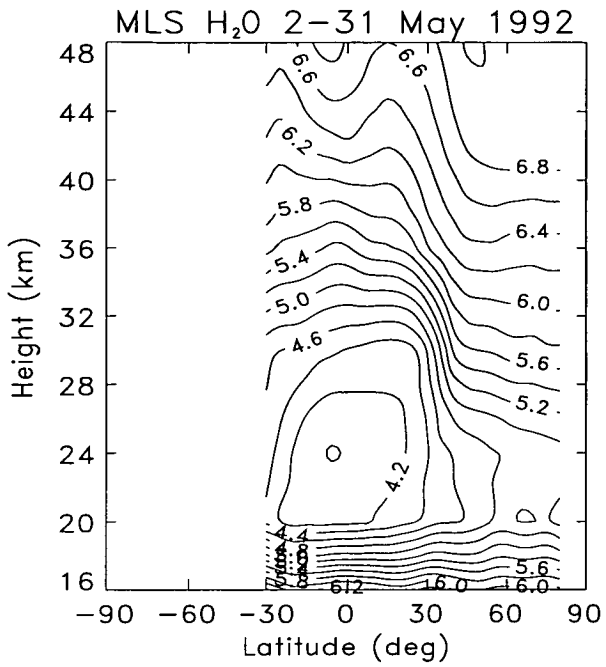


Figure 5.2: Zonal-mean latitude-height cross sections of MLS H₂O (v0003) for May and November 1992 and LIMS H₂O for November 1978 and May 1979. The blank areas in the plots are regions where no measurements were available. Contours every 0.2 ppmv

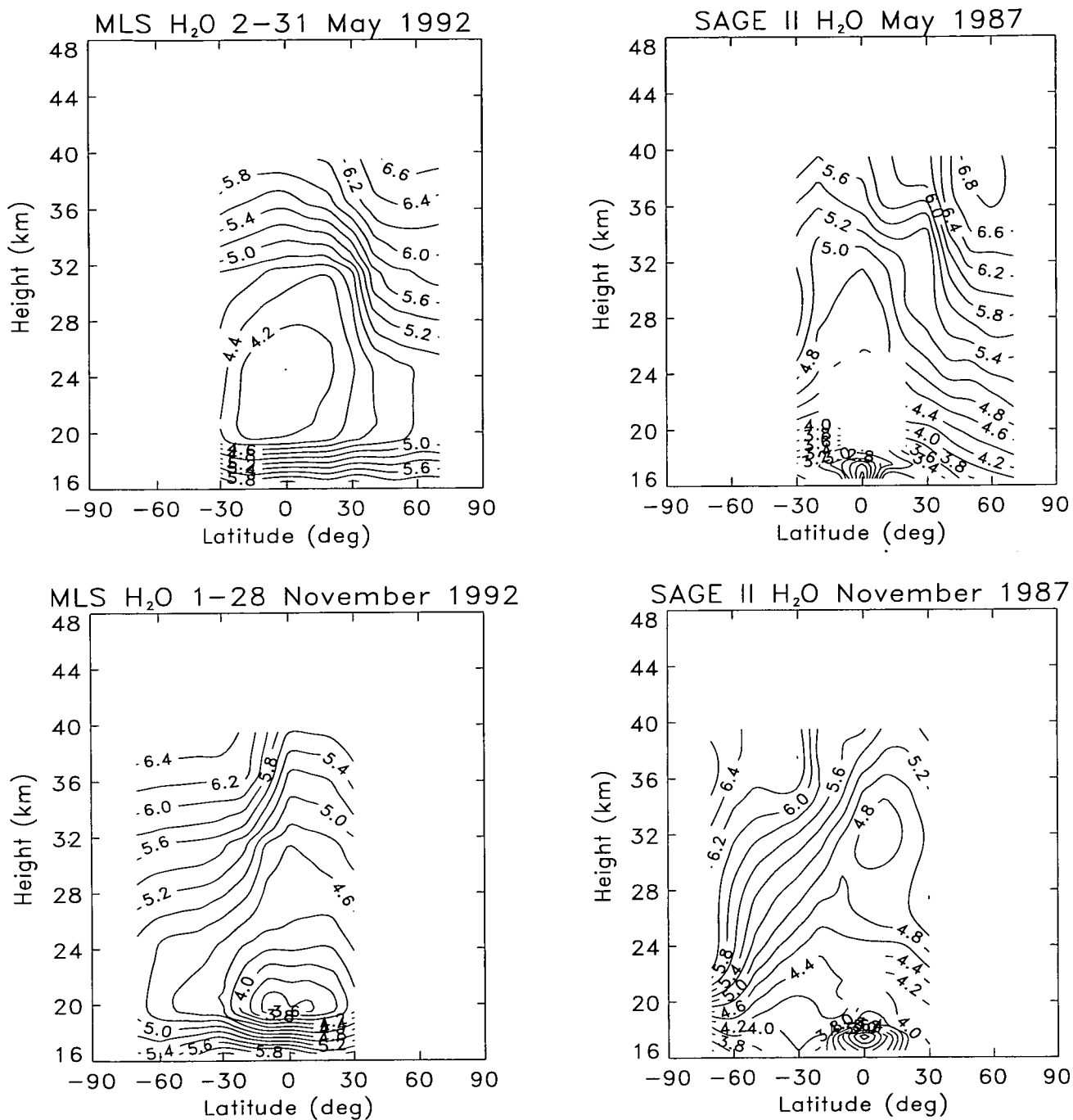


Figure 5.3: Zonal-mean latitude-height cross sections of MLS H₂O (v0003) for May and November 1992 and SAGE II H₂O for May and November 1987. The blank areas in the plots are regions where no measurements were available. Note that for MLS, the data below 20 have a large contribution from the *a priori*. Contours every 0.2 ppmv

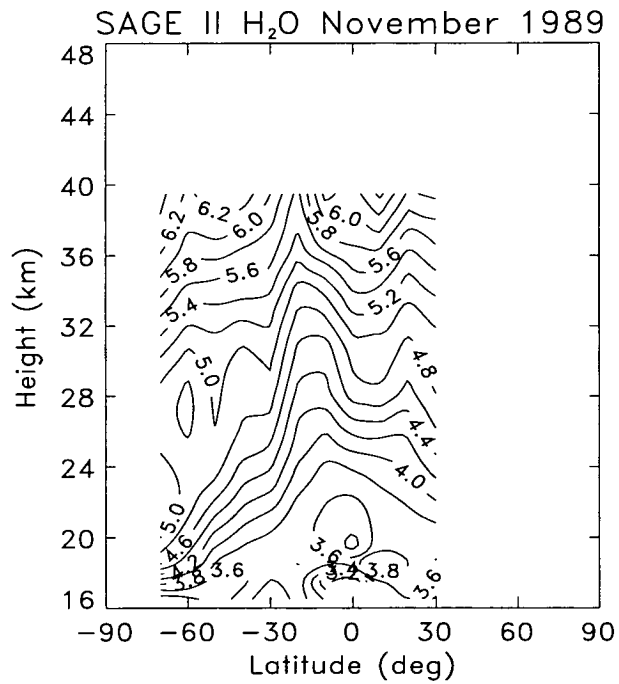
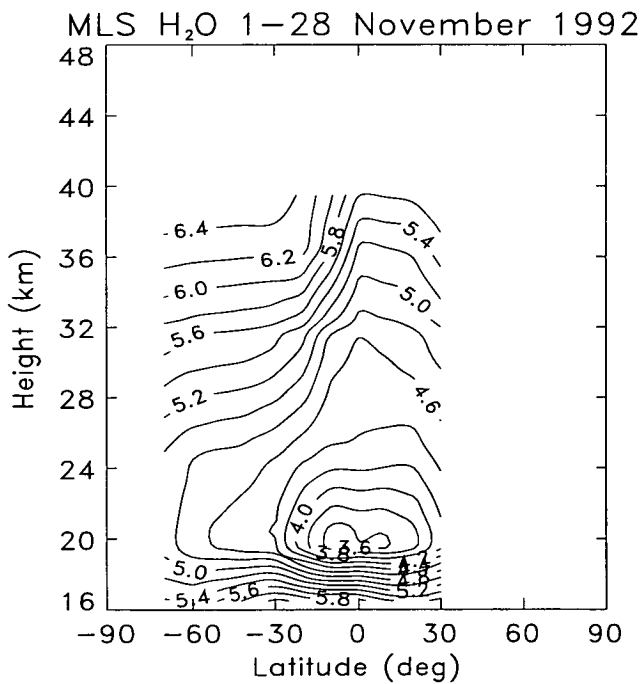
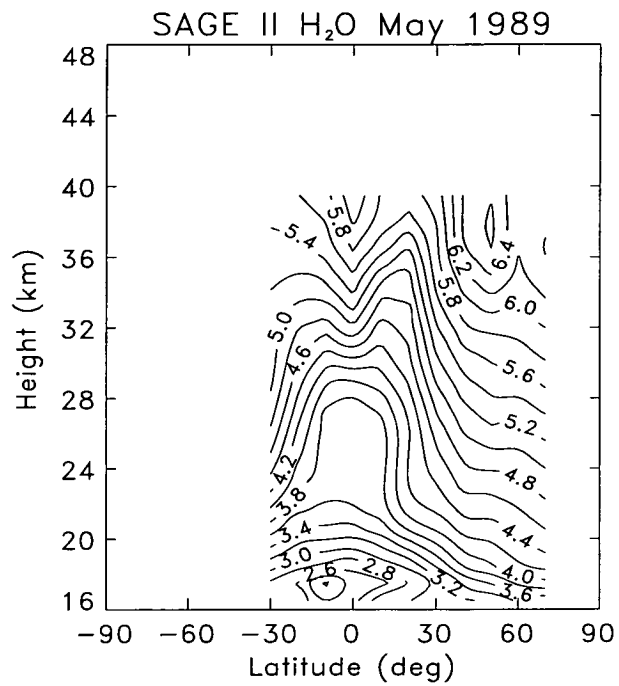
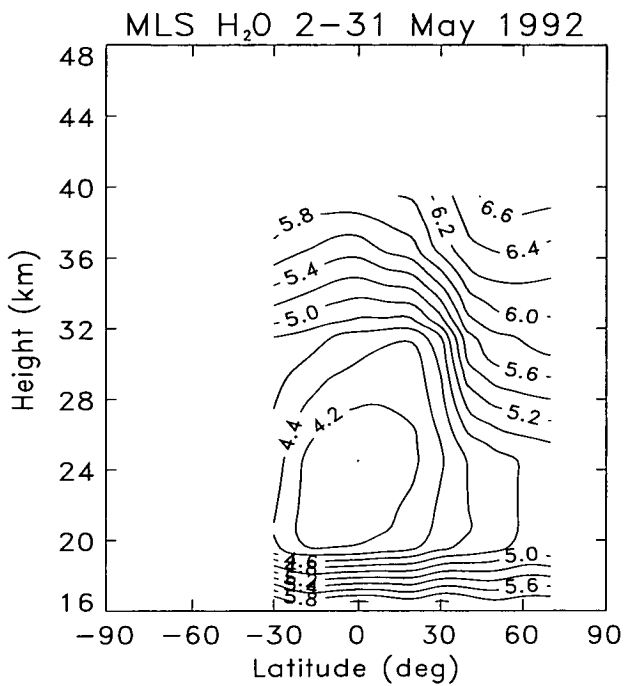


Figure 5.4: Same as Figure 5.3 but for SAGE II data from 1989

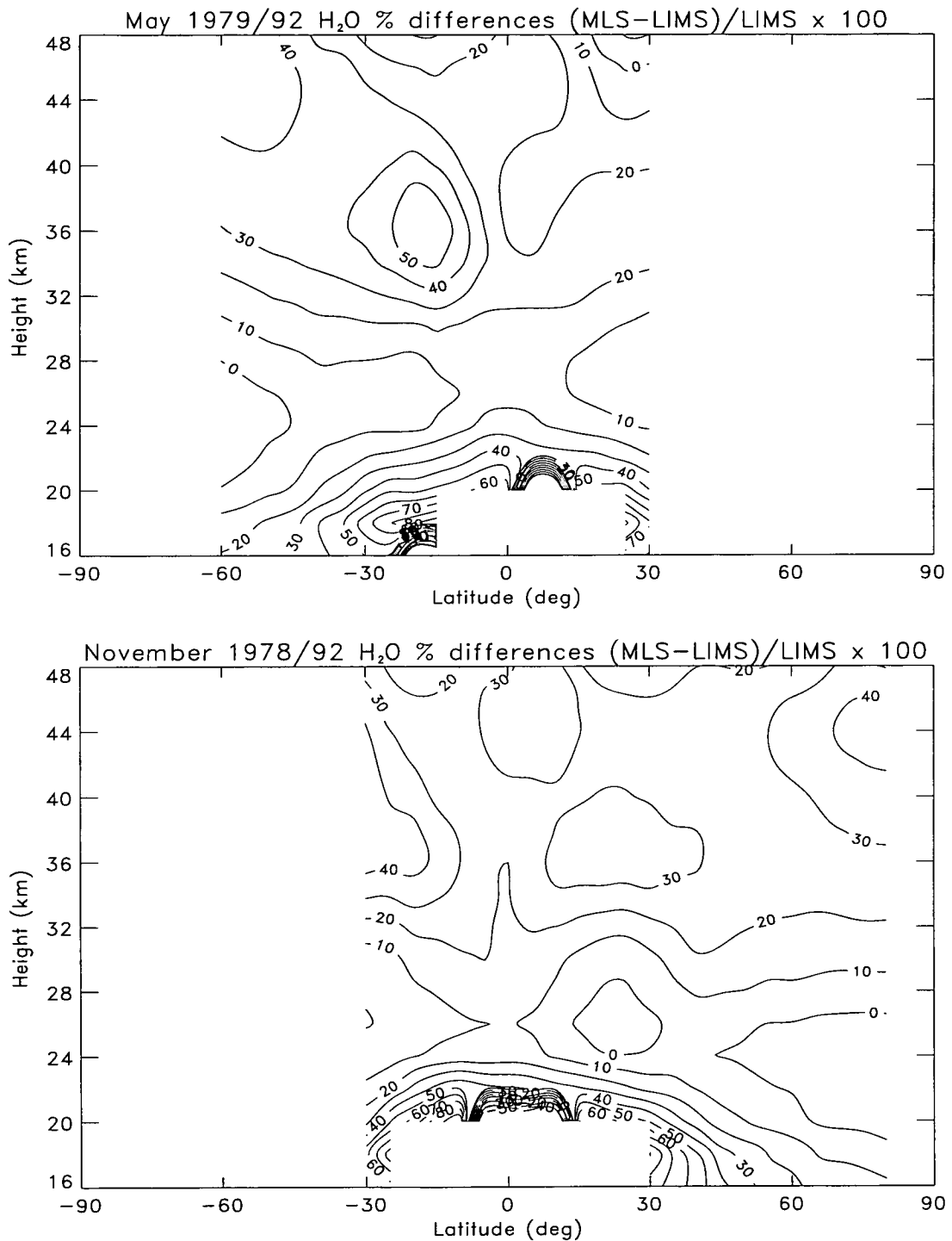


Figure 5.5: Percentage differences between MLS and LIMS water vapour ($(\text{MLS-LIMS})/\text{LIMS} \times 100$). Solid contours are where MLS H₂O is greater than LIMS H₂O. Top panel is for November differences and bottom panel is for May differences. Contours are every 10%

distributions, particularly in November show a narrower flank (in terms of latitude) of implied ascent (Figure 5.1). Another reason for the differences is that LIMS has a more pronounced “dry-tongue” (WMO, 86) than MLS. In May, LIMS shows mixing ratios of ~ 4.0 ppmv near 40 km at $\sim 30^\circ\text{S}$ generally consistent with the seasonal variation in the Brewer-Dobson circulation. In contrast, the distribution of MLS H_2O in May is consistent with a fairly weak circulation; the contours are fairly flat over much of the tropics between 28 and 40 km. Analysis of the UKMO zonal-mean winds for this time show that there was a period of westerly vertical shear in the middle-tropical stratosphere. This would tend to dampen the velocity of air parcels in the Brewer-Dobson cell and thus may explain some of the difference with LIMS.

Another important issue to consider is the extent to which changing atmospheric methane levels have altered the water vapour distribution between the time of LIMS (1978/79) and the time of MLS (1991–93). Although Steel et al (1992) suggest that the growth rate of methane has sharply declined in recent years, over the period 1978/79 to 1991/93 methane levels of air entering the stratosphere are calculated, using estimates from Hansen and Robinson (1989) and Dessler et al. (1994), to have increased by ~ 0.2 ppmv. Assuming that direct conversion of one CH_4 molecule leads to two molecules of H_2O (Dessler et al., 1994, Le Texier et al., 1988) this would lead to an increase of roughly 0.4 ppmv in H_2O mixing ratios, particularly in the upper stratosphere where methane oxidation is more prevalent.

Now, as discussed in the previous chapter, preliminary results from MLS (v0004) retrievals have seen a decrease in stratospheric mixing ratios of 0.1–0.2 ppmv between 46 and 10 hPa and 0.2–0.4 ppmv between 4.6 and 1.0 hPa. Combining these results with the estimated rise in H_2O mixing ratio due to increasing methane levels reduces the differences (Figure 5.5), between MLS and LIMS, by ~ 10 percentage units. Thus, from the above discussion, the unresolved differences between the two instruments are, in fact, relatively small when compared to the accuracy of their measurements..

MLS v SAGE II

The differences between MLS and SAGE II (1987 and 1989) data are less than 10% everywhere (Figures 5.6 and 5.7) apart from at the lowermost height levels (where MLS does not retrieve) and in the lower tropical stratosphere (for the same reasons outlined above in the LIMS comparison)

Although the agreement is generally excellent one should note that the SAGE II data were gridded at 10° latitude intervals and so some real differences may have been masked by the averaging process. However this is unlikely to have a large impact on the scale of the features discussed here.

Another point, worth bearing in mind, is that since SAGE II is an occultation instrument far fewer measurements have made up each monthly average and thus the distribution is not a true monthly-mean. This should not have a great effect on the percentage differences but it would be prudent in further work to perhaps repeat the investigation by using only the MLS data at latitudes where SAGE II measures on each particular day in the month.

5.3 Summary

In this chapter the zonal-mean climatology of the MLS water vapour (v0003) distribution was presented for the first time. Many of the broad features present have been observed in previous satellite measurements and give rise to confidence in the data.

Compared to LIMS, MLS zonal-mean water vapour measurements are much larger (10-50%). A rough calculation of the increase in stratospheric methane levels shows that part of this difference can be explained by the greater volume of methane in the atmosphere in 1991–1993 than in 1978/1979.

Another reason for the difference is that MLS (v0003) water vapour mixing ratios are believed to be too large (Lahoz et al., 1996). The retrieval software has recently been improved (See section 3.8). Initial comparison of current MLS results with those from the new retrieval (v0004) suggest that mixing ratios are currently ~ 5 -10% too big. Even allowing for this decrease, MLS mixing ratios, compared to correlative data (Lahoz et al., 1996) still appears too ‘wet’.

Furthermore, at least some of the difference must be due to natural variability.

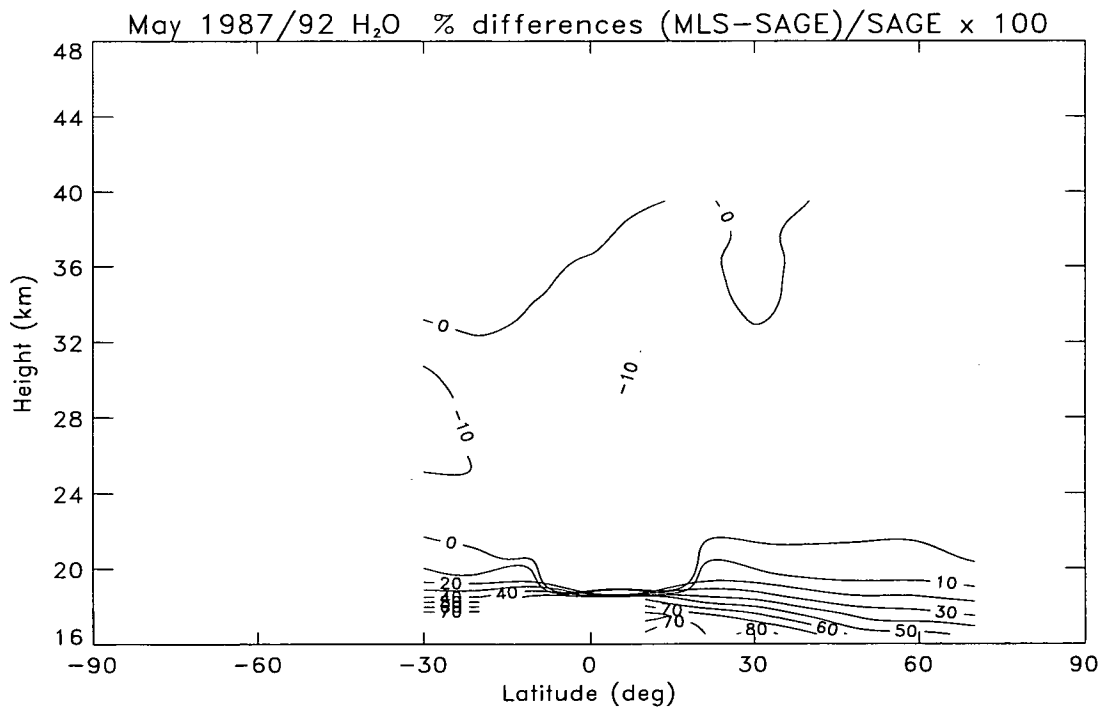
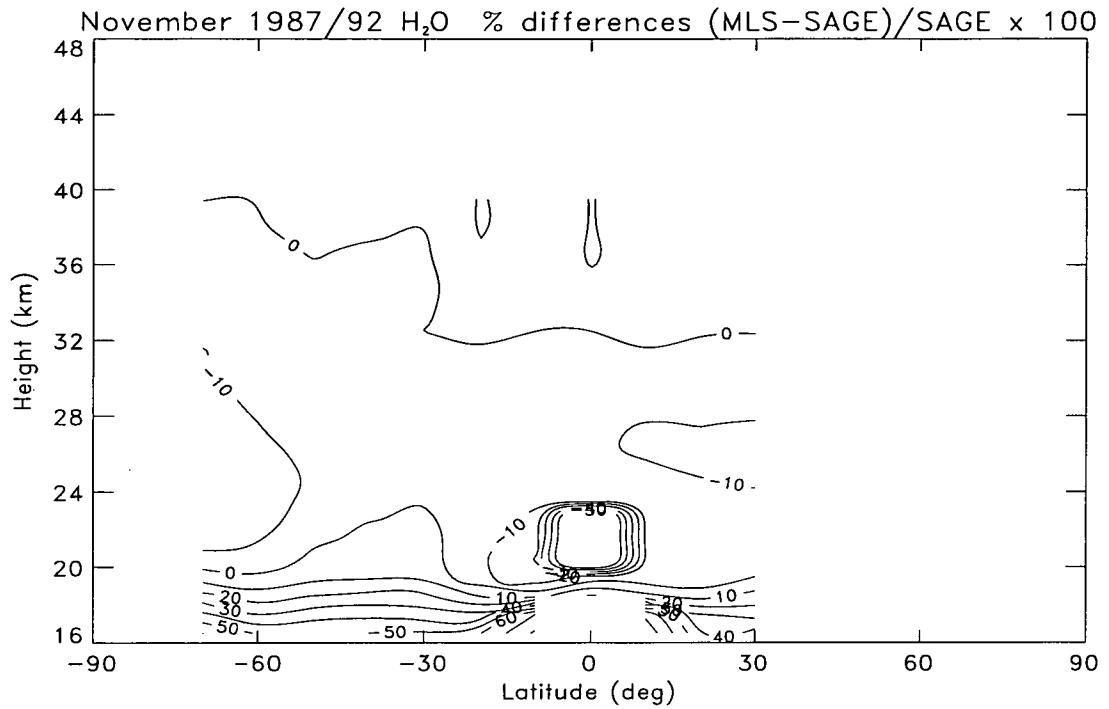


Figure 5.6: Percentage differences between MLS and SAGE II (1987) water vapour ($(\text{MLS}-\text{SAGE})/\text{SAGE} \times 100$). Solid contours are where MLS H₂O is greater than SAGE II H₂O. Top panel is for November differences and bottom panel is for May differences. Contours are every 10 %

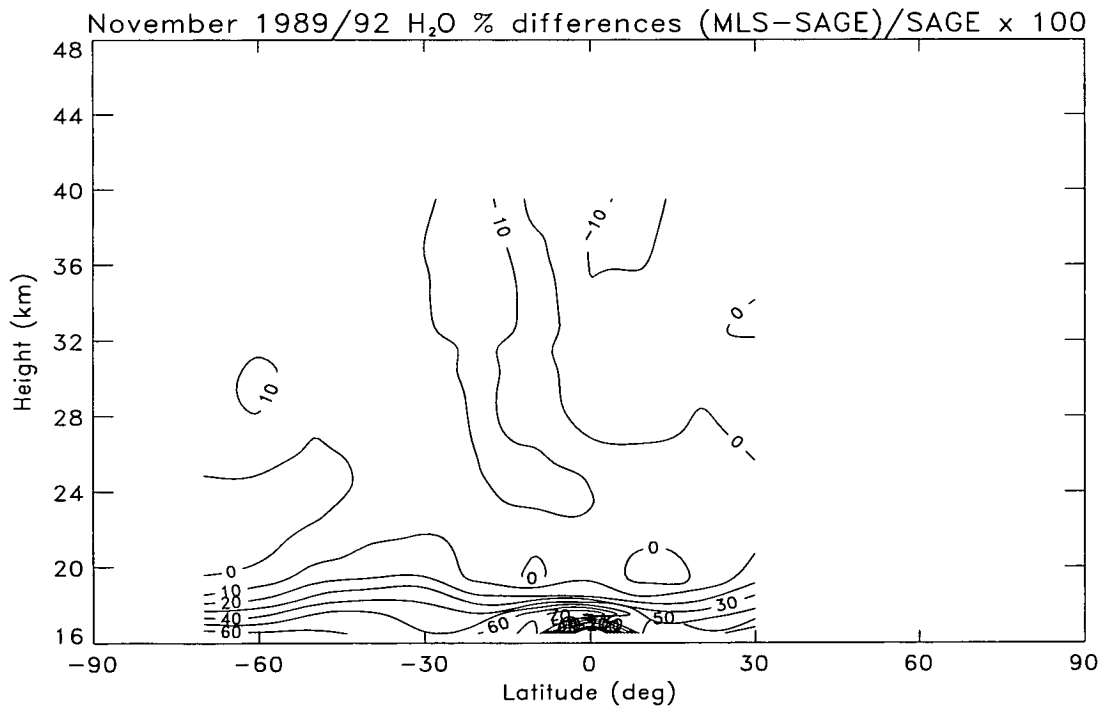
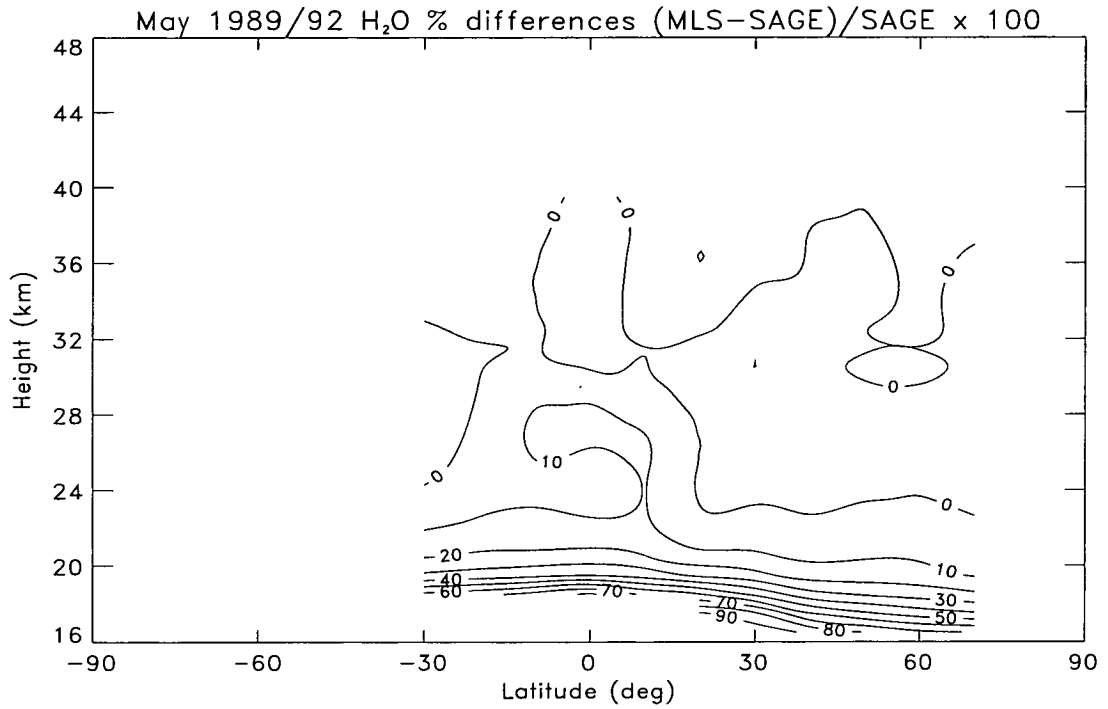


Figure 5.7: Percentage differences between MLS and SAGE II (1989) water vapour ($(\text{MLS}-\text{SAGE})/\text{SAGE} \times 100$). Solid contours are where MLS H₂O is greater than SAGE II H₂O. Top panel is for November differences and bottom panel is for May differences. Contours are every 10 %

For example, it was noted in the previous section that implied transport in the Brewer-Dobson cell differed between MLS and LIMS.

Combining the reasons above illustrates that the unresolved differences are relatively small, at least in terms of the estimated accuracy of each measurement-set.

The zonal-mean distributions from MLS were also quantitatively compared to results from SAGE II. MLS mixing ratios are predominantly larger ($\sim 10\%$) in much of the stratosphere but the differences are generally within the accuracy of measurements. The better agreement between MLS and SAGE II than MLS and LIMS is what might be expected since the MLS and SAGE II measurements are, compared to LIMS, contemporaneous and hence increasing methane levels would have much less of an effect in any differences.

It is also worth noting that zonal-mean mixing ratios generally increase from 1978/79 (LIMS) to 1987/89 (SAGE II) to 1991–93 (MLS), consistent with, but not fully accounted for, increases in methane over the time period.

The main difference between each of the datasets is in the tropical lower stratosphere where each instrument measures its minimum values. The altitude and magnitude of these minima differ between instruments and results in the large percentage differences observed. Part of the reason for this is that satellite instruments cannot adequately resolve the true structure in a region of the atmosphere where there is a large vertical gradient in the distribution. The difference in the magnitude of the minima is, in part, related to the variabilities in the tropopause temperatures since small changes in temperature can have a large impact on saturation mixing ratios.

A feature not previously observed by satellites, and uniquely observed by MLS, was the extensive dehydration that occurs in the Antarctic lower stratosphere during winter. MLS observed this phenomenon at high southern latitudes in August and September 1992.

The following chapter will describe in more detail some of the points raised above. Furthermore, the variability of the data at different latitudes and different altitudes will be examined.

Chapter 6

Variability of Stratospheric MLS H₂O

6.1 Introduction

This chapter concentrates on a detailed description and discussion of the seasonal-scale variations of water vapour at various pressure levels and in various latitudinal bands.

6.2 Seasonal scale variations in MLS H₂O

This section takes the form of two separate sub-sections; one will deal with the variations observed in the lower stratosphere: the other will discuss upper stratospheric variations.

6.2.1 Lower stratospheric variations

Tropical latitudes

We now consider the temporal and latitudinal variations of tropical water vapour as observed by MLS, beginning with the lower stratospheric tropics.

Figure 6.1 shows the time-latitude variation of the zonal mean MLS water vapour ($v0003$) at 22 and 46 hPa. Data were averaged every 4° in latitude and were screened to remove any profiles flagged by the retrieval as bad (See section 4.2). The large gap in the figure during June and July of 1992 was a period when the spacecraft experienced some problems with its solar arrays and was hence temporarily shut down.

The averaging process greatly improves precision since each 4°-mean value is comprised of approximately 40 measurements. Also, calculation of the standard deviation around the mean mixing ratio in each 4° band, for each day, revealed no significant trends with values of between 0.2 and 0.3 ppmv seen at both 46 and 22 hPa throughout the tropics. Note also, that at 22 hPa there is a yaw-related problem which manifests itself as a quasi-monthly cycle in most of the time series in the tropics (and, on occasion, beyond). Future versions of the retrieval should correct this artifact.

At both pressure levels, a well-defined tropical minimum is present, which in some months is flanked by sharp gradients poleward of 10° or 20°. In other months, the well-defined tropical minimum and sharp gradients are not present (e.g. July and August at 22 hPa and May and June at 46 hPa).

At 46 hPa, the equatorial variations more nearly follow an annual cycle than at 22 hPa (Figure 6.2) with minima in November/December of 1991/1992 of 3.8 ppmv and 3.6 ppmv respectively. The smaller minimum in 1993 suggests that the region of the tropical tropopause where air entered the stratosphere in this year was colder than in 1992. However, analysis of UKMO 100 hPa temperature data reveals, in general, that minimum temperatures are similar in both years. This implies either that the 100 hPa pressure is non-representative of the true tropopause or that the resolution of UKMO is not fine enough to capture the true temperature minima or that equatorial MLS mixing ratios in either 1992 or 1993 contain a systematic error. The latter reason seems unlikely since mixing ratios polewards of the equator are similar in both years. The second possibility is also unlikely since Frederick and Douglass (1983) point out that during northern winter, when the tropical tropopause is coldest and around the time that MLS measures minima at 46 hPa, the 100 hPa pressure surface accurately represents the tropopause. Thus it seems probable that true temperature minima are on a scale simply not resolvable by UKMO data.

There also exists a sub-tropical gradient in mixing ratios in both 1991/92 and 1992/93 that moves in a seasonal fashion towards the south in the months September/October to January and then weakens after February. We will return to this later (see Figure 6.7).

The maximum mixing ratios, at 46hPa, are observed in March/April 1992

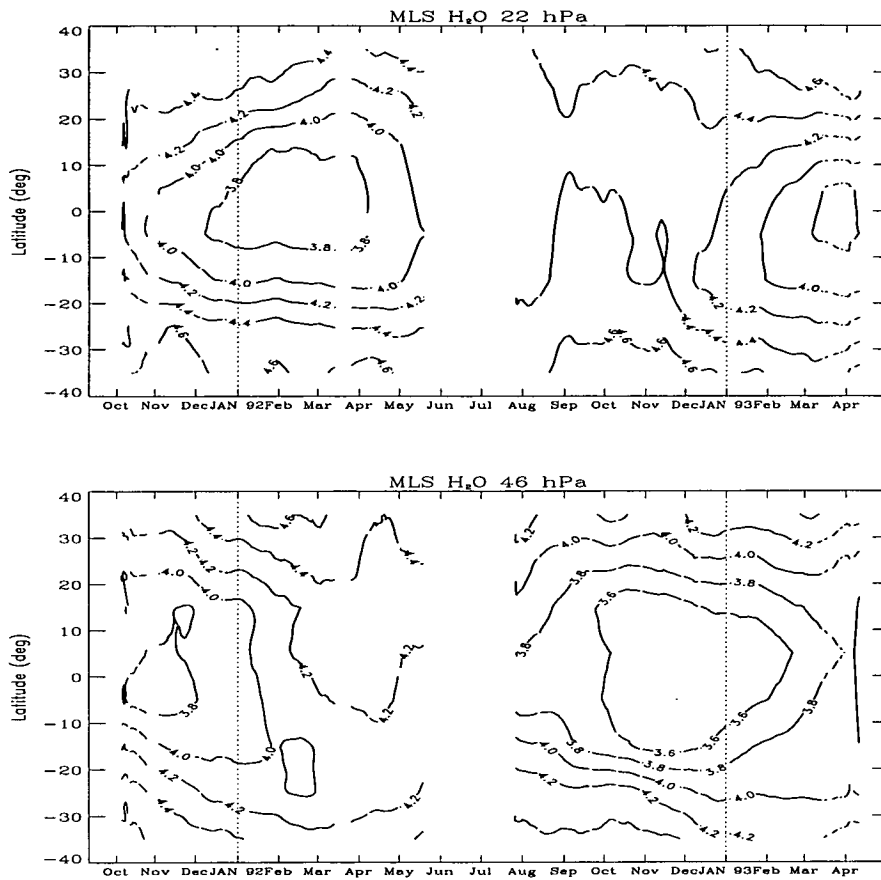


Figure 6.1: Time-latitude cross section of MLS (v0003) water vapour at 46 and 22 hPa. Data were averaged every 4° in latitude. The series in each latitude band have also been smoothed using a low pass filter. The gap in the centre of the plot was a period when the MLS 183 GHz radiometer was not working

(~ 4.2 ppmv) and sometime after April 1993.

At 22 hPa, the minimum mixing ratios, during 1992, occur from January to April and are approximately ~ 3.8 ppmv, while in 1993, minima (~ 3.8 ppmv) first occur sometime during March, at least two months later than in 1992. Thus the time between minima at 22 hPa is at least 14 months.

The sub-tropical gradient is weaker than at 46 hPa and its drift is less apparent, although there is some poleward movement of tropical values in both hemispheres.

Maximum mixing ratios are found around September 1992 (~ 4.5 ppmv) and sometime before October 1991.

The variations in HALOE (v0017) water vapour (Figure 6.3) are qualitatively similar to MLS at both 46 and 22 hPa except for earlier in the record where

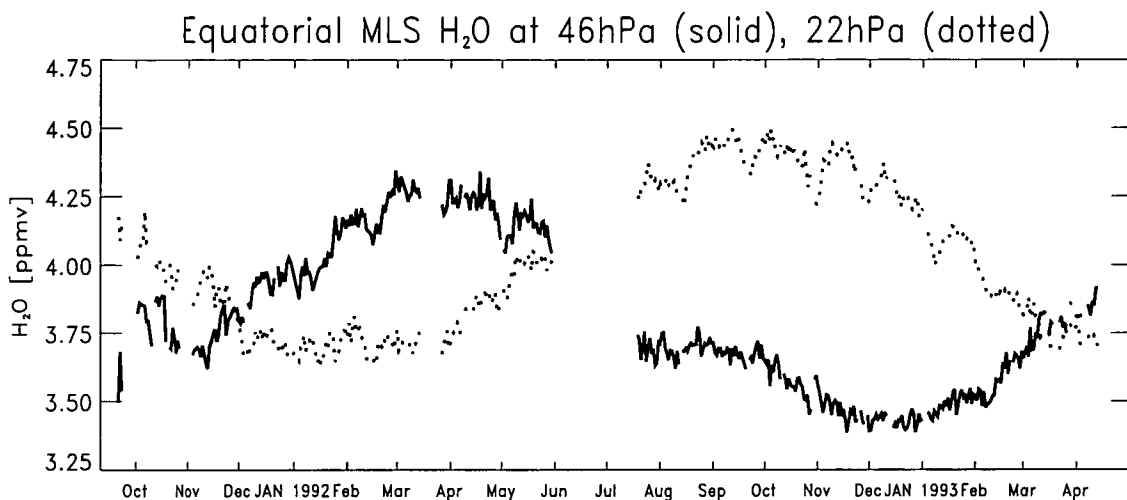


Figure 6.2: Time-series of equatorial MLS water vapour at 46 and 22 hPa. Typical average precision values for mixing ratios are between 0.7 and 0.9 ppmv at 46 hPa and 22 hPa

equatorial HALOE values suffered due to Pinatubo aerosol contamination. At 22 hPa, CLAES (v0007) mixing ratios are close to HALOE and are systematically ~ 0.5 ppmv lower than those from MLS. CLAES retrievals at 46 hPa were poor as mentioned in Chapter 4. The longer HALOE record indicates that a minimum at 22 hPa occurred in March/April 1993 with a maximum at 46 hPa around the same time.

Figure 6.4 shows a time-height contour plot of MLS water vapour in the equatorial lower stratosphere. The figure illustrates a very interesting feature in the distribution. That is, the 22 hPa minimum which is first observed in January 1992 appears to be the remnant of the 46 hPa minimum which occurred earlier in the year (from October to November/December). Although the movement of the minimum between these levels appears abrupt it is likely to be an artifact of the retrieval grid having adjacent grid points at these positions. Inspection of HALOE data (not shown) which are retrieved on a finer grid indicates the lower stratospheric minimum sometimes to occur on an intermediate level at 32 hPa.

The 1992/93 minimum at 46 hPa appears at a similar time of year to the previous one but is sustained for a longer period, some four and half months. Hence, the minimum at 22 hPa, if it were to be a remnant of this 46 hPa minimum, would appear somewhat more than a year after the previous one.

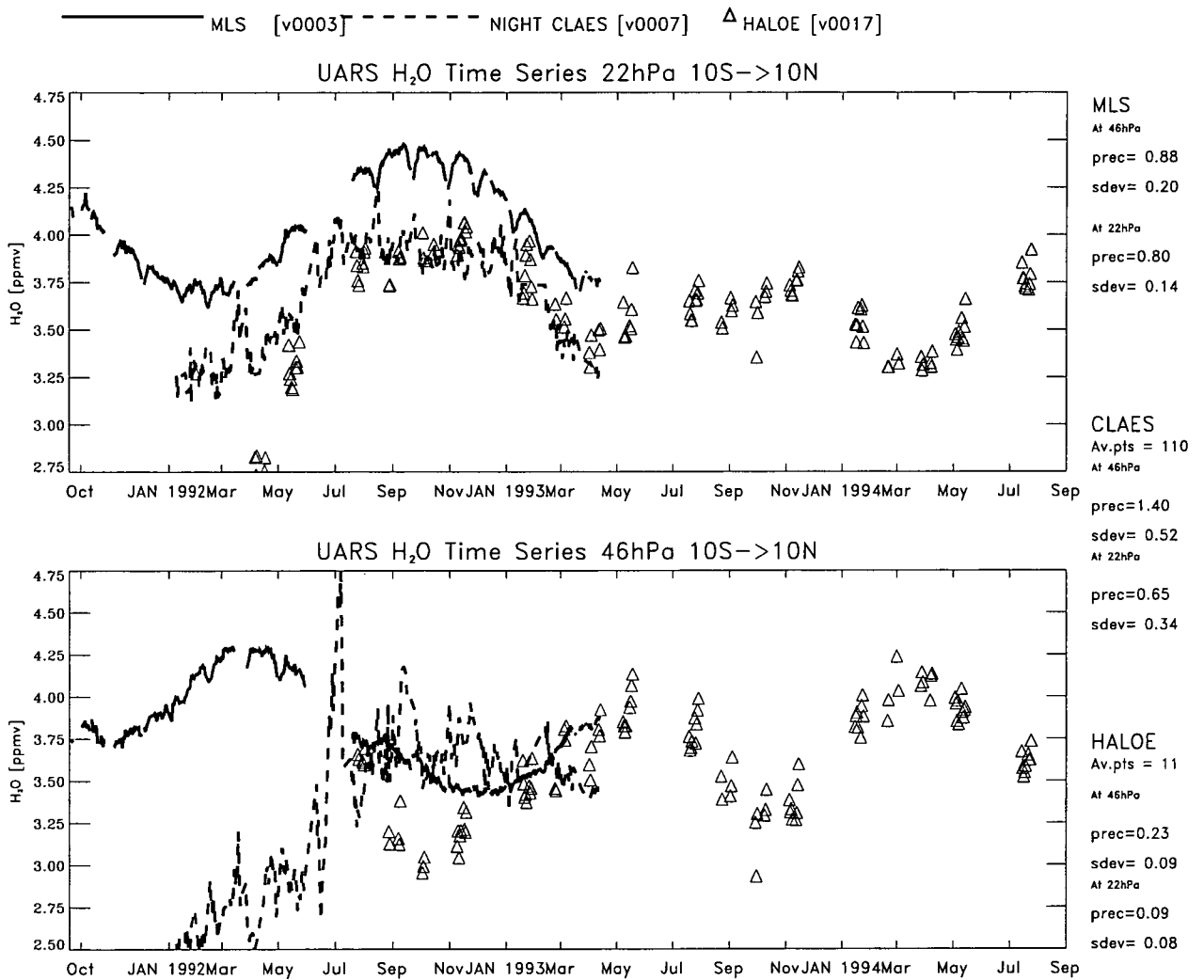


Figure 6.3: Comparison of daily tropical (10deg S to 10deg N) measurements for MLS (solid curve), HALOE (triangles) and CLAES (dashed curve) for the period October 1991 to September 1994. Top and bottom panels show time series at 22 and 46 hPa respectively.

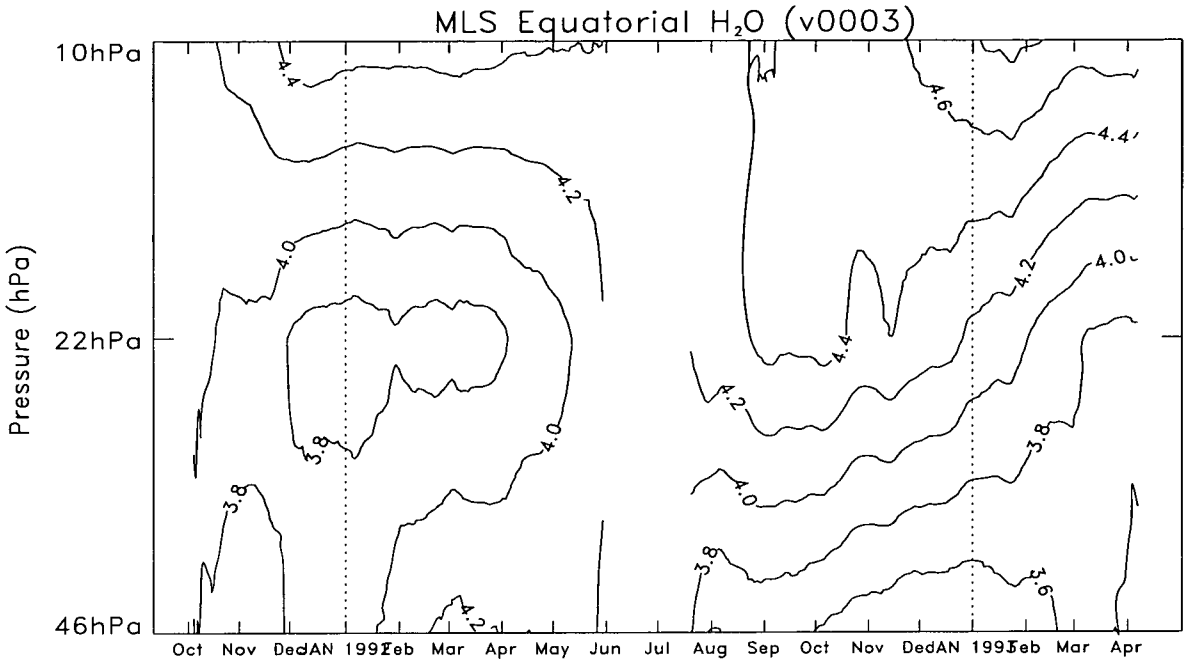


Figure 6.4: Time series of lower stratospheric MLS H₂O (v0003).

Using this equatorial feature as a starting point, the temporal variations in the lower stratospheric tropics (Figure 6.2) were first examined for any QBO influence. The equatorial 22 hPa water vapour was found to be well correlated (c.coeff=0.90) with the vertical shear of zonal mean zonal wind (Figure 6.5) between 10 hPa and 50 hPa (using winds from the UK Met. Office assimilation which is part of the UARS correlative data base (Swinbank and O'Neill, 1994)).

Furthermore, to ascertain whether the variation in equatorial water vapour was more like the variation in wind shear or more like an annual cycle, two different curves were fitted to the water vapour data (Figure 6.6). One curve represented a fit to an annual cycle ($\text{constant} + A\sin(t/365) + B\cos(t/365)$), the other a fit to an annual cycle plus a scaled wind shear term ($C(U(t)_{10} - U(t)_{50})/M$), where M was the absolute maximum value in the shear time series). The scaling was to ensure that the size of wind shear term lay between 0 and 1, thus ensuring a sensible comparison of A, B and C .

It turned out that the amplitude of the wind shear term was several times larger than the contribution from the annual cycle and thus it was initially concluded

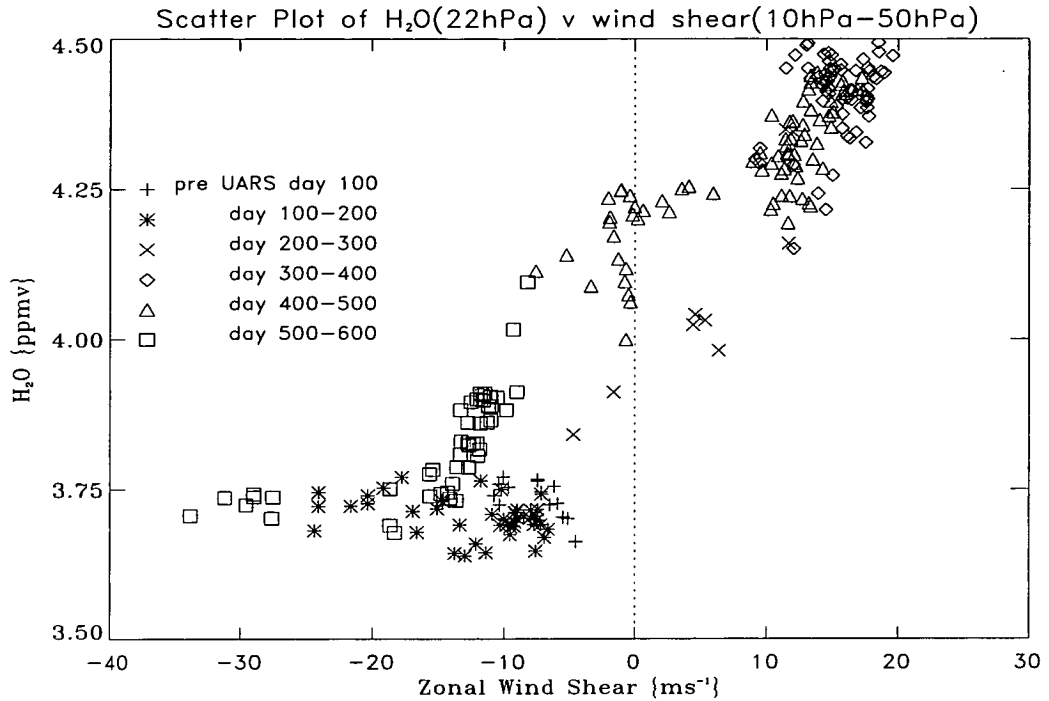


Figure 6.5: Scatter plot of H₂O at 22hPa versus wind difference (10-50hPa).

that the mechanism responsible for the variation in the zonal winds (i.e. the QBO) was also modulating the variation in equatorial mixing ratios.

However, during the research and as more HALOE water vapour data became available, the zonal-wind shear (10-50 hPa) variation looked less and less like the variability in the HALOE data. The high correlation cited above was thought to be coincidental, partly due to the fact the MLS water vapour record, on which the correlation calculation was based, was relatively short.

Further analysis showed that water vapour in the lower stratosphere is very sensitive to the seasonal variations of tropopause temperature (Mote et al., 1995). They showed that the timing of the features in Figure 6.2 was largely determined by the time at which air crossed the tropical tropopause. In January or February the tropopause is coldest and air passing through it has more water vapour removed than in summer when tropopause temperatures are higher.

The QBO was found to play a role but it was less important than originally thought. Its main affect on the variation of water vapour is to delay or accelerate the arrival of a minimum; this explains why the variations at 22 hPa were farther from a pure annual cycle than the variations at 46 hPa since the air was under the

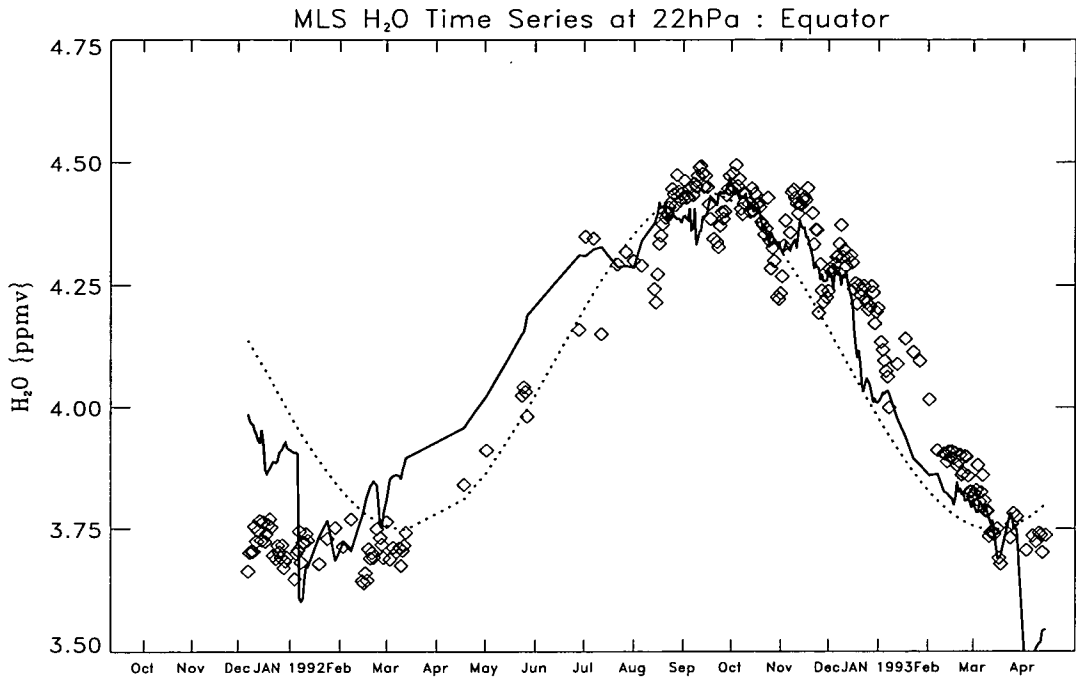


Figure 6.6: Curve fits through MLS H₂O at 22hPa. Solid curve is an annual cycle fit plus a wind shear term $(4.09 - 0.07\sin(T/365) - 0.02\cos(T/365) + 0.41(\text{shear}/15))$. The dotted line is an annual cycle fit only $(4.08 - 0.22\sin(T/365) + 0.23\cos(T/365))$

QBO influence for a longer period of time.

Mote et al. (1996) describe how stratospheric water mixing ratios are, in fact, marked by the temperatures they encountered at the tropical tropopause; the so-called “tape-recorder” hypothesis. Direct evidence, using MLS data, is given of the upwards advection of the annually varying tropopause saturation mixing ratios. This is a possible explanation for the elevated hygropause first observed by Kley et al. (1979,1982) and now observed in MLS data (Figure 6.4).

The tropical tape-recorder

In 1993, at a NATO Science Workshop, Michael McIntyre first put forward his “tape-recorder” theory. This argued that air passing through the tropical tropopause should be marked with the prevailing minimum saturation mixing ratio, similar to the way in which a magnetic tape is marked by a tape-recorder head. Evidence to support the “tape recorder” hypothesis is revealed in the MLS water vapour

measurements.

Mote et al (1995) first suggested that the larger-scale view revealed by the MLS water vapour data showed the signature of upwards advection by the mean circulation. Moreover this circulation appeared not to be significantly degraded by mixing. To check their conclusions they calculated, from MLS ozone and water vapour and UKMO temperature fields, a residual transformed Eulerian mean (TEM) circulation and also ran trajectories from levels in the stratosphere to 100 hPa. From these trajectories, saturation mixing ratios at 100 hPa could be used to estimate the mixing ratios at the trajectory starting points. They found that the mixing ratios observed by MLS varied temporally in a similar fashion to those of the trajectory calculation and thus demonstrated consistency with a tape-recorder-like connection between the annual cycle in tropopause temperature and the annual cycle in MLS lower stratospheric water vapour. However, there were sometimes large discrepancies between the amplitudes of the observed and calculated variation. This was initially thought to be due to the neglect of mixing in the TEM calculation but more detailed investigation by Mote et al. showed that the main reason for the differences was the failure of the 100hPa pressure surface to represent accurately enough the height of the tropopause. The height of tropical tropopause varies seasonally. In northern winter, it mainly occurs at pressures less than 100hPa and in northern summer at pressures more than 100hPa (Reid and Gage, 1981). Hence, if the temperature profile minimum is above 100 hPa then the minimum saturation mixing ratio is overestimated by $T_{100\text{hPa}}$ and underestimated by the 100 hPa surface, thus resulting a small net error (Frederick and Douglass, 1983). The large differences, between the calculated and observed variations, in northern summer are because both $T_{100\text{hPa}}$ and 100hPa pressure surface overestimate the minimum saturation mixing ratio. Thus there is no cancellation as in winter.

Mote, myself and others (Mote et al., 1996) discuss this issue in more detail and also discuss further the role of the QBO in the variability of tropical MLS H_2O (Carr et al., 1995). Moreover, an investigation of whether the water vapour observations between the tropopause and 46 hPa were marked by the tape recorder (MLS does not currently retrieve in this region) was carried out. Using additional data from a 2-D model (Kinnersley, 1995), from HALOE (twice the vertical reso-

lution of MLS (v0003)), from CLAES and from the NOAA lyman- α hygrometer aboard the ER-2 aircraft (Kelly et al., 1989), they provide strong evidence to support their case that air is indeed marked by its stratospheric entry temperature and that it rises relatively unmixed upwards through the lower stratosphere.

Summary

As noted above there is annual cycle in MLS lower stratospheric tropical water vapour and this cycle is somewhat modified by the quasi-biennial oscillation. The QBO acted to delay or accelerate air parcels and so had a greater affect on the 22 hPa variability, which was further from an annual cycle than the variability at 46 hPa. Mote et al. (1996) looked further into the role of the QBO by comparing the variability to results from a 2D model. The time between successive minima in the model compared favourably with those from MLS (and HALOE) and *Mote et al* suggested that this fact and the fact that the shape of HALOE profiles was consistent with their hypothesis shows that the QBO stretches or compresses the “tape recorder” signal.

Sub-tropical and middle latitude variations

We now turn our attention to the variations observed outside the tropics. We begin by discussing the precision and accuracy of measurements in these regions since this will give an indication of the level at which any real variation is detectable. The average precision values of MLS measurements in the lower stratosphere at extratropical and middle latitude water vapour show little variation with latitude and lie between 0.8 and 1.0 ppmv at 46 and 22 hPa and between 0.4 and 0.6 ppmv at 10 and 4.6 hPa. Moreover, the standard deviations from the daily-means shown in Figure 6.7 are generally constant at between 0.2 and 0.3 ppmv for all retrieved levels in the lower stratosphere.

At subtropical and middle latitudes the relatively strong quasi-annual signal observed in tropical latitudes becomes less apparent (Figure 6.1 and 6.7). Although McCormick et al. (1993) found the opposite to be true in SAGE II water vapour their results were based on measurements at altitudes below which MLS can currently retrieve. Above 18 km, where MLS does retrieve, SAGE II data at

middle latitudes showed only a faint sign of the delayed tropical signal that was observed at lower altitudes. At those lower stratospheric levels where MLS does retrieve it is only at 46 hPa that some horizontal transport is implied (Figure 6.7). From the start of the record to March 1992, average mixing ratios in the southern sub-tropics decrease while those in the north increase. The greatest difference is observed in mid-February where the south is drier by ~ 0.5 ppmv. The situation reverses after March 1992 and the northern hemisphere becomes drier and the south wetter. Looking again at Figure 6.1 one can see the reason for this is seasonal transport from the tropics. Note also, the direction of the transport reverses at approximately the same time as the winter equinox. At 22 hPa, as is evident from Figure 6.1, there is a greatly reduced sign of this seasonal motion. This is somewhat consistent with the so-called “lowermost stratosphere” discussed in Holton et al. (1995). They claimed that there are two distinct transport regimes which occur in stratosphere. Net transport in the lowermost stratosphere has a large horizontal component whereas above this height vertical motions, controlled by non-local dynamical processes, dominate the transport. The main difference here, in MLS data, is that the height demarkating the lowermost stratosphere and the “over-world” beyond is higher than that suggested by *Holton et al*; 46 hPa (~ 465 K) for MLS compared to 380 K for Holton.

There is also some degree of variability and hemispheric difference that can be attributed to the seasonal variations of the Brewer-Dobson circulation.

In the zonal-mean cross-sections of MLS water vapour discussed in the previous chapter it was seen that the implied tropical ascent was much greater in some months than in others (Figure 5.1). For example, the distribution in yaw period 10 (14 August - 20 September 1992) shows a large upwards bulge in the contours over much of the northern tropics. Correspondingly, there is implied descent at latitudes immediately polewards which includes, in this case, the southern tropics. The opposite scenario is seen in yaw month 3 (5 December 1991 - 13 January 1992) with ascent over the southern tropics and descent over the northern tropics.

These variations in the Brewer-Dobson cell also manifest themselves quite clearly in the time series at 10 hPa and 4.6 hPa (Figure 6.8 and 6.9).

Note the sudden rise during January and February 1992/1993, at both 10 and 4.6 hPa in the northern extratropical latitudes. The variation in southern tropical

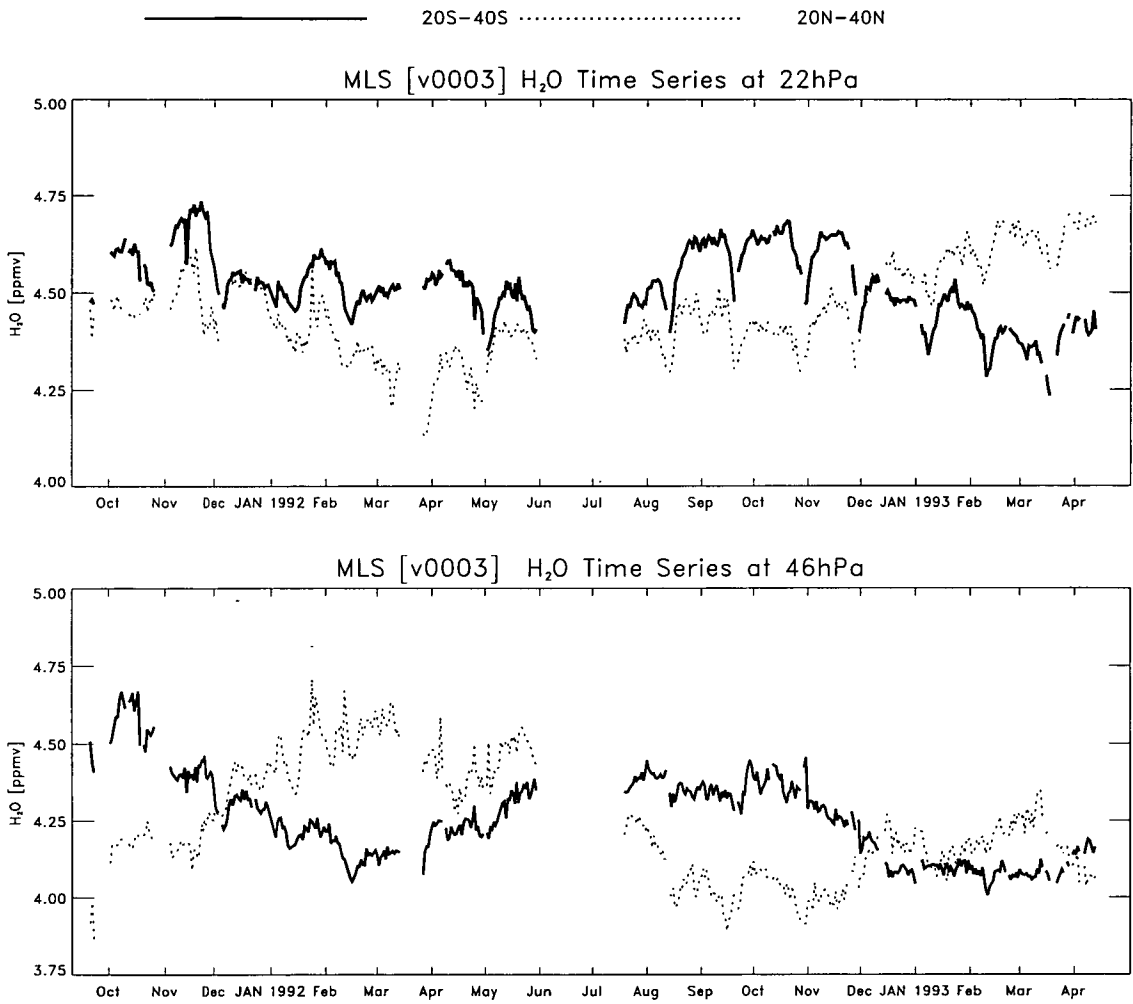


Figure 6.7: Time series of MLS water vapour at 46 and 22 hPa in the latitude bands 20N-40N (dotted) and 20S-40S (solid). Note the yaw-related glitches at 22 hPa mentioned in Chapter 4

———— at Equator 10N->20N - - - - 20N->30N - . - . 30N->40N

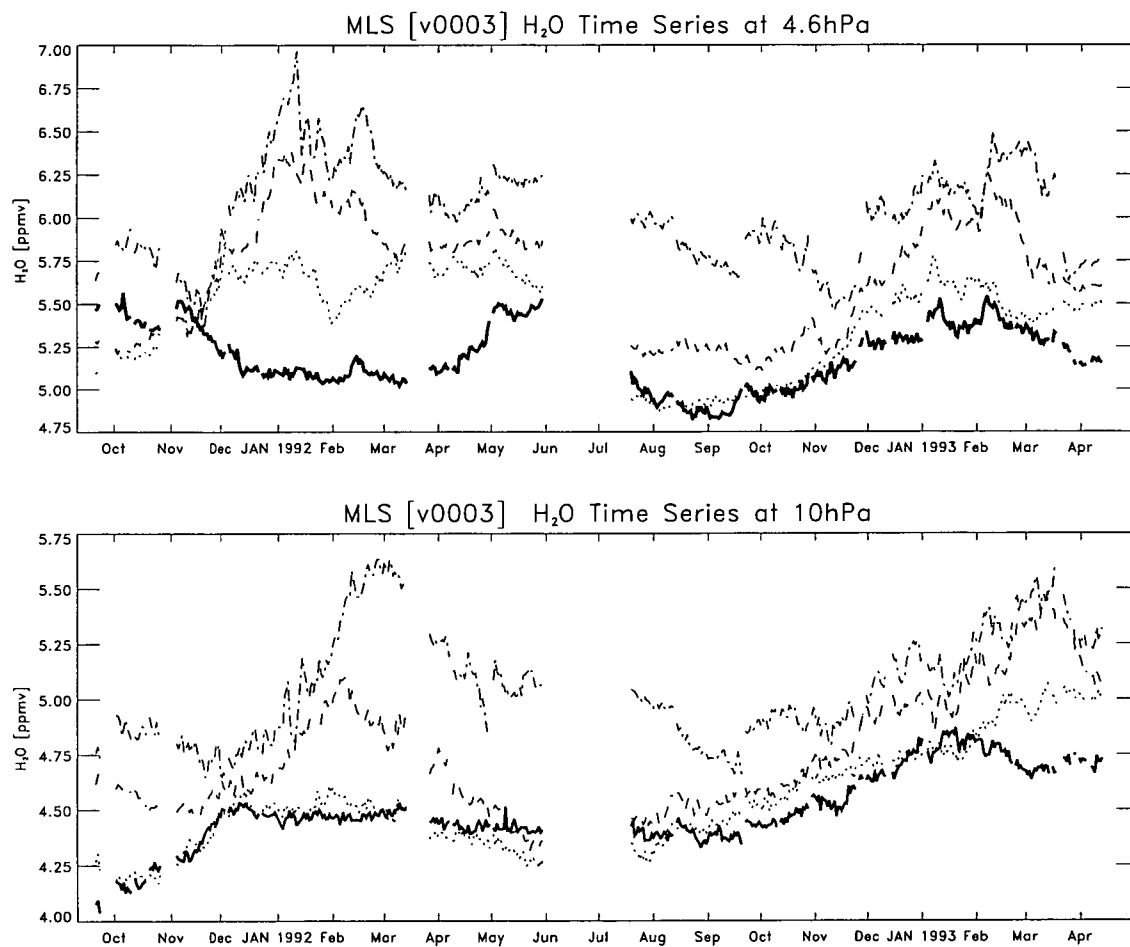


Figure 6.8: Time series of MLS water vapour at 10 and 4.6 hPa in the latitude bands, equatorial (solid), 10N-20N (dotted), 20N-30N(dashed), 30N-40N (dot-dashed).

— at Equator 10S->20S - - - - - 20S->30S - · - · - · 30S->40S

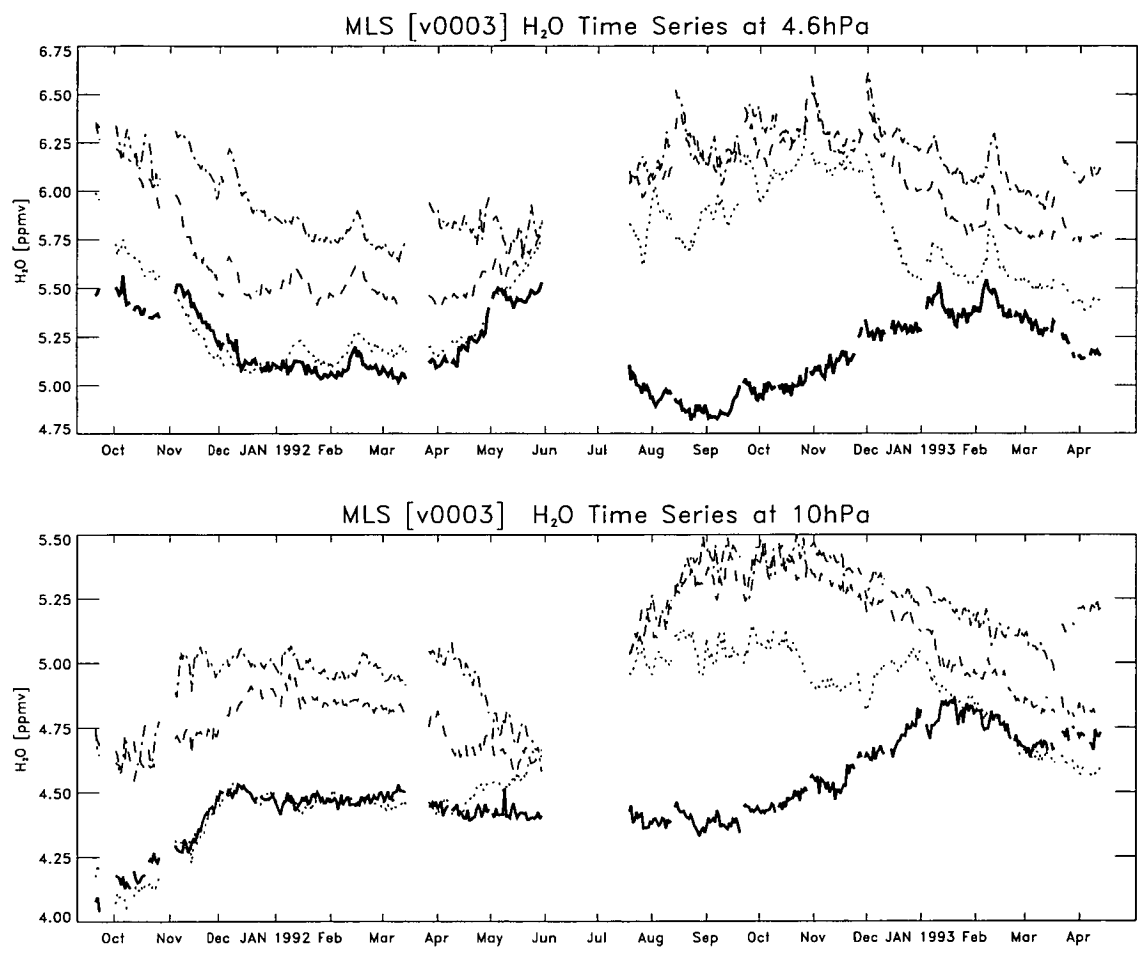


Figure 6.9: Same as above but for southern latitudes

latitudes during this period more closely follows the equatorial cycle. As the main flank of the Brewer-Dobson circulation moves seasonally towards the north a contrasting picture is observed, with, this time, the northern tropical variation more closely following the equatorial cycle. The rise during January and February of 1992 is more dramatic than in 1993 since it occurred during a period of easterly acceleration in the vertical zonal-wind shear, a period when upwards transport in the Brewer-Dobson cell is enhanced.

To summarise, mixing ratios in the lower stratospheric tropics follow a annual cycle slightly modulated by the QBO. Hemispheric differences just outwith these latitudes can be explained in terms of the latitudinal extent of the Brewer-Dobson cell, the seasonal drift of dry air between hemispheres, and upwards advection of the minimum through the stratosphere. The mixing ratios gradients suggest, at least qualitatively, that there is more horizontal mixing from the tropics at 46 hPa than at 22 hPa. The exact height at which horizontal transport becomes less dominant is, from MLS results, higher than the height suggested by Holton et al (1995). Whether this difference is due to the relatively large vertical resolution of MLS measurements in the lower stratosphere, may be answered when a non-linear retrieval for MLS water vapour becomes fully operational. At such a time a better comparison could also be made with SAGE II lower-stratospheric latitudinal variations.

Possible effects from Mount Pinatubo

Figure 6.10 shows latitude-height cross sections of tropical MLS water vapour for four days in October 1991. In each of these plots there exists a well-defined and broad minimum at 46 hPa and also a secondary minimum, at 10 hPa, in the tropics, particularly in the south, which persists well into November. The occurrence of this second minimum is unusual and has not been observed in any other water vapour measurements. Moreover it does not appear to be consistent with the tape recorder theory discussed above.

In the first month that MLS operated there was a change to the scan pattern so that the vertical resolution of lower stratospheric measurements was increased. It might be thought that this would explain the low values at 10 hPa but, as the

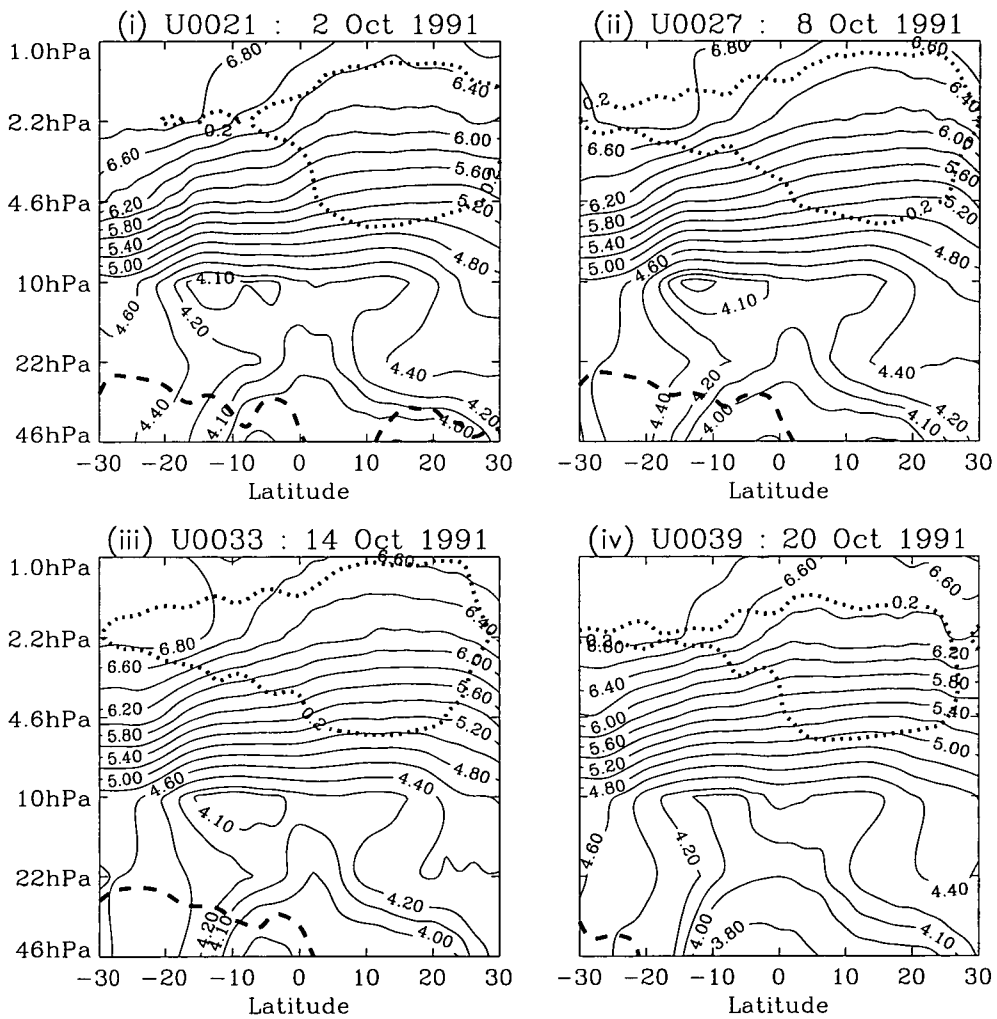


Figure 6.10: Zonal-mean latitude-height cross sections for tropical MLS water vapour for four days in October 1991. Also plotted is the error ratio (ER). Dashed line is $ER=0.5$ and dotted line is $ER = 0.2$

plot below (Figure 6.11) shows, there was no dramatic change in the mixing ratios after the alteration to the scan, which occurred on October 16th 1991.

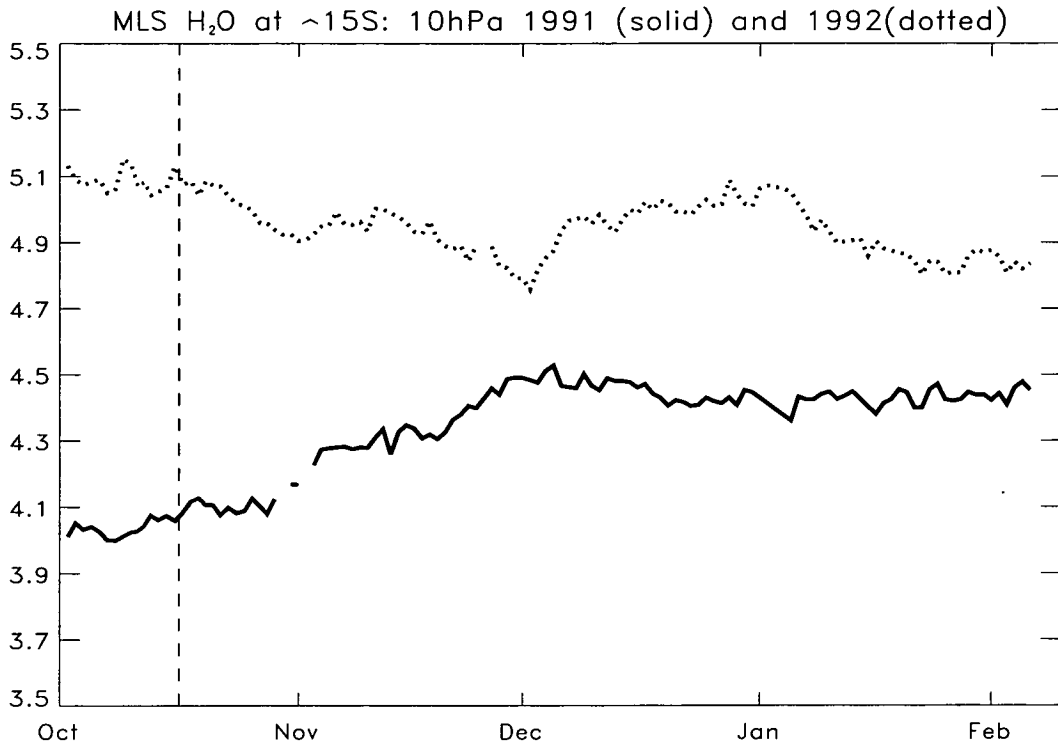


Figure 6.11: Time series of MLS water vapour at 15S and 10hPa. The solid line is for 1991/1992 data and the dotted line is for 1992/93 data. The vertical dashed line marks the day when the scan pattern was changed, October 15th 1991

One possible explanation is that in the months following the eruption of Mount Pinatubo (15°N,120°E) in June 1991 there was a modification to the water vapour distribution. Labitske and McCormick (1992) showed that after the eruption the lower stratosphere was greatly perturbed due to the sudden influx of large amounts of aerosols. This led to temperature increases (compared to 20 year averages) for several months afterwards reaching maxima of between 3.5 and 4 K at 30-50 hPa in the northern tropics in September/October 1991. Similar increases were expected south of the equator. One effect of the temperature increase was to enhance the vertical velocities in the Brewer-Dobson circulation. Thus, it is possible that the

10 hPa minimum in MLS water vapour was due to the uplift of drier air, from below, in this enhanced circulation.

SAGE II measured aerosol extinction ratios before and after the eruption and the subsequent evolution of the volcanic plume was described by Trepte et al (1993). Interestingly, they showed high aerosol extinction ratios in southern tropics, centred near 15S in the latter part of 1991. In October 1991 there is ridge of high values near 32 km and by December this ridge had risen to 40 km. The MLS water vapour values in December 1991 show little sign of this ridge, however the values of water vapour in December 1991 are consistently lower than those in December 1992.

At the time of writing the presence of this secondary minimum in MLS water vapour has still to be fully understood or, indeed, confirmed. Further work should investigate this in more detail. This work should consider examining trace-gas measurements of other instruments as well as further analysis of the MLS results themselves. Also, work in the department is well under way to develop a non-linear retrieval scheme. This will also aid the investigation since it will provide measurements of a finer vertical resolution.

Our attention is now turned to the observed variations at high latitudes beginning with the northern hemisphere.

High-latitudes

The variations at northern high-latitudes are now described. Before this discussion a brief recap on the precision and accuracy of measurements in these regions is given.

At high northern latitudes average precision values are approximately 1.0 ppmv for most of the year at 46 hPa and 22 hPa but often reach ~ 1.5 ppmv during winter periods, when the retrieval quality in these regions degrades. Note that the precision values given here differ from those quoted in Chapter 4. This is because the values quoted in that chapter were issued as a general guide only.

At 10 hPa the precision is ~ 0.7 ppmv. Standard deviations around the mean daily value in each latitudinal band remain fairly constant at ~ 0.3 – 0.4 ppmv at all lower stratospheric levels. However, note that at 4.6 hPa (and 2.2 and 1.0 hPa - see later) the deviations from the daily zonal-means get quite large (not shown) between $\sim 40\text{N}$ – 80N during January/February 1992 and 1993. This is because descent occurred in the highly non-zonal polar vortex during these periods (Lahoz et al., 1993, 1994). Moreover mixing ratios were further perturbed by the presence of the Aleutian high, which regularly extended to middle and extratropical latitudes in winter.

At higher latitudes the variations in mixing ratios are harder to ascertain since data are only available in alternate yaw months. To help clarify the variability, HALOE water vapour data are also utilised. Although HALOE measures less frequently than MLS, in a particular latitude band, measurements were made over a longer period than MLS and thus are included in the discussion.

Figure 6.12 shows the variability of MLS water vapour in northern high latitudes at 46 and 22 hPa. There is an annual cycle in each of the bands with the largest mixing ratios observed around February/March (5.25–5.50 ppmv) and the lowest mixing ratios observed in the summer (4.25–4.50 ppmv). This is consistent with descent in the winter polar vortex (Lahoz et al., 1993, 1994) bringing wetter air from aloft. During spring and summer the differences between mixing ratios at the highest and lowest latitudes (in Figure 6.12) are at their smallest ($< \sim 0.5$ ppmv) since descent is weaker during these times.

HALOE data, in high latitudes, are generally consistent with this picture at

46hPa (Figure 6.13) with maxima of ~ 4.6 - 4.7 ppmv in April of 1992, 1993 and 1994 and minima of ~ 4.5 ppmv in Aug/Sept 1992, 1993 and 1994. However at 22 hPa, agreement is, in general poor. Future work is needed to investigate fully the differences at 22 hPa. However the work is beyond the scope of this thesis.

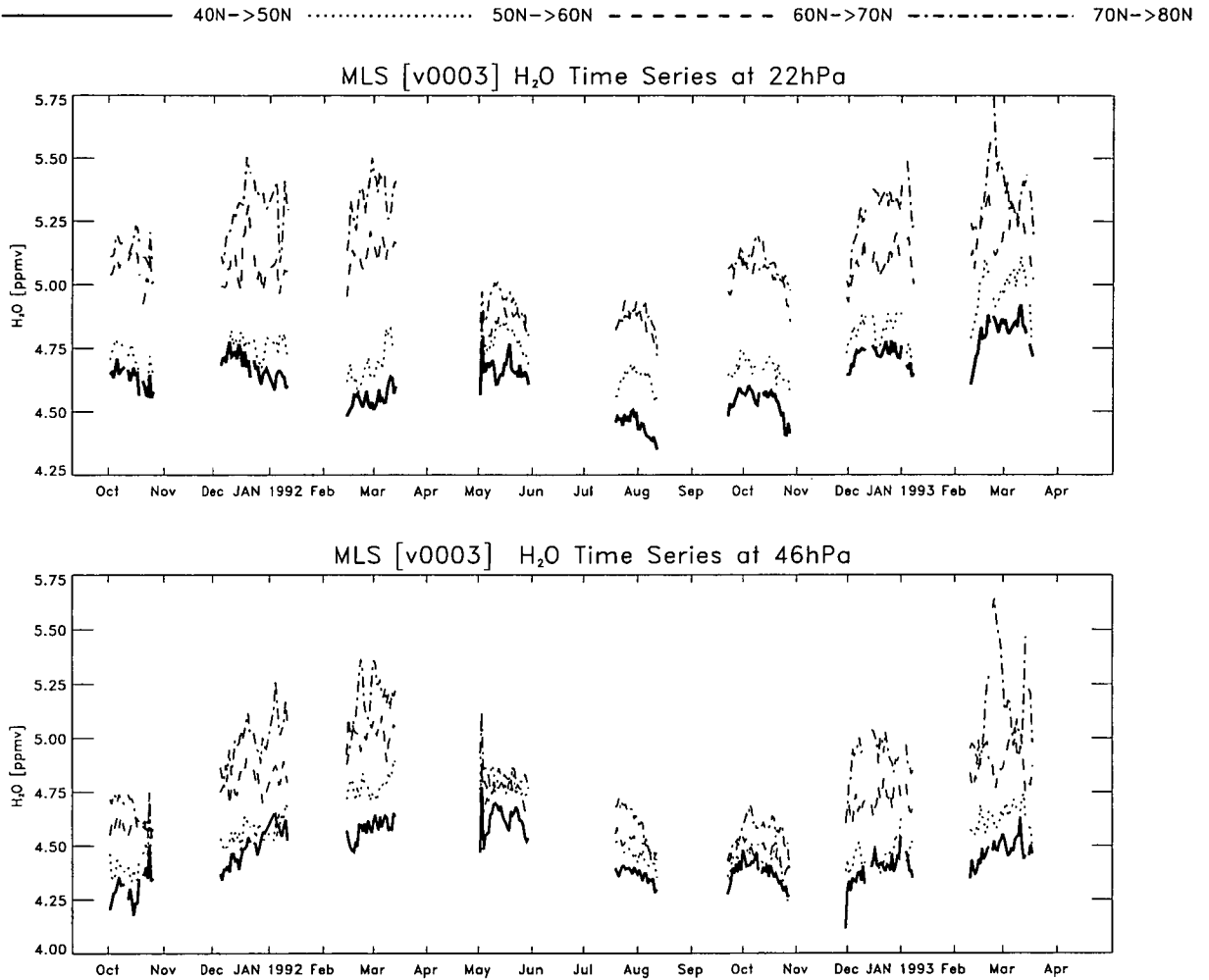


Figure 6.12: Time series of MLS Water Vapour at 46 and 22 hPa in the latitude bands 40N-50N, 50N-60N, 60N-70N and 70N-80N.

The time-series at 46 and 22 hPa show no obvious sign of dehydration but Manney et al. (1994) show that the lowest temperatures in the 1992 arctic winter vortex occurred during a period when MLS was viewing southern high latitudes. These low temperatures were below the PSC threshold value during early 1992 and were accompanied by enhanced levels of vortex ClO and decreased levels of ozone (partially dynamically induced). Santee et al. (1995) compare and describe in

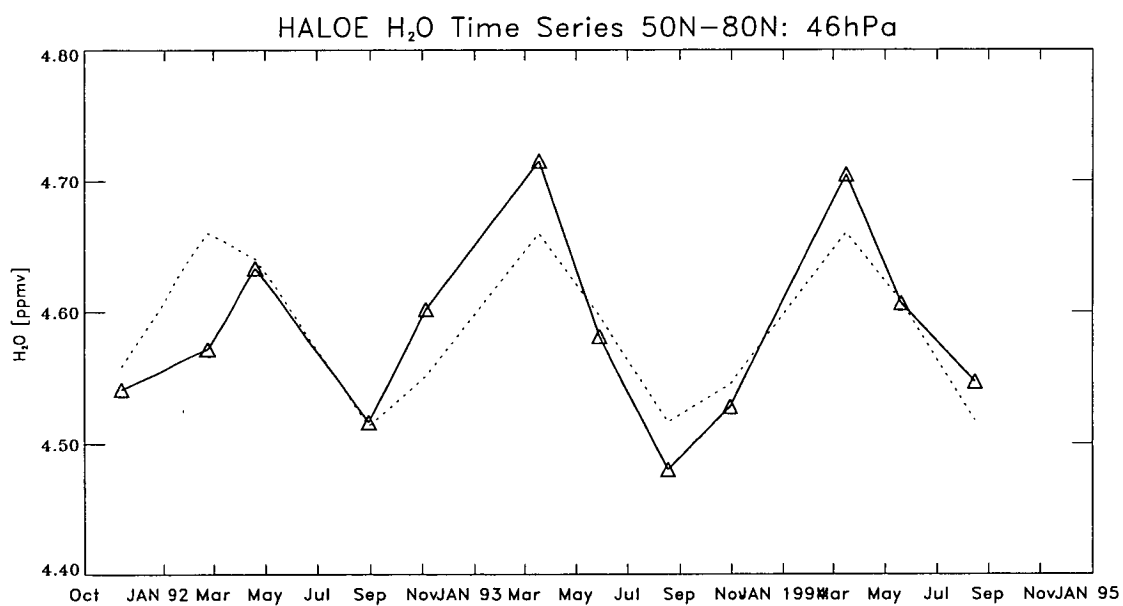
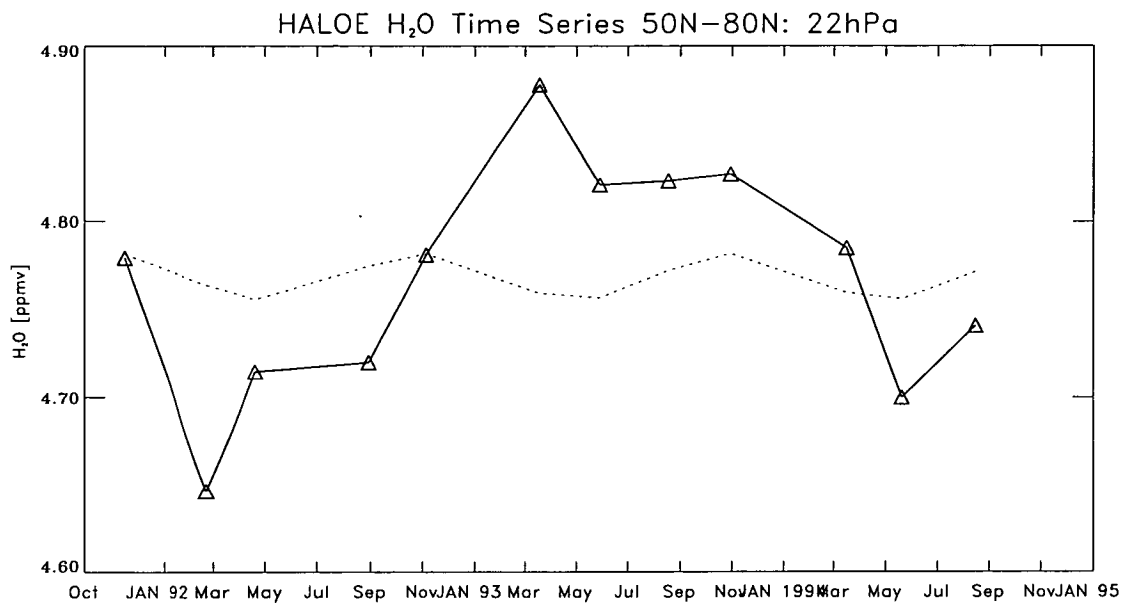


Figure 6.13: Time series of HALOE 75-day mean water at 46 hPa and 22 hPa (middle). Data were averaged over the latitude range 50N-80N every 75 days. The dotted curve represents a simple annual-cycle least-squares-fitted to the HALOE-means

great detail the chemistry and dynamics of the antarctic and arctic winter periods observed by MLS. They point out that, although winter temperatures were low enough for PSC formation and activation of chlorine, they were not sufficiently low and persistent to permanently denitrify the vortex. This is one of the reasons why ozone depletion in the arctic is not as acute as in the antarctic.

At higher altitudes diabatic descent in the vortex increases (Rosenfield et al., 1994, Schoeberl et al., 1992) and clear signs of this are observed in winter at 70N-80N in the time-series at 10 and 4.6 hPa (Figure 6.14) where the peaks are sharper and happen slightly earlier than at 46 and 22 hPa. From October 1991 to mid-December 1991 mixing ratios at 10 hPa increase rapidly (~ 5.75 ppmv to ~ 6.5 ppmv). In 1992 the maxima at 10 hPa occur at a similar time and are slightly lower in value (~ 0.25 ppmv)

The sudden decrease from mid-December to mid-January at 10 hPa has been noted by Lahoz et al. (1994) and is indicative of the descent of H_2O -poor air from the mesosphere. During February and March mixing ratios in each latitude band remain fairly constant at ~ 5.75 ppmv and as spring, and eventually summer, approaches the vortex breaks up and the average mixing ratio in each band slowly decreases; the decrease being due in part to the Brewer-Dobson circulation which during this period transports dry air upwards and northward away from the tropics. Mixing ratios rise sharply once more in December/January 1993, as descent occurs the following winter.

To summarise, the variability of lower-mid stratospheric MLS water vapour in middle and high northern latitudes is annual with the largest mixing ratios observed during winter when large-scale descent brings wet air from the mesosphere. During spring the summer the variations at 4.6 hPa are relatively small but at 10 hPa there is a clear seasonal variation linked with the seasonal variation in the meridional circulation of the lower stratosphere.

We now focus on the corresponding variations in the southern hemisphere.

At middle and high southern latitudes the time-series in the lower stratosphere (Figure 6.15) demonstrate vividly the large-scale dehydration that occurred in August/September 1992 (Ricaud et al., 1995). During this period antarctic ozone levels were observed to decrease (Waters et al., 1993) as enhanced levels of chlorine monoxide were seen and temperatures fell well below the PSC threshold for ~ 4

————— 40N->50N 50N->60N - - - - - 60N->70N - - - - - 70N->80N

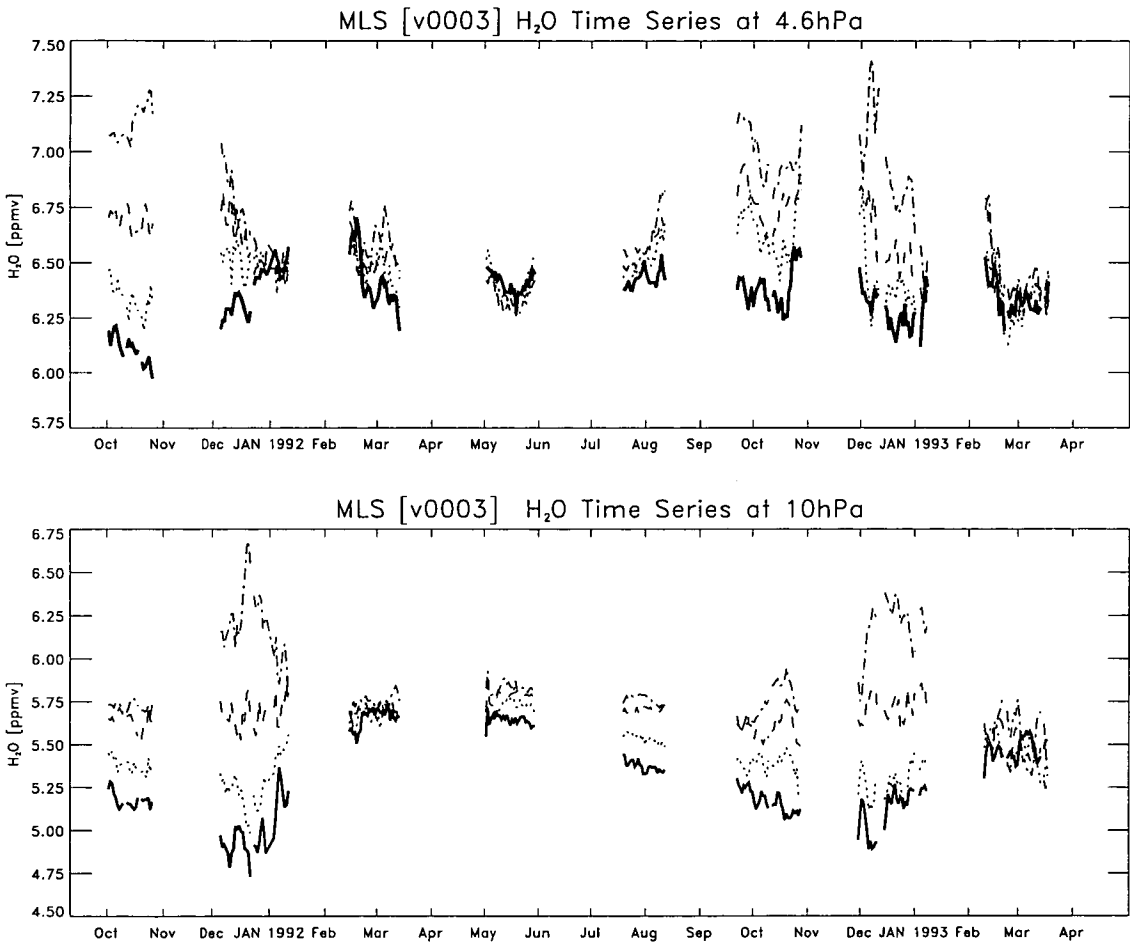


Figure 6.14: Time series of MLS Water Vapour at 10 and 4.6 hPa in the latitude bands 40N-50N, 50N-60N, 60N-70N and 70N-80N.

months.

Ricaud et al. have used MLS data and CLAES aerosol data in a case study of dehydration and ozone depletion in the antarctic vortex for five days in August/September 1992. Their results will be discussed in the next chapter.

The dehydration in Figure 6.15 is clear to see and in fact masks some of the variation present at lower latitudes (Figure 6.16) when plotted at this scale. The mixing ratios at the higher latitudes drop from around 4.5–4.75 ppmv during non-winter periods to around 2.25–2.5 ppmv at their lowest in August/September. The timing and severity of dehydration are consistent with the results of Kelly et al. (1989) who measured minimum antarctic mixing ratios in the lower stratosphere of 1.5 ppmv during August/September 1987.

Once again, it should be borne in mind that MLS does have some trouble in retrieving in regions where the atmosphere is very cold (Lahoz et al., 1996). Precision estimates, at 46 hPa, rise to ~ 1.5 ppmv during these cold periods. Throughout the rest of the measurement record the values remain at 0.8–1.0 ppmv at both 46 and 22 hPa. The standard deviation of the daily means varies little at both heights and is 0.3–0.5 ppmv.

HALOE data, which do not suffer from this cold retrieval problem give a similar picture at 46 hPa (Figure 6.17) with minima during August/September of 1992, 1993 and 1994. The minimum in the southern hemisphere winter of 1993 is particularly low reaching 3.8 ppmv in the band average from 50S–80S. At 22 hPa unlike MLS there is no dehydration present and, in fact, the variability is almost exactly out of phase with that at 46 hPa, indicating descent of older wetter air.

As temperatures rise during September/October (Manney et al., 1993) mixing ratios get larger indicating that the PSC may have evaporated and in the lower stratosphere, polewards of 60S, mixing ratios eventually exceed typical values observed prior to dehydration. This is indicative of moist air descending from aloft. The time series at higher altitudes support this interpretation with the evolution of the polar water vapour distribution at 10 hPa showing large increases (~ 1.25 ppmv) in August/September 1992 (Figure 6.18).

Compared to their northern counterparts, the lower stratospheric mixing ratios in the 40S–50S and 50S–60S bands show less variation, with values of around 4.5 and 4.75 ppmv throughout much of the measuring period, and, unlike HALOE

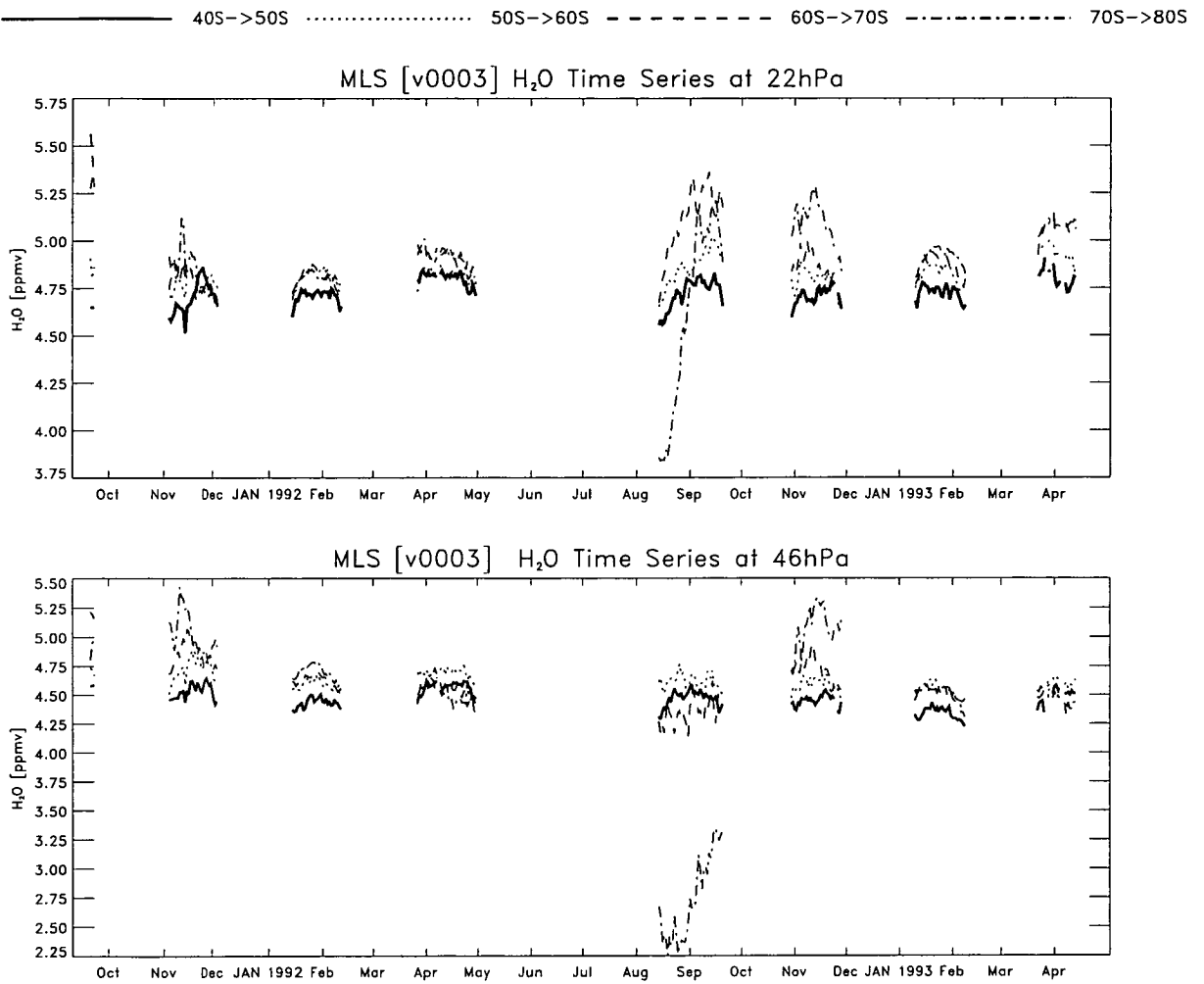


Figure 6.15: Time series of MLS water vapour at 46 and 22 hPa in the latitude bands 40S-50S, 50S-60S, 60S-70S and 70S-80S.

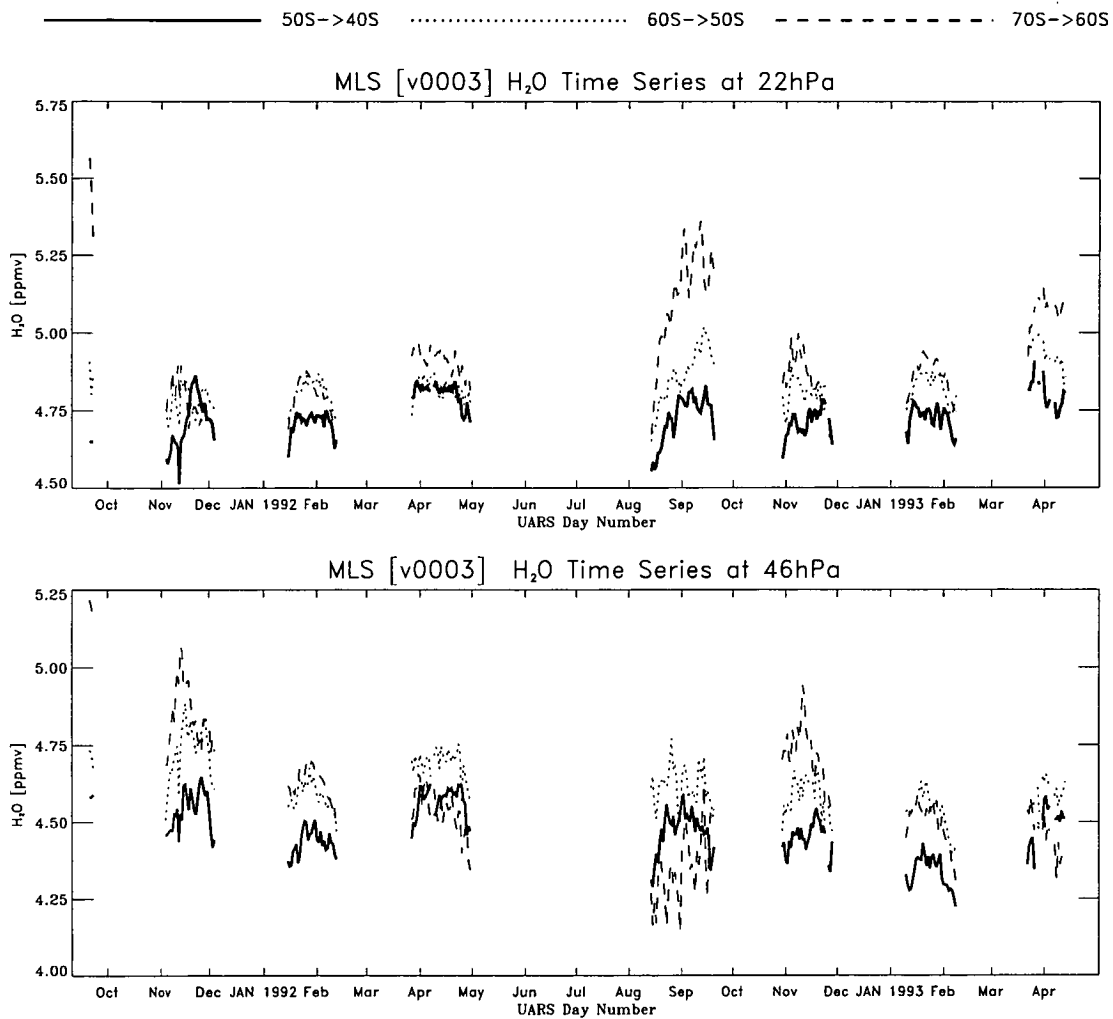


Figure 6.16: Time series of MLS water vapour at 46 and 22 hPa in the latitude bands 40S-50S, 50S-60S, 60S-70S

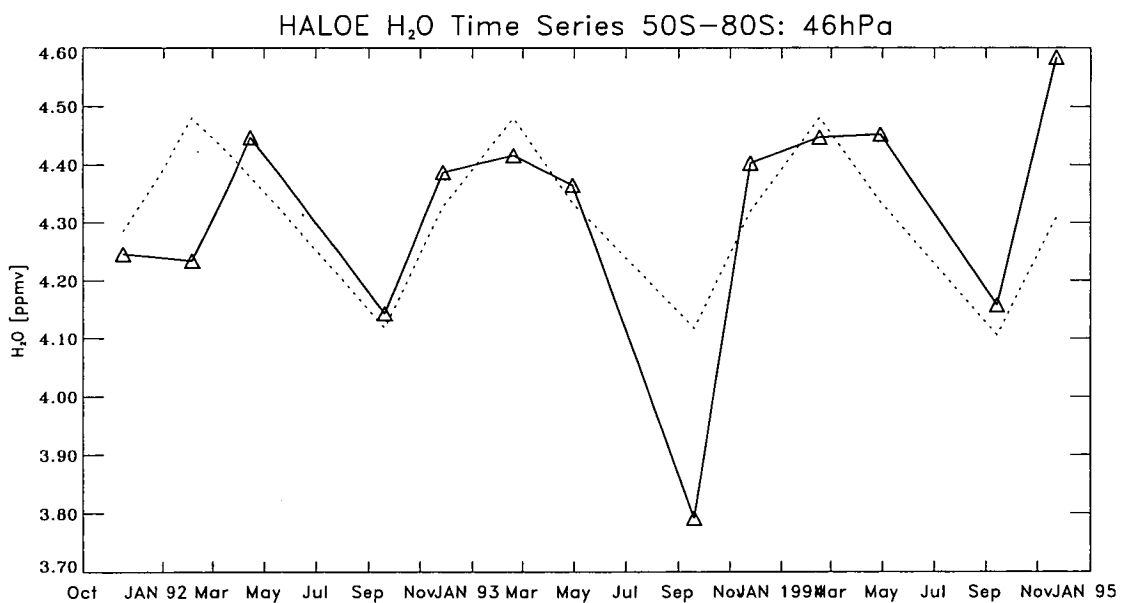
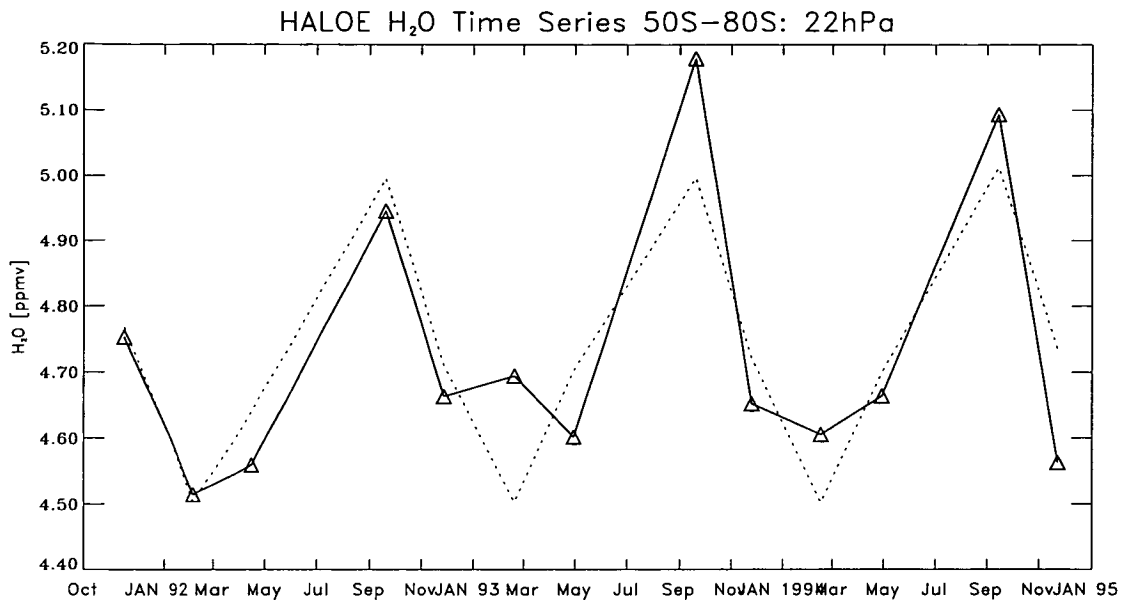


Figure 6.17: Time series of HALOE 75-day mean water at 46 hPa (bottom) and 22 hPa (top). Data were averaged over the latitude range 50S-80S every 75 days. The dotted curve represents a simple annual-cycle least-squares-fitted to the HALOE-means

— 40S->50S 50S->60S - - - - - 60S->70S - · - · - · 70S->80S

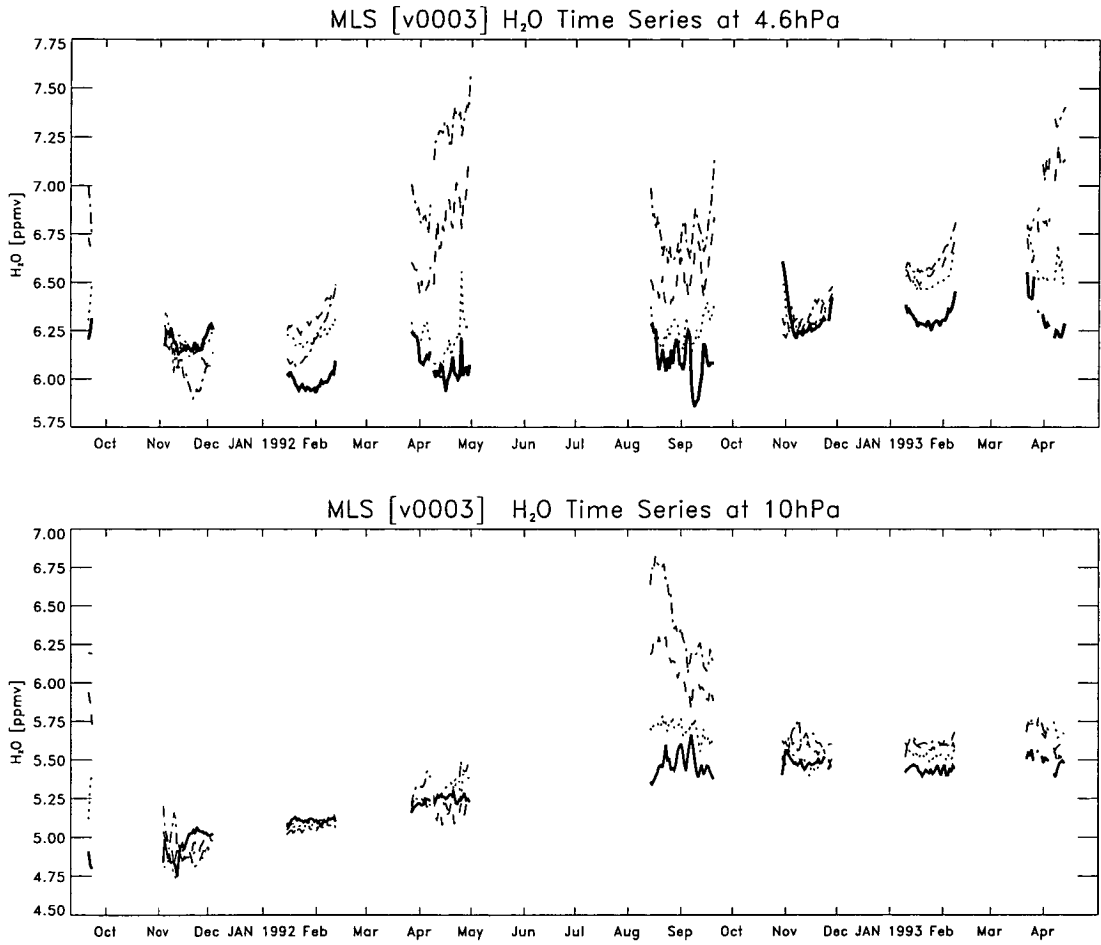


Figure 6.18: Time series of MLS water vapour at 10 and 4.6hPa in the latitude bands 40S-50S, 50S-60S, 60S-70S, 70S-80S

data (Mote, 1995), there is no evidence for any significant transport of dehydrated air to middle latitudes following vortex-break-up; mid-latitude band averages of MLS H₂O show little change during southern hemisphere spring.

6.2.2 Upper stratospheric variations

Low latitudes

As with the QBO, the zonal forcings which cause the semi-annual oscillation (SAO) in the tropical upper stratosphere also produce thermal anomalies and a meridional circulation. This meridional circulation has a clear signal in equatorial MLS water vapour in the upper stratosphere with the largest amplitudes occurring at 2.2 and 1 hPa (Figure 6.19), qualitatively consistent with the SAO in zonal-mean wind and temperature which have been observed to have maximum amplitudes near the stratopause. The variations at each level also correlate well with the corresponding variation in UKMO winds and cause the well-known equinoctial double peak in the zonal mean latitude height cross sections of tracer distributions (Figure 5.1). The MLS temperature and ozone measurements also exhibit this semi-annual oscillatory signal (Ray et al., 1995).

We now look at the variability in more detail.

Figure 6.20 shows time-series of the variations in MLS water vapour averaged over the latitude band 20S-20N at the pressure levels 4.6 hPa, 2.2 hPa and 1.0 hPa (top panel). The variations are given as the percentage differences between the daily average and the 1992 average.

Also shown are time-series of UKMO zonal-mean winds at these same pressure levels and averaged over the same latitude band (bottom panel). Additionally, shown on the same figure (dot-dashed line) is a time series of the vertical wind shear between 4.6 and 1.0 hPa (i.e. zonal-wind at 4.6 hPa minus the zonal wind at 1.0 hPa).

Dry anomalies (or minima) are observed in February/March 1992, August/September 1992 and February/March 1993. The minima in Feb/March 1992 and 1993, at 2.2 and 1.0 hPa, are $\sim 2.5\%$ of the mean deeper than in the summer 1992 dry phases. This is typical of the SAO which is normally stronger during the first cycle of each year. Also, note that the winter 1992 minimum is deeper than the

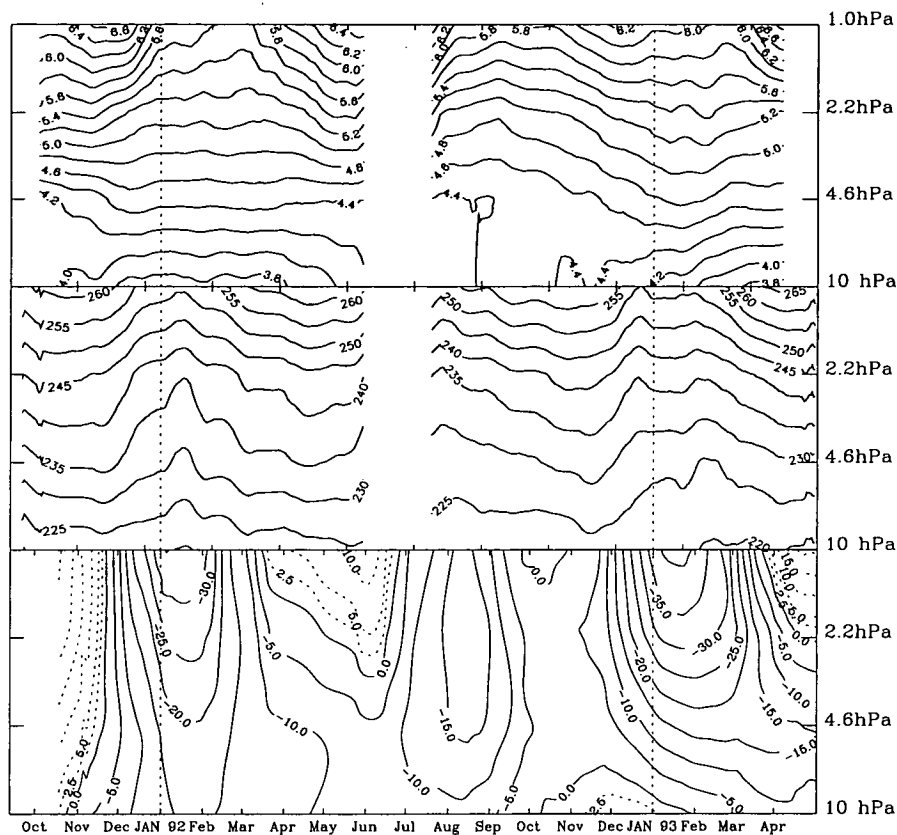


Figure 6.19: Time series of upper stratospheric equatorial MLS water vapour (upper panel); MLS temperature (middle panel); UKMO zonal-mean wind (lower panel)

winter 1993 minimum. This highlights some of the interannual variability in the strength of the SAO. Analysis of the UKMO zonal-mean wind field for this period reveals that the SAO is in a strong easterly phase (the temperature SAO is thus in its cold phase) and hence upwards motion is stronger and brings drier air from below at a faster rate than in 1993. The variation in winds is also consistent with the relatively weak minima in water vapour in August/September 1992, a period when the wind shear throughout the upper stratosphere is negligible.

Wet anomalies (or maxima) occur in December/January 1991/92, May/June 1992 and December 1992/93 with by far the largest amplitude at 2.2 hPa in December 1991 (more than 10% or 0.75 ppmv). Elson et al (1996) originally discovered this and felt that it was an anomalous occurrence and concluded that the amplitude was atypical. However, as Ray et al (1995) point out there is a large degree

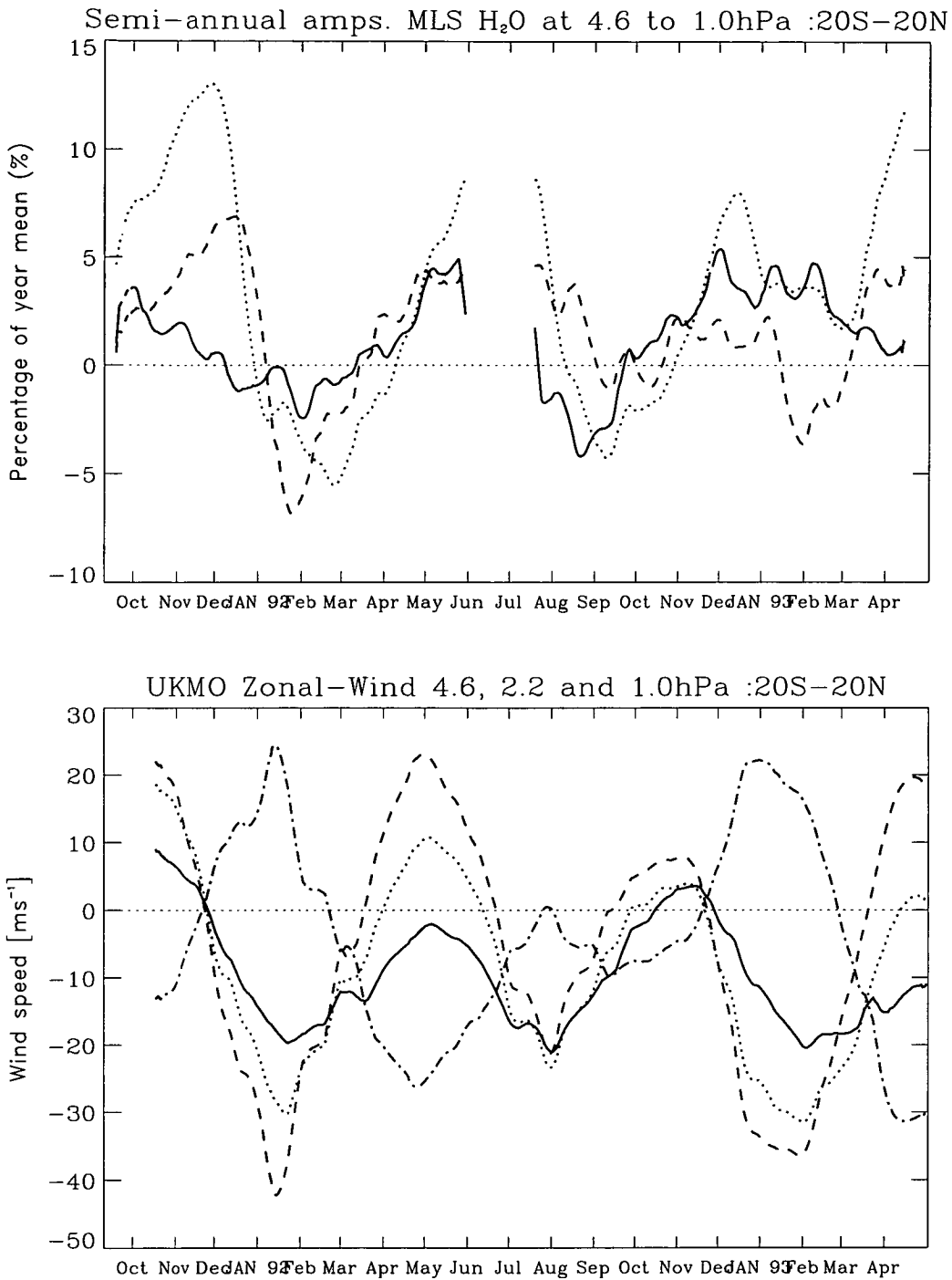


Figure 6.20: Time series of percentage amplitudes of the MLS water vapour variability at 4.6hPa (solid), 2.2hPa (dotted) and 1.0hPa (dashed) over the latitude range 20S-20N (top panel). Also shown (bottom panel) are time series of the UKMO zonal-mean wind averaged over the same latitude range and at the same pressure levels. The “dot-dashed” line is the wind at 4.6 hPa minus the wind at 1.0 hPa (i.e. 4.6 hPa - 1.0 hPa)

of inter-annual variability in the strength of the SAO as well as some feedback from the QBO. As it happens, during late 1991 the SAO was in a strong westerly phase whereas winds in the lower stratosphere were easterly. This created a large perturbation in temperature in the middle and upper stratosphere (Ray et al., 1995) and also allowed the propagation of Kelvin waves to extend higher into the stratosphere; this would tend to strengthen the westerly SAO phase (Dunkerton, 1979) and thus the perturbation in water vapour.

McCormick and Chiou (1994) have recently completed a limited investigation into the SAO amplitudes of SAGE II water vapour in the 0-10N latitude band. A multi-regression curve fitting technique was applied to the data and revealed semi-annual amplitudes of 5.3% and 4.2% at 2.2 hPa and 4.6 hPa respectively. In the MLS results discussed above the average amplitude, in the 20S-20N, band at 4.6 hPa was $\sim 2.2\%$ and at 2.2 hPa it was $\sim 4.9\%$

An analysis of HALOE data also reveals semi-annual signals in the upper stratosphere. Figure 6.21 shows 30-day means in the 20S-20N band, at 4.6 hPa, 2.2 hPa and 1.0 hPa. Superimposed on the figure is a simple least-squares fit curve. The curve represents an attempt to fit a semi-annual cycle to the data. As is clearly observed, the variability of tropical HALOE water vapour is primarily semi-annual in nature in the upper stratosphere but there is also some degree of variability between each year. The minima that MLS observed in Feb/March 1992 and 1993 are observed in HALOE data at approximately the same time and with approximately the same severity.

The average amplitudes at 4.6 hPa, 2.2 hPa and 1.0 hPa are approximately 3.6%, 6.1% and 3.3% respectively; in reasonable agreement with MLS.

There also appears to be an overall increase in mixing ratio from around March 1993 onwards with averages typically at least 0.5 ppmv higher than in 1991 and 1992. I thought that this may have been due to a sampling bias but with few exceptions the average latitude for each 30-day mean shown above oscillates near the equator (Figure 6.22). Analysis of UKMO wind and temperature fields in the period after March 1993 shows nothing unusual or atypical and although the rise may be real more work is needed before this trend can be confirmed (or not).

We now turn to an investigation of how the SAO in upper stratospheric water vapour varies with latitude.

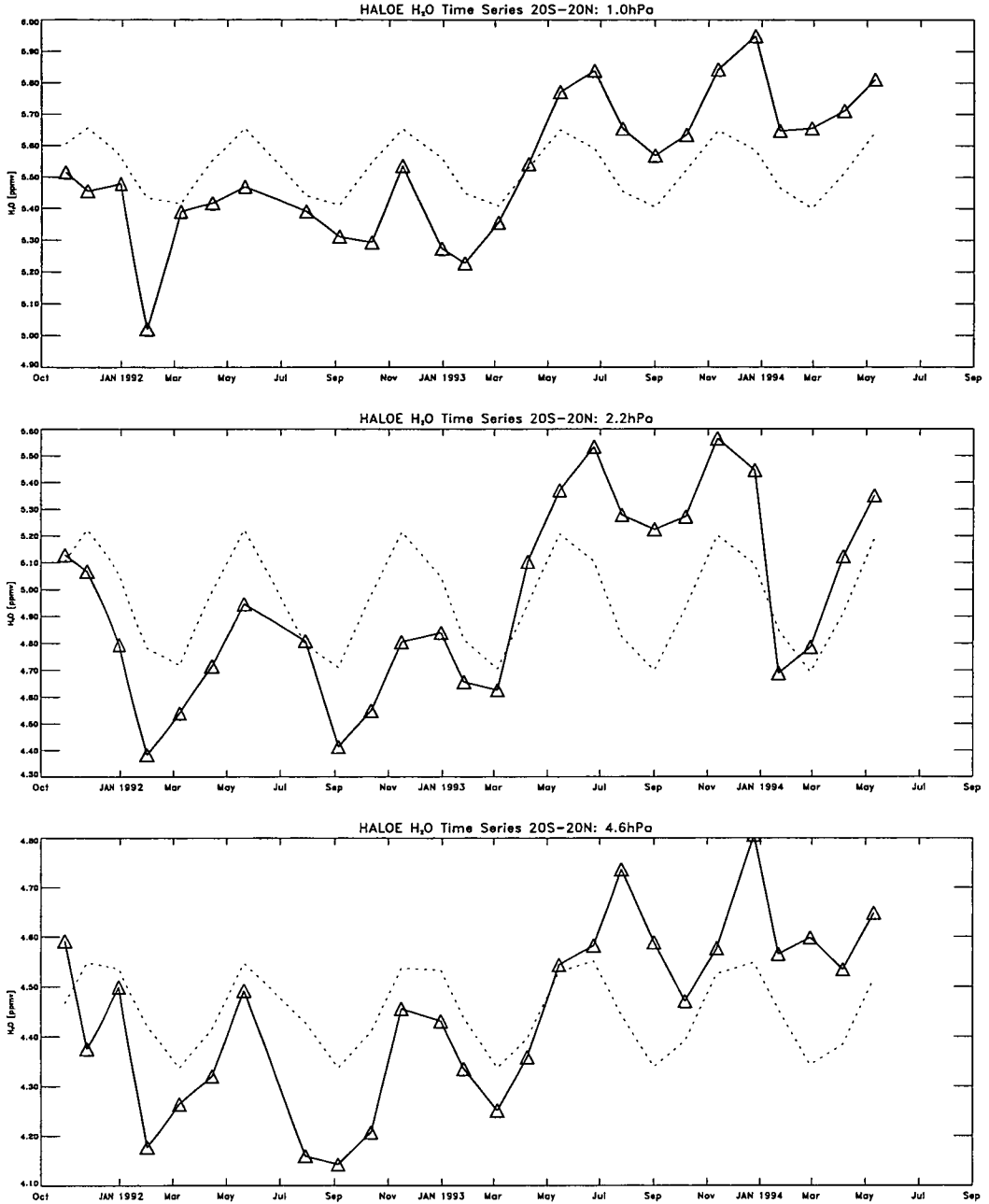
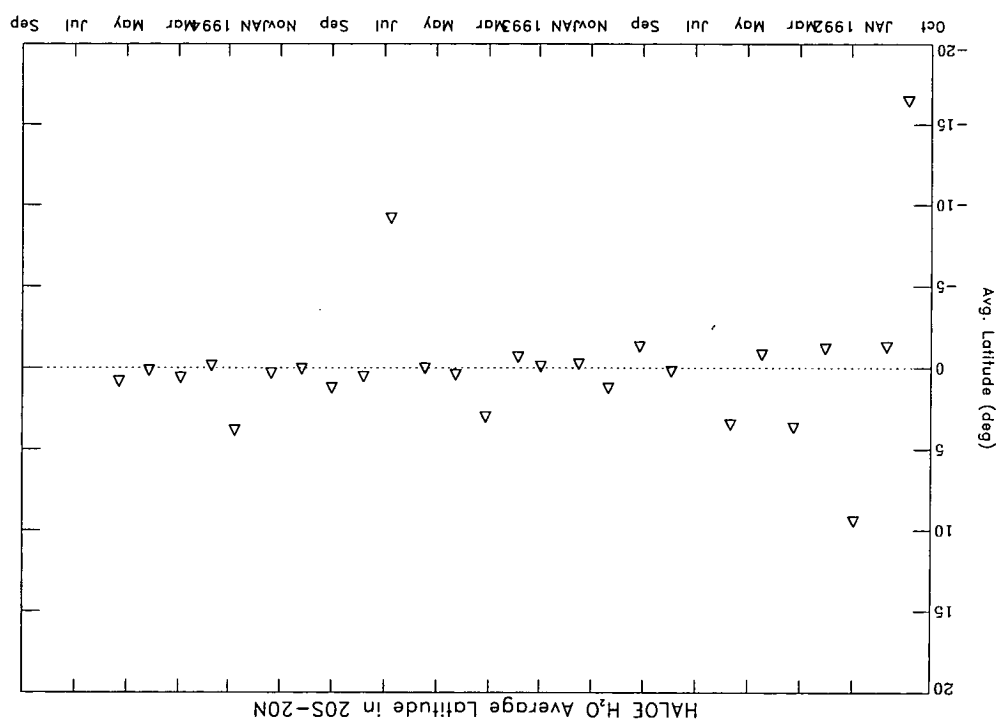


Figure 6.21: Time series of HALOE 30-day mean water at 1.0hPa (top), 2.2hPa (middle) and 4.6hPa (bottom) averaged over the latitude range 20S-20N. The dotted line in each panel is a simple least-squares semi-annual fit through the series of 30-day means

Figure 6.22: Average latitudes at which the 30-day means of HALOE water vapour plotted above (Figure 6.21) were measured



Latitudinal structure of SAO

The SAO in MLS water vapour shows a large degree of seasonal variability in its latitudinal structure (Figure 6.23). The smallest mixing ratios generally occur around the period of the strongest easterlies (Figure 6.24) and thus where the strongest perturbations exist. Maximum mixing ratios correspondingly occur during the strongest westerly SAO phases. Moreover, since maxima in upper stratospheric easterlies and westerlies occur near the solstices and equinoxes respectively (Swinbank and O'Neill, 1994) asymmetries are created about the equator in the upper stratospheric water vapour distribution.

During December 1991 and January 1992 there is a rapid decrease in mixing ratios, throughout the tropics at both 2.2 and 1.0 hPa with values dropping more than 0.5 ppmv, to minima of ~ 5.6 ppmv and ~ 6.2 ppmv respectively in less than a month. Regions of minimum values, at each pressure level, are broader in the southern tropics (i.e. the summer tropics) than in the northern tropics, coinciding with the presence of strong easterlies south of the equator (Figure 6.23). Note also that Ray et al (1995) point out that during each of the easterly phases there were warming events at high northern latitudes. During these phases there was increased vertical motion over the tropics. This is possibly one reason for the rapidity of the decrease in water mixing ratios ratios at 2.2 and 1.0 hPa. At 4.6 hPa there is a less rapid decrease with values decreasing about 0.2 ppmv, the decrease primarily occurring south of the equator.

As the easterlies recede during March and April, so the temporal gradient in water vapour diminishes. For most of the spring and summer of 1992 there is very little vertical wind shear (Figure 6.20) and hence perturbations in the vertical component of the circulation are smaller than usual. Consequently the water vapour distribution during this period is less variable. As the easterlies extend towards the northern tropics during summer, water vapour starts to decrease once more. In this case the minimum mixing ratios (~ 6.2 ppmv at 1 hPa, ~ 5.6 ppmv at 2.2 hPa and ~ 5.0 ppmv at 4.6 hPa) are observed in the northern tropics. In particular, the region of minimum values at 1.0 hPa is relatively small and confined to the latitudes $\sim 15\text{N}$ - 30N .

Interestingly, at the onset of the next easterly phase, in December/January

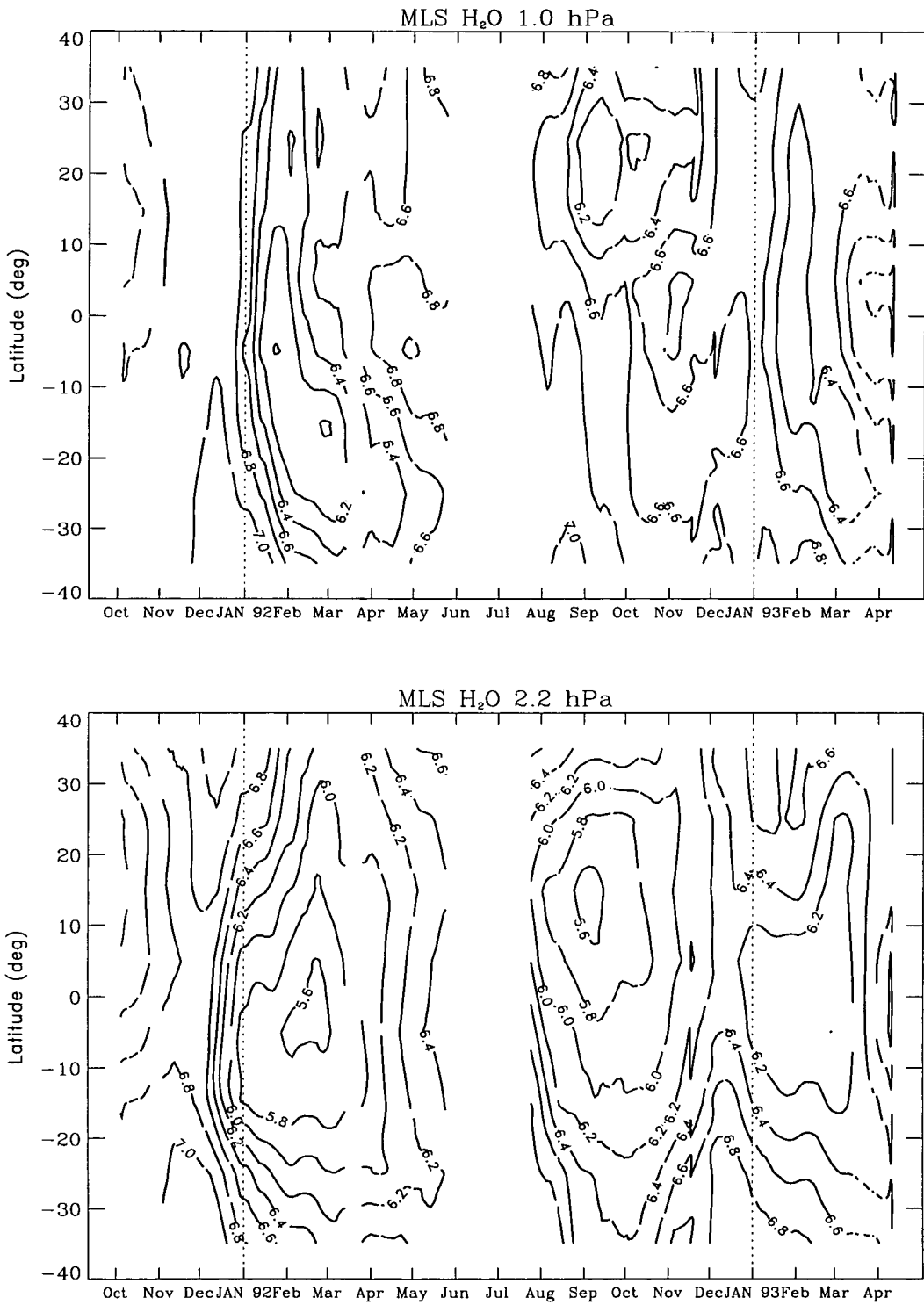


Figure 6.23: Time-latitude series of upper stratospheric tropical MLS water vapour at 4.6 hPa(bottom), 2.2 hPa(middle) and 1.0 hPa(top). Contour intervals are every 0.2 ppmv

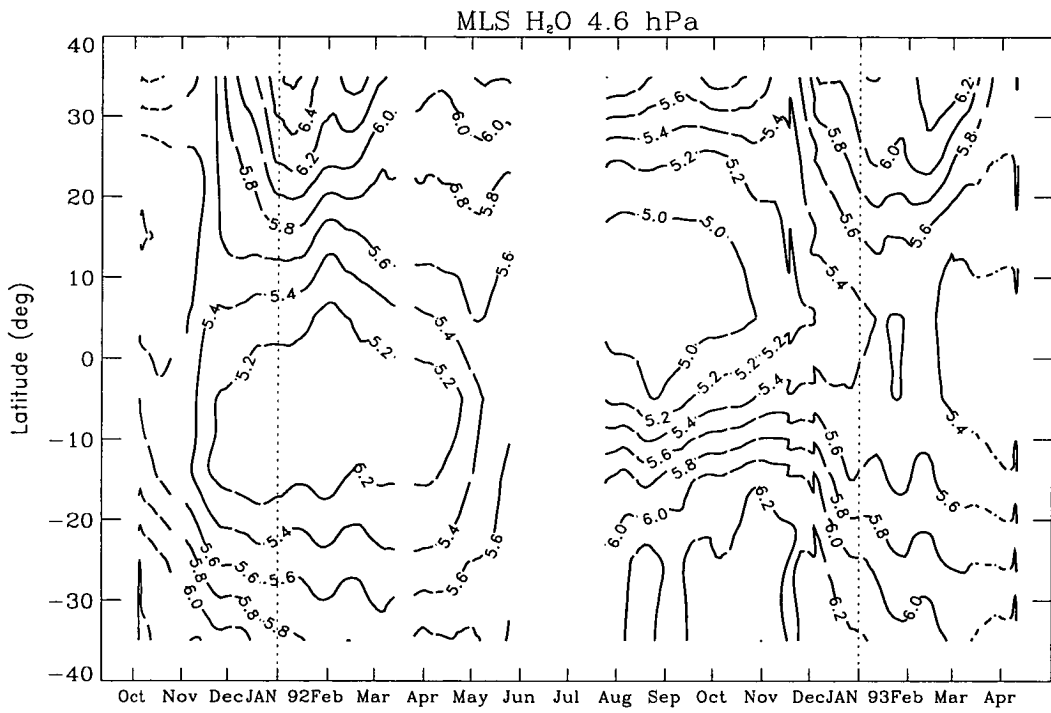


Figure 6.23: Continued

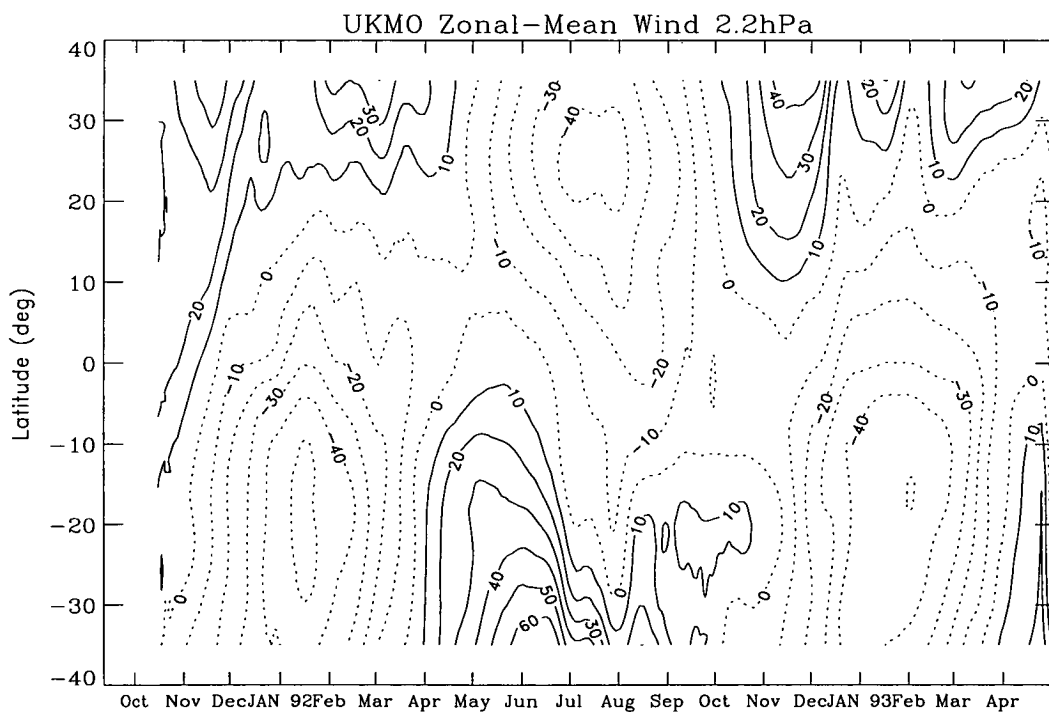
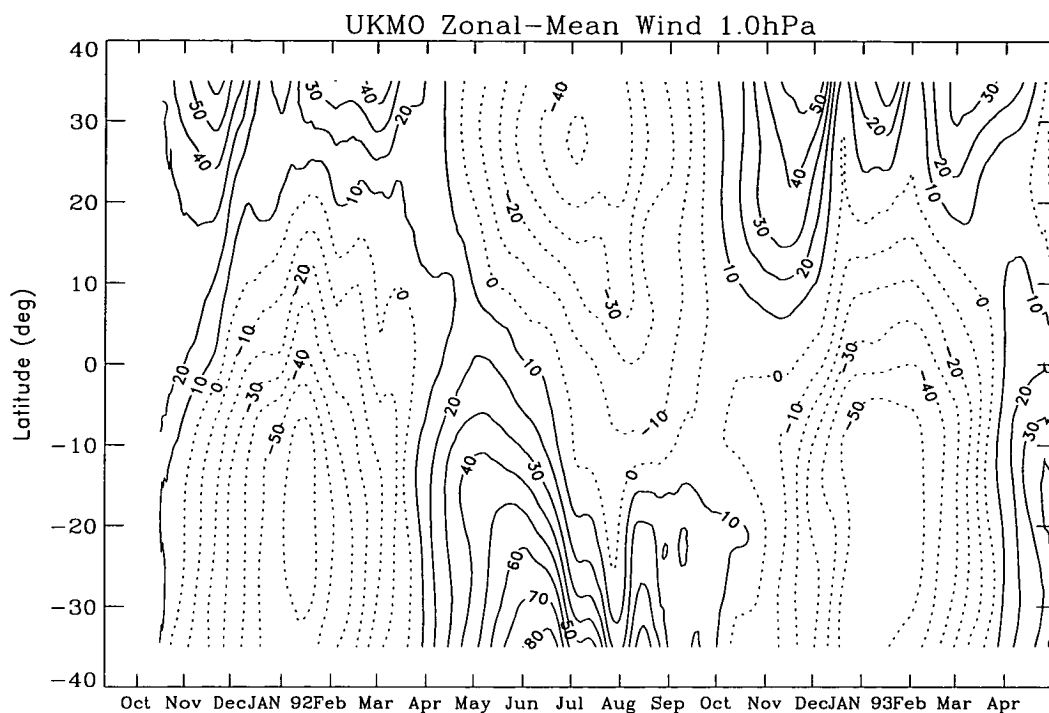


Figure 6.24: Time-latitude series of upper stratospheric tropical UKMO zonal-mean winds at 4.6hPa, 2.2hPa and 1.0hPa. Contour intervals are every 10ms^{-1}

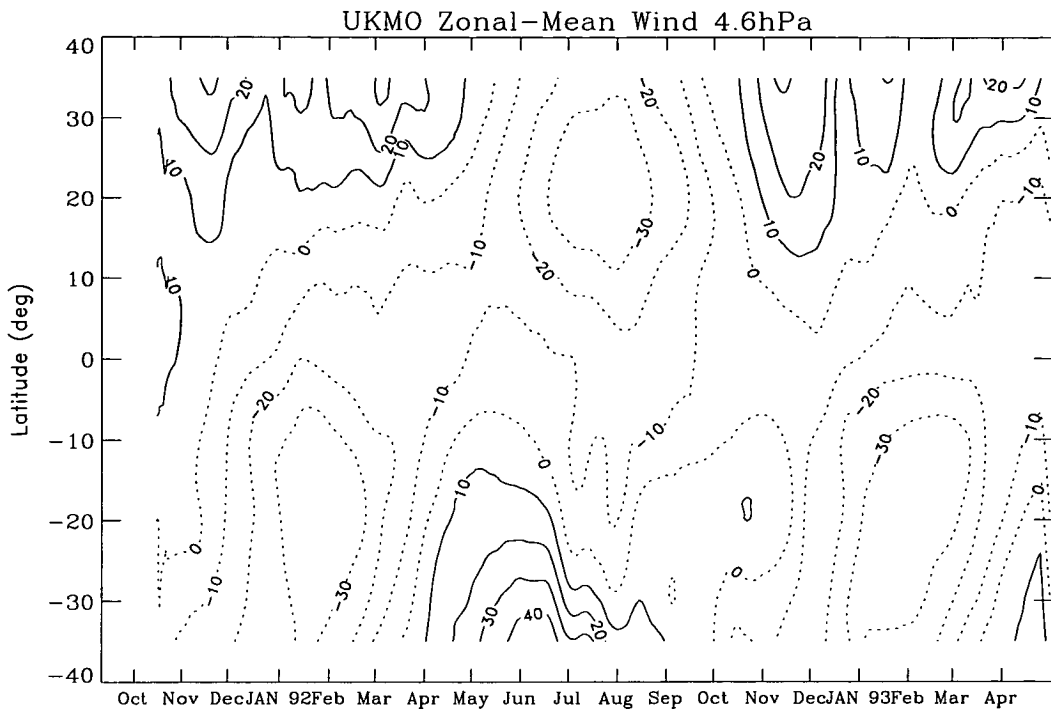


Figure 6.24: Continued

1992/93, the rapid decrease in mixing ratios which was observed during the previous December/January is not present. Note that during December/January 1992/93 the QBO was in its westerly phase (and westerlies increased with height in the lower stratosphere) and hence vertical velocities in the Brewer-Dobson (BD) cell were likely to have been damped. In December/January 1991/92 the QBO was in an easterly phase and hence velocities in the BD cell may have been enhanced. Evidence for the damping/enhancing of vertical velocities may be seen, at least qualitatively, in the zonal-mean latitude-height cross-sections of Chapter 5 (Yaw months 3 and 13). The proposed enhancement to the upwards velocities in the BD-cell may be the reason for the rapid reduction in mixing ratios in the 1991/92 winter, since the vertical component of the tropical circulation, in the middle and upper stratosphere, had a relatively large (compared to during a westerly phase) “upwards” contribution from the QBO.

Outwith tropical regions the variability in upper stratospheric MLS water vapour is more annual. This is now examined in more detail in the section below.

Middle and high latitudes

At latitudes polewards of the tropics the variation is largely annual, primarily through descent during the year and particularly in the vortex each winter. The variation is discussed further below beginning with the northern hemisphere.

In northern high latitudes, at 1.0 hPa, (Figure 6.25) there are maxima (~ 7.5 – 7.75 ppmv) around October 1991 and in late September 1992 where, initially, descent has brought wetter air from aloft. However, towards October in both 1992 and 1993 mixing ratios rapidly decrease as dry air descends from the mesosphere (Lahoz et al., 1993) and eventually reaches this altitude. Minimum mixing ratios are approximately 6.0 ppmv in 1992 and 5.75 ppmv in 1993 and occur in both years around January.

At 2.2 hPa a similar pattern is present but the maxima (~ 7.75 ppmv in 1991/92 winter and ~ 8.25 ppmv in 1992/93 winter) occur slightly later than at 1.0 hPa, consistent with the longer transit time of wetter air descending from aloft. Similarly at 4.6 hPa there is descent of air from above with maxima of ~ 7.25 ppmv occurring in November/December 1991 and 1992.

Variations in upper stratospheric HALOE water vapour (Figure 6.26) are qualitatively consistent with those from MLS. Maxima, at 2.2 and 1.0 hPa, typically occur around September in each year with each annual minimum occurring in March.

The variability at southern high latitudes is similar to that at northern high latitudes but it occurs approximately six months out of phase (Figures 6.27)

At 1.0 hPa there are maxima in the autumn of 1992 and 1993 (~ 8.0 ppmv); maxima, on the whole, increasing in size with latitude. With the onset of the southern winter of 1992 descent from the mesosphere decreases the average mixing ratio in each latitude band and by August/September 1992 mixing ratios are ~ 6.25 – 6.50 ppmv. During the next few months, and as the vortex breaks up, mixing ratios increase as descent continues and as vortex air mixes with wetter air from lower latitudes.

An almost identical picture is observed at 2.2 hPa with maxima of ~ 8.0 ppmv in spring 1992 and a minimum in September/October 1992 of ~ 6.5 ppmv. Similarly at 4.6 hPa, maxima of ~ 7.5 ppmv occur in spring 1992 and 1993 and a minimum

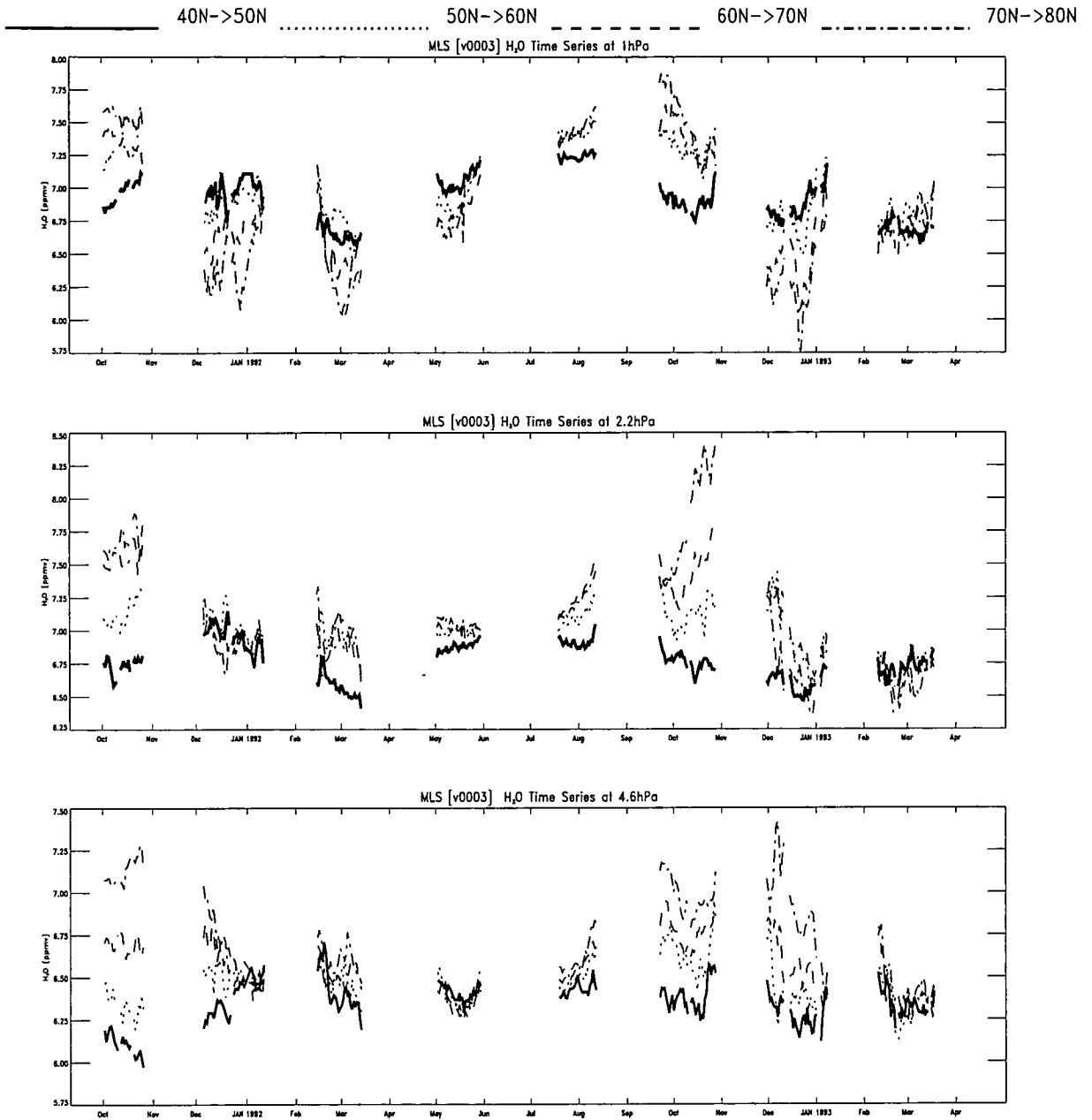


Figure 6.25: Time series of MLS water vapour in the latitude bands, 40N-50N, 50N-60N, 60N-70N and 70N-80N at 4.6, 2.2 and 1.0hPa

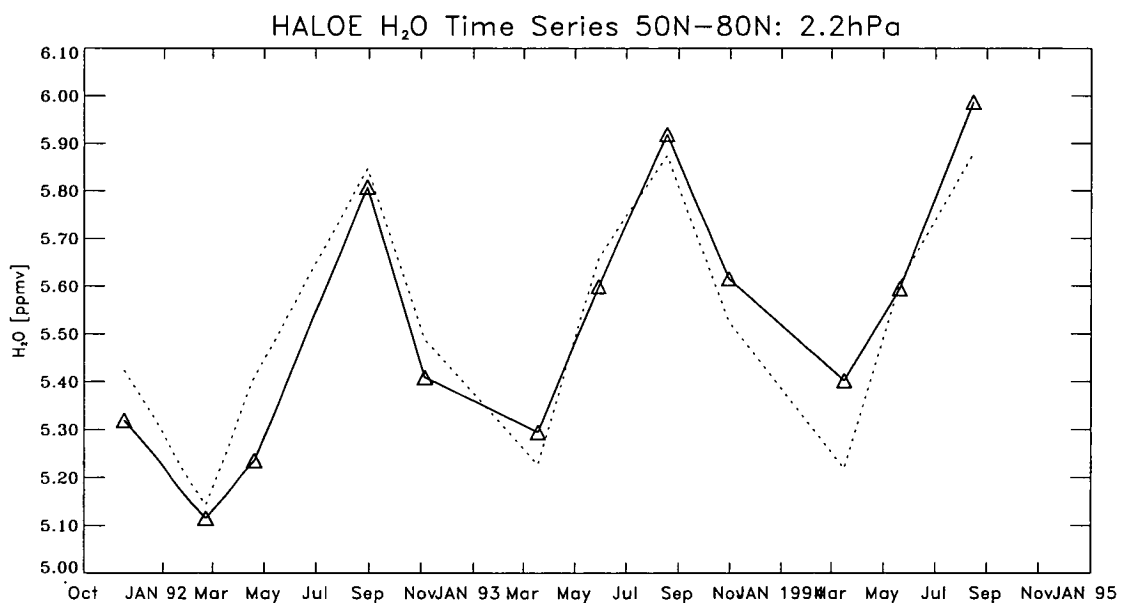
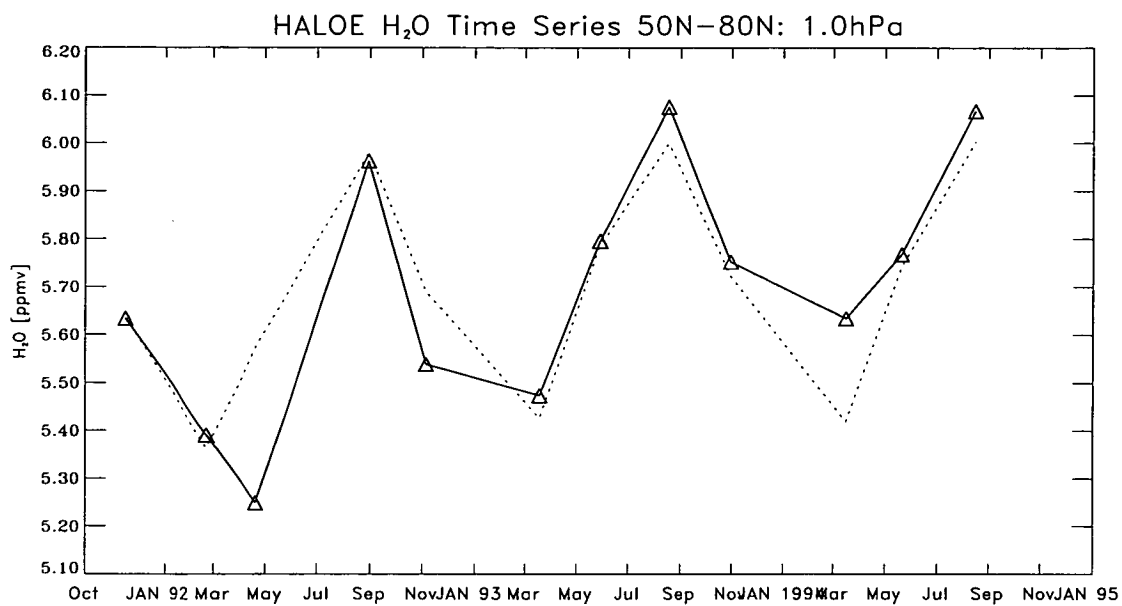


Figure 6.26: Time series of HALOE 75-day mean water at 2.2 hPa (bottom) and 1.0 hPa (top). Data were averaged over the latitude range 50N-80N every 75 days. The dotted curve represents a simple annual-cycle least-squares-fitted to the HALOE-means

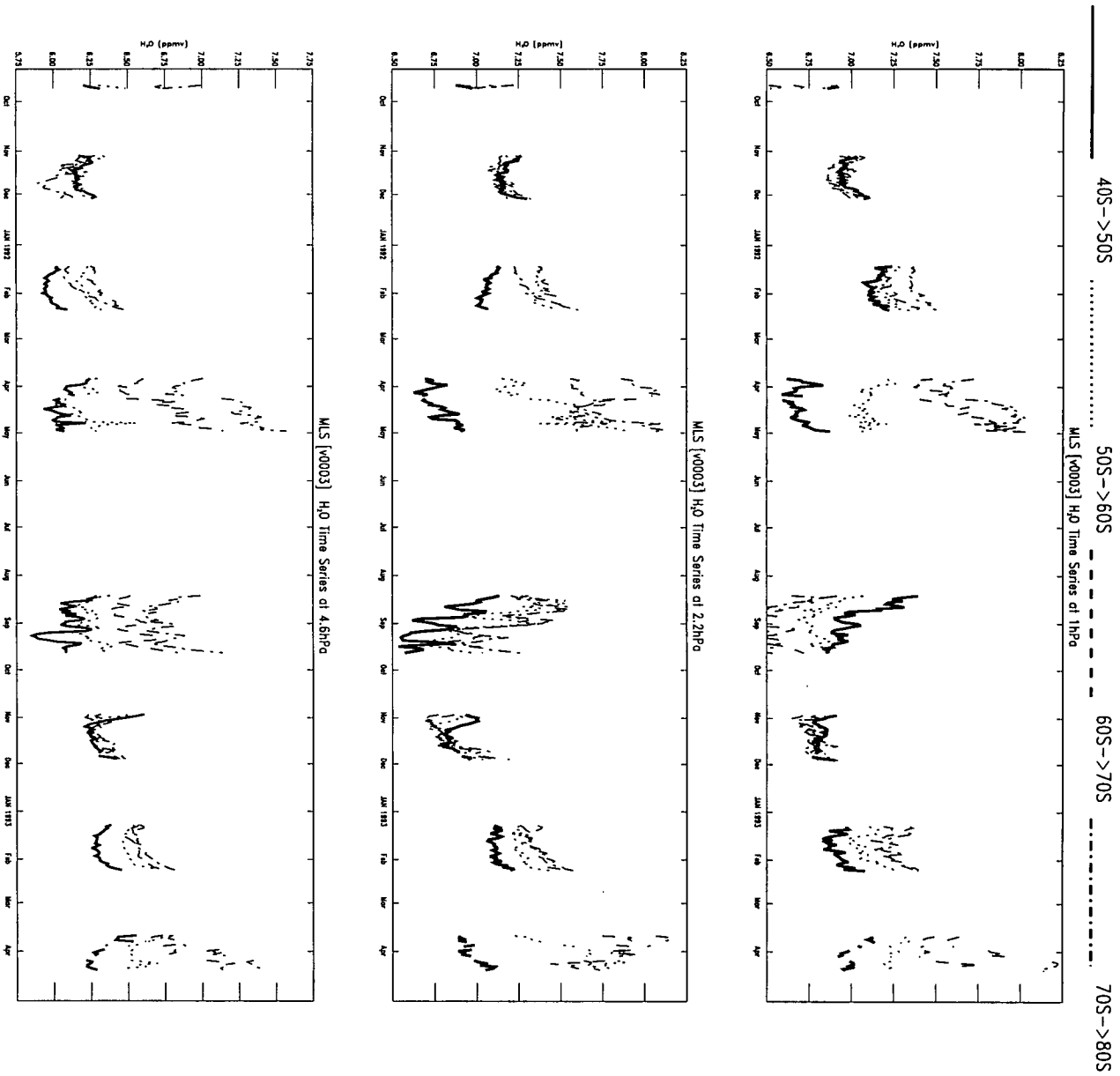


Figure 6.27: Time series of MLS water vapour in the latitude bands, 40S-50S, 50S-60S, 60S-70S and 70S-80S at 4.6, 2.2 and 1.0hPa

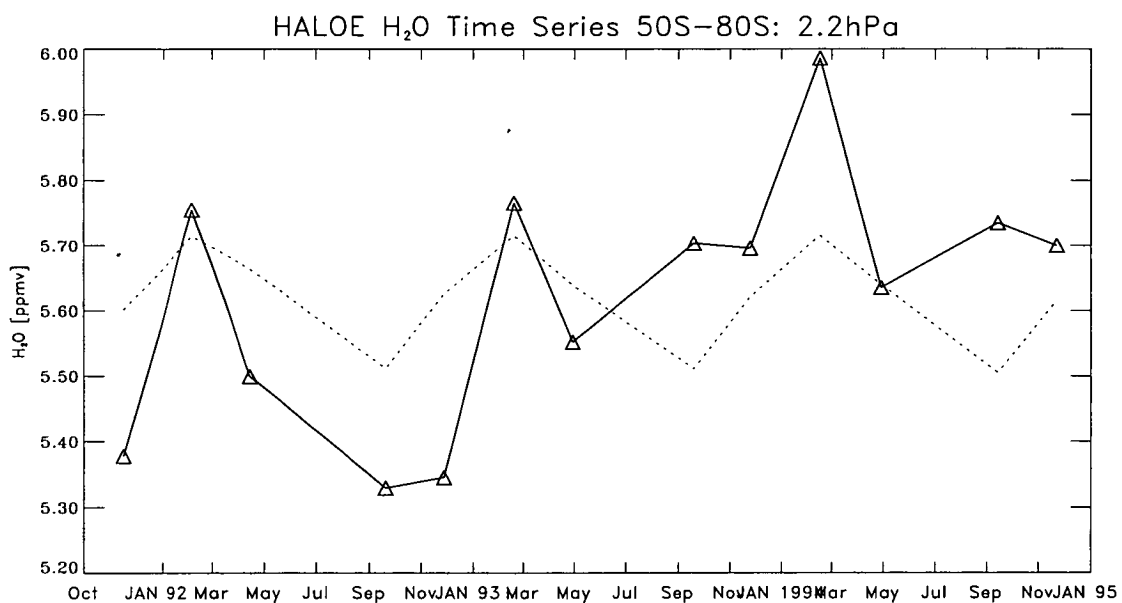
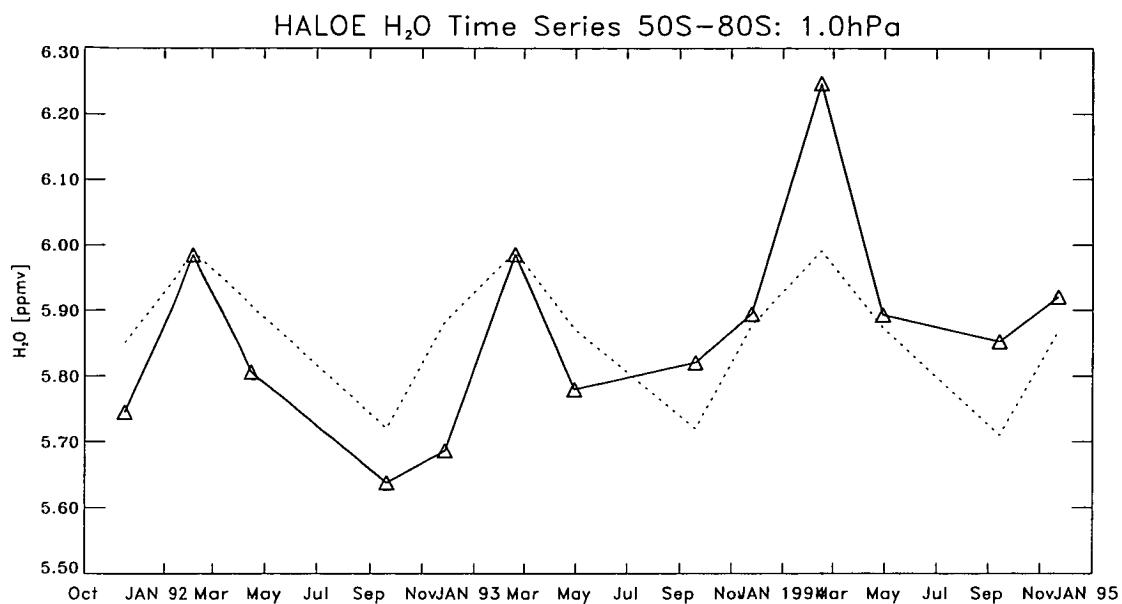


Figure 6.28: Time series of HALOE 75-day mean water at 2.2 hPa (bottom) and 1.0 hPa (top). Data were averaged over the latitude range 50S-80S every 75 days. The dotted curve represents a simple annual-cycle least-squares-fitted to the HALOE-means

occurs of ~ 6.0 ppmv occurs in September/October 1992.

Variations in HALOE data are similar (Figure 6.28) with maxima and minima in March and October respectively.

6.3 Summary

Lower stratosphere

Variability in the lower stratospheric tropics and sub-tropics is primarily annual with some modulation by the QBO, which acts to delay or accelerate air parcels according to its phase. At latitudes poleward, and at 46 hPa, there is some sign of transport, from the tropics, of the annual signal. At 22 hPa this is less clear.

There is also some degree of variability and hemispheric difference that can be related to seasonal variations in the Brewer-Dobson circulation. Ascent, implied by the upwards-bowing of the contours in the zonal-mean latitude-height distributions, is observed to be more acute in the summer hemisphere than in the winter hemisphere.

The variation at high latitudes in the northern hemisphere shows a clear annual cycle, mainly because of strong descent of wetter air in winter periods. At southern high latitudes, particularly at 46 hPa, the largest amplitudes of the variability are as a result of the severe dehydration which occurred during the winter of 1992.

Upper stratosphere

At tropical latitudes, MLS water vapour variability shows very distinct semi-annual oscillations (SAO) with the strongest amplitudes at 2.2 hPa and 1 hPa. The oscillations are qualitatively consistent with variations in UKMO equatorial zonal-mean wind fields and with tropical mixing ratios of upper stratospheric HALOE data.

There is also a large degree of seasonal variability in the latitudinal structure of the SAO. The smallest mixing ratios are observed around the period of the strongest easterlies and thus where the strongest perturbations exist. Maximum mixing ratios correspondingly occur during the strongest westerly SAO phases. Moreover, since maxima in upper stratospheric easterlies and westerlies occur near

the solstices and equinoxes respectively (Swinbank and O'Neill, 1994) asymmetries are created about the equator in the upper stratospheric water vapour distribution.

Furthermore, qualitative evidence exists for QBO-modulation of the SAO perturbations in MLS mixing ratios. During times when the QBO and SAO are in their easterly phases, the upper stratospheric mixing ratios in the tropics rapidly decrease, presumably because of the rapid ascent of drier air from below. During the westerly phase of the QBO the decrease in mixing ratios is much less acute.

At higher latitudes the variations mainly follow an annual regime with winter descent having a large impact on the observed variations. The implied descent in the northern hemisphere was greater than in the south, consistent with previous studies of the vortex descent rates (e.g. Rosenfield et al., 1994). Variations in upper stratospheric HALOE water vapour were similar.

In the next chapter, we look at a case study during August/September 1992 where, as shown earlier, there was severe dehydration (and ozone depletion) in the lower stratosphere at high southern latitudes.

Chapter 7

Arctic and Antarctic dehydration case studies

7.1 Introduction

In this chapter two case studies are examined. Each of the studies will cover a period when polar stratospheric temperatures were low enough for condensation of water vapour to be expected and hence for the existence of polar stratospheric clouds (PSC). Using MLS water vapour, and a variety of data from other sources, this expectation is now investigated.

The first period discussed is from the southern winter of 1992 and will concentrate specifically on measurements in the five days between August 30 and September 3 1992. These measurements have been reported by Ricaud, myself and others in *Ricaud et al.*, 1995, and are briefly reiterated, in more detail, making use of better graphics which help reinforce the arguments published previously.

The second period discussed is from the northern winter of 1992/93. The focus of the discussion will concern measurements made during the five days between February 10 and February 14 1993. MLS measurements, in the arctic, although not specifically in this five day period, have been discussed by Manney et al. (1994), Santee et al (1995) and others. These papers concentrated, in the main, on the chemical evolution of MLS species throughout northern winter. The main aim of the present study is to show that the dynamical situation in the troposphere had a strong bearing on the variability of the MLS measurements during the five-day-period.

Before the main discussion a brief introduction to PSC's, the role that water

vapour plays in their formation and their importance in ozone chemistry, is given.

7.2 Polar Stratospheric Clouds

Water vapour plays an important role in the depletion of ozone in the polar stratosphere since under extreme temperatures it can condense to ice and may combine with other chemical compounds to form clouds of crystals. Depending on the exact temperature, the time those temperatures persist and the concentration of other chemical species (e.g. nitric acid) present, these clouds, known as polar stratospheric clouds (PSC) can be categorised into various types.

7.2.1 Type I

The most common kind of PSC are type I clouds (Toon et al., 1986) which are thought to be primarily composed of nitric acid trihydrate (NAT) or perhaps, as more recent work has shown, nitric acid dihydrate (NAD) crystals (Toon et al., 1995).

They form at temperatures below $\sim 195\text{K}$ and make up a large majority of cloud sightings (McCormick et al., 1982). Toon et al. (1990) sub-divided type I PSC into two classes. One of these corresponds to a “condensation stage” where small spherical droplets are formed (type 1a), the other corresponds to a final “frozen stage”, where larger, and less regular particles are formed. However there still remains some uncertainty as to the mechanism (or mechanisms) by which they actually form (e.g. MacKenzie et al. (1995))

7.2.2 Type II

Type II PSC are composed of water/ice crystals (Poole and McCormick, 1988) and are rarer than type I since they form at temperatures of less than $\sim 188\text{K}$. Temperatures this low occur less frequently than those that allow the formation of type I PSC. The actual temperature at which PSC form is dependent on a number of factors including the water concentration, the nitric acid concentration, and the availability of condensation nuclei. This is why the literature sometimes quotes a small range of temperatures for the threshold of type II-PSC. However, a temperature of 188 K is commonly used as the threshold in the lower stratosphere.

7.2.3 Type III

The third type of PSC, type III (Cariolle et al., 1989), are really just a subset of type II and are formed over orographic features such as mountains. They are extremely transient in comparison to either type I or type II and are created on a much shorter time scale.

7.2.4 Importance in ozone destruction

PSC are important in the catalytic destruction of ozone since they provide a suitable platform for the series of complex heterogeneous reactions that result in a chemical loss of ozone. Without their existence some reactions could not occur and others would be very slow. In fact, failure to include the effects of PSC was one of the main reasons why many early computer models severely underestimated polar ozone loss.

The bulk of the literature regarding PSC's and their implication in the depletion of ozone has focussed on their occurrence in the antarctic, since heterogeneous ozone depletion was first noticed there (Farman et al., 1985) and also, at present, is more acute than in the arctic. This is primarily because the antarctic vortex is stronger and generally is colder than the arctic vortex. Moreover antarctic temperatures tend to remain below the thresholds for type I and type II PSC for a much longer period (Schoeberl et al., 1992). For example, during the southern hemisphere winter of 1992 temperatures remained below $\sim 190\text{K}$ for nearly four months while during the northern hemisphere winter of 1991/92 temperatures only occasionally dropped below this threshold (Waters et al., 1993). The main reason for the difference in temperatures between hemispheres is that the northern hemisphere has greater orography and is thus subject to greater planetary wave activity (e.g. Schoeberl and Hartman, 1991) which may cause sudden and dramatic warmings throughout the winter period. Note also, chemical destruction in the arctic vortex can be more difficult to detect than in the antarctic since there is greater dynamical variability which may lead to catalytical depletion being masked by advection. Such problems do occur in the southern vortex too (Waters et al., 1993) but are less prevalent.

The differences in arctic and antarctic winter temperatures are also believed

to be the main reason for the differences that occur in the extent of denitrification in the polar stratospheres (Fahey et al., 1990). Although “denoxification” (conversion of NO_x to HNO_3) occurs in both hemispheres, the time that temperatures remain below PSC thresholds means that denitrification (permanent removal of total nitrogen, NO_y , by sedimentation) is significantly stronger in the southern winter vortex, and so, when sunlight increases, there is little conversion of HNO_3 to active nitrogen leading to a longer period of chemical ozone loss.

In the northern vortex, the shorter period that air has been exposed to low temperatures means that, when sunlight increases in late winter, evaporation of PSC’s occur before sedimentation can remove total nitrogen. Thus, HNO_3 is released and is photolysed to NO_2 which removes active chlorine by conversion to chlorine nitrate. This limits the ozone loss in the northern hemisphere.

We now turn to a discussion of the southern polar winter of 1992, concentrating on the five day period August 30 to September 3. During this period MLS water vapour measurements showed the atmosphere to be severely dehydrated. Correspondingly, enhanced levels of chlorine monoxide and depleted ozone concentrations were observed.

7.3 Case Study I: August 30 to September 3

The southern winter of 1992 (~ May to September) has been studied, from a different point of view, at great length (e.g. Manney et al., 1993, Waters et al., 1993b, Roche et al, 1993b,), not least because it was the first complete southern winter that UARS measured in great detail. For large periods of this winter lower stratospheric temperatures were low enough for PSC to be expected. One such period was August 30 to September 3. Measurements during this episode are now examined and the existence of PSC investigated.

7.3.1 Introduction

In this section, the main part of the discussion will look at UARS and UKMO measurements in the five day period from August 30 to September 3 1992. During this period the water vapour and temperature fields from MLS indicated that PSC could have formed in the southern polar vortex. This was further supported by

ozone and chlorine monoxide observations whose concentrations suggested that heterogeneous processing had occurred.

Using MLS observations, aerosol data from the CLAES instrument (Mergenthaler et al., 1993) and UKMO geopotential heights and temperature, the presence of polar stratospheric clouds is examined.

Figure 7.1 shows a time series, from April to October 1992, of the average ten lowest southern polar temperatures from MLS (solid line) at 46 hPa. Also shown is a similar series for UKMO temperatures (dashed line). Note that the MLS temperatures are not retrieved at 46 hPa and so the values shown are, in fact, *a priori* data which, in this case, are from the National Meteorological Center (NMC).

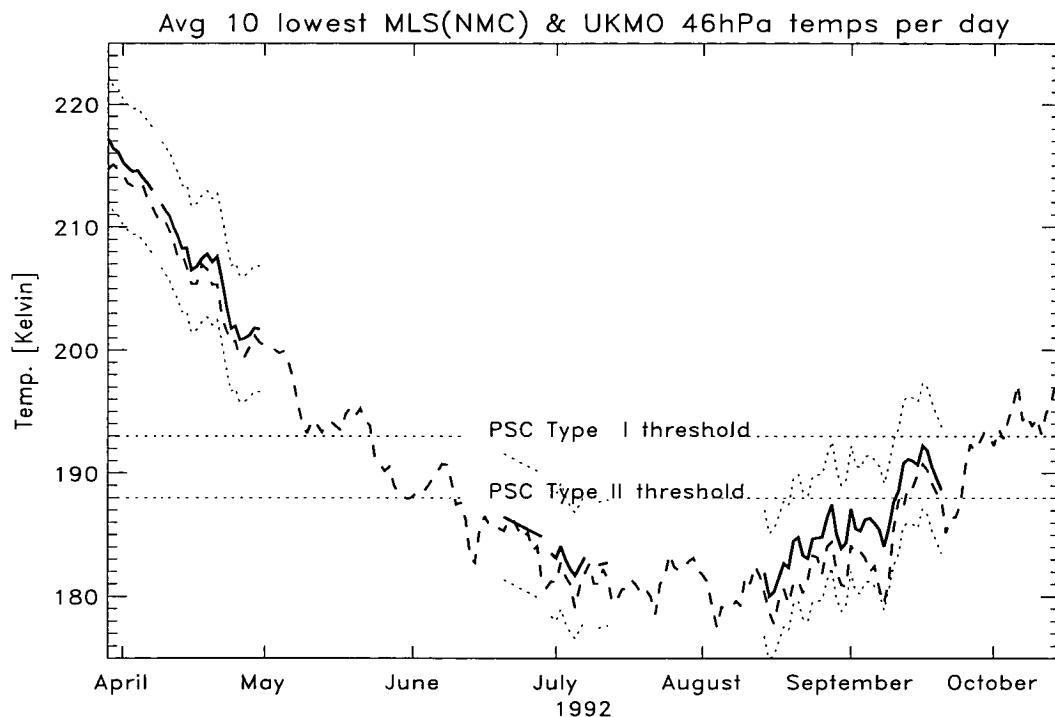


Figure 7.1: Average of 10 lowest 46 hPa polar (60-80S) temperatures from NMC (solid) line and UKMO (dashed). The dotted lines flanking the NMC time-series are 1-sigma error bars. The two horizontal dotted lines represent nominal PSC type I and II thresholds, 193 K and 188 K respectively. The actual PSC thresholds may, of course, vary from the nominal ones.

Temperatures at 46 hPa were below the nominal frost point of 188 K for ~4 months (Manney et al., 1994) steadily decreasing from the beginning of April, falling below 188 K in mid-June and remaining there until early in September

1992.

Accompanying this decline in temperature were dramatic changes in the polar concentration of ozone, water vapour, chlorine monoxide (Waters et al., 1993) and aerosol extinction ratios (Figure 7.2). The aerosol extinction ratios, measured by the CLAES instrument (Mergenthaler et al., 1993), if high can indicate the presence of PSC.

Water vapour mixing ratios remained relatively constant until temperatures approached PSC thresholds (Figure 7.2). Mixing ratios plummeted during July; the viewing pattern of MLS made it impossible to specify exactly when this happened. Concentrations of 4.0–5.0 ppmv were observed from ~April to ~June and by August/September were less than 1.0 ppmv.

Frost point measurements by Vogel et al. (1995), made over McMurdo Sound (~77°S, 165°E) (1995) over the years 1990 to 1994, follow a similar trend with dehydration starting in mid-June, at ~20–25 km, and lasting until the end of July. Vogel et al. also showed that ice particles in early winter were rehydrated at ~12–15 km since mixing ratios at these altitudes were enhanced. However this was thought to be a transient, although chemically important stage, since as the winter progressed dehydration became more widespread throughout the lower stratosphere. They also noted that on a couple of occasions, and well after the dehydration started, ice-saturation was reached, suggesting that the dehydration over McMurdo was not locally induced but was a result of the transportation of air through a small “cold” region elsewhere in the vortex.

Returning to the MLS results, since air enters the stratosphere with a mixing ratio much higher than the lowest antarctic values observed by MLS (~1.0 ppmv) (e.g. Kley et al., 1982) the mixing ratios observed in August/September 1992 suggest that condensation must have occurred. This is supported by observations of CLAES aerosol extinction coefficients (790 cm^{-1}) which, in general, are higher where MLS measures low water vapour concentration (Figure 7.2).

As the temperature increases during late-August and September, water vapour mixing ratios start to rise. There are two possible mechanisms for this:-

The first possibility is that the slowly-sedimenting ice-particles have evaporated before they have left the stratosphere.

The second possibility, which may have occurred in tandem with the first,

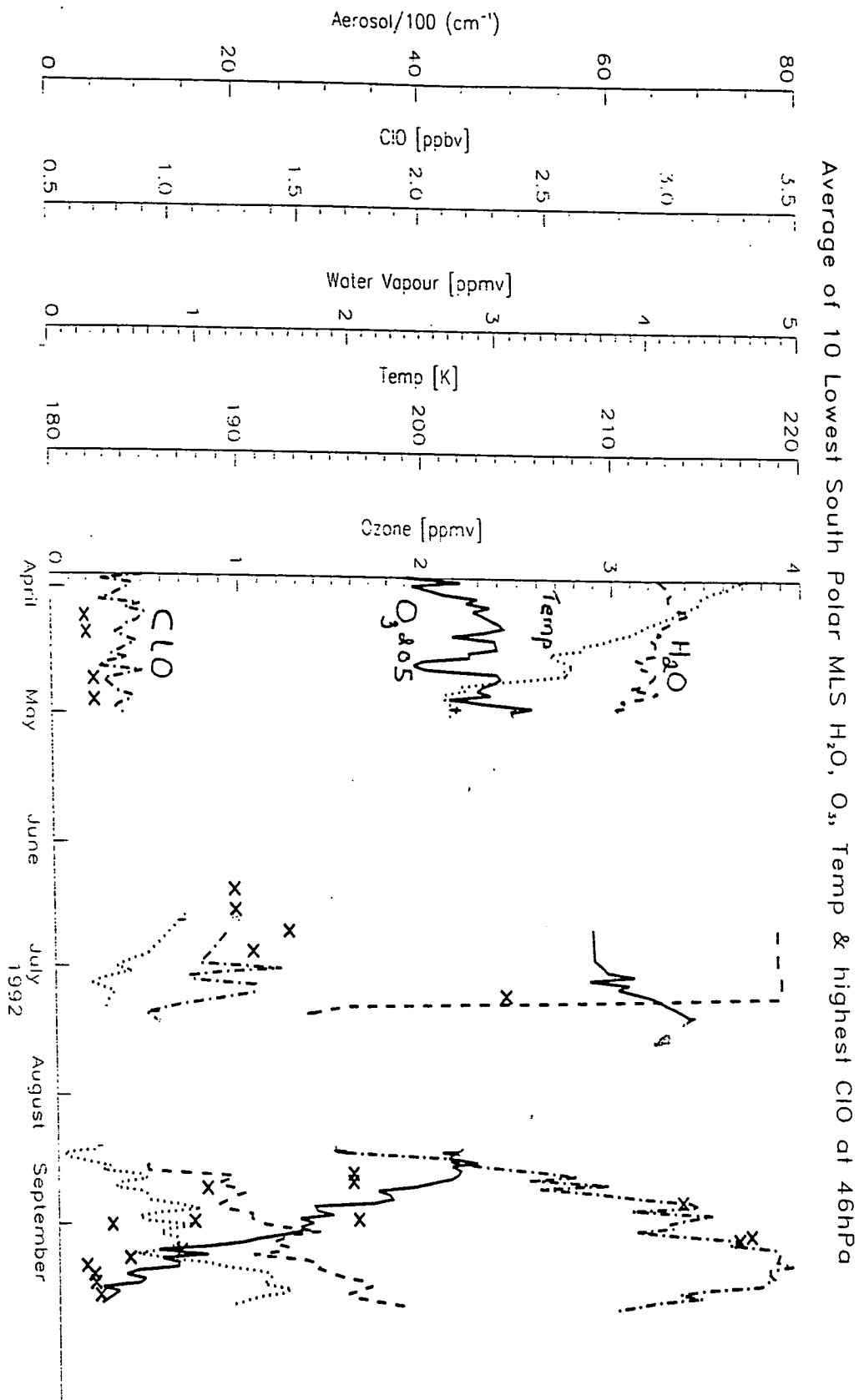


Figure 7.2: Average of 10 lowest 46 hPa polar NMC temperatures, MLS ozone and water vapour and highest ClO. CLAES maximum aerosol measurements are marked by crosses (every ~50 days and every second day, where possible, in August and September). The gaps in the plot are where MLS was viewing northern high latitudes except in the period May/June when the instrument experienced difficulties.

is that descent in the polar vortex had occurred as the temperature increased, bringing wetter air from aloft.

The first possibility is certainly likely since, if sedimentation had entirely removed all the water vapour from the stratosphere, then one would expect a signal of the dehydrated air to be observed subsequently at middle and high latitudes. There is no such signal apparent in MLS water vapour. Furthermore, recent work by Mote (1995) using HALOE water vapour data, which extends lower into the stratosphere than MLS (v0003), has shown that there is only a minimal impact, at least in 1992, of dehydrated vortical air on the zonally averaged distribution at lower latitudes.

The second possibility is certainly true since evidence of descent is, in fact, observed in MLS water vapour and was discussed in the previous chapter (e.g. see Figure 6.12). Thus it is likely that both mechanisms contributed, in part, to the increase in observed mixing ratio during late-August.

Ozone mixing ratios followed a similar pattern to water vapour with mixing ratios falling sometime between July and August (see Figure 7.2). In early August, when the instrument returned to viewing high southern latitudes, mixing ratios were ~ 2.0 ppmv. They continued to decrease for the next couple of months reaching a minimum of less than 0.5 ppmv in early-September.

Maximum chlorine monoxide values were fairly steady at values near the noise level of the measurements (~ 0.4 – 0.5 ppbv) through April and May and increased to ~ 1.0 ppbv by July. During July, August and September mixing ratios increased dramatically reaching a maximum of ~ 3.0 – 3.5 ppbv by the middle of September.

Note that chlorine monoxide mixing ratios continued to increase for about a month after the water vapour had reached its lowest concentrations (mid-August) suggesting that, although evaporation was presumably taking place, PSCs of type I were still present.

During the period August 30 to September 3, well after the the onset of dehydration, water vapour concentrations and temperatures were such that a region in the southern vortex was supersaturated with respect to ice. This suggested that the region was likely to contain PSC (Ricaud et al., 1995).

This suggestion is now investigated.

7.3.2 Discussion

Work performed with Ricaud and reported in Ricaud et al (1995) showed that MLS water vapour and temperature measurements, during the five day period defined above, suggested the presence of PSC over western Antarctica. This was supported by showing measurements from the CLAES instrument, which measured high aerosol extinction coefficients near, or in, the region where MLS water vapour indicated supersaturation. Furthermore, chlorine monoxide concentrations were enhanced downstream from the supposed area of PSC, suggesting that it had been activated through this region.

It was shown that the PSC could be attributed to a slow moving tropospheric anti-cyclone which forced adiabatic cooling underneath the vortex. This anti-cyclone also caused a minimum in columnar ozone (less than 200 DU) which was observed in the region of inferred PSC.

Lahoz et al (1995) noted that MLS water vapour retrievals were poor inside the polar vortex at 46 hPa in winter, measurements being largely dominated by 'wet' climatological values. This resulted in an overestimation of supersaturation (ice-cloud) throughout the winter. Thus, for Ricaud et al., (1995) a non-linear retrieval algorithm was used (Read et al., 1995) to reprocess the water vapour data (for latitudes poleward of 50S) for the five day period above.

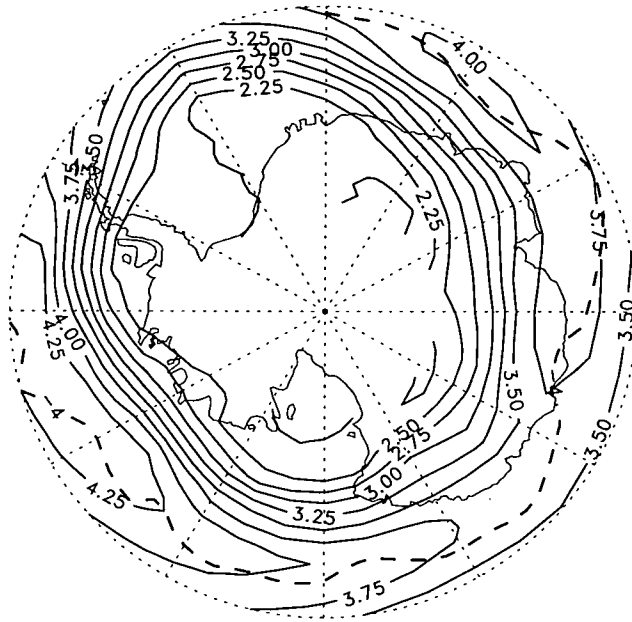
Figure 7.3 shows the reprocessed MLS water vapour fields, interpolated to the 465 K potential temperature surface, for each of the five days in the study. Superimposed on each map is a potential vorticity contour at $-4 \times 10^{-5} \text{Km}^{-2}\text{kg}^{-1}\text{s}^{-1}$. This was representative of the edge of the conservative polar vortex during this time.

Mixing ratios of less than 2.5 ppmv are observed over a large part of Antarctica indicating wide-spread dehydration in the southern polar vortex.

HALOE measurements, although only sampling in high southern latitudes for short periods, also show strong evidence of dehydration (see previous chapter) with mixing ratios of ~ 2.75 ppmv occurring in early October 1992.

Moreover, during this five day period there was a region inside the polar vortex where MLS water vapour and temperature measurements implied supersaturation. Supersaturation is assumed to occur when the partial pressure of MLS

MLS H₂O (non-lin) 465K :Aug 30



MLS H₂O (non-lin) 465K :Aug 31

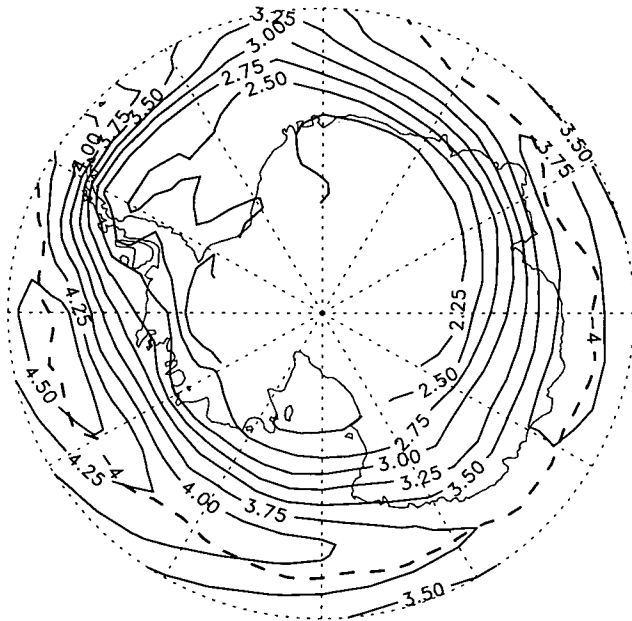
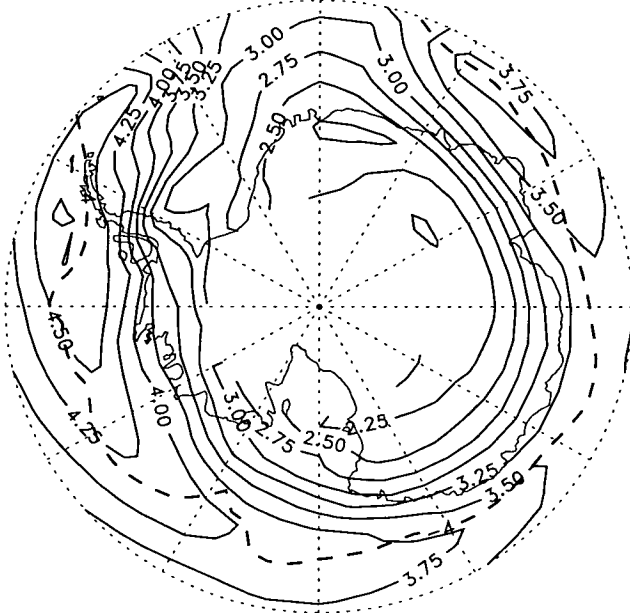


Figure 7.3: Polar stereographic projections (60S to pole) of reprocessed MLS water vapour at 465K for August 30–September 2 1992. The dashed line is UKMO potential vorticity at $-4 \times 10^{-5} \text{Km}^{-2}\text{kg}^{-1}\text{s}^{-1}$ and represents the edge of the conservative polar vortex as defined by Ricaud et al. (1995)

MLS H₂O (non-lin) 465K :Sep 01



MLS H₂O (non-lin) 465K :Sep 02

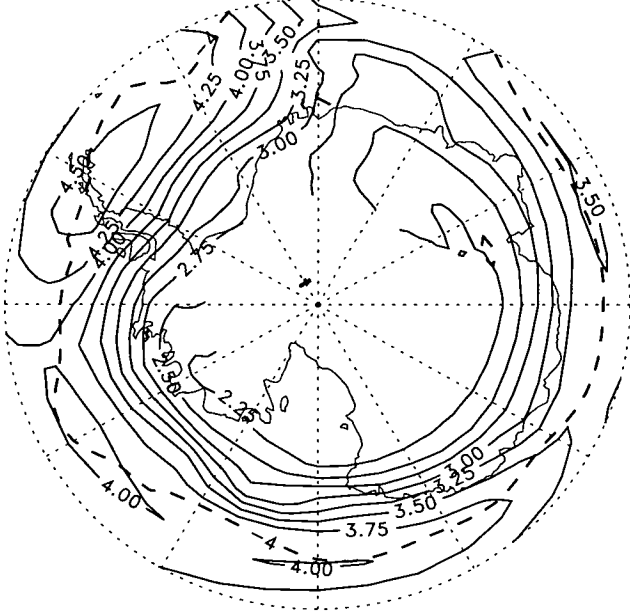


Figure 7.3: (Continued)

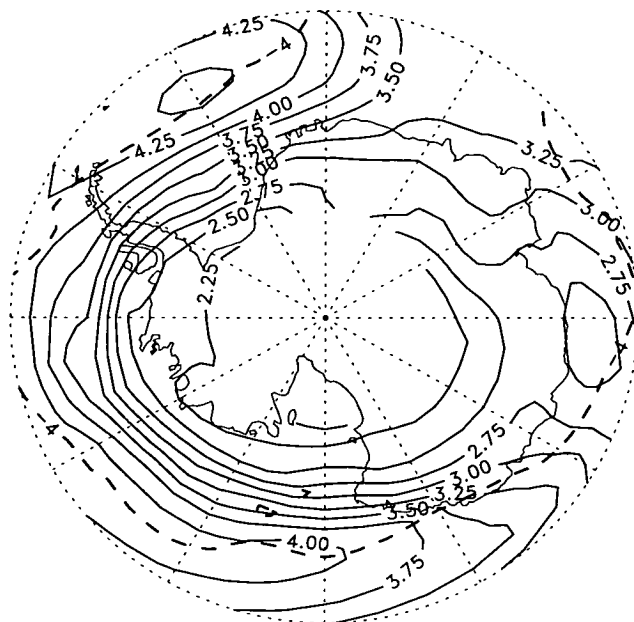


Figure 7.3: (Continued)

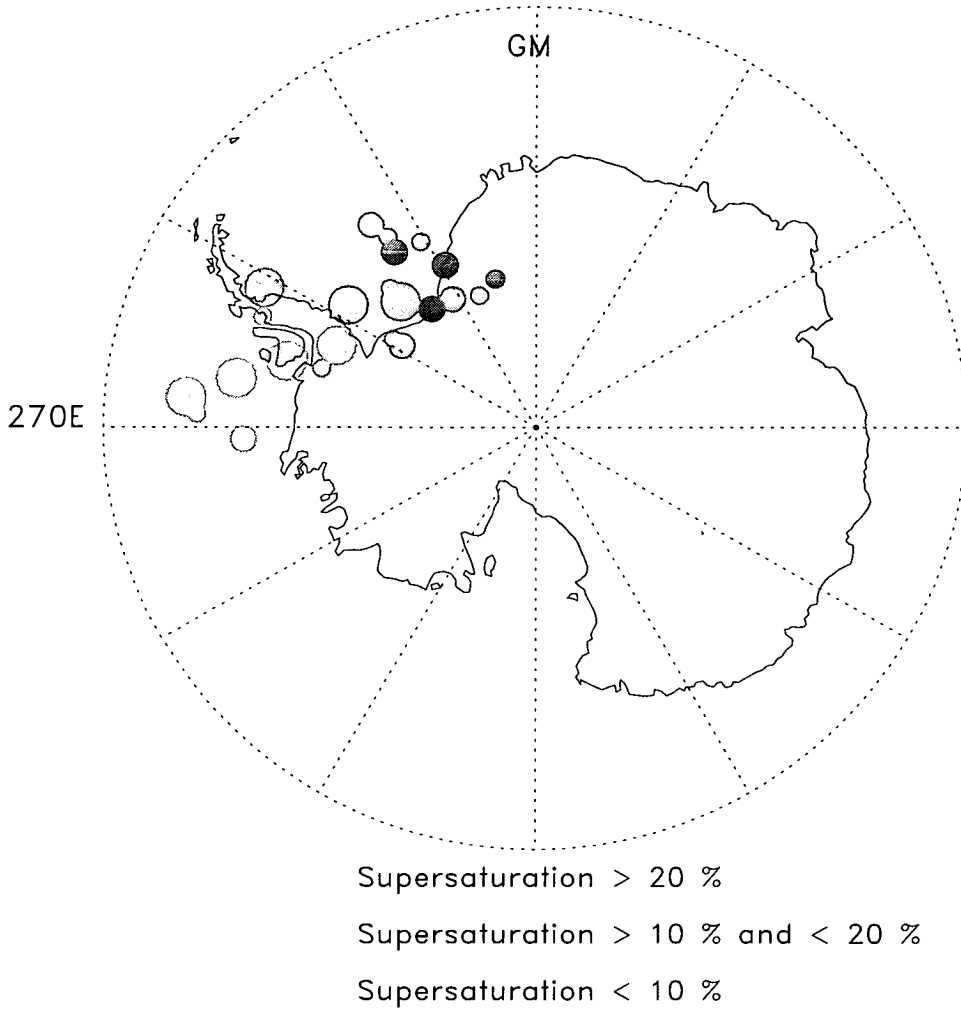
water vapour, (P_{H_2O}), exceeds E_i , the saturation vapour pressure of water over a plane surface of pure ice. E_i was calculated using the empirical formula from the *Smithsonian Tables* (1958).

Figure 7.4 shows the progression of the 465 K percentage supersaturation (%), defined as $s_i = 100 \times ((P_{H_2O}/E_i) - 1)$, over each of the five days. Note that data used in this plot are the actual retrieved profiles and have not been subject to averaging or gridding. Measurements of supersaturation, on Figure 7.4, are depicted as shaded circles of different sizes, the size and darkness of shade of each circle increases with magnitude of supersaturation and time; the lightest and darkest circles represent measurements on August 30 and September 2 respectively.

A supersaturated region is first observed on August 30 at $\sim 260E$ over the Bellinghousen Sea and then moves slowly eastwards over Palmer Land, the Antarctic Peninsula, the Weddell Sea and by September 2 is over Coats Land ($\sim 330E$). The amount of supersaturation (s_i), in general, diminishes over the five days; there are greater number of occasions where s_i is greater than 20% at the start of the period than at the end.

It should be borne in mind, at this stage, that supersaturation calculations are extremely sensitive to temperature. Using UKMO temperatures which are, in general, lower than NMC throughout the winter (Figure 7.1) leads to a greater

MLS H₂O Supersaturation 465K: Aug 30 – Sep 3



Circles get darker towards September 3

Figure 7.4: Polar stereographic projections (60S to pole) of supersaturation (and NMC temperatures). The largest circles are for supersaturation measurements (s_i) greater than 20%; the smallest ones are for s_i less than 10%. Time is indicated by the darkness of the circles which increases from August 30 to September 2.

amount of calculated supersaturation for each day. However, the slow eastward progression of s_i is maintained (not shown) using UKMO data. There are other factors which may have some effect on the amount of deduced supersaturation and these are discussed by Ricaud et al (1995).

Figure 7.5 shows a similar plot but for CLAES aerosol extinction coefficients (version 7) at 465 K. There is a clear similarity with Figure 7.4 with high aerosol values initially observed slightly more westwards than for supersaturation but the progression over the five days is similar with a slow eastward movement towards $\sim 340\text{E}$ by September 2.

Analysis of UKMO wind fields show that the areas of supersaturation and high aerosol do not move with the circulation at this level. The average wind speed at these latitudes, during this period, was $\sim 40 \text{ ms}^{-1}$. A rough approximation of the “velocity” of the supersaturated area at 465K, using the approximate distance that the supersaturated region travels in five days is only 8 ms^{-1} , five times smaller than the true wind speed.

We now look at the possibility that the inferred PSC regions were induced by a slower moving tropospheric weather system similar to that reported by McKenna et al. (1989) They showed that a slow eastward moving region of total ozone and temperature minima over Antarctica could be attributed to the forcing of an anti-cyclonic ridge underneath the polar vortex.

7.3.3 The cooling influence of a tropospheric anti-cyclone

The effects of tropospheric weather systems on stratospheric dynamics and temperature have been known for a long time (Dobson, 1928) and have been observed in several stratospheric observations.

For example, McKenna et al (1989) discussed the evolution of ozone “mini-holes” which were discovered over Antarctica in September 1987 during the Airborne Antarctic Ozone Experiment (AAOE). These holes would form rapidly, move slowly eastwards and last a few days before diminishing. Realising that proposed chemical destruction rates were extremely unlikely to account for the rapid decline observed in columnar ozone levels (from $\sim 250\text{DU}$ to $\sim 150\text{DU}$) McKenna and co-workers sought and found a dynamical solution.

By observing the geopotential height fields at 500 hPa (used as a diagnostic

CLAES Aerosol Extinction Coeffs. 465K: Aug 30 – Sep 3

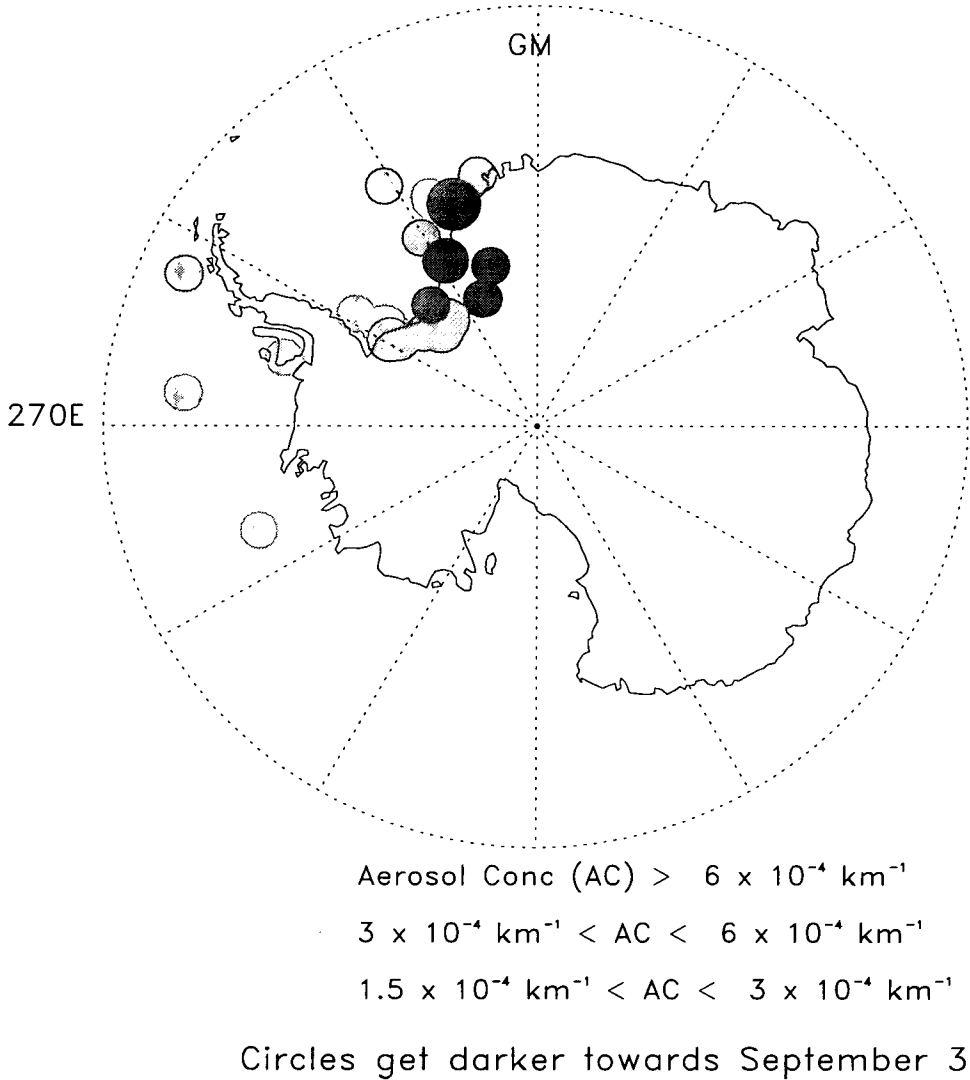


Figure 7.5: Polar stereographic projections (60S to pole) of CLAES aerosol extinction coefficients interpolated to 465 K. The circles increase in size with the magnitude of aerosol concentration. Time is indicated by the darkness of the circles which increases from August 30 to September 2.

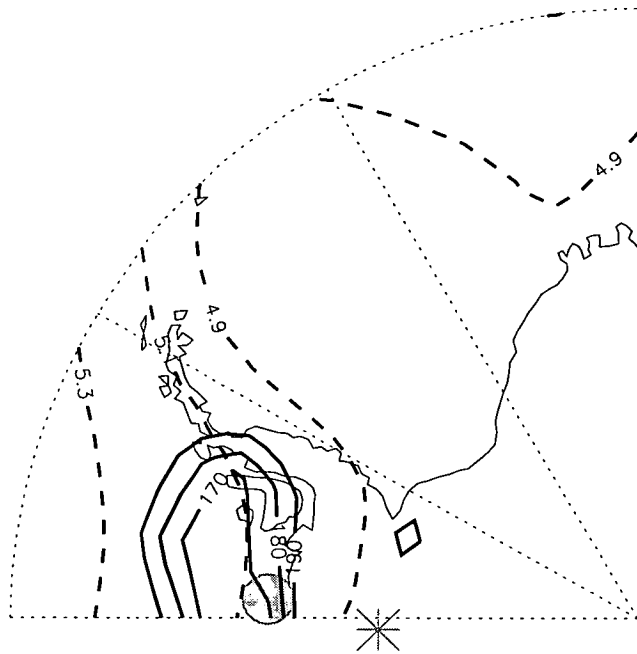
tool to locate synoptic-scale weather systems) they found a striking correlation in both the location and movement of the miniholes and an eastward moving anti-cyclonic ridge. The main reason why columnar ozone levels were so low was a product of the higher tropopause in anticyclonic regions. That is, the ozone columns contained more tropospheric ozone-poor air than normal.

In the vicinity of this ridge, isentropes were lifted upwards, resulting in air above being adiabatically cooled. The effects of this adiabatic forcing were apparent in the stratosphere with temperatures of less than 195 K seen at 50 hPa above the centre of the ridge. They pointed out that, since the area of low temperatures is quasi-stationary and the zonal-winds are strong in this region, this has important implications for PSC formation (and hence ozone depletion) because a large volume of air can pass through this region and be processed. In fact, aerosol extinction ratios measurements from the Stratospheric Aerosol Measurement II instrument (Poole and McCormick, 1988) suggest that PSC occurred within the neighbourhood of the low temperatures.

We now return to the case study in the southern winter of 1992 and look for a similar dynamical feature that might explain the progression of deduced supersaturation described above

Figure 7.6 shows the geopotential 500 hPa-height fields, for longitudes 270E to the Greenwich Meridian, for each of the five days in the case study. Superimposed onto each plot is the total ozone 190 Dobson Units contour for each day (calculated from MLS 205 Ghz ozone. Measurements have been vertically integrated from 100 hPa). Also shown are the average supersaturation and the average location of high aerosol concentration for each day. Supersaturation is marked by a shaded circle, the size of which is determined by the magnitude (M) of the aerosol concentration; a large circle is for $M > 20\%$; a small circle is for $M < 20\%$. The aerosol location is marked by a grey asterisk.

There is a clear correlation between the location (and hence motion) of each of the fields above. The area of supersaturation and low columnar ozone, in general, overlap and each quantity is seen to slowly drift with a large anti-cyclonic ridge in geopotential heights. Moreover, apart from September 1 when there were few CLAES aerosol measurements available, there is good agreement between the locations of supersaturation and high aerosol extinction coefficients.





August 30

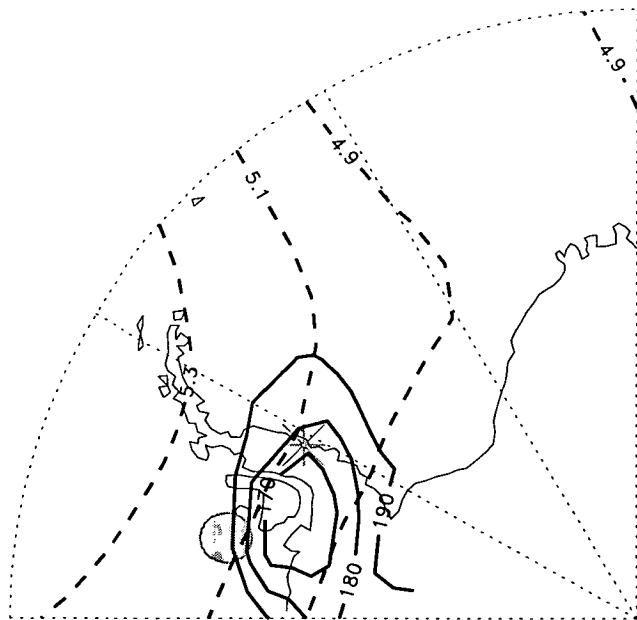
MLS Total Ozone at 190 (DU): solid line

UKMO Geopotential Hghts (km): dashed line

MLS Supersaturation (%):

-  > 20%
-  < 20%

Avg. Location of CLAES Aerosol *





August 31

MLS Total Ozone Minimum (DU): solid line

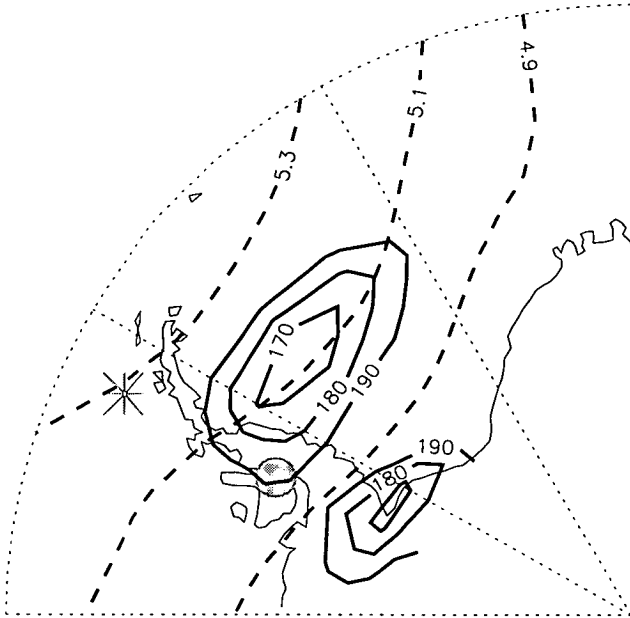
UKMO Geopotential Hghts (km): dashed line

MLS Supersaturation (%):

-  > 20%
-  < 20%

Avg. Location of CLAES Aerosol *



Figure 7.6: See September 3 plot for figure caption



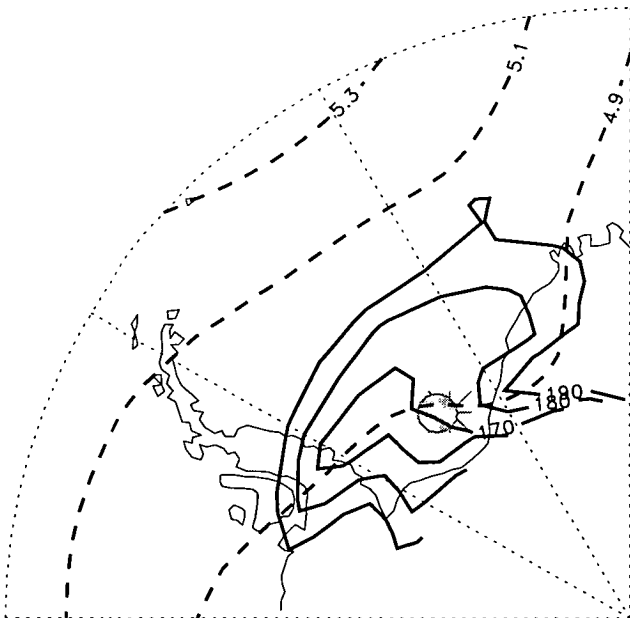
September 01

MLS Total Ozone at 190 (DU): solid line
 UKMO Geopotential Hghts (km): dashed line

MLS Supersaturation (%):

-  > 20%
-  < 20%



Avg. Location of CLAES Aerosol *



September 02

MLS Total Ozone Minimum (DU): solid line
 UKMO Geopotential Hghts (km): dashed line

MLS Supersaturation (%):

-  > 20%
-  < 20%

Avg. Location of CLAES Aerosol *

Figure 7.6: Continued

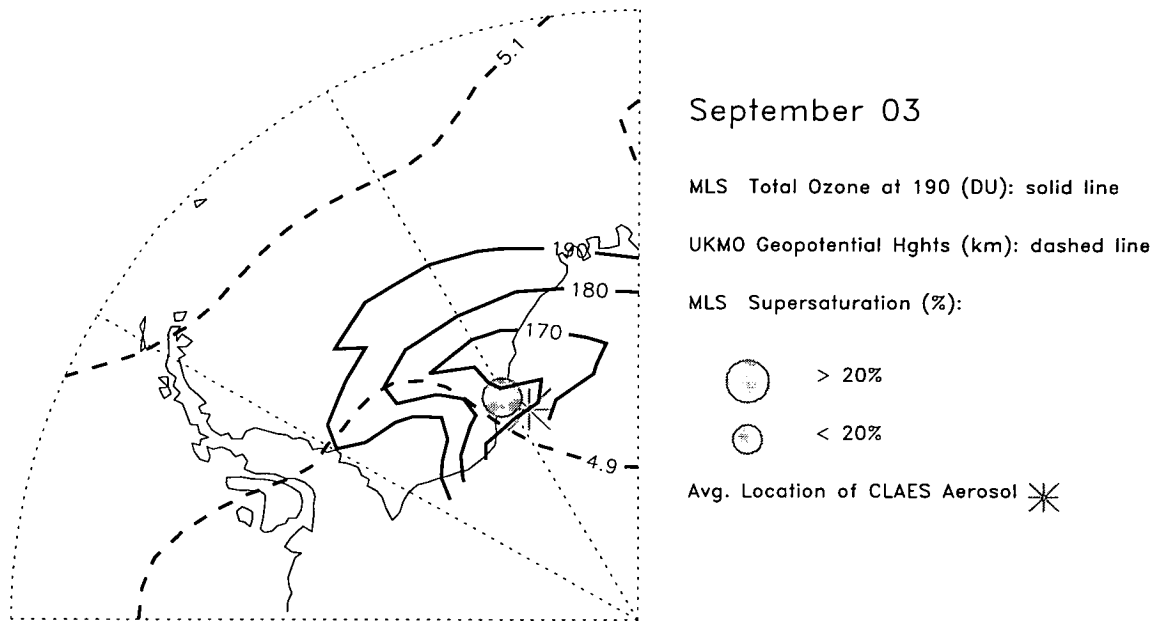


Figure 7.6: UKMO 500hPa-height fields (km) for August 30 to September 3 1992 (dashed lines) from 270E to the Greenwich Meridian. The 190 DU contour for MLS total ozone (from 205 GHz radiometer) is also shown (solid line). The column was calculated by integrating the vertical column from 100hPa. The shaded circle is the average supersaturation of all measurements during that day. A small circle indicates an average of less than 20%, large one more than 20%. The grey asterisk is positioned at the average location of high aerosol concentration for each day.

This strongly suggests that the areas of supersaturation, high aerosol and low ozone are not, in themselves, advected by the mean stratospheric flow but are in fact quasi-stationary regions created by the penetration of an tropospheric ridge underneath the vortex.

Further evidence for this is seen in Figure 7.7 which shows that, in the 270E-0E longitude sector, isentropes from the the troposphere to the lower stratosphere, under the vortex, are raised. There is thus adiabatic cooling in these regions.

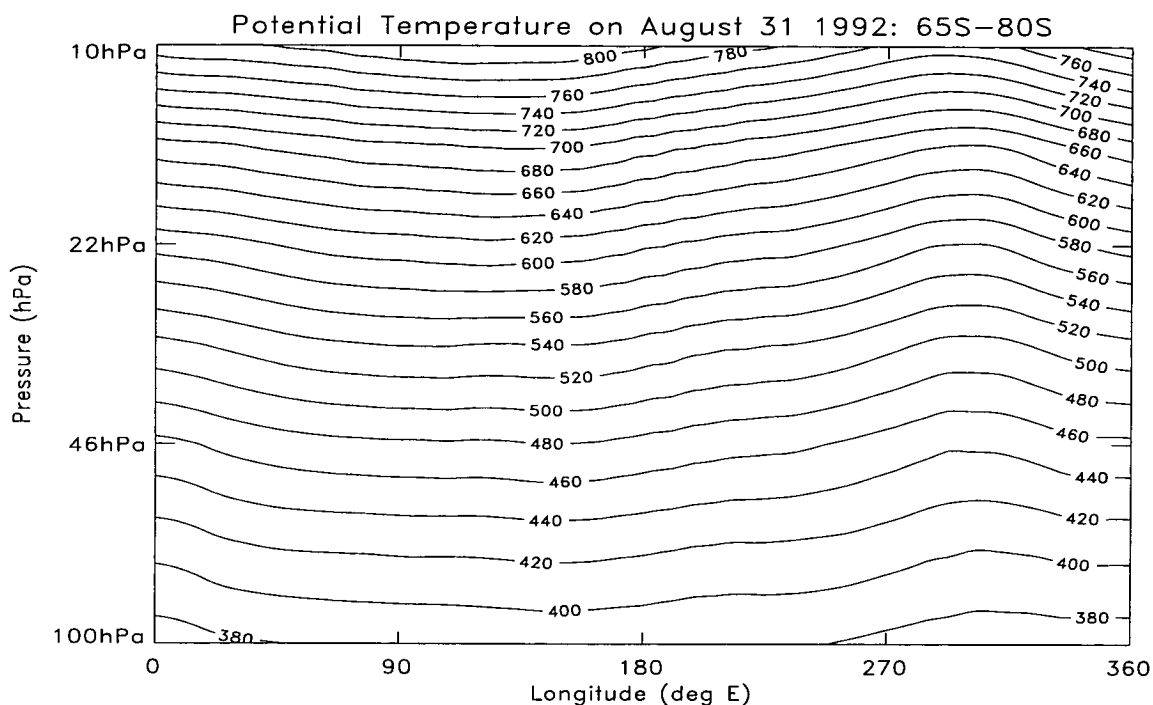


Figure 7.7: UKMO potential temperature [K] for August 31 1992 averaged between 65S and 80S

This has important implications for chlorine activation since it means that a large volume of air is capable of being processed through this area. And, in fact, Ricaud et al. (1995) showed that enhanced levels of CLO were indeed observed downstream from the inferred area of PSC.

CLO amounts during this time are generally very high with mixing ratios of more than 2.5 ppbv observed. The high levels are consistent with chemical processing on PSC.

7.3.4 Summary

To summarise, it has been shown that, during the period August 30 - September 3 1992, lower stratospheric measurements of water vapour and temperature in the southern vortex were such that it was extremely likely that polar stratospheric clouds were present. This view was supported by evidence from the CLAES instrument, which showed high aerosol extinction coefficients in the regions where MLS inferred PSC. The areas of enhanced aerosol and supersaturation were linked to the cooling action of a slow moving anti-cyclone in the troposphere. This anti-cyclone also caused minima in total ozone.

The second case study will discuss a five day period during a northern winter when temperatures are generally warmer than during southern winter (e.g. Manney et al., 1994).

7.4 Case Study 2: February 12 to February 16

7.4.1 Introduction and overview of winter 1992/93

In this section we look at a five day period, during the northern winter of 1992/93, when arctic polar temperatures were very low enough to expect the occurrence of PSC. Minimum temperatures in the lower stratospheric arctic vortex typically occur in January and February. In the winter of 1992/93 it appears, from UKMO data (Figure 7.8), that minimum temperatures occurred in mid-January; a period when MLS was viewing high southern latitudes. The period discussed in this study is February 12 to February 16; just after MLS yawed to the north. It will be shown that, during this period, type I PSC were present. This will be achieved using CLAES aerosol data, as well as data from MLS and the UKMO. The low temperatures that caused the PSC will be shown to be due, in part, to a similar tropospheric forcing event as in the southern winter of 1992. Moreover, the occurrences of supersaturation are found to be much rarer than in the southern hemisphere and are less persistent, leading to a lesser degree of dehydration and subsequent ozone loss. It is suggested that future work could investigate further the nature of tropospheric anti-cyclones as their future behavior can indirectly affect chemical ozone loss.

7.4.2 Discussion

Minimum MLS and UKMO arctic temperatures, at 46 and 22 hPa, are shown in Figure 7.8. The figure covers the period October 1992 to April 1993 (N.B. the MLS temperatures at 46 hPa are strongly biased towards those from NMC)

At 46 hPa, the UKMO and MLS (\sim NMC) time series are very similar, temperatures decreasing from \sim 210 K in November to \sim 190 K in January/February. In mid-January, when MLS was viewing high southern latitudes, UKMO temperatures fall below 188 K for a few days. From the middle of February MLS and UKMO temperatures steadily increase and by the end of April are \sim 220 K.

At 22 hPa, the UKMO series oscillates about temperatures near the PSC type I threshold for much of December to mid-February and increases sharply from then onwards. For a short period in mid-January the temperature minima touch 188 K.

The MLS 22 hPa temperatures vary in a nearly identical way but are systematically lower by as much as 10 K. Temperatures below 188 K are observed between December 1992 and February 1993.

The accuracy of MLS temperatures has been addressed by Fishbein et al (1996). They suggest that arctic winter temperatures at 22 hPa may be underestimated. The reasons for this are varied. A bias of 2 K arises from using incorrect values of O₂ pressure broadening coefficients in the current **v0003** retrieval. Another factor is thought to be the non-retrieval of 46 hPa temperatures. If the temperature in the atmosphere at 46 hPa is lower than in the NMC (or MLS) analysis the MLS retrieval, being sensitive to conditions at 46 hPa, attempts to reduce its estimated radiances by decreasing the 22 hPa temperature. It is thought (Evan Fishbein, personal communication, 1995) that where MLS 22 hPa temperatures are lower than NMC, are the same places where the 46 hPa NMC temperature may also be too warm. Hence, although MLS temperatures at 22 hPa indicate that the stratosphere is cooler than what is reported by the NMC (and UKMO) analysis, they may be, in fact, too cold because they are compensating for the positive temperature bias in NMC at 46 hPa.

Another reason for doubting the validity of 22 hPa temperatures is that the MLS water vapour values show no significant dehydration. The nominal frost

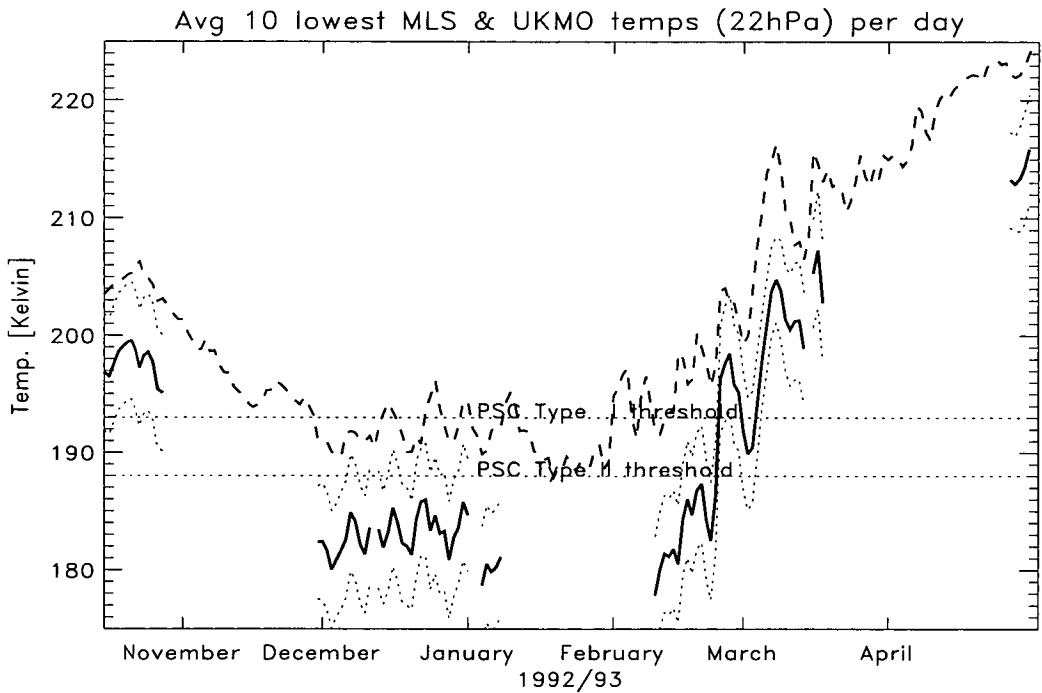
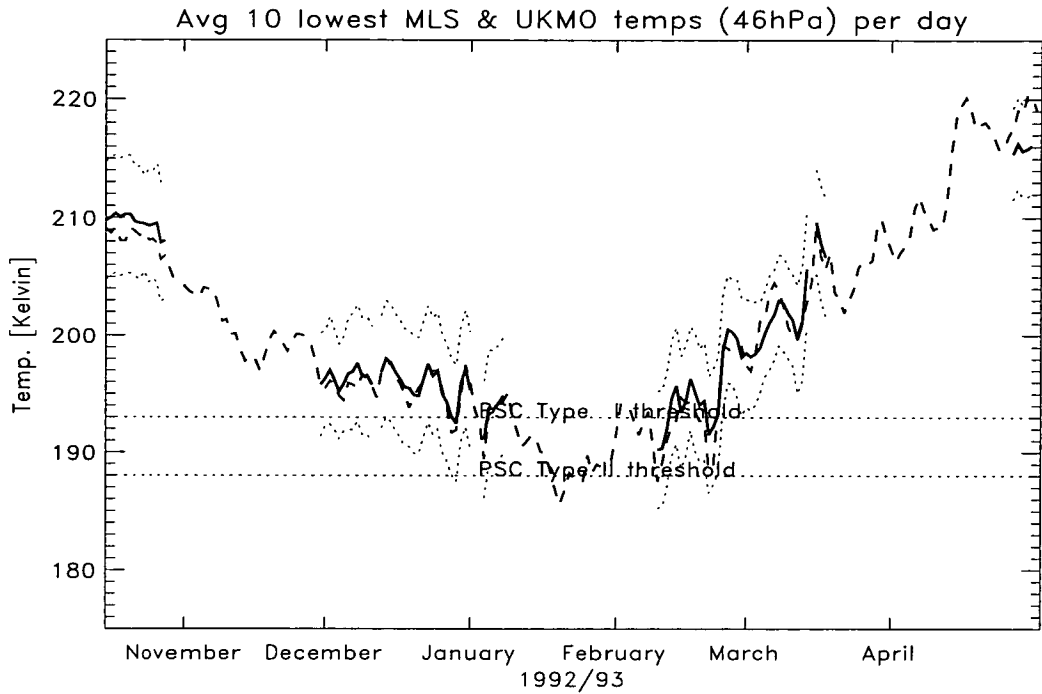
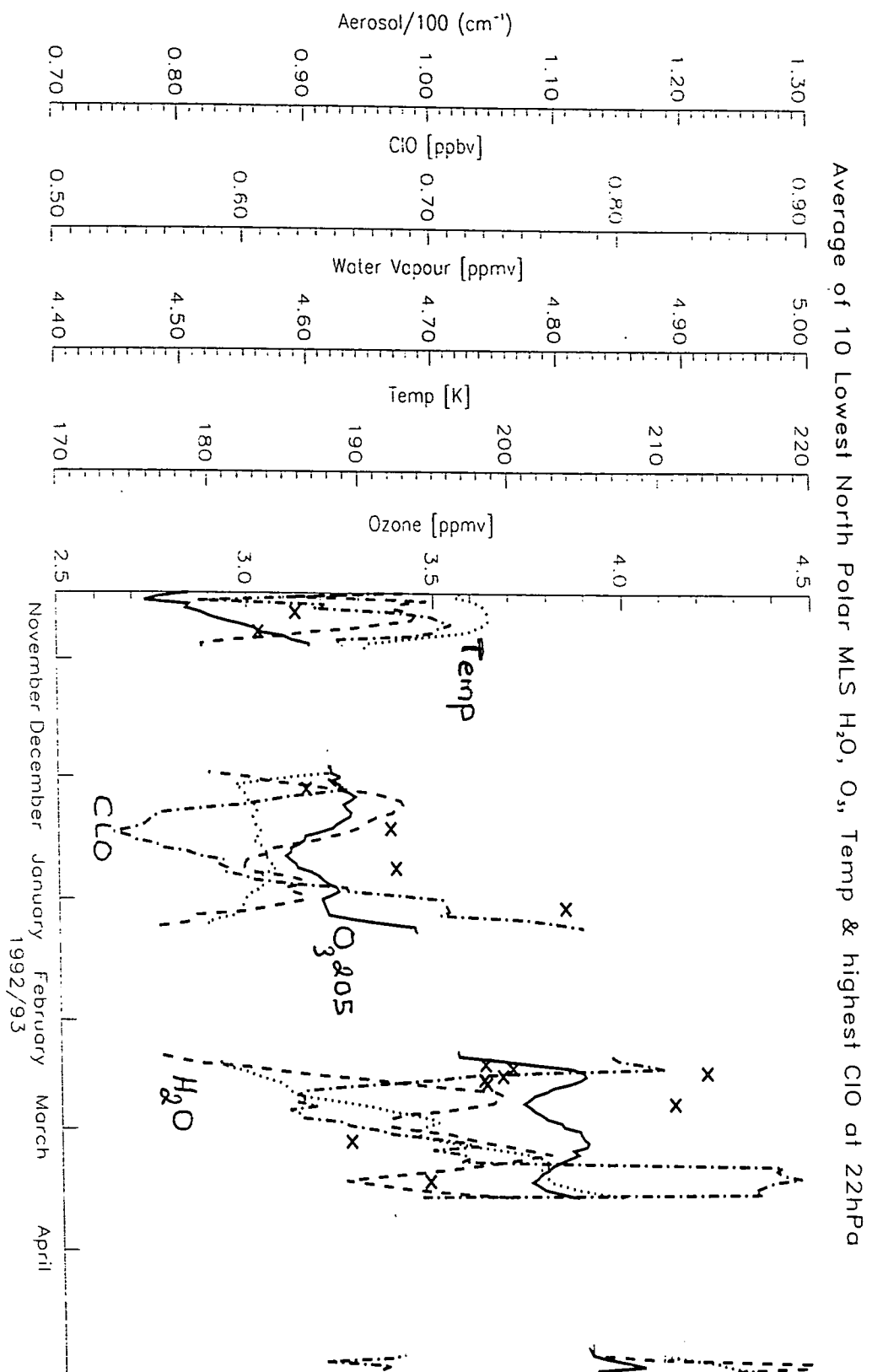


Figure 7.8: Average of 10 lowest 46hPa and 22hPa polar temperatures from MLS (solid) line and UKMO (dashed). 1-sigma error bars are also given for MLS values. Note, MLS temperatures at 46 hPa are strongly biased to the NMC values. NMC data make up the large majority of *a priori* temperatures in the lower stratosphere

point at 22 hPa is 184 K and as MLS temperatures were below this for large periods of the winter there should have been wide-spread condensation. Calculation of supersaturation indicates that ice-cloud was present throughout December to February; water vapour values were at times ~ 2.0 ppmv in excess of supersaturation. However this contradicts the lack of significant dehydration present (Figure 7.8). This can be partly explained by the fact that the v0003 mixing ratios are too high during winter, similar to the southern winter case discussed above. To estimate how important this was, in terms of reducing the estimated supersaturation, a non-linear retrieval was used to recalculate mixing ratios on a day where supersaturation (in v0003 data) was especially high in a large region of the vortex (Read: personal communication). The non-linearly retrieved water vapour values resulted in the magnitude of estimated supersaturation being approximately halved, leaving values of approximately 1.0 ppmv of supersaturation in a smaller but non-negligible area of the vortex. Hence, assuming that similar results would be obtained for other days throughout the winter, MLS temperatures at 22 hPa are almost certainly too low. In a test, where arctic temperatures were increased by 2 K, the number of days throughout this northern winter when supersaturation was observed previously was greatly reduced. Moreover, although supersaturation events were still observed on days in December, January and February, they were sporadic, lasting for a few days at most. Compare this to the southern winter of 1992 discussed above, where extensive dehydration (and heterogeneous ozone loss) occurred and where long periods of supersaturation were observed. It is likely that although type II PSC formation may have occurred during the winter it was infrequent and unable to sustain significant dehydration. This is consistent with measurements made during the Airborne Arctic Stratospheric Experiment (AASE) which ran from January to February 1989 (Kawa et al., 1992) and showed that, only rarely, was ice-saturation observed. Below, we discuss a five-day-period, in the 1992/93 northern winter, where MLS, UKMO and CLAES measurements indicate type I PSC were present.



Average of 10 Lowest North Polar MLS H₂O, O₃, Temp & highest ClO at 22hPa

Figure 7.9: Average of 10 lowest 22 hPa north polar NMC temperatures, MLS ozone and water vapour and highest ClO. CLAES maximum aerosol measurements are marked by crosses (every ~50 days). The gaps in the plot are where MLS was viewing southern high latitudes

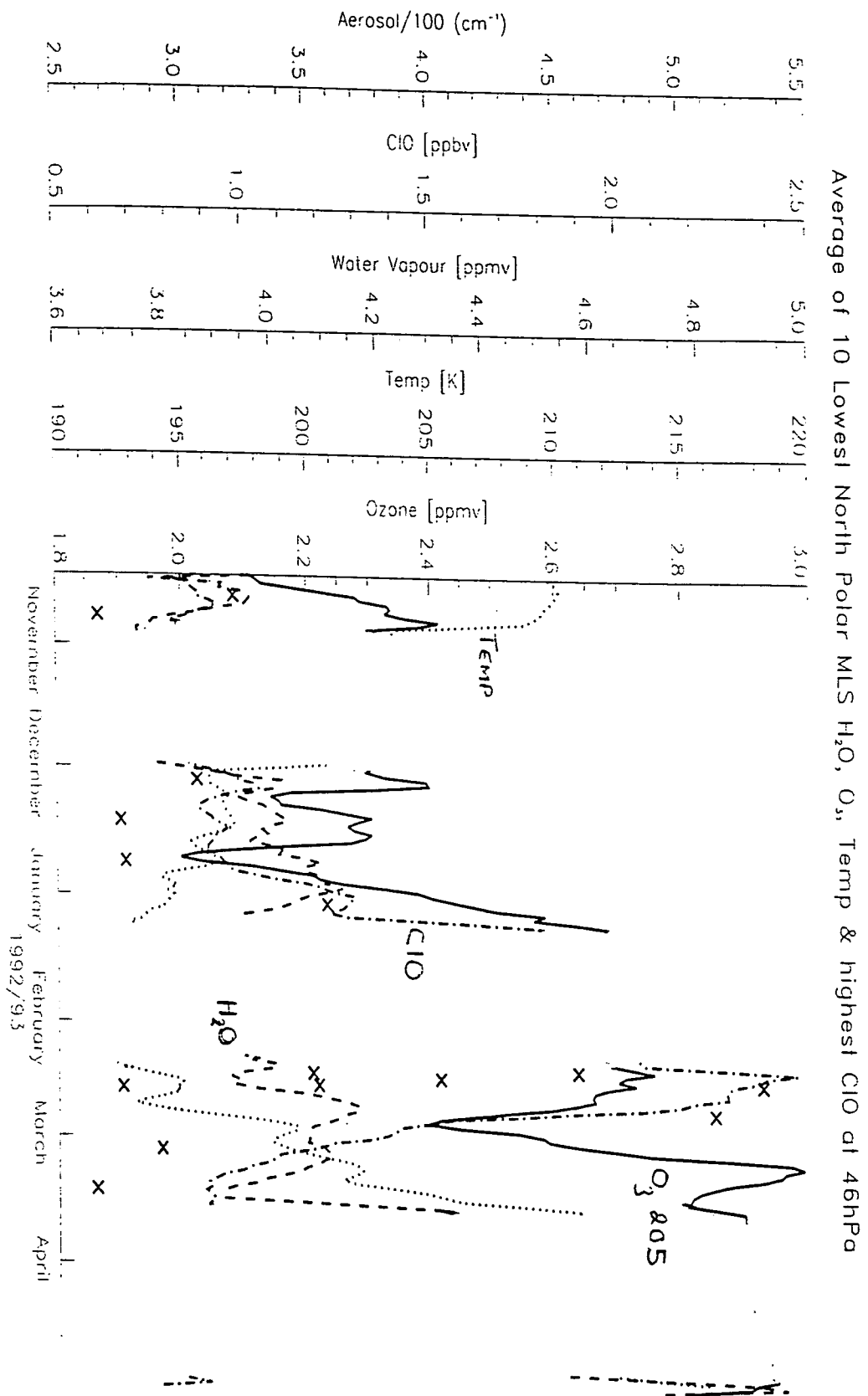


Figure 7.10: Average of 10 lowest 46 hPa north polar NMC temperatures, MLS ozone and water vapour and highest ClO. CLAES maximum aerosol measurements are marked by crosses (every ~50 days). The gaps in the plot are where MLS was viewing southern high latitudes

Figures 7.9 and 7.10 show the average of the 10 lowest measurements (north of 65°N) of MLS water vapour, ozone and temperature at 22 and 46 hPa respectively. Also shown are the average of the 10 highest ClO measurements. Crosses represent maximum CLAES aerosol extinction coefficients for several days throughout the winter. High coefficients may indicate the presence of PSC.

Water vapour measurements at 46 and 22 hPa show no obvious large downward trends that would indicate dehydration over the winter. However, at 22 hPa and, to a lesser extent, 46 hPa the behavior of mixing ratios just before the instrument yawed towards the south, in early January, and just after the yaw towards the north, in early February, give the impression that mixing ratios may have been at their lowest during this south-looking period. Just before the spacecraft yawed south in January, temperatures were decreasing towards PSC-formation temperatures. The UKMO time series shows temperatures as low as 188K in mid-January at 46 hPa (Figure 7.8). CLAES aerosol extinction ratios are generally highest when temperatures are lowest and are indicative of PSC.

Moreover, chlorine monoxide mixing ratios reach values greater than 2.0 ppbv, at 46 hPa, throughout February indicating conversion of chlorine reservoir species on PSC. Furthermore, Santee et al (1995) describe a short period where HNO₃ was low at 465 K in the northern vortex of 1992/1993 indicating a phase-change of HNO₃ to NAT. Although ozone mixing ratios are observed to increase during early winter, Manney et al report that vortex-averaged ozone at 465 K had decreased by 20 % by late-February. This decrease they attribute to heterogeneous chemical destruction.

We now look in more detail at a five day period when lower stratospheric temperatures are below 195 K in regions of the arctic vortex. This temperature is the typical value at which PSC of type I form.

It is shown that the CLAES instrument measures high aerosol extinction coefficients in the vicinity of these low temperatures. Furthermore, evidence is given to suggest that the low temperatures are, in part, due to a similar tropospheric forcing event which caused the cooling in the southern vortex of 1992.

Figure 7.11 shows 465 K polar stereographic projections, over northern Europe, of UKMO 195 K temperature contours for February 12 to February 16 1993. Also shown are 465K CLAES aerosol extinction coefficient contours at 4.5 and 5.0

$\times 10^{-5} \text{ km}^{-1}$. The dotted line is the 465 K potential vorticity contour at $2.5 \times 10^{-5} \text{ Km}^{-2} \text{ kg}^{-1} \text{ s}^{-1}$ and is representative of the conservative edge of the arctic polar vortex (Manney et al., 1994)

In general, for each day, the region of maximum aerosol values are observed where UKMO has minimum temperatures. There is also a slow eastwards progression of these regions over the five days.

On February 12, high aerosol values lie over north western Scandinavia and overlap the large region of low temperatures which occurs over much of northern Scandinavia, eastern Greenland and Svalbard. The high-aerosol and low-temperature regions are also located near to the edge of the polar vortex.

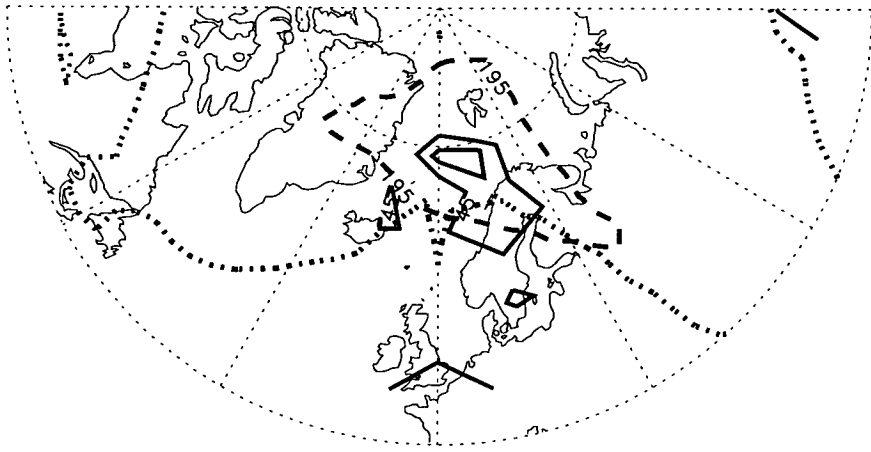
By February 13 and 14 the regions of low temperatures and high aerosol had moved slowly eastward, extending towards western Asia.

On February 15, there are two distinct areas where temperatures are low and aerosol concentrations are high. One region is at a similar location to that observed on the previous day, but is larger in size and extends further west than on February 14. The other region is centred over Iceland and has a smaller area of high aerosols than the region further east.

By February 16, the region of high aerosols over Iceland had decreased greatly in size. There was a also region of high aerosols over the USSR which is not contained by the 195 K contour but where temperatures are still below 200 K. The UKMO temperatures have an approximate root-mean-square error of 1 K which may be larger at winter latitudes (Swinbank and O'Neill, 1994). So it is not impossible that the high aerosols are signatures of PSC.

The chlorine monoxide concentrations for these five days (Figure 7.12) are enhanced (greater than 1.0 ppbv) throughout the polar vortex. These high concentrations are indicative of heterogeneous processing of reservoir chlorine on polar stratospheric clouds. Moreover, the size of the region of low temperatures/high aerosols is small compared to the region where ClO concentrations are high and indicates that the area of low temperatures/high aerosols may have acted as a chemical processor. This is supported by the magnitude of the zonal-mean winds in the lower polar stratosphere which are much larger than that implied by the motion of low temperatures. This is an important factor in the chlorine activation (and resulting ozone loss) since it means that a large proportion of air in the polar

Feb 12



Feb 13

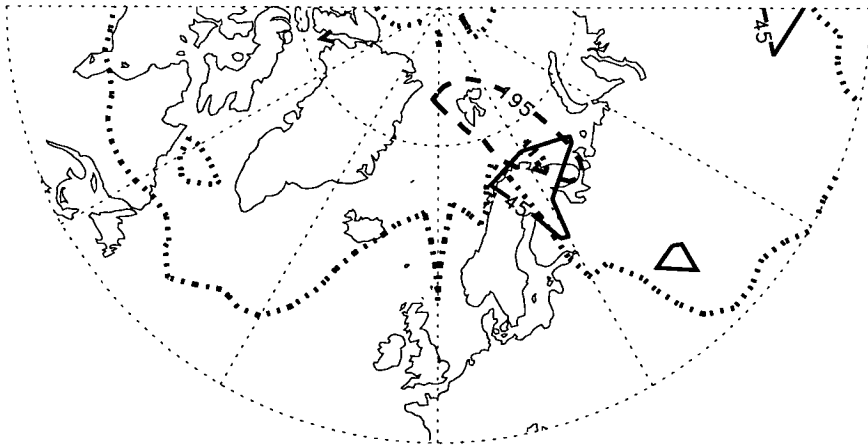
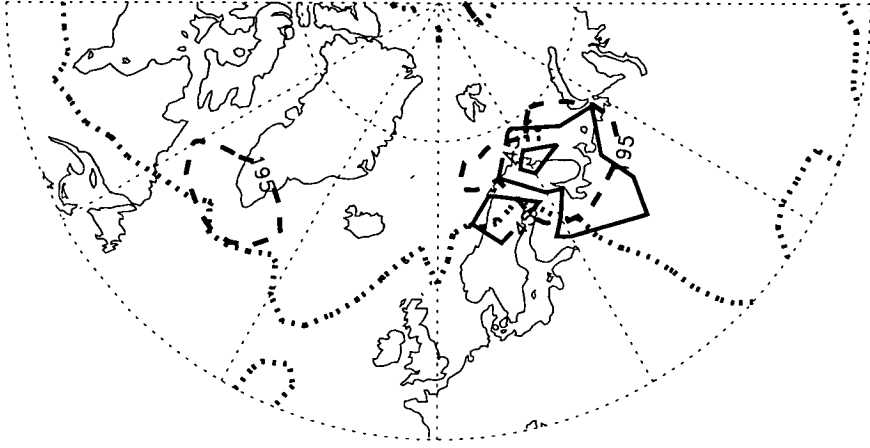


Figure 7.11: See February 16 plot for caption

Feb 14



Feb 15

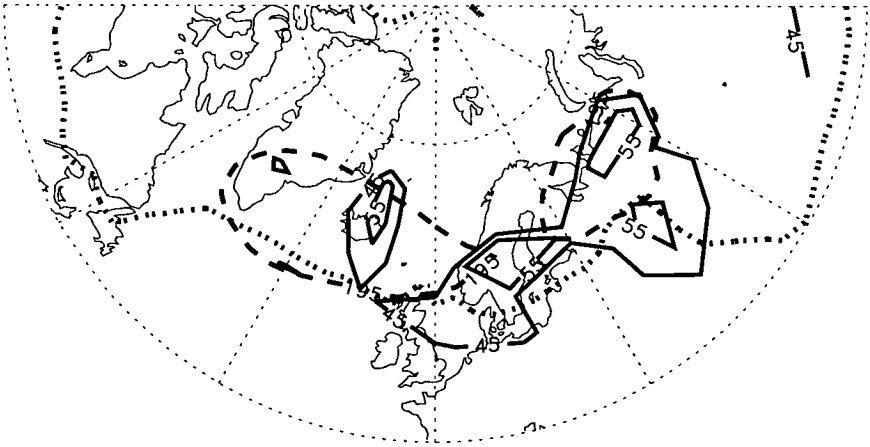


Figure 7.11: Continued

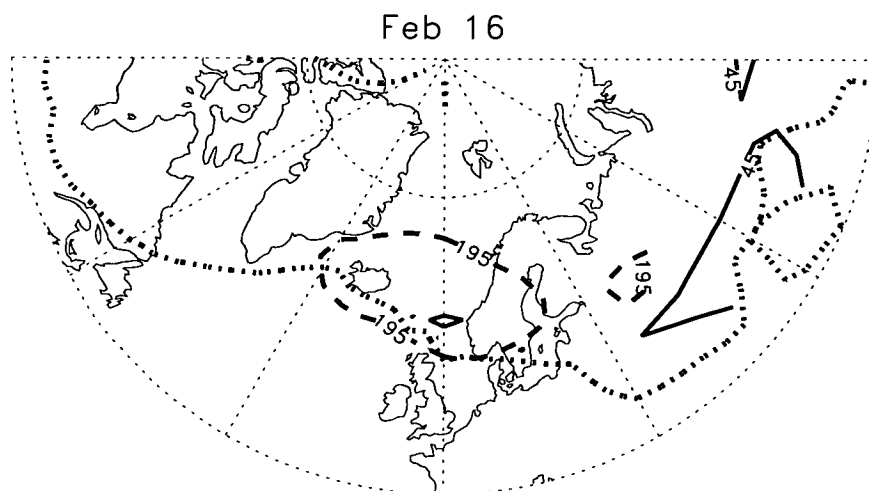


Figure 7.11: Polar stereographic projections (45N to pole and 90 W to 90 E) of the 465 K UKMO temperature contour at 195 K (dashed line), 465 K CLAES aerosol extinction coefficient contours at 4.5 and $5.0 \times 10^{-5} \text{ km}^{-1}$ (solid lines) and the UKMO derived potential vorticity contour (dotted line) at $2.5 \times 10^{-5} \text{ Km}^{-2}\text{kg}^{-1}\text{s}^{-1}$ for February 12 to 16 1993.

vortex is likely to have been processed through this region.

Thus it seems that PSC of type I were present at periods during the northern winter of 1992/93. However because sequestration of water in type I PSC is limited by the concentrations of HNO_3 , and those concentrations are generally small at these levels, no significant dehydration was expected, and was observed.

Santee et al (1995) and others have pointed out that future cooling of the arctic vortex could lead to greater ozone loss since dehydration and denitrification may be more intense.

We now show that the low temperatures and supposed PSC were caused, in part, by the cooling influence of a tropospheric anti-cyclonic ridge under the vortex. There was also a reduction in total ozone in the vicinity of this ridge.

7.4.3 The cooling influence of a tropospheric anti-cyclone

The effects of a tropospheric anti-cyclone on the arctic vortex has been noted previously.

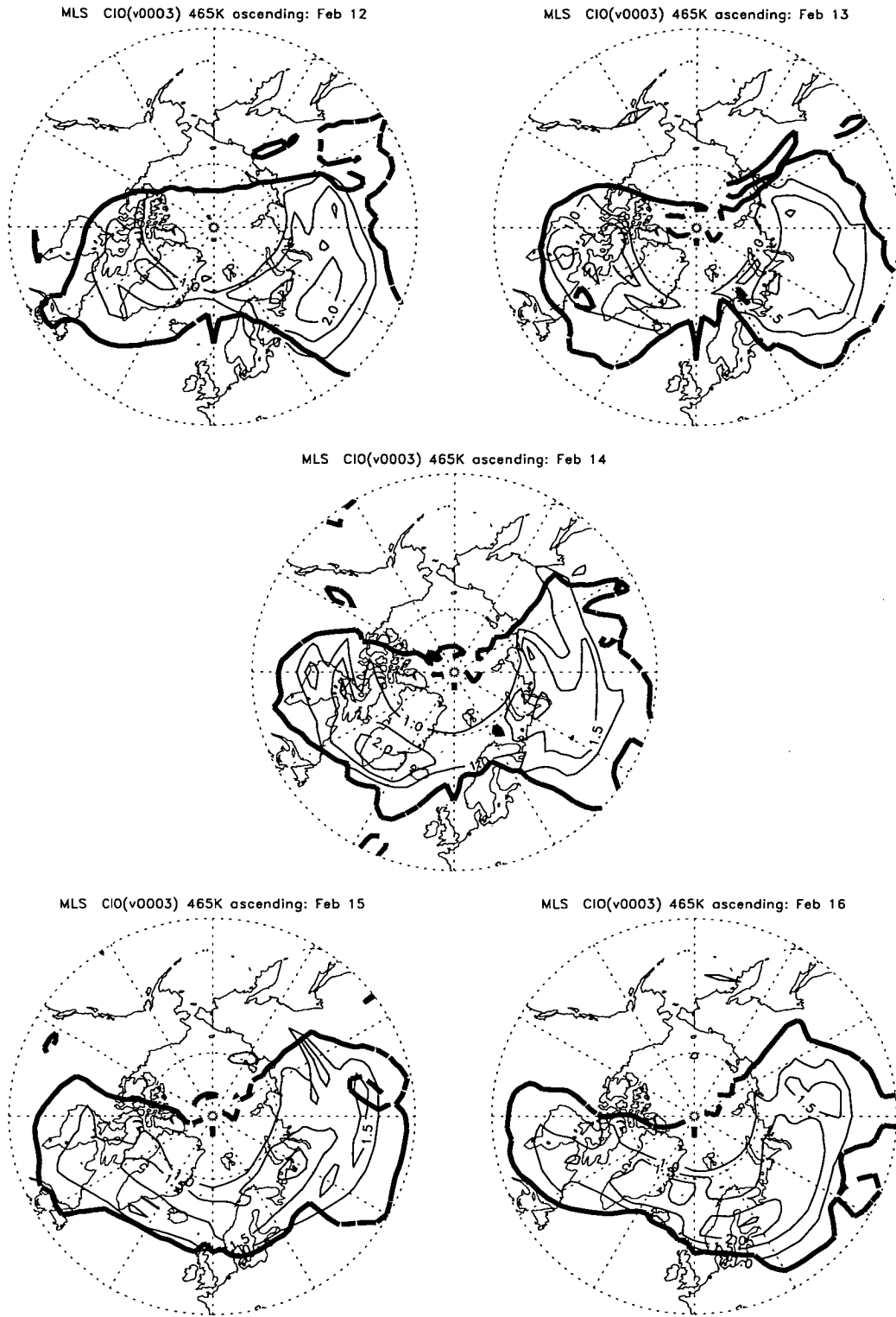


Figure 7.12: Polar stereographic projections (45N to pole) of daytime MLS chlorine monoxide at 465K for February 12–February 16 1993. The thick dark contour is the potential vorticity contour at $2.5 \times 10^{-5} \text{ Km}^{-2} \text{ kg}^{-1} \text{ s}^{-1}$. The thinner contours are for CIO at 1.0, 1.5 and 2.0 ppbv

In the northern winter of 1991/92 Orsolini et al (1995) found that total ozone values over northern Europe were very low throughout January 1992. By using a high-resolution general circulation model they showed that these low values were linked to an anti-cyclonic ridge penetrating the stratosphere. They also showed that where the ridge penetrated the stratosphere model temperatures were very low (~ 193 K).

Figure 7.13 shows the geopotential 500 hPa height fields for the five days in this case study, February 12 to February 16. Also shown are total ozone minima derived from MLS ozone (vertically integrated from 100 hPa).

For the five days shown, the geopotential height fields (dashed lines) imply the presence of a large eastward moving anti-cyclone over northern Europe. The location of the ridge of the anticyclone approximately follows the location of the high-aerosols and low temperature discussed above. Similar to the case in southern winter, isentropes are lifted above the ridge causing adiabatic cooling (Figure 7.14)

Also associated with this anti-cyclonic ridge is a region where total ozone values (heavy dark line) are low. Also, since the lowest total ozone values are found on the outside edge of the vortex, similar to previous arctic mini-holes (Orsolini et al., 1995), it would appear that the adiabatic forcing from below is offset somewhat by diabatic descent inside the vortex.

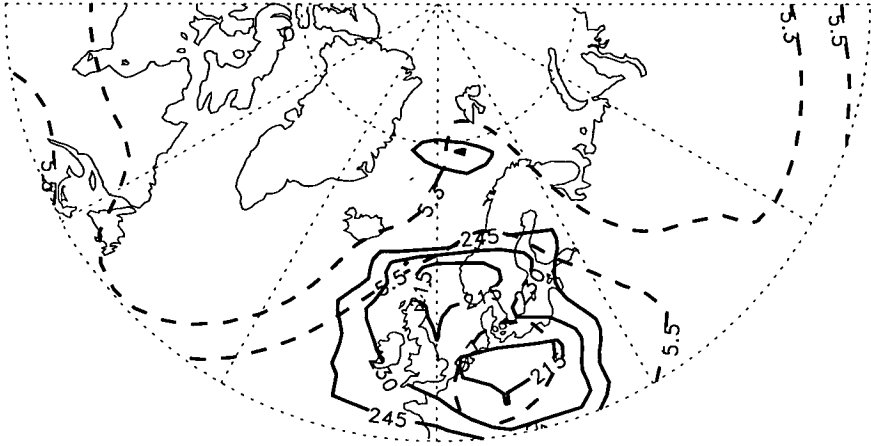
7.4.4 Summary

During the northern winter of 1992/93 MLS water vapour measurements, UKMO data, and CLAES aerosol data have been used to indicate the presence of PSC. The low polar temperatures were in part due to the presence of a tropospheric weather system which forced adiabatic cooling beneath the vortex. The occurrence of supersaturation events is more sporadic than in the antarctic and no significant dehydration was observed. This lack of extensive dehydration is consistent with previous studies (e.g. Kawa et al., 1992)

7.5 Conclusions from Case Studies

During August 30 – September 3 1992 there was widespread dehydration throughout the lower stratospheric antarctic polar vortex. Temperatures from the NMC

Feb 12



Feb 13

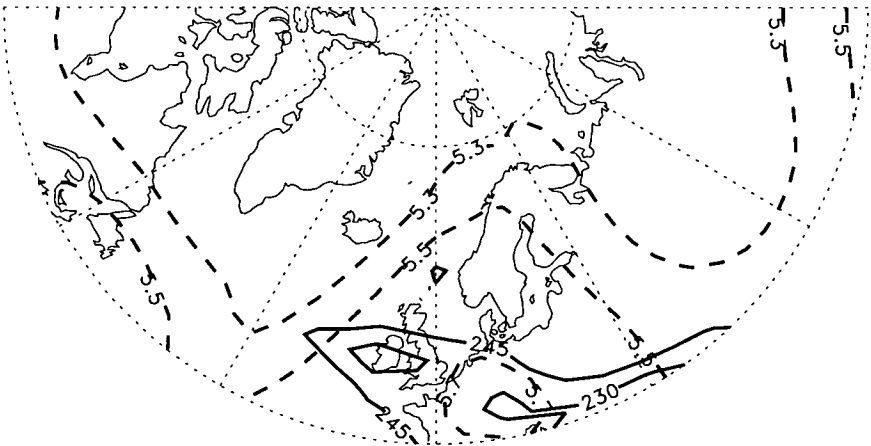
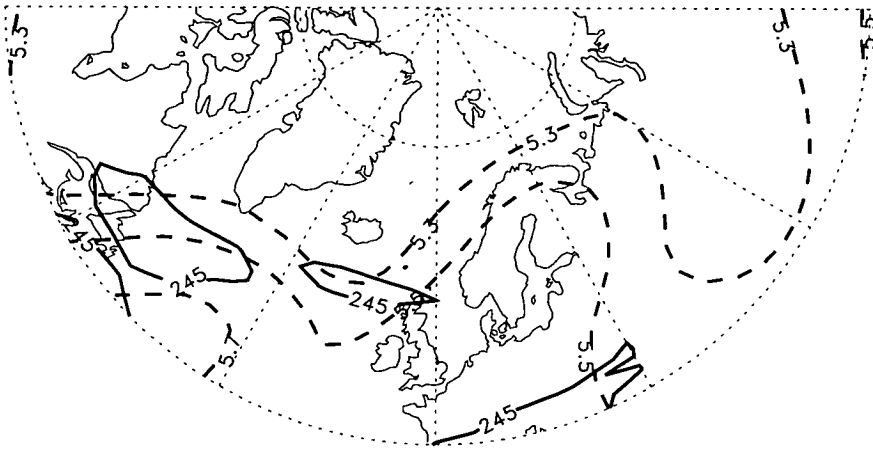


Figure 7.13: See February 16 plot for caption

Feb 14



Feb 15

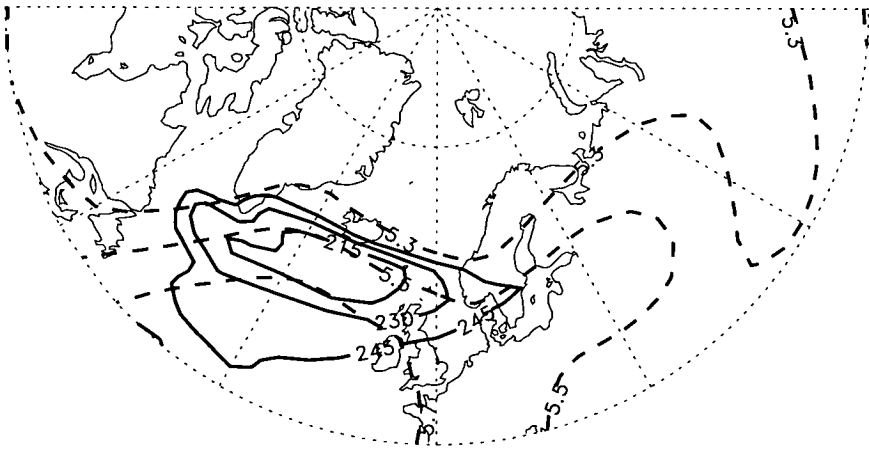


Figure 7.13: Continued

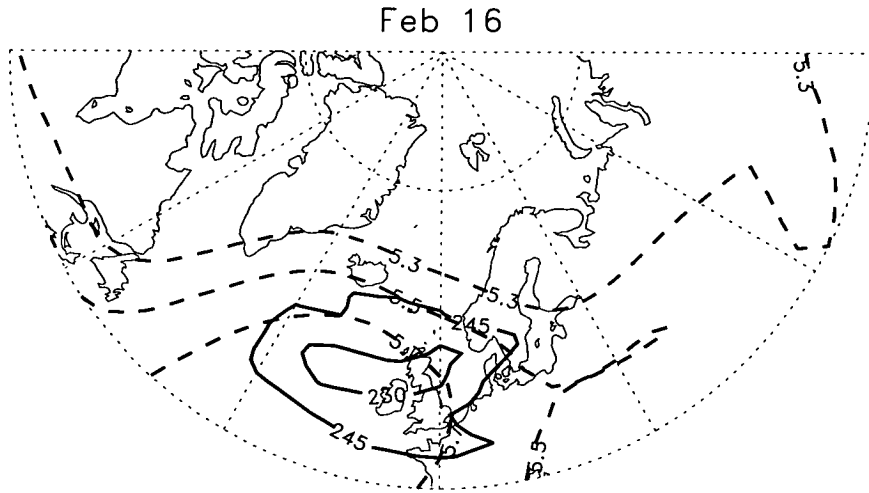


Figure 7.13: Polar stereographic projections (45N to pole and 90W to 90E) of UKMO 500 hPa geopotential heights in km (dashed) and MLS total ozone (solid) in Dobson units (vertically integrated from 100 hPa).

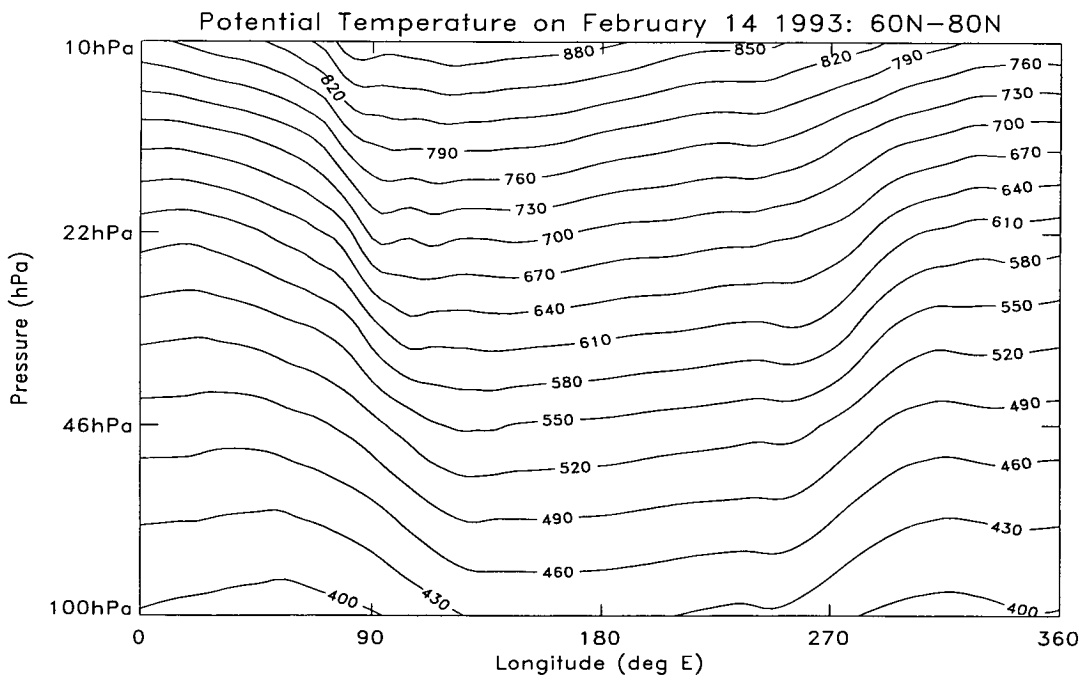


Figure 7.14: UKMO potential temperature [K] for February 14 1993 averaged between 60N and 80N

analysis, water vapour measurements from MLS and aerosol data from CLAES suggested that PSC type II were present at certain areas within the polar vortex. Enhanced measurements of ClO were observed in the polar vortex and suggested that air had been processed on PSC. The small region of very low temperatures was caused by adiabatic cooling following the penetration of a tropospheric anti-cyclone into the polar stratosphere.

In the northern winter of 1992/93 MLS temperatures at 22 hPa suggested that widespread dehydration should be present at high northern latitudes throughout the winter. However, the temperatures at this altitude are believed to be underestimated (Fishbein et al., 1996). A study using more realistic temperatures significantly reduced the number of likely supersaturation events, and hence the likelihood that type II PSC were widespread during this winter.

However, it was shown that, during the period of the case study, PSC type I were present at 465 K (\sim 46 hPa). CLAES aerosol concentrations were consistent with this notion since they were high where temperatures were low, but not as high as in the southern winter, where PSC type II were present. A tropospheric anti-cyclonic ridge was discovered beneath the area where temperatures were low similar to the previous northern winter (Orsolini et al., 1995) and the southern winter of 1992.

As was shown above, tropospheric weather systems can impact greatly on the polar stratospheres since they can provide suitable conditions for PSC to form. The regularity and endurance of these weather systems are thus an important topic for future research since they can indirectly modulate the amount of dehydration and hence, ozone destruction. At present, at least in the case of the MLS results, supersaturation events, and subsequent heterogeneous processing on PSC, are much rarer in the arctic than in the antarctic. Thus, any mechanism which has the potential to sustain low arctic temperatures for longer than at present is worthy of future investigation.

Chapter 8

Summary and Conclusions

This thesis was primarily concerned with the zonal-mean measurements of water vapour from the Microwave Limb Sounder (MLS). It has shown, for the first time, near-global zonal-mean distributions of stratospheric water vapour over the course of a year and a half. It is also the first time that a satellite instrument has extensively measured water vapour at antarctic and arctic latitudes during winter.

Also described were the temporal variations in MLS water vapour at individual pressure levels and at different latitudes. Two winter case studies described the conditions, and in particular the changes in water vapour concentration, that prevailed during the arctic and antarctic winters of 1992/93 and 1993 respectively.

The zonal-mean distributions of MLS water vapour, for each yaw-month (~ 36 days), were shown to exhibit many of the features present in the monthly-means from LIMS and SAGE II. Mixing ratios in the stratosphere increased upwards and polewards from a broad minimum in the lower stratospheric tropics. This pointed towards a zonal-mean distribution consistent with the Brewer-Dobson circulation and with methane oxidation being a source of stratospheric water vapour. Moreover, in the upper stratosphere there was evidence of the equinoctial double-peaked structure over the equator, a consequence of perturbations to the circulation caused by the semi-annual oscillation in wind and temperature.

It was shown that, compared to LIMS, MLS zonal-mean water vapour measurements were much larger (10-50 %). An estimate of the increase in stratospheric methane levels showed that part of this difference (~ 10 percentage units) could be explained by the greater volume of methane in the atmosphere in 1991–1993

than in 1978/1979. The differences with SAGE II were much smaller, than for LIMS, and were generally less than 10 % throughout the stratosphere except in the lower stratospheric tropics where SAGE II values are known to be less accurate and where remote sensing from satellite is notoriously difficult. Another reason for the difference was that MLS (v0003) water vapour mixing ratios are believed to be too large (Lahoz et al., 1996). Results from a newer version of the retrieval (v0004) suggests that MLS stratospheric mixing ratios should be at least 5–10 % smaller. Furthermore, at least some of the difference could be attributed to the natural variability in the atmosphere (e.g. the affects of the QBO on the Brewer-Dobson circulation).

One of the largest differences between MLS, LIMS and SAGE II results was in the size and altitude of their stratospheric minima. The value of the retrieved MLS minimum was typically $\sim 3.5\text{--}4.0$ ppmv and was located over the tropics at either 22 hPa (~ 25 km) or 46 hPa (~ 20 km), adjacent grid points in the retrieved profile. For SAGE II, minimum mixing ratios of ~ 3.0 ppmv occur at ~ 16 km over the equator. For LIMS, the minimum was typically ~ 2.5 ppmv and was located at ~ 18 km. Part of the reason for these differences was attributed to the problem of inadequate measurement resolution. Another reason is due to the different times that measurements were made. MLS results implied that dry (and wet) air in the tropics rises slowly through the lower stratosphere and is relatively unmixed; minimum mixing ratios at 22 hPa were shown to be as a result of the upwards advection of dry air previously at 46 hPa (Carr et al., 1995). Hence, depending on the time measurements were made, minima (and maxima) would be observed at different altitudes.

The difference in the magnitude of the minima may also be related to the variabilities in the tropopause temperatures since small changes in temperature have a large impact on saturation mixing ratios and hence the mixing ratio of air entering the stratosphere.

A feature not previously observed by satellites, and uniquely observed by MLS, was the extensive dehydration that occurred in the Antarctic lower stratosphere during the summer of 1992. Zonal-mean mixing ratios of less than 1.0 ppmv were observed in southern high latitudes (65°S to 80°S) at 46 hPa. The values were comparable with previous *in-situ* results (e.g. Kelly et al., 1989).

Variability of H₂O in the lower stratospheric tropics and sub-tropics was shown (Chapter 6) to be primarily annual with some modulation by the QBO, which acted to delay or accelerate air parcels according to its phase. At latitudes poleward, and at 46 hPa, there was some sign of transport, from the tropics, of the annual signal. At 22 hPa this was less clear.

There was also some degree of variability and hemispheric difference that could be related to seasonal variations in the Brewer-Dobson circulation. Ascent, implied by the upwards-bowing of the contours in the zonal-mean latitude-height distributions, was observed to be more acute in the summer hemisphere than in the winter hemisphere.

The variation at high latitudes in the northern hemisphere showed a clear annual cycle, mainly because of strong descent of wetter air in winter periods. At southern high latitudes, particularly at 46 hPa, the largest amplitudes of the variability were as a result of the severe dehydration which occurred during the winter of 1992. The period when the southern vortex of 1992 broke up was a time when MLS was viewing northern high latitudes so nothing certain can be concluded about the impact, if any, that dehydrated air had on the middle latitude distribution. However at the time when southern high latitudes were next observed (some 6 weeks later), there was little sign of any decrease in average mixing ratios, indicating that any spread of dehydrated air had, at most, a minimal impact when mixed with air from mid-latitudes. This was consistent with studies by Mote (1994) using HALOE data

In the upper stratosphere, the variability could be separated into two distinct latitudinal regions; tropical and higher latitudes.

In tropical latitudes, MLS water vapour variability showed very distinct semi-annual oscillations (SAO) with the strongest amplitudes at 2.2 hPa and 1 hPa. The oscillations were qualitatively consistent with variations in UKMO equatorial zonal-mean wind fields and with tropical mixing ratios of upper stratospheric HALOE data. There was also a large degree of seasonal variability in the latitudinal structure of the SAO. The smallest mixing ratios were observed around the period of the strongest easterlies and thus where the strongest perturbations existed. Maximum mixing ratios correspondingly occurred during the strongest westerly SAO phases. Moreover, since maxima in upper stratospheric easterlies

and westerlies occur near the solstices and equinoxes respectively (e.g. Swinbank and O'Neill, 1994) asymmetries were created about the equator in the upper stratospheric water vapour distribution.

At higher latitudes the variations mainly followed an annual regime with winter descent having a large impact on the observed variations. The implied descent in the northern hemisphere was greater than in the south, consistent with previous studies of the vortex descent rates (e.g. Rosenfield et al., 1994). Variations in upper stratospheric HALOE water vapour were similar.

Case studies of 5-day periods in the northern and southern winters of 1992/93 and 1992 found temperatures in both vortices were extremely low but dehydration was limited to the southern vortex (Chapter 7). Temperature and water vapour data indicated that episodes of supersaturation (and hence type II PSC formation) probably occurred throughout this southern winter. This was supported by the extensive chemical ozone loss in the vortex observed during this time (Waters et al., 1993).

Although, temperature and water vapour measurements indicated that supersaturation should have been widespread in the northern vortex too, it was subsequently discovered that MLS temperatures were colder than the 'truth' by at least 2 K (Fishbein, *personal communication*). Recalculation of supersaturation values, assuming the temperature to be 2 K greater, revealed that episodes of supposed ice-cloud were greatly reduced and persisted for only short periods of time (a few days). This meant that any sustained dehydration was unlikely.

However, using CLAES aerosol data it was shown that, during the study-period, February 12 - February 16 type I PSC were present in the boreal vortex. The low temperatures causing the PSC were found to be induced by a tropospheric weather system which penetrated underneath the vortex and adiabatically cooled air passing over it. It was concluded that such weather systems should be studied since any change in their variation may indirectly lead to greater dehydration and subsequent ozone depletion.

At the beginning of 1996, a new version of MLS retrieval software became operational (v0004). This, coupled with the fact that a full non-linear retrieval may not be too far off, will mean that much of the work in this thesis will have to be updated. In particular, if retrievals are possible below 46 hPa, a better comparison

may be made with the variations in lower stratospheric SAGE II data. Moreover, this comparison could be extended to include CLAES, since future versions of its H₂O retrievals should be greatly improved.

Discussion of MLS measurements in the mesosphere (above ~50 km) were not included in this thesis. However, there is a lot of scope for future study in this area and it is hoped that somebody will make full use of this data.

References

- Andrews, D. G., Holton, J. R., and Leovy, C. B., *Middle Atmosphere Dynamics*, Academic Press, 489pp, 1987
- Angell, J. K., and Korshover, J., Quasi-biennial and long term fluctuations in total ozone, *Month. Weath. Rev.*, **101**, 426-443, 1973
- Barath, F.T., Chavez M. C., Cofield R. E. et al., The upper atmosphere research satellite microwave limb sounder instrument, *J. Geophys. Res.*, **98**, 10751-10762, 1993
- Barclay, F. R., Elliott, M. J. W., Goldsmith, P. and Jelley, J. V., A direct measurement of the humidity in the stratosphere using a cooled vapor trap, *Quart. J. Roy. Meteorol. Soc.*, **86**, 259-264, 1960
- Barrett, E. W., Herndon L. R. and Carter, H. J., Some measurements of the distribution of water vapor in the stratosphere, *Tellus*, **2**, 320-311, 1950
- Bates, D. R., and Nicolet, M., Atmospheric hydrogen, *Atmospheric Hydrogen, Plan. Spa. Sci.*, **13**, 905-909, 1965
- Beagley, S.R., Harwood, R. S., The residual circulation: interhemispheric differences and heating and eddy components, in *Transport Processes in the Middle Atmosphere*, edited by G Visconti and R Garcia, published by Reidel, pg 387-400, 1987
- Brewer, A. W., Air Ministry Meteorological Research Ctte., MRP, No.940, 1955
- Brewer, A. W., Evidence for a world circulation provided by the measurements of helium and water vapour distribution in the stratosphere, *Quart. J. Roy. Meteorol. Soc.*, **75**, 351-363, 1949
- Brown, F., Goldsmith, P., Green, H. F., Holt, A. and Parham A. G., Measurements of the water vapour, tritium and carbon-14 content of the middle atmosphere over southern England, *Tellus*, **13**, 407-416, 1961
- Carr, E. S., Harwood, R. S., Mote, P. W., Peckham, G. E., Suttie, R. E., Lahoz, W. A., Lahoz, O'Neill, A., Froidveaux, L., Jarnot, R. F., Read, W. G., Waters, J. W., and Swinbank, R., Tropical stratospheric water vapour measured by the microwave limb sounder (MLS), *Geophys. Res. Lett.*, **22**, 691-694, 1995
- Cariolle, D., Muller, S., and Cayla, F. Mountain waves, polar stratospheric clouds, and the ozone depletion over Antarctica, *J. Geophys. Res.*, **94**, 11233-11240, 1989
- Chiou, E. W., McCormick, M. P., McMaster, L. R., Chu, W. P., Larsen, J. C., Rind, D. and Oltmans S., Intercomparison of stratospheric water vapor observed by satellite experiments: stratospheric aerosol and gas experiment II versus limb infrared monitor of the stratosphere and Atmospheric Trace Molecule Spectroscopy, *J. Geophys. Res.*, **98(D3)**, 4875-4887, 1993

- Cluley, A. P. and Oliver M. J., Aircraft measurements of humidity in the low stratosphere over southern England 1972–1976, *Quart. J. Roy. Meteorol. Soc.*, **104**, 511–526, 1978
- Danielsen, E.F., In situ evidence of rapid, vertical, irreversible transport of lower tropospheric air into the lower stratosphere by convective cloud turrets and by larger scale upwelling in tropical cyclones, *J. Geophys. Res.*, **98(D5)**, 8665–8681, 1993
- Danielsen, E. F., A dehydration mechanism for the stratosphere, *Geophys. Res. Letts.*, **9**, 605–608, 1982
- Davis, G. R., Remote sensing of atmospheric water vapour by pressure modulation radiometry, *D. Phil. Thesis*, Oxford University, 1987
- Dessler, A. E., Weinstock, E. M., Hintsa, E. J., Anderson, J. G., Webster, C. R., May, R. D., Elkins, J. W., and Dutton, G. S., An examination of the total hydrogen budget of the lower stratosphere, *Geophys. Res. Letts.*, **21(23)**, 2563–2566, 1994
- Dobson, G. M. B., Brewer A. W. and Cwilong, B.M., Meteorology of the lower stratosphere, *Proc. Royal Soc. (London)*, **A185**, 144–175, 1946
- Dobson, G. M. B., Harrison, D. N., and Lawrence, J., Measurements of the amount of ozone in the Earths atmosphere and its relation to other geophysical parameters, *Proc. Royal Soc. (London)*, **122**, 456–486, 1928
- Douglass, A. R., and Stanford, J. L., A model of the antarctic sink for stratospheric water vapour, *J. Geophys. Res.*, **87(NC7)**, 5001–5008, 1982
- Drummond, J. R., Houghton, J. T., Peskett, G. D., Rodgers, C. D, Wale, M. J., Whitney, J. and Williamson, E. J., The stratospheric and mesospheric sounder on Nimbus 7, *Phil. Trans. Roy. Soc. London.*, *A296*, 219–242, 1980
- Dunkerton, T. J., On the role of kelvin wave in the westerly phase of the semi-annual zonal wind oscillation, *J. Atmos. Sci.*, **36**, 32–41, 1979
- Ellsaesser, H. W., Stratospheric water vapour, *J. Geophys. Res.*, **88**, 3897–3906, 1983
- Ellsaesser, H. W., Harries, J. E., Kley, D. K., and Penndorf, R., Stratospheric H₂O, *Planet. Space. Sci.*, **28**, 827–835, 1980
- Ellsaesser, H. W., Water vapor budget of the stratosphere, CIAP 3, DOT-TSC-OST-74-15, NTIS, Springfield, VA, 273–283, 1974
- Elson, L. S., Read, W. G., Waters, J. W., Mote, P. W., Kinnersley, J. S., Harwood, R. S., Space-time variations in water vapor as observed by the UARS microwave limb sounder, *J. Geophys. Res.*, **101 (D4)**, 9001–9015, 1996
- Fahey, D. W., Kelly, K. K., Kawa, S. R., Tuck, A. F., Loewenstein, M., Chan, K. R., and Heidt, L. E., Observations of denitrification and dehydration in the winter polar stratospheres, *Nature*, **344**, 321–324, 1990
- Fishbein, E.F., Read, W. G., Froidevaux, L., and Waters, J. W., Validation of temperature and pressure measurements by the Upper Atmosphere Research Satellite Microwave Limb Sounder, *J. Geophys. Res.*, **101 (D6)**, 9983–10016, 1996
- Frederick, J. E., and Douglass, A. R., Atmospheric temperatures near the tropical tropopause: temporal variations, zonal asymmetry and implications for stratospheric water vapor, *Mon. Weath. Rev.*, **111**, 1397–1403, 1983

- Gille, J. C. and Russell III, J. M., The limb infrared monitor of the stratosphere: experiment description, performance and results, *J. Geophys. Res.*, **89** (D4), 5125–5140, 1984
- Gray, L. G., Ruth, S., The modelled latitudinal distribution of the ozone quasi-biennial oscillation using observed equatorial winds, *J. Atmos. Sci.*, **50**(8), 1033–1046, 1993
- Gray, L. G., Pyle, J. E., Two-dimensional studies of equatorial dynamics and tracer distributions, *Quart. J. Roy. Meteorol. Soc.*, **113** (no. 476), 635–651, 1987
- Gunson, M. R., Farmer, C. B., Norton, R. H., Zander, R., Rinsland, C. R., Shaw, J. H. and Gao B. C., Measurements of CH₄, N₂O, CO, H₂O and O₃ in the middle atmosphere by the atmospheric trace molecular spectroscopy experiment on spacelab 3, *J. Geophys. Res.*, **95**, 13867–13882, 1990
- Hansen, A. R., and Robinson, G. D., Water vapor and methane in the upper stratosphere: An examination of some of the Nimbus 7 measurements, *J. Geophys. Res.*, **94**(D6), 8474–8484, 1989
- Hansen, J., Lacis, A., Rind, D., Russell, G., Stone, P., Fung, I., Reudy R. and Lerner, J., Climate sensitivity: Analysis of feedback mechanisms, in *climate Processes and Climate Sensitivity*, edited by Hansen, J. and Takahashi, T., *Geophys. Monogr. Ser.*, vol 29, 73–91, 1984
- Harries, J. E., Russell III, J. M., Tuck A. F., Gordley, L. L., et al., Validation of measurements of water vapour from the halogen occultation experiment, HALOE, *J. Geophys. Res.*, **101** (D6), 10205–10216, 1996
- Harries, J. E., The distribution of water vapour in the stratosphere, *Rev. Geophys. Space Phys.*, **14**, 565–575, 1976
- Hasebe, F., The global structure of the total ozone fluctuations observed on the time scales of two to several years. *Dynamics of the middle atmosphere*, J.R. Holton, t. Matsuno, Eds., Terra Scientifica, 445–464, 2984
- Hayashi, E., Water vapor distribution in the stratosphere by the dew-point radiosonde observation, *J. Meteor. Res.*, **13**, 905–916, 1961
- Holton, J.R., and Lindzen, R. An updated theory for the quasi-biennial cycle of the tropical stratosphere, *J. Atmos. Sci.*, **29**(2), 1972
- Houghton, J. T. and Seeley, J. S., Spectroscopic observations of the water vapour content of the stratosphere, *Quart. J. Roy. Meteorol. Soc.*, **86**, 358–370, 1960
- Hyson, P., Stratospheric water vapour over Australia, *Quart. J. Roy. Meteorol. Soc.*, **109**, 285–294, 1983
- Jarnot, R.F., R.E. Cofield, G.E. Peckham, and J.W. Waters, Calibration of UARS MLS, *J. Geophys. Res.*, submitted, 1994.
- Johnston, H.S. and Solomon, S., Thunderstorms as possible micro-meteorological sinks for stratospheric water, *J. Geophys. Res.*, **84**, 3155–3158, 1979
- Johnson, D.J., Jucks, K. W., Traub W. A., and Chance, K. V., The Smithsonian stratospheric far-infrared spectrometer and data reduction system, J.G.R., in press, (1994).
- Jones, P. D., Recent warming in global temperature series, *Geophys. Res. Lett.*, **21**(12), 1149–1152, 1994
- Jones, R. L., Pyle, J. A., Harries, J. E., Zavody, A. M., Russell III, J. M. and Gille, J. C., The water vapour budget of the stratosphere studied using LIMS and SAMS satellite data, *Quart. J. Roy. Meteorol. Soc.*, **112**, 1127–1243, 1986

- Jones, R. L. and Pyle, J. A., Observations of CH₄ and N₂O by the Nimbus 7 SAMS: A comparison with in-situ data and two dimensional numerical model calculations, *J. Geophys. Res.*, **89**, 5263–5279, 1984
- Kawa, S. R., Fahey, D. W., Kelly, K. K., Dye, J. E., Baumgardner, D., Gandrud, B. W., Loewenstein, M., Ferry, G. V., and Chan, K. R., The arctic polar stratospheric cloud aerosol: aircraft measurements of reactive nitrogen, total water, and particles, *J. Geophys. Res.*, **97(D8)**, 7925–7938, 1992
- Kelly, K.K., A.F. Tuck, D.M. Murphey, M.H. Proffitt, D.W. Fahey, R.L. Jones, D.S. McKenna, M. Loewenstein, J.R. Podolske, S.E. Strahan, G.V. Ferry, K.R. Chan, J.F. Vedder, G.L. Gregory, W.D. Hypes, M.P. McCormick, E.V. Browell, and L.E. Heidt, Dehydration in the lower Antarctic stratosphere during late winter and early spring, 1987, *J. Geophys. Res.* **94**, D9, 11317–11357, 1989.
- Kerridge, B. J., and Remsberg, E. E., Evidence from the limb infra-red monitor of the stratosphere for non-local thermodynamic equilibrium in the v₂ mode of mesospheric water vapour and the v₃ mode of stratospheric nitrogen dioxide, *J. Geophys. Res.*, **94 (D13)**, 1989
- Kinne, S, O.B. Toon and M.J. Prather, Buffering of Stratospheric Circulation by Changing amounts of tropical ozone: A Pinatubo case study, *Geophys. Res. Lett.*, **19(19)**, 1927–1930, 1992
- Kinnersley, J.S., A realistic three-component planetary wave model, with a wave breaking parameterisation, *Quart. J. Roy. Meteorol. Soc.*, **121(a)**, 853–881, 1995
- Kley, D., Schmeltekopf, A. L., Kelly, K., Winkler, R. H., Thompson, T. L. and McFarland, M., Transport of water vapor through the tropical tropopause, *Geophys. Res. Lett.*, **9**, 617–620, 1982
- Kley, D. E., Stone, J., Henderson, W. R., Drummond, J. W., Harrop, W. J., Schmeltekopf, A. L., Thomson, T. M. and Winkler, R. H., *In-situ* measurements of the mixing ratio of water vapor in the stratosphere, *J. Atmos. Sci.*, **36**, 2513–2524, 1979
- Labitzke, K., McCormick, M. P., Stratospheric temperature increases due to pinatubo aerosols, *Geophys. Res. Lett.*, **19(2)**, 207–210, 1992
- Lahoz, W.A., M.R. Suttie, L. Froidevaux, R.S. Harwood, C.L. Lau, T.A. Lungu, G.E. Peckham, H.C. Pumphrey, W.G. Read, Z. Shippony, R.A. Suttie, J.W. Waters, G.E. Nedoluha, S.J. Oltmans, J.M. Russell III, and W.A. Traub, Validation of UARS MLS 183 GHz H₂O measurements, *J. Geophys. Res.*, **101 (D6)**, 10129–10149, 1996
- Lahoz, W.A., O'Neill, A., Carr, E. S., Harwood, R. S., Froidevaux, L., Read, W. G., Waters, J. W., Kumer, J. B., Mergenthaler, J. L., Roche, A. E., Peckham, G. E., and Swinbank, R., 3-dimensional evolution of water vapor distributions in the northern hemisphere stratosphere as observed by the MLS, *J. Atmos. Sci.*, **51(20)**, 2914–2930, 1994
- Lahoz, W. A., Carr, E. S., Froidevaux, L., Harwood, R. S., Kumer, J. B., Mergenthaler, J. L., Peckham, G. E., Read, W. G., Ricaud, P. D., Roche, A. E., Northern hemisphere mid-stratosphere vortex processes diagnosed from H₂O, N₂O and potential vorticity, *Geophys. Res. Lett.*, **20(23)**, 2671–2674, 1993
- Lindzen, R. S., Holton, J. R., A theory of the quasi-biennial oscillation, *J. Atmos. Sci.*, **25**, 1095–1107, 1968

- Manney, G.L., Froidevaux, L., Waters, J. W., Zurek, R. W., Read, W. G., Elson, L. S., Kumer, J. B., Mergenthaler, J. L., Roche, A. E., O'Neill, A., Harwood, R. S., MacKenzie, I., and Swinbank, R., Chemical depletion of ozone in the Arctic lower stratosphere during winter 1992–93, *Nature* **370**, 429–434, 1994.
- Manney, G.L., Froidevaux, L., Waters, J. W., Fishbein, E. F., Zurek, R. W., Harwood, R. S., Lahoz, W.A., The evolution of ozone observed by UARS MLS in the late 1992 winter southern polar vortex, *Geophys. Res. Lett.*, **20(12)**, 1279–1282, 1993
- Mason, GARP Publ. Ser., **26**, vol II, 295–311, 1986
- Mastenbrook, H. J., and Oltmans, S. J., Stratospheric water vapour variability for Washington, DC/Boulder, CO: 1964–82, *J. Atmos. Sci.*, **40**, 2157–2165, 1983
- Mastenbrook, H. J., Water vapor measurement in the lower stratosphere, *Can. J. Chem.*, **52**, 1527, 1974
- Mastenbrook, H. J., Water vapor distribution in the stratosphere and high troposphere, *J. Atmos. Sci.*, **25**, 299–311, 1968
- Mastenbrook, H. J., Frost-point hygrometer measurements in the stratosphere and the problem of moisture contamination, *Humidity and moisture measurement and control in science and industry*, Vol II, New York, Rheinhold Publishing Co., 480–485, 1965
- McCormick, M. P., Chiou, E. W., McMaster, Chu, W. P., Larsen, J. C., Rind, D., and Oltmans, s., Annual variations of water vapor in the stratosphere and upper troposphere observed by the stratospheric aerosol and gas experiment II, *J. Geophys. Res.*, **98(D3)**, 4867–4874, 1993
- McCormick, M. P., and Chiou, E. W., Annual variations of water vapor in the stratosphere and upper troposphere based on SAGE II observations made during 1986–1992, paper presented at *Chapman conference on atmospheric water vapour*, 1993
- McCormick, M. P., Steele, H. M., Hamill, P., Chu, W. P., Swissler, T. J., Polar stratospheric cloud sitings, *J. Atmos. Sci.*, **39(6)**, 1387–1397, 1982
- McKenna, D. S., Jones. R. L., Austin, J., Browell, E. V., McCormick, M. P., Krueger, A. J., and Tuck, A. F., Diagnostic studies of the antarctic vortex during the 1987 airborne antarctic ozone experiment: ozone miniholes, *J. Geophys. Res.*, **94(D9)**, 1989
- McKenzie, A. R., Kulmala, M., Laaksonen, A., Vesala, T., On the theories of type-I polar stratospheric cloud formation, *J. Geophys. Res.*, **100(D6)**, 11275–11288, 1995
- Mergenthaler, J. L., Kumer, J. B., Roche, A. E., CLAES south-looking aerosol observations for 1992, *Geophys. Res. Lett.*, **20(12)**, 1295–1298, 1993
- Mote, P. W., Rosenlof, K. H., McIntyre, M. E., Carr, E. S., Holton, J. R., Kinnersley, J. S., Pumphrey, H. C., III Russell, J. M., Waters, J. W., and Gille, J. C., An atmospheric tape recorder: the imprint of tropical tropopause temperatures on stratospheric water vapour, *J. Geophys. Res.*, **101 (D2)**, 3989–4006, 1996
- Mote, P.W., K.H. Rosenlof, J.R. Holton, R.S. Harwood, and J.W. Waters, Seasonal variations of water vapor in the tropical lower stratosphere, *Geophys. Res. Lett.* **22**, No. 9, 1093–1096, 1995
- Mote, P.W., A reconsideration of the cause of dry air in the southern middle latitude stratosphere, middle latitude stratosphere, *Geophys. Res. Lett.*, **22(15)**, 2025–2028, 1995

- Mote, P.W., Holton, J.R., Russell, J. M., Boville, B. A, A comparison of observed (HALOE) and modelled (CCM2) methane and stratospheric water-vapour, *Geophys. Res. Lett.*, **20(14)**, 1419-1422, 1993
- Munro, R. and Rodgers, C. D., Latitudinal and season variations of water vapour in the middle atmosphere, *Geophys. Res. Lett.*, **21(8)**, 661-664, 1994
- Murcray, D. G., Kyle T. G. and Williams W. J., Distribution of water vapor in the stratosphere as determined from setting sun absorption data, *J. Geophys. Res.*, **74**, 5369-5373, 1969
- Murcray, D. G., Murcray F. H. and Williams W. J., Distribution of water vapor in the stratosphere as determined from infrared absorption measurements, *J. Geophys. Res.*, **67**, 759-766, 1962
- Mutlow, C. T., Studies of atmospheric water vapour using satellite data, *D. Phil. Thesis*, Oxford University, 1984
- Newell, R. E. and Gould-Stewart, S., A stratospheric fountain ?, *J. Atmos. Sci.*, **38**, 2789-2796, 1981
- Oltmans, S. J., and D. J., Hofmann, Increase in lower stratospheric water vapour at a mid-latitude northern hemisphere site from 1981 to 1994, *Nature*, **374 (no. 6518)**, 146-149, 1995
- Orsolini, Y., Cariolle, D., Deque, M., Ridge formation in the lower stratosphere and its influence on ozone transport: A general circulation model study during late January 1992, *J. Geophys. Res.*, **100(D6)**, 11113-11135, 1995
- Ovarlez, J., Ovarlez, H., and Teitelbaum, H., In situ measurements, and a case study of the drying mechanism of the tropical lower stratosphere, submitted to *Quarterly Journal of the Royal Meteorological Society*, 1996
- Pawson, S., R. S. Harwood, Monthly mean diabatic circulations in the stratosphere, *Quart. J. Roy. Meteorol. Soc.*, **115**, 807-840, 1989
- Penndorf, R., Analysis of ozone and water vapor field measurement data, Report No. FAA-EE-78-29, NTIS, Springfield, VA, 1978
- Poole, L. R., and McCormick, M. P., Polar stratospheric clouds and the antarctic ozone hole, *J. Geophys. Res.*, **93(ND7)**, 8423-8430, 1988
- Ray, E.A., J.R. Holton, E.F. Fishbein, L. Froidevaux, and J.W. Waters, The tropical semi-annual oscillation in temperature and ozone as observed by the MLS, *J. Atmos. Sci.*, **51**, 3045-3052, 1994.
- Reber, C. A., Trevathan, C. E., McNeal, R. J., Luther, M. R., The upper atmosphere research satellite (UARS) mission, *J. Geophys. Res.*, **98(D6)**, 10643-10647, 1993
- Reber, C. A., The upper atmosphere research satellite, *Eos Trans.*, AGU, **71**, 1867, 1990
- Reid, G. C., and Gage, K. S., On the annual variation in height of the tropical tropopause, *J. Atmos. Sci.*, **38**, 1928-1938, 1981
- Remsberg, E.E., Improved absorption cross sections for the retrieval of Nimbus 7 LIMS water vapor, *Technical Digest Optical Remote Sensing of the Atmosphere*, 458-460, 1990
- Remsberg, E.E., J.M. Russell III, and C.-Y. Wu, An interim reference model for the variability of the middle atmosphere water vapor distribution, *Adv. Space Res.* **10**, 51-64, 1990.
- Remsberg, E. E., Russell. J. M., Gordley, L. L., Gille J. C. and Bailey P. L., Implications of the stratospheric water vapor distribution as determined from the Nimbus 7 LIMS experiment, *J. Atmos. Sci.*, **41**, 2934-2945, 1984

- Read, W.G., J.W. Waters, L. Froidevaux, D.A. Flower, R.F. Jarnot, D.L. Hartmann, R.S. Harwood, and R.B. Rood, Upper tropospheric water vapor from UARS MLS, *Bull. Amer. Met. Soc.*, submitted, 1994.
- Reed, R. J., Campbell, W. J., Rasmussen, L. A., and Rogers, D. G., Evidence of downward propagating annual wind reversal in the tropical stratosphere, *J. Geophys. Res.*, **66**, 813–818, 1961
- Ricaud, P. D., Carr, E. S., Harwood, R. S., Lahoz, W. A., Froidevaux, L., Read, W. G., Waters, J. W., Mergenthaler, J. L., Kumer, J. B., Roche, A. E., Peckham, G. E., Polar stratospheric clouds as deduced from MLS and CLAES measurements, *Geophys. Res. Lett.*, **22(15)**, 2033–2036, 1995
- Rind, D. and Lonergan, P., Modeled impacts of stratospheric ozone and water vapor perturbations with implications for high-speed civil transport aircraft, *J. Geophys. Res.*, **100(D4)**, 7381–7396, 1995
- Rind, D., Chiou, E. W., Chu, W. P., Oltmans, S., Lerner, J., Larsen, J., McCormick M. P., and McMaster L., Overview of the stratospheric aerosol and gas experiment II water vapor observations: Method, validation, and data characteristics, *J. Geophys. Res.*, **98(D3)**, 1993
- Rind, D., and Lacis, A., The role of the stratosphere in climate change, *Surv. Geophys.*, **14**, 133–165, 1993
- Rinsland, C. P., Smith, M. A. H., Seals, R. K., Goldman, A., Murcray, F. J. and Murcray, D. G., Stratospheric measurements of collision-induced absorption by molecular oxygen, *J. Geophys. Res.*, **87 (C4)**, 3119–3122, 1982
- Robbins, D., Waters, J., Zimmermann, P., Jarnot, R., J. Hardy, H. Pickett, S. Pollitt, W. Traub, K. Chance, Louisnard, N., Evans, W., and Kerr, J., Ozone measurements from the balloon intercomparison campaign, *J. Atmos. Chem.* **10**, 181–218, 1990.
- Robinson, G.D., and Atticks Schoen M. G., , The formation and movement in the stratosphere of very dry air, *Quart. J. Roy. Meteorol. Soc.*, **113**, 653–679, 1987
- Roche, A. E., Kumer, J. B., Mergenthaler, J. L., Ely, G. A., Uplinger, W. G., Potter, J. F., James, T.C., and Sterrit, L. W., The cryogenic limb array etalon spectrometer (CLAES) on UARS: Experiment description and performance, *J. Geophys. Res.*, **98(D6)**, 10763–10775, 1993a
- Roche, A. E., Kumer, J. B., Mergenthaler, J. L., CLAES observations of ClONO₂ and HNO₃ in the antarctica stratosphere, *Geophys. Res. Lett.*, **20(12)**, 1223–1226, 1993b
- Rodgers, C.D., Characterisation and error analysis of profiles retrieved from remote sounding measurements, *J. Geophys. Res.*, **95(D5)**, 5587–5595, 1990.
- Rodgers, C.D., Retrieval of atmospheric temperature and composition from remote measurements of thermal radiation, *Rev Geophys. and Space Phys.* **14**, 609–624, 1976b.
- Rosenfield, J. E., Newman, P. A., Schoeberl, M. R., Computations of diabatic descent in the stratospheric polar vortex, *J. Geophys. Res.*, **99(D8)**, 16677–16689, 1994
- Russell III, J. M., Gordley, L.L., Park, J. H., Drayson, S. R., Hesketh, W. D., Cicerone, R. J., Tuck. A. F., Frederick, J. E., Harries, J. E. and Crutzen, P. J., The halogen occultation experiment, *J. Geophys. Res.*, **98(D6)**, 10777–10797, 1993a

- Russell III, J. M., Tuck, A. F., Gordley, L.L., Park, S. J., Drayson, S. R., Harries, J. E., Cicerone, R. J., and Crutzen, P. J., HALOE antarctic observations in the spring of 1991, *Geophys. Res. Lett.*, **20**, 719–722, 1993b
- Russell, J. M., An interim reference model for the middle atmosphere water vapor distribution, *Adv. Space Res.*, **7(9)**, 1987
- Russell, J. M., Gille J. C., Remsberg, E. E., Gordley, L. L., Bailey P. L., Fisher, H., Girard, A., Drayson, S. R., Evans, W. F. J. and Harries J. E., Validation of water vapour results measured by the limb infrared monitor of the stratosphere experiment on Nimbus 7, *J. Geophys. Res.*, **89 (D4)**, 5115–5124, 1984
- Santee, M.L., Read, W. G., Waters, J. W., Froidevaux, L., Manney, G. L., Flower, D. A., Jarnot, R. F., Harwood, R. S., and Peckham, G. E., Inter-hemispheric differences in polar stratospheric HNO₃, H₂O, ClO, and O₃, *Science* **267**, 849–852, 1995.
- Schoeberl, M. R., Lait, L. R., Newman, P. A., Rosenfield, J. E., The structure of the polar vortex, **97(D8)**, 7859–7882, 1992
- Schoeberl, M. R., and Hartmann, D. L., The dynamics of the stratospheric polar vortex and its relation to springtime ozone depletion, *Science*, **251(4989)**, 46–52, 1991
- Smithsonian Institution, Smithsonian Meteorological Tables, 6th rev .ed., prepared by R.J. List, *Smithson. Inst. Publ.*, 1958
- Solomon, S., The mystery of the antarctic ozone hole, *Rev. Geophys.*, **26**, 131–148, 1988
- Stanford, J. L., Possible sink for stratospheric water vapour at the winter antarctic pole, *J. Atmos. Sci.*, **30**, 1431–1436, 1973
- Steele, L. P., Dlugokencky, E. J., Lang, P. M., Tans, P. P., Martin, R. C., Masarie, K. A., Slowing down of the global accumulation of atmospheric methane during the 1980's, *Nature*, **358(6384)**, 313–316, 1992
- Suttie, M. R., Characterisation and error analysis for the H₂O retrieval from the upper atmosphere research satellite microwave limb sounder, *Ph. D. Thesis*, Edinburgh University, 1995
- Swinbank, R., and O'Neill, A., A stratosphere-troposphere data assimilation system, *Mon. Wea. Rev.*, **122**, 686-702, 1994.
- Taylor, F. W., Rodgers, C. D., Whitney, J. G., Werret, S.T., Barnett, J. J. et al, Remote sensing of atmospheric structure and composition by pressure modulator radiometry from space: The ISAMS experiment on UARS, *J. Geophys. Res.*, **98(D6)**, 10799–10814, 1993
- Toon, O. B., and Tolbert, M. A., Spectroscopic evidence against nitric acid trihydrate in polar stratospheric clouds, *Nature*, **375**, 218–221, 1995
- Toon, O. B., Turco, R.P., Hamill, P., Denitrification mechanisms in the polar stratospheres, *Geophys. Res. Lett.*, **17(4)**, 445–448, 1990
- Toon, O. B., Hamill, P., Turco, R. P., and Pinto, J., Condensation of HNO₃ and HCl in the winter polar stratospheres, *Geophys. Res. Lett.*, **13**, 1284–1287, 1986
- Trepte, C.R., Veiga, R.R., and McCormick, M. P. The polewards dispersal of Mount Pinatubo volcanic aerosol, *J. Geophys. Res.*, **98(D10)**, 18563–18573, 1993

- Tuck, A.F., Russell, J. M., Harries, J. E., Stratospheric dryness - antiphased dessication over Micronesia and Antarctica, *Geophys. Res. Lett.*, bf 20(12), 1227-1230, 1993
- Tucker, G. B., An analysis of the humidity measurements in the upper troposphere and lower stratosphere over southern England, MRP 1052, Meteorological Research Committee, London, 35pp, 1957
- Veryard, R. G., and Ebdon, R. A., Fluctuations in tropical stratospheric winds, *Meteorol. Mag.*, **90**, 125-143, 1961
- Vomel, H., Oltmans, S. J., Hofmann, D. J., Deshler, T. and Rosen, J. M., The evolution of the dehydration in the Antarctic stratospheric vortex, *J. Geophys. Res.*, **100(D7)**, 13919-13926, 1995
- Waters, J.W., Microwave Limb Sounding, in *Atmospheric Remote Sensing by Microwave Radiometry*, (M.A. Janssen, ed.), ch. 8, John Wiley & Sons, New York, 1993a.
- Waters, J.W., Froidevaux, L., Manney, G. L., Read, W. G., Elson, L. S., MLS observations of lower stratospheric ClO and O₃ in the 1992 southern-hemisphere winter, *Geophys. Res. Lett.*, **20(12)**, 1219-1222, 1993b
- Waters, J.W., A proposal for the Earth Observing System Microwave Limb Sounder, submitted to NASA A.O. No. OSSA-1-88, 1988.
- Waters, J., Hardy, J., Jarnot, R., Pickett, H., and Zimmermann, P., A balloon-borne microwave limb sounder for stratospheric measurements, *J. Quant. Spectrosc. Radiat. Transfer*, **32**, 407-433, 1984
- Waters, J., Gustinic, J., Swanson, P., and Kerr, A., Measurements of upper atmospheric H₂O emission at 183 GHz, in *Atmospheric Water Vapor*, edited by Wilkerson and Ruhnck, pp 229-240, 1980
- Waters, J.W., Absorption and emission by atmospheric gases, in *Methods of Experimental Physics, 12B*, (L. Meeks, ed.), 142-176, Academic Press, New York, 1976.
- WMO, Atmospheric Ozone 1985: WMO global ozone research and monitoring project, Report No. 16, vol II, Geneva, 1985
- WMO, *The stratosphere 1981 Theory and Measurements*. WMO global ozone research and monitoring project, Report No. 16, Geneva, 1981
- Wuebbles, D. J., F. M. Luther and J. E. Penner, Effect of coupled anthropogenic perturbations on stratospheric ozone, *J. Geophys. Res.*, **88**, 1444-1456, 1983.
- Zawodny, J. M., and McCormick, M. P., Stratospheric Aerosol and Gas Experiment II measurements of the quasi-biennial oscillations in ozone and nitrogen dioxide, *J. Geophys. Res.*, **96(D5)**, 9371-9377, 1991